Chapter I

Microelectrode Voltammetry

Introduction

Microelectrodes have been defined as electrodes having at least one physical dimension (the critical dimension) of the electrochemically active surface measuring in the low microns- 50 microns (e.g. radius of a disc or cylinder electrode) and lower. This definition is based not on the physical dimensions of the electrode but on the electrochemical properties that arise due to their small size.[1-3] When the critical dimension is lower than 10 nm –nanodes-the electrochemical properties undergo a further change.[4] The microelectrode definition originally applied to amperometric detectors; however the physical size criterion has been adopted to include physically small electrodes such as selective ion potentiometric detectors. The small physical size of the microelectrode allows accurate spatial location of the electrochemically active surface near the area of interest. It also reduces perturbation and in living organisms reduces damage in the adjacent regions. Applications of these physically small electrodes are: pH changes in a living cell,[5] K^+ in plant root hairs[6] and barley leaves,[7] NO_3^- in barley root cells,[8] heavy metals[9]and pesticides[10] in frog's eggs, probes for a combined scanning electrochemical-atomic force microscope to characterise the surface of a carbon electrode,[11] and monitoring neurotransmitter concentration changes in the mammalian brain.[12] It is the latter example that is the ultimate use of the physically small microelectrode fabricated and modified by the techniques presented in this thesis.

It is the aim of this work is to develop a method of fabricating a microelectrode, based on the *in situ* pyrolysis of acetylene to form a carbon film surface on a pulled quartz capillary substrate, to monitor the efflux of the neurotransmitter dopamine in the mammalian brain.

Additional to the fabrication is the modification of the carbon film surface to provide an anionic barrier with anti-fouling properties.

Neurotransmitters, such as large peptides, indoleamines, catecholamines and nitric oxide[13] are chemical messengers within the central nervous system. In this thesis work it is the catecholamine neurotransmitter dopamine that is of interest. Dopamine (4-(2-Aminoethyl)-1,2-benzenediol) has been associated with motor, cognitive and limbic functions, the early stages of Parkinson's disease, schizophrenia and attention deficit hyperactivity disorder.[14] Recently the release of dopamine into the extracellular fluid within the brain has been connected with drugs of abuse.[15-17]

To study neurotransmitters *in vivo*, freely moving[18;19] and anaesthetised rats,[20;21] together with brain slices[22;23] , release from a single cell[24] and absorption by a single cell in a picolitre vial[25] have been used. The relaying of messages (neurotransmission) is by the release of dopamine by a neuron and the uptake of it by an adjacent neuron with up to 4 μM being passed in one second[26], across the synapse, which is 100 nm wide and filled with extracellular fluid in a rat's forebrain nucleus accumbens region. The basal level of dopamine is ~ 5 nM rising to 1.6 μM during transient bursts. The nucleus accumbens region is located approximately 10mm down from the brain surface.

To stimulate the release of neurotransmitters in anesthetised animal or brain tissues, a series of electrical pulses (typically 5 pulses at 10 Hz), which mimics a neurological signal, is applied to the dopamine axons in the midbrain. Depending on the type of investigation the release of dopamine may occur over milliseconds to minutes.[23]

This understanding of the role of dopamine has been achieved using analytical techniques, such as microdialysis probes to collect extracellular samples which are then analysed by electrophoresis[27], HPLC[15] or GC/MS after derivatisation[28], together with electrochemical monitoring. (Dopamine is electrochemically active being easily oxidisable by a two electron transfer going from a 1,2-diol to a 1,2-dione.) The chromatography has provided an accurate

qualitative and quantitative analysis of the chemistry associated with the release and uptake of neurotransmitters. However chromatography has two disadvantages. The analysis requires minutes to obtain a sample and the dialysis probe is large. A recent paper has cast doubts on the reliability of quantitative results obtained by using a dialysis probe.[29] Due to its size (240 nm radius) it has been described as causing stab wound trauma.[30] The large size of the dialysis probe (150 μm) is reported to elicit higher levels of evoked dopamine efflux in the extracellular fluid than that obtained using a carbon fibre microelectrode.[29;31] Besides causing minimal damage on insertion into the brain, the microelectrodes provide accurate spatial location and temporal measurements[23] and when used in the fast scanning cyclic voltammetric mode the type of neurotransmitter can be verified.[32;33] The temporal resolution is important when the release and uptake occurs in time spans of less than one second.

In vivo monitoring of neurotransmitters in a mammalian brain was first achieved in 1973 using a 50 μm radius Teflon tube with a carbon paste tip in an anaesthetised rat's brain.[34] The lack of selectivity of this electrode prevented the discrimination of catecholamines from the endogenous ascorbic acid, in the extracellular fluid of the brain. This is a continuing challenge which is the subject of Chapter V in this thesis.

The 50 μm carbon paste electrode, having a flat disc surface, resulted in excessive tissue damage causing extracellular fluid leakage during *in vivo* implantation.[35] Although small metal electrodes were available they were found to be unsuitable for *in vivo* applications due to fouling, with consequential reduction in analytical signal in a very short period of time.[36-38]

In 1979 *in vivo* monitoring was improved by fabricating a carbon fibre electrode, 8 μm radius and 500 μm long.[39] Being of a smaller radius, damage during implanting and perturbation of the adjoining cells was minimised. This basic structure has remained unchanged and is the most popular form of microelectrode for experimentation, both *in vivo* and *in vitro*.[40] It is used as a fibre or cut to form a disc in aqueous and non-aqueous[41] solvents, etched and coated to

form nanodes.[42] Changes have occurred in its construction for specialised applications. A recent publication[43] details an improved technique for the fabrication of carbon fibre microelectrodes which includes the use of Wood's metal to improve the contact between the carbon fibre and recording instrument wire resulting in the reduction of background electrical noise. This reduction of electrical background noise is important, as measurement of neurotransmitters *in vivo* frequently requires the measurement of currents in the low picoampere range.

Other microelectrode configurations developed for *in vivo* monitoring have been a carbon ring[44] and carbon disc[45] electrodes. Both are based on the *in situ* pyrolysis of methane in a pulled quartz capillary. In the forming of the carbon ring the methane was pyrolysed by heating the pulled quartz capillary, in a Bunsen flame, such that a carbon film was formed on the inside walls. The remaining void was filled with resin and the tip cut to expose a ring of pyrolysed methane. The carbon disc electrode was formed by continuing to pyrolyse the methane until the tip completely sealed the pulled capillary orifice.

It is from the fabrications of the *in situ* pyrolysed methane ring and disc electrodes that this thesis has evolved. Instead of using methane as the hydrocarbon source acetylene was used. The rationale for the use of acetylene is that during pyrolysis of methane acetylene is the major species formed in the reaction pathway to the formation of carbon.[46] To form an electrochemically active surface, without oxides forming on the surface or complete loss of the carbon formed due to extensive oxidation, the pyrolysis was carried out under a blanket of nitrogen in a quartz tube. By varying the direction and flow rate of the nitrogen blanket both cylindrical (similar to carbon fibres) and disc electrodes can be formed. The details of this fabrication technique are given in Chapter III.

The use of a coated quartz substrate for carbon film formation has a physical strength advantage over that of carbon fibre. During insertion of the microelectrode into the rat's brain tissue great care must be taken to prevent breakage, as the tip must pass through 10 mm of

brain tissue. Carbon fibre, when in a polymer matrix has exceptional physical strength, however when used uncoated as a single fibre it is prone to breakage and care is required when handling. If breakage occurs re-insertion will result in additional tissue damage with consequential leakage from these cells thus casting doubts on the validity of the results. The alternative is the preparation of another animal, with consequential loss of time and animal.

An attempt to improve the fragility of carbon fibres was the coating of the carbon fibre with a silica film.[47] This coating, from 1 μm to 600 μm thick, enabled the construction of "mechanically stable" disc electrodes. This type of construction is limited to *in vivo* applications where the target analyte is of sufficiently high concentration, to yield a detectable signal. The fabrication of the disc electrodes presented in this thesis is of similar form. These amperometric microelectrodes, besides giving greater spatial resolution with smaller physical dimensions has consequential changes in electrode properties due to their small size, which is fortuitous for *in vivo* analysis. During electroanalysis molecules reach the electrode surface by migration, convection and diffusion. At microelectrodes surface diffusion predominates [48;49] and migration effects (conduction to the surface arising from the ionic charges) are minimised by using a supporting electrolyte. Convection (solution flow due to pressure gradients) is reduced by allowing a three minute quiescence time and supporting the reaction vessel on a vibration dampening surface. As the electrode size is reduced the diffusion pathways occur predominantly at the edge of the electrochemically active surface. This is illustrated in Figure I-i. In the case of a large electrode inlaid into a surface, such as a polished 3 mm radius glassy carbon disc electrode, the principal diffusion pathway is perpendicular to the surface. As the radius of the disc electrode decreases, the diffusion pathways to the edge predominate over the perpendicular paths. The curved surface of the hemisphere and cylinder also undergoes the same pathway changes as the radius decreases.

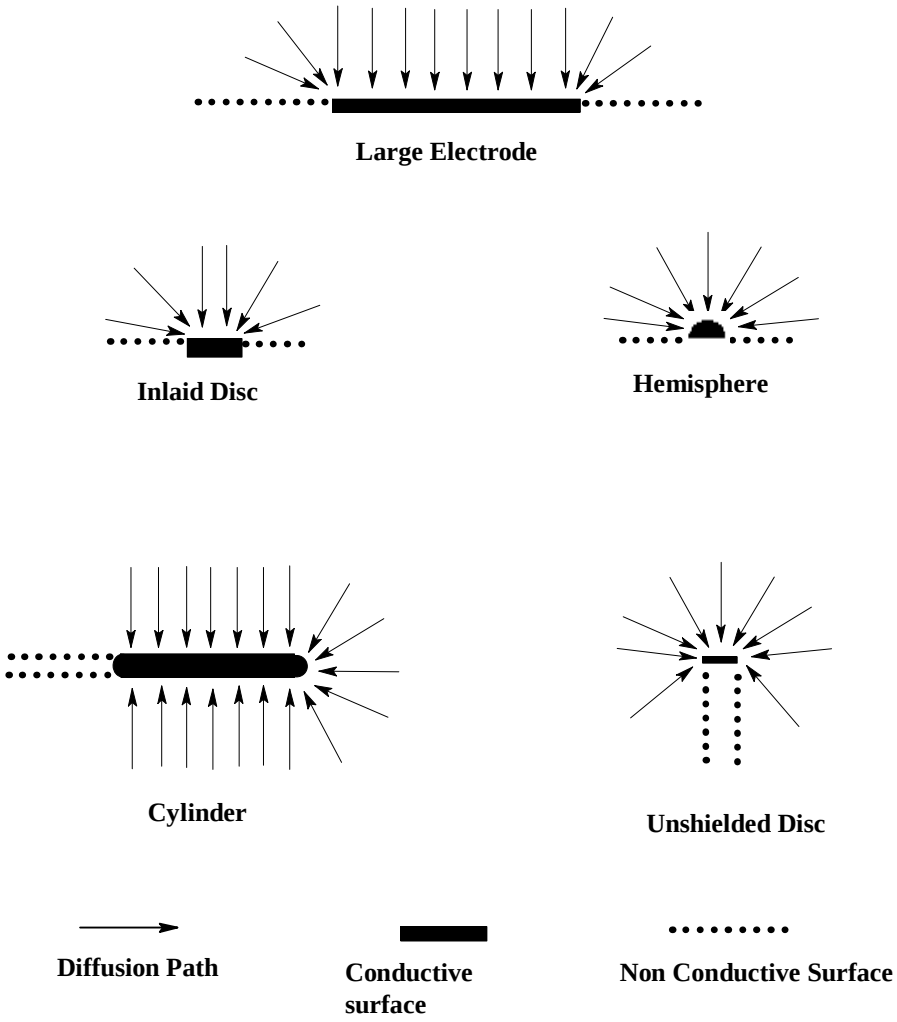

Figure I-i

Diffusion pathways at electrode surfaces

The unshielded disc electrode probably best represents the surface formed by *in situ* pyrolysis of acetylene in a pulled quartz capillary as the surface is formed *in situ* in a flowing gas stream. As the diffusion pathways to the unshielded electrode are closer to that of a hemisphere than that of an inlaid disc, this shape was used in this thesis for calculations of the electrode radius for non cylindrical electrodes.

The changes in diffusion pathways, when the electrochemically active surface becomes micrometre in size, confer unique properties on amperometric microelectrodes, such as the rapid attainment of steady state,[50] small IR drop[51] and a high signal to noise ratio.[51] This occurs due to the analytical signal becoming a function of the smallest electrochemically

active dimension of the electrode, whereas other properties, such as resistance and capacitance remain a function of the electrochemically active area.

The rapid attainment of steady state arises from the Cottrell decay,[4] being dependent on the diffusion currents exceeding the convective currents. The ability to reach steady state permits quantification of analyte concentration in a short time, such as monitoring the release and uptake of neurotransmitters, which occurs in milliseconds. Another example of rapid attainment of steady state is measurement of glucose with an enzyme glucose oxidase coated sensor in less than 85 milliseconds.[52] Using enzyme coated larger electrodes will take many minutes. The small physical size together with together with rapid attainment of steady state makes carbon fibre microelectrodes suitable for amperometric detectors for HPLC analysis [53] detecting 5-hydroxy-tryptophan down to 10 ppb. A further improvement in detection limits can be obtained by using different flow configurations in the HPLC detector, such as tubular and microjet.[54]

The small IR drop at the microelectrode surface solution interface is due to the very small currents, in nanoampere to picoampere range used by these electrodes. This compares to that of a conventional electrode (1 mm-5 mm radius) operating in the microampere range.[1] The low IR drop occurring at the electrode solution interface permits electrochemical measurements to be carried out in high electrical resistance solvents, such the oxidation of ferrocene in acetonitrile at a 25 μm radius platinum electrode or at a 0.3 μm electrode in dichloromethane and the oxidation of krypton in acetonitrile,[55] using a 20 μm radius 0.75 μm thick gold ring electrode on a glass fibre substrate, without the deliberate addition of a supporting electrolyte.[56] With conventional electrodes an ionic salt is used as a supporting electrolyte, at concentrations approximately hundred times that of the analyte. This high concentration of supporting electrolyte ensures that the current measured is predominately diffusion of the analyte and the ohmic polarisation of the cell is reduced. In the experimental work for this thesis, supporting electrolytes were used to ensure that only diffusion current

was measured as the sizes of microelectrodes fabricated in this thesis ranged from sub micron to 60 μm radius and 800 μm length for cylindrical microelectrodes.

Noise originating from the electrode surface (as distinct from equipment noise- Johnson, AC hum or EMI) arises from the surface capacitance. As capacitance is a function of surface area ($\propto r^2$) and current is dependent on the radius ($\propto r$) (Equation (ii) and (iii) this chapter) for disc and hemispherical electrodes, reducing the radius rapidly reduces capacitance ($\propto r$). For carbon fibre (cylindrical) electrodes this effect is similar as capacitance is directly proportional to electrode radius and length and with the current almost proportional to length. (Equation iv this chapter)

In addition to disc and cylinder electrodes these unique properties may be obtained by other electrode geometries having only one dimension measured in microns. These include band,[57;58] ring,[44]cylinder,[59] carbon paste filled microporous membranes [60] and RAM (random assemblies of microdiscs- 400 carbon 7 μm discs).[61] These electrode configurations, whilst maintaining the unique microelectrode properties also have a "large surface area". As a consequence the response to the analyte is in the microampere range enabling measurement with standard laboratory amperometers.

With the physically small size and unique properties of amperometric microelectrodes the detection and monitoring in real time, *in vivo* of neurotransmitters in a mammalian brain is an ideal application for such devices.

The unique properties, which arise due to the diffusion profile of the microelectrodes (see Figure 1-i), are illustrated by comparing the cyclic voltammogram of a 3 mm diameter glassy carbon electrode to that of a 0.5 μm radius carbon film microelectrode in Figure I-ii.

Theory of Electron Transfer at a Microelectrode

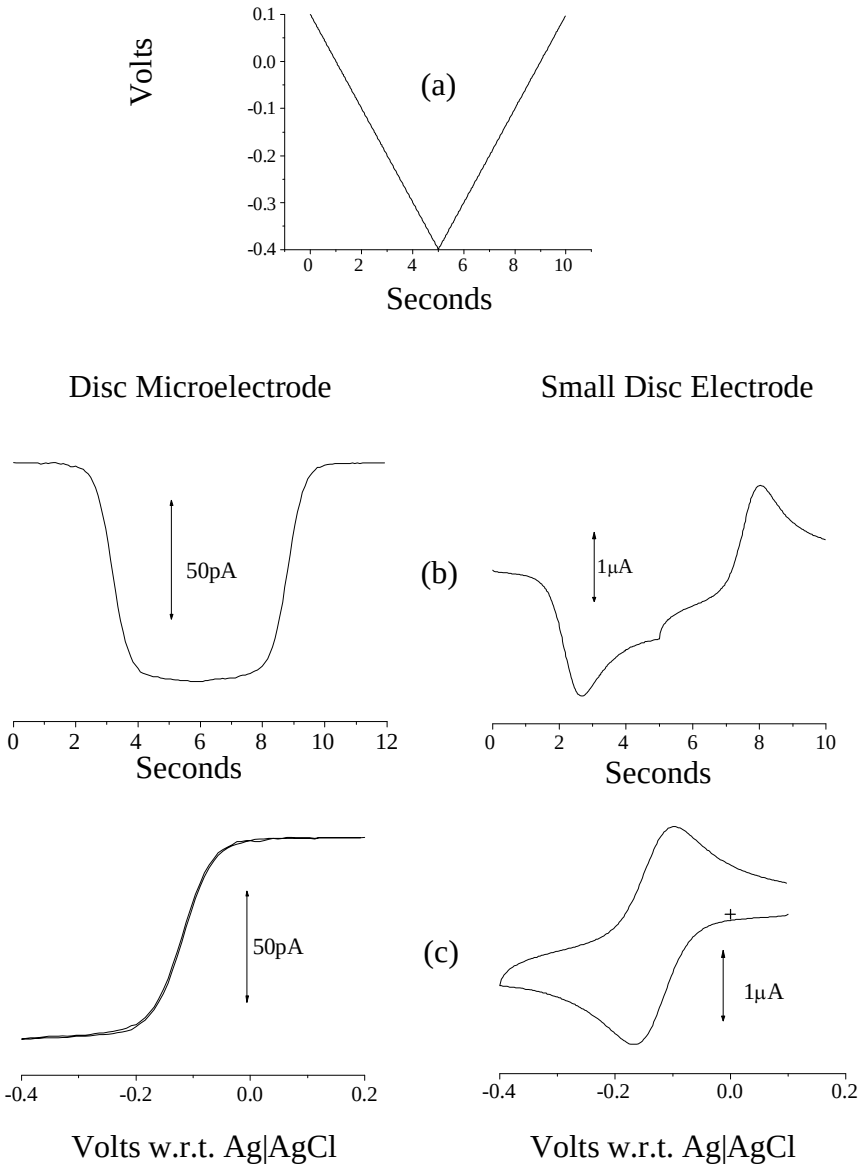

Figure I-ii

Voltage ramp (a), chronoamperograms (b) and cyclic voltammograms (c) of the reduction of 10^{-4} M $Ru(NH_3)_6Cl_3$ in 0.05 M KCl supporting electrolyte (scan rate 0.1 V s^{-1}) at disc microelectrode and small disc electrode.

The cyclic voltammograms were obtained (see Chapter II for experimental details) using a 3-electrode cell. The voltage was ramped (Figure I-ii(a)), measured between the reference electrode and the working electrode, from the non-Faradaic region (0.2 V to 0 V) to the Faradaic region (-0.25 V to –0.4 V), with the current measured between the working electrode and the auxiliary electrode, resulting in the current-time scan shown in Figure I-ii(b). The cyclic voltammograms were obtained by correlating the current and voltage, which is shown in Figure I-ii(c).

The shape of the resultant cyclic voltammograms illustrates the effect of electrode size. The disc microelectrode displays a sigmodial voltammogram, whereas that obtained for a small disc electrode is peak shaped voltammogram. The small disc electrode is controlled by both diffusion and kinetics whereas the disc microelectrode is diffusion controlled only.

The Sigmodial Shape

The sigmodial response of the disc microelectrode (Figure I-ii(c)) is described by equation (i) for a Nerstian reduction.[62]

$$\frac{i_{E\ app}}{i_{ss}} = \frac{1}{1 + e^{(E_{app} - E^{0'})\, nF / RT}} \qquad \text{(i)}$$

Where i_{Eapp} is the current at applied voltage, i_{ss} the steady state current (maximum Faradaic current), E_{app} is the voltage applied, $E^{0'}$ the formal potential of the electrode, n electrons per mole oxidised or reduced, F the Faraday constant, R the gas constant and T is temperature in degrees absolute. This relationship applies when the microelectrode radius is considerably less than $(Dt_c)^{½}$, where t_c is RT/nFv, D is the diffusion coefficient and v is the scan rate.

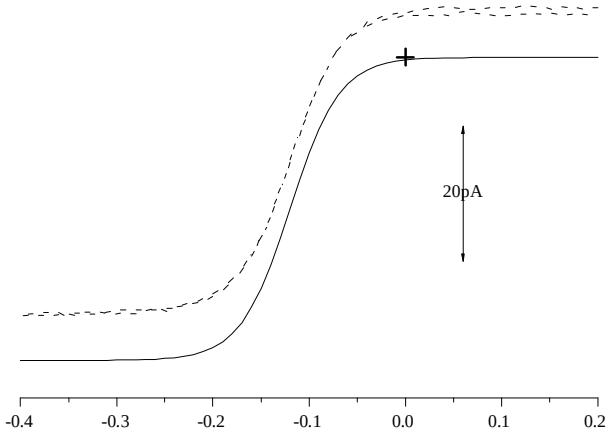

Volts w.r.t. Ag|AgCl

Figure I-iii

Voltammograms of the reduction of $Ru(NH_3)_6Cl_3$ 10^{-4} M in KCl $5x10^{-2}$ M supporting electrolyte at a microelectrode 1.3 μm radius (---)and calculated from equation (i) (—). Scan rate 0.1 V s^{-1}

Using the limiting current and $E\,½$ ($\approx E^{0'}$)[4] of a carbon film microelectrode, fabricated as outlined in Chapter III, the calculated sigmodial voltammogram is in excellent agreement with the observed cyclic voltammogram obtained from the reduction of $Ru(NH_3)_6Cl_3$ 10^{-4} M. The comparisons of calculated and experimental results are shown in Figure I-iii.
The experimental cyclic voltammogram has a slight offset 6-8 pA, possibly arising from instrument zero offset.

Limiting Current

The sigmodial shape generated during cyclic voltammetry of microelectrodes leads to a limiting current, which is dependent on electrode shape, radius and the number of electrons in the redox reaction, and is independent of reaction kinetics.

The maximum Faradaic current for an inlaid disc, (see Figure 1) with a bulk solution concentration $C_{0,}$ where D is the diffusion coefficient and r the radius, which is less than 1μm, is given in equation (ii).[63]

$$i_{ss} = 4nrFDC_0 \qquad \text{(ii)}$$

The 1 μm radius restriction arises from experimental evidence that the limiting current is not influenced by solution flow.[63]

For a hemispherical electrode the equation for the limiting current is similar to that of a disc, with a "spherical correction". The equation for the limiting current flow at a hemispherical microelectrode is given by equation (iii).[4]

$$i_{ss} = 2\pi nrFDC_0 \qquad \text{(iii)}$$

The limiting current for other shapes can be determined from an "accessibility factor". The numerical difference between a disc (the lowest) and a thin toroid (the highest) is two, i.e. by changing the surface of a disc electrode radius r to a thin toroid of the same radius the limiting current will double.[64;65]

For cylinder microelectrodes although being micrometres in the critical dimension, the equation for the steady state contains a time function. The limiting current for a cylindrical microelectrode is therefore a quasi limiting current (i_{qss}) which is given in equation (iv).[4]

$$i_{qss} = \frac{2nFADC_0}{r \ln \tau} \qquad \text{(iv)}$$

Where $\tau = \frac{4Dt}{r^2}$, with t being time. For experimental applications the quasi steady state is considered to be equivalent to steady state conditions.[4]

Equations (ii), (iii) and (iv) are the simplest forms and will be used in calculations of dimensions of electrodes fabricated in this thesis work for comparison with results from scanning electron microscopy (SEM).

The more complex forms of the equations (ii), (iii) and (iv) consider current flow from t=0 to steady state and include the initial Cottrell decay terms.[51;62] These empirically derived

equations provide an accuracy of less than 1.3%, which is in excess of that necessary for correlation with SEM studies on electrodes fabricated by the techniques outlined in Chapter III.

Cottrell Decay

When a Nerstian electrochemical system has a voltage applied to it, such that the working potential is in the Faradaic region, the current overshoots the eventual steady state current before decreasing to the steady state current. The decrease in this current (proportional to $t^{-½}$) is the Cottrell decay, the rate of decay depends on the size and shape of the electrode. In this thesis work the Cottrell decay is used to determine the radius and length of cylindrical electrodes formed using the techniques outlined in Chapter III. The use of Cottrell decay to determine the dimensions of the cylindrical electrodes was within the measurement capabilities (pA) of the equipment used, whereas the use of equation (iv) for disc microelectrodes, requires measurement in the femtoamperes. The Cottrell decay for cylindrical electrodes is given by equation (v).[66]

$$i = \frac{nFADC_0}{r}\left[0.5 + \frac{r}{\sqrt{\pi Dt}}\right] \qquad \text{(v)}$$

Using this equation, good correlations with scanning electron micrograms, over the time interval 1 to 6 seconds, was obtained to determine the electrode length and radius, (Chapter III Table III-(i) and (ii)).

Uncertainty of the equipment measurements and the presence of non-Faradaic currents [66] were reduced by omitting the time interval zero to 2 seconds. Times greater than six seconds resulted in very small current changes for the smaller cylindrical electrodes. These effects can be seen in Figure I-iv.

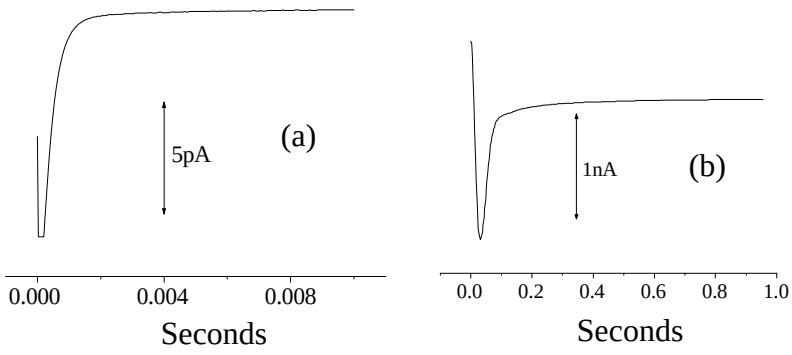

Figure I-iv

Cottrell current decay during the reduction of $Ru(NH_3)_6Cl_3$ 10^{-4} M in KCl $5x10^{-2}$ M at a disc microelectrode (a) and a small cylinder microelectrode (b).

In Figure I-iv the small disc electrode has a radius 0.6 μm calculated from equation (iii) and the small cylinder electrode was calculated to be 30 μm long with a 1μm radius, using equation (v). The rapid decrease in current with time (less than 8 milliseconds) for the 0.6 μm makes the use of equation (iii) appropriate, whereas the longer time to reach equilibrium for the small cylinder electrode permits the use of equation (v).

The calculations of cylinder dimensions were required to determine the capacitance of the fabricated and modified electrodes.

Steady State

Ideally all electrochemical measurements should be measured under steady state conditions. Microelectrodes by virtue of their small critical dimension achieve steady state very quickly, as can be seen in Figure I-iv. The small disc electrode, calculated radius 0.6 μm, is very close to steady state after only 8 milliseconds, whereas a slightly larger electrode, 1.2 μm radius (calculated equation (iii)) requires 60 milliseconds. The Cottrell decay of this "larger electrode" is shown in Figure I-v.

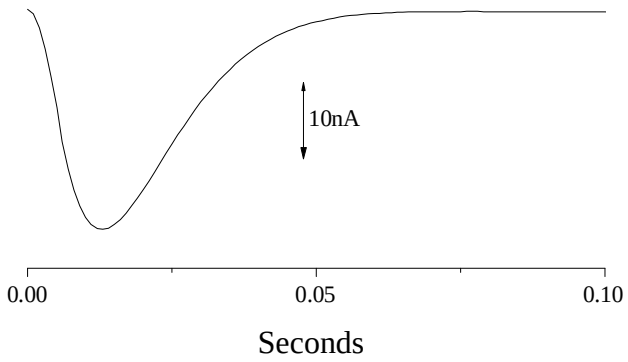

Figure I-v

Cottrell current decay at a 1.2 μm radius disc electrode during the reduction of $Ru(NH_3)_6Cl_3$ 10^{-4} M in KCl $5x10^{-2}$ M supporting electrolyte

Defining steady state at microelectrodes requires the definition of the "closeness" to steady state, usually within 1% and 5% of the steady state limiting current. The time to reach steady state, for any point on a voltammetric scan, using a hemispherical microelectrode, in a potentiostatic experiment is given by equation (vi) derived from Nerstian equations,[50;67]

$$t_{\varepsilon} = \frac{10^4 (2r)^2}{\pi^3 D \varepsilon^2} \qquad \text{(vi)}$$

where ε is the numerical value for the percentage difference between steady state current and measured current. Using equation (vi) and a diffusion coefficient of $5.48x10^{-6}$ cm^2 s^{-1} ($Ru(NH_3)_6Cl_3$) the steady state (within 5% of limiting current at t_∞) is reached in 34 milliseconds and 136 milliseconds for 0.6 μm and 1.2 μm radius disc electrodes, respectively. The calculated results are greater than those obtained experimentally especially in the case of the 0.6 μm radius electrode. If only Cottrell decay is considered and equated to steady state current at a microelectrode the time to reach steady state occurs in the nanosecond region.[68-70] It therefore appears the results obtained for a small hemispherical electrode indicates behaviour between these two regimes.

The rapid attainment of steady state is an ideal property for measuring the release of neurotransmitters *in vivo* [22] as these events occur in less than one second. (Chapter VI-Figure VI-ii) Unfortunately to measure these low concentrations requires the use of larger electrodes, such as carbon film cylindrical shaped pulled quartz capillaries or carbon fibres, with the critical dimension in micrometre range, to obtain the shortest time to reach quasi steady state. (Equation (iv)) Although the cylindrical electrodes take "longer time" to reach steady state, they provide accurate monitoring in real time of dopamine release and uptake, as demonstrated in Chapter VI of this thesis.

Capacitance

The magnitude of the double layer capacitance provides an indicator to the possible types of carbon crystal surfaces exposed on the electrode surface. A glassy carbon surface has been reported to have a capacitance of 35 μF cm^{-2} [71] and a basal plane of highly orientated pyrolytic graphite 6 μFcm^{-2}.[72] This large difference in capacitance, together with electron transfer characteristics of model analytes, has enabled the possible surface structures of the carbon film formed by the *in situ* pyrolysis of acetylene to be proposed. (Chapter IV-(xiii)) Changes to the surface, such as oxidation[73], presence of edge planes[71] and determining the area of chemical modifications (carbodiimide after surface oxidation), can also be detected by changes in capacitance.[74] In this thesis work the changes in capacitance will be used to define the location of the electrochemical and chemical reaction sites.

Double layer capacitance is also important in electrochemical measurements and particularly for *in vivo* monitoring of neurotransmitters, as it is a source of noise.[26;75] *In vivo* monitoring requires measurements in the 10 pA range over one millisecond to detect exocytotic events, therefore noise elimination from the equipment and electrode is of paramount importance especially when detecting zeptomoles in real time.[75]

Two techniques have been used to determine the capacitance of electrode surfaces. The first is the more rigorous approach using AC voltages.[76] The second is a simple cyclic

voltammetric scan using a standard three electrode system (Chapter II Electrochemical Equipment) in a non Faradaic solution. The difference in results shows that the AC technique results are approximately 50% higher than those obtained with the cyclic voltammetric technique, which was used in this thesis.[77] The equation (vii) for the determination of double layer capacitance was:

$$C_{dl} = \frac{\Delta i}{2Av} \qquad \text{(vii)}$$

Where Δi is the difference in current between the forward and reverse scans, A is the area of the electrode and v the scan rate.

The dependence of limiting current for microelectrodes on one critical dimension and on two dimensions (area) for capacitance results in an increase in signal to noise ratio as the microelectrode becomes smaller. This is another fortuitous feature of using microelectrodes for *in vivo* applications.

E½

The potential at half the limiting current, under steady state conditions, provides an indication of the energy at which the redox reaction at the electrode takes place. It is used in this thesis work to monitor changes taking place on the electrode surface, either due to fabrication techniques or surface modification. It also provides an indication of the crystal planes formed on the surface during pyrolysis.

Wave Slope

As with *E ½* the wave slope has been used to provide information on the nature of the surface formed during the pyrolysis, using different fabrication conditions and as an

indicator of surface modifications. It can be used to suggest the number of electrons involved in the redox reaction occurring at the surface and the reversibility of the reaction.[4] The wave slope, under steady state conditions, is related to $E_{1/2}$ and limiting current as shown in equation (viii).[4]

$$E = E_{1/2} + \frac{RT}{nF} Ln\left(\frac{i_{\infty} - i(t)}{i(t)}\right) \qquad \text{(viii)}$$

Where i_{∞} is the limiting current and $i(t)$ is current after t seconds. Plotting E with respect to $\log[(i_{\infty}-i/i)]$ will yield the wave slope. For a reversible reaction the slope will be $0.0591/n$ V at 25°C for. The value of n also provides an insight into the processes occurring due to surface changes.

Heterogeneous Electron Transfer Rate

Determination of electron kinetics was not carried out due to time limitations and availability of equipment, such as computer modeling,[78] and AC voltammetry[79]. Simple techniques using $E_{1/2}$, $E_{1/4}$ or $E_{3/4}$, were not applicable as the wave slope was too symmetrical,[80] and electrode radii[65] required precise measurement of E^0 beyond the accuracy of the equipment available.

The knowledge of the electron transfer coefficient k^0 would have provided additional information for understanding the nature of the carbon film formed during pyrolysis of acetylene.

Conclusion

The reduction of electrodes to the micron size has not only enabled accurate spatial location in living tissues it has also dramatically changed the electrochemical response of

analytes at solid electrodes. These changes have resulted in: a sigmodial shape of the current to voltage curve which has provided a wide voltage plateau for constant potential ammperometry, the rapid attainment of steady state enabling real time measurements to accurately track neurotransmitter concentration changes and provided a high signal to noise ratio without electrode kinetics restrictions.

Further improvements in instrumentation, such as "femtostats" will enable microelectrodes as small as 100 nm to provide more insight into the complex workings of the central nervous system.

References

1. Scharifer B.R. In Microelectrode Techniques in Electrochemistry. No 22; edited by Brockis J.O.M.; Plenun Press: New York, 92.
2. Pons S.; Fleischmann M. *Analytical Chemistry* **1987,** *59,* 1391A-9A.
3. Bond A.M. *Analyst* **1994,** *119,* R1-R21.
4. Bard A.J.; Faulkner L.R. *Electrochemical Methods,* 2nd ed.; John Wiley & Sons: U.S.A., 2001.
5. Saito M.; Matsuoka H. *Analytica Chimica Acta* **2000,** *404,* 223-29.
6. Ivashikina N.; Becker D.; Ache P.; Meyerhoff O.; Felle H.H.; Hedrich R. *FEBS Letters* **2001,** *508,* 463-69.
7. Cuin T.A.; Miller A.J.; Laurie S.A.; Leigh R.A. *Journal of Experimental Biology* **2003,** *54,* 657-61.
8. Walker D.J.; Smith S.J.; Miller A.J. *Plant Physiology* **1995,** *108,* 743-51.
9. Fung Y.S.; Wong C.C.W.; Deng J.Q. *Electrochimica Acta* **1997,** *42,* 3257-64.
10. Fung Y.S.; Mak J.L.L. *Analytica Chimica Acta* **1999,** *44,* 3855-64.
11. Macpherson J.V.; Unwin P.R *Analytical Chemistry* **2000,** *72,* 276-85.
12. Troyer K.P.; Heien M.L.A.V.; Venton B.J.; Wightman R.M. *Current Opinion in Chemical Biology* **2002,** *6,* 696-703.
13. Stuart J.N.; Hummon A.B.; Sweedler J.V. *Analytical Chemistry* **2004,** *April,* 122A.
14. Nieoullin A *Progress in Neurobiology* **2002,** *67,* 53-83.
15. Rouge-Pont F.; Usiello A.; Benoit-Marand M.; Gonon.F.; Piazza P.V.; Borrelli E. *Journal of Neuroscience* **2002,** *22,* 3293-301.

16. Davidson C.; Lee T.H.; Ellinwood E.H. *Neurochemistry International*, **2005,** *46*, 189-203.

17. Zhou F-M.; Liang Y.; Salas R.; Zhang L.; Biassi M.B.; Dani J.A. *Neuron* **2005,** *46*, 65-74.

18. Yavich L.; Tiihonen J. *Journal of Neuroscience Methods* **2000,** *104*, 55-63.

19. Adams R.N. *Analytical Chemistry* **1976,** *48*, 1128A-37A.

20. Gonon F. *Neuromethods*, Boulton A.; Baker G.Adams R.N., Eds.; Humana Press: 1995.

21. Benoit-Marand M.; Borrelli E.; Gonon F. *Journal of Neuroscience* **2001,** *21*, 9134-41.

22. Stamford J. S.; Justice J. B. Jr. *Analytical Chemistry News & features* **1996,** 359A-63A.

23. Baufreton J.; Garret M.; Rivera A.; de la Calle A.; Gonon F.; Dufy B.; Bioulac B.; Taupignon A. *Journal of Neuroscience* **2003,** *23*, 816-25.

24. Venton B.J.; Troyer K.P.; Wightman R.M. *Analytical Chemistry* **2002,** *74*, 539-46.

25. Troyer K.P.; Wightman R.M. *Analytical Chemistry* **2002,** *74*, 5370-75.

26. Venton B.J.; Wightman R.M. *Analytical Chemistry* **2003,** *1st Oct*, 414A-21A.

27. Powell P.R.; Ewing A.G.. *Analytical Bioanalytical Chemistry* **2005,** *382*, 581-91.

28. Bergquist J.; Sciubisz A.; Kaczor A.; Silberring J. *Journal of Neuroscience Methods* **2002,** *113*, 1-13.

29. Khan A.S.; Michael A.C. *Trends in Analytical Chemistry* **2003,** *22*, 503-08.

30. Kadota E.; Nonaka K.; Karasuno M.; Nishi K.; Nakamura Y.; Namikwa K.; Okazaki Y.; Teramura K.; Hashimot S. *Acta Neurochirurqica* **1994,** *60*, 162-64.

31. Blaha C.D.; Coury A.; Phillips A.G. *75*, 543-50.

32. Michael D.J.; Wightman R.M. *Journal of Pharmaceutical and Biomedical Analysis* **1999,** *19*, 33-46.

33. Cahill P.S.; Walker Q.D; Finnegan J.M.; Mickelson G.E.; Travis E.R./Wightman R.M. *Analytical Chemistry* **1996,** *68*, 3180-86.

34. Kissinger P.T.; Hart J.B.; Adams R.N. *Brain Research* **1973,** *55*, 209-13.

35. Stamford J.A.; Crespi F.; Marsden C.A. *Monitoring Neuronal Activity. A Practical Approach*, Stamford J.A., Ed.; Oxford Press: 1992.

36. Mattson S.J.; Jones T.T. *Analytical Chemistry* **1976,** *48*, 2164-67.

37. Chen T.K.; Lau Y.Y.; Wong D.K.Y.; Ewing A.G. *Analytical Chemistry* **1992,** *64*, 1264-68.

38. Lau Y.Y.; Wong D.K.Y.; Ewing A.G. *Microchemical Journal* **1993,** *47*, 308-16.

39. Ponchon J.; Cespuglio R.; Gonon F.; Jouvet M.; Pujol J. *Analytical Chemistry* **1979,** *51*, 1483-86.

40. Clark R.A.; Ewing A.G. *Analytical Chemistry* **1998,** *70*, 1119-25.

41. Schwarz J.; Kaden H.; Enseleit U. *Electrochemical Communications* **2000,** *2*, 606-11.

42. Schulte A.; Chow R.H. *Analytical Chemistry* **1998,** *70*, 985-90.

43. Millar J.; Pelling C.W.A. *Journal of Neuroscience* **2001,** *110*, 1-8.

44. Lau Y.Y.; Chein J.B.; Wong D.K.Y.; Ewing A.G. *Electroanalysis* **1991,** *3*, 87-95.

45. Wong D.K.Y.; Xu L.Y.F. *Analytical Chemistry* **1995,** *67*, 4086-90.

46. Gueret C.; Daroux M.; Billaud F. *Chemical Engineering Science* **1997,** *52*, 815-27.

47. Zhao G., Giolando D.M., and Kirchoff J.R. 95; Vol. 67, pp. 2592-2598.

48. M.I. Montenegro , Compton R.G. & Hancock G., Ed.; Elsevier: 1994.

49. Wightman R.M.; Wipf D.O. *Electroanalytical Chemistry*, Bard A.J., Ed.; 1989.

50. Zoski C.G. *Journal of Electroanalytical Chemistry* **1990,** *296*, 317-33.

51. Amatore C. *Physical Electrochemistry. Principle Methods and Applications*, Rubinstein I. Ed.; Marcel Dekker Inc.: 1995.

52. Meyerhoff J.B.; Ewing M.A.; Ewing A.G. *Electroanalysis* **1999,** *11*, 308-12.

53. Agrafiotou P.; Sotiropoulos S. *Analytica Chimica Acta* **2003,** *497*, 1758-189.

54. Macpherson J.V.; Simjee N.; Unwin P.R. *Electrochimica Acta* **2001,** *47*, 29-45.

55. Dibble T., Bandyopadhyay S., Ghoroghchian J., Smith J.J., Sarfarazi F., Fleischmann M., and Pons S.; *Journal of Physical Chemistry*, **1986**; *90*, 5275-5277.

56. Bond A.M., Fleischmann M., and Robinson J. *Journal of Electroanalytical Chemistry* **1984**; Vol. 168, pp. 299-312.

57. Bond A.M.; Henderson T.L.E.; Thormann W. *Journal of Physical Chemistry* **1986,** *90*, 2911-17.

58. Tabel H.; Takahashi M.; Hoshino S.; Niwa O.; Horiuchi T. *Analytical Chemistry* **1994,** *66*, 3500-02.

59. Aoki K.; Honda K.; Tokuda K.; Matsuda H. *Journal of Electroanalytical Chemistry* **1985,** *186*, 79-86.

60. Cheng I.L.; Whitely L.D.; Martin C.R. *Analytical Chemistry* **1989,** *61*, 762-66.

61. Nirmaier H.P.; Henze G. *Electroanalysis* **1997,** *9*, 619-24.

62. Kissinger P.T.; Heineman W.R. *Microelectrodes*, Michael A.C.; Wightman R.M., Eds.; 2nd ed.; Marcel Dekker: U.S.A., 1996.

63. Satio Y. *Review of Polarography (Japan)* **1968,** *15,* 177-86.

64. Oldham K.B. *Journal of Electroanalytical Chemistry* **1992,** *323,* 53-76.

65. Zoski C.G. *Modern Techniques in Electroanalysis.*, Vanysek P., Ed.; Wiley-Interscience: U.S.A., 1996.

66. Bard A.J.; Faulkner L.R. *Electrochemical Methods. Fundamentals and Applications,* ed.; John Wiley & Sons: USA, 1980.

67. Bond A.M.; Oldham K.B.; Zoski C.G. *Analytica Chimica Acta* **1989,** *216,* 177-230.

68. Aoki K. *Electroanalysis* **1993,** *5*, 627-39.

69. Montenegro et als (eds) *Why Microelectrodes*, Pletcher D., Ed.; Academic Publishers: Netherlands, 1991.

70. Andrews M.K.; Harris P.D. *Electroanalysis* **1998,** *10*, 1112-18.

71. McDermott M.T.; Kneten K.; McCreery R.L. *Journal of Physical Chemistry* **1992,** *96,* 3124-30.

72. Xu J.; Chen Q.; Swain G.M. *Analytical Chemistry* **1998,** *70,* 3146-54.

73. McCreery R.L. *Electroanalytical Chemistry*, Bard A.J., Ed.; Dekker: 1991.

74. Fujihira M.; Tamura A.; Osa T. *Chemistry Letters* **1977,** 361-66.

75. Hochsteltler S.E.; Puopolo M.; Gustincich S.; Raviola E.; Wightman R.M. *Analytical Chemistry* **2000,** *72,* 489-96.

76. Tshernikovski N.; Gileadi E. *Electrochimica Acta* **1971,** *16,* 579-84.

77. Eriksson A.; Norekrans A.; Carlsson J. *Journal of Electroanalytical Chemistry* **1992,** *324,* 291-305.

78. Mahon P.J.; Oldham K.B. *Electrochimica Acta* **2001,** *46,* 953-65.

79. Rosvall M. *Electrochemical Communications* **2000,** *2,* 791-95.

80. Mirkin M.V.; Bard A.J. *Analytical Chemistry* **1992,** *64,* 2293-302.

Chapter II

Experimental

Introduction

This chapter covers two major experimental methods which are the basis of this thesis. Also described is the preparation of the analyte solutions prior to electrochemical analysis. The first experimental method is the laser heated puller which draws down a quartz capillary 1mm O.D. and 0.5 mm I.D. to a tip size of 0.5 µm to 1 µm radius. The second is the standard three electrode setup which was used to carry out voltammetric characterisation and constant potential oxidation of the microelectrodes.

Puller

The pulled capillaries form the substrate onto which the pyrolysing acetylene forms the carbon film. The shape is important for *in vivo* applications, as a tapering shank permits easy penetration into the brain tissue reducing extracellular fluid leakage. For *in vitro* evaluation the tapering is not important, however the shank should ideally be less than 25 µm radius for the length of the carbon film.

The Sutter P-2000 (Sutter Instrument Co) puller converts a 7 cm long and 1mm O.D. x 0.5 mm I.D. quartz capillary into two tapered electrode bodies after heat is applied to the centre of the quartz capillary. A laser beam is used as the heat source, rather than a resistance wire, as high temperatures are required to reach the softening point of quartz. The schematic diagram of the Sutter P-2000 puller is shown in Figure II-i

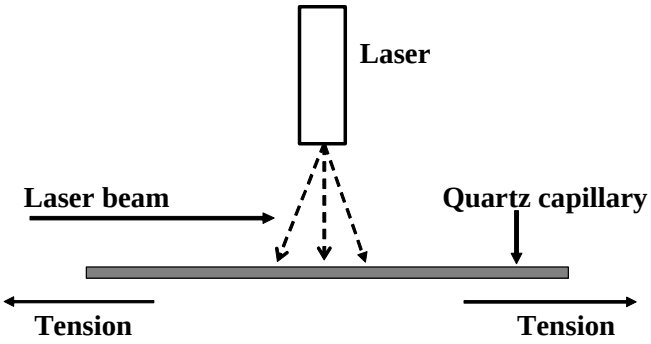

Figure II-i

Schematic of Sutter P-2000 Puller

As the tip diameter and tip body profile are important for *in vivo* and *in vitro* applications the Sutter P2000 Puller has five variable inputs to control the heat input, length heated, melt viscosity, cooling period and the final or "hard pull". By selecting a "weak" final pull, such that the capillary does not separate, the heating and stretching cycle can be repeated – looped. This looping provides additional control to ensure the final diameter is repeatable. The five variable inputs used to control the drawing down of the quartz capillary into two separate electrode bodies are: -

Heat Input. (Range 0 to 999) It is a numerical value used to control the power output from the laser.

File. The numbers (Range 1 to 15) are programs, which control the laser beam scan length along the quartz capillary and dwell time over that scanned section.

Velocity (Range 0-255) This is a measure of the quartz viscosity under static load.

Delay (Range 0-255) The delay setting is the cooling period between when the laser is switched off and when the "hard pull" commences.

Pull (0-255) This controls the force of the final pull i.e. the "hard pull", which occurs after the delay period.

After drawing down the quartz capillary the shape is assessed using an optical microscope (400X magnification).

Typical values (which require daily adjustment) used to form electrode bodies with an orifice less than 1μm radius are presented in Table II-i.

Table II-i Typical values for Sutter P2000 puller**.**

	Electrode Profile		
	Cylindrical Tapered tip		Hemispherical Less than 100nm radius orifice
Variable settings	Loop 1	Loop 2	Loop 1
Heat	625	625	800
File	4	4	5
Velocity	55	40	50
Delay	130	125	150
Pull	50	35	125

Electrochemical Equipment

All experiments were carried out in a Faraday cage using an eDAQ (eDAQ Pty. Ltd.) picostat connected to eDAQ digital to analogue interface. The interface was controlled by eDAQ EChem (Version 2) software.

The electrochemical cell was a standard three electrode system, a reference electrode Ag|AgCl (3 M KCl), an auxiliary platinum coil and the working electrode, either hemispherical or cylindrical microelectrode. Connections to the electrodes were made with eDAQ supplied small alligator clips.

To reduce convection currents caused by vibrations, the reaction vessel (55 ml) was supported by a hard wood block on two layers of foamed rubber (of differing hardness). These, together with the eDAQ picostat were placed in the Faraday cage to minimise extraneous noise.

A schematic diagram of the electrochemical apparatus is shown in Figure II-ii.

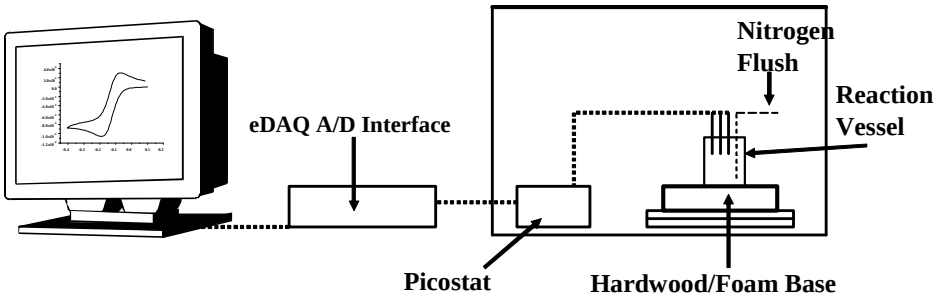

Figure II-ii

Schematic of electrochemical experimental layout

Cyclic Voltammetry

The potential of the working electrode was cycled between preset limits with respect to the reference electrode. The voltage output to the picostat was in the form of a staircase. This was a consequence of computer digital control and necessitates an integral number of voltage steps between the preset scan limits. To control the scan three variables were selected, scan rate (V s^{-1}), step width (msec) and step height (V).

The priority in settings was given to the scan rate and the default setting was 0.1 V s^{-1}. The step width was selected as 80 milliseconds as this time interval reduced AC hum. The step height was then adjusted by the software to give an integral number of steps. A further data acquisition parameter is the sampling speed and sampling time during the step period. The sampling speed could be selected from 100 Hz to 100 kHz and the sampling period from 1millisecond to the full step width.

Scan rate of 0.1 V s^{-1} was used as a compromise between obtaining steady state, convection currents and to evaluate a large number of electrodes. (A total exceeding 1500 microelectrodes were fabricated, characterised, modified and characterised again.)
The effect of scan rate was examined using two extremes in electrode size, fabricated by the methods detailed in Chapter III, a hemispherical tip 0.9 μm radius and a cylindrical microelectrode with a calculated length of 340 μm and 14 μm radius. The variation in microelectrode size with scan rate can be seen in Figure II-iii. The small hemispherical

electrode has minimal change with scan rate, whereas the cylindrical electrode shows a significant change in waveslope. These changes are summarised in Table II-ii.

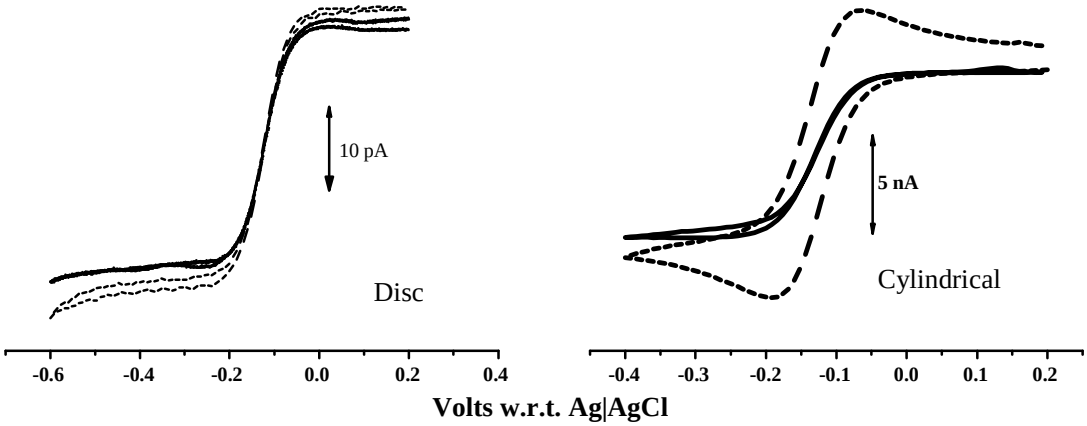

Figure II-iii

Effect of scan rate on cyclic voltammetric shape of the reduction of $Ru(NH_3)_6Cl_3$ 10^{-4} M
Scan rate 0.1 V s^{-1} (----) and 0.05 V s^{-1} (—)
Supporting electrolyte 0.05 M KCl

Table II-ii Effect of scan rate on *E½* and waveslope.

	Electrode Shape			
	Hemispherical		Cylindrical	
	E½	Waveslope	*E½*	Waveslope
Scan Rate	w.r.t. Ag|AgCl	V/decade	w.r.t. Ag|AgCl	V/decade
V s^{-1}	(3 M KCl)		(3 M KCl)	
0.005	-0.124	0.06	-0.129	0.059
0.01			-0.131	0.054
0.02	-0.124	0.061		
0.025			-0.134	0.043
0.05	-0.114	0.054	-0.134	0.043
0.1	-0.124	0.061	-0.135	0.041

To obtain the values in Table II-ii an "average" scan was obtained by averaging the forward and reverse scans prior to measuring *E½* or calculating the waveslope. The values obtained are in agreement with theory, i.e. *E½* is independent of scan rate whereas the wave slope is dependent on scan rate for "large electrodes under non steady state.[1]

In this thesis *E½* and waveslope are used to quantify changes before and after modification on the same electrode. Therefore, the use of 0.1 V s^{-1} as the default scan rate, does not introduce significant errors

The step width was set at 80 milliseconds to provide sufficient data points (10-15) to define the waveslope, while providing time for Cottrell decay to be minimised after each voltage step.

The default settings used were: - scan rate, 0.1 V s^{-1}; step width, 80 milliseconds; step height, 0.008 V; sampling period, 20 milliseconds (between 60 milliseconds and 80 milliseconds of the step width) and sampling rate 100 kHz (2000 samples per data point).

Solution Preparation

All chemicals, which are listed in the experimental section in following chapters and sub-chapters, were used as received without further purification.

All solvents and buffers were deoxygenated, using nitrogen, prior to making up the stock solution. (Dopamine and ascorbic acid react with molecular oxygen.)

Analytes were dissolved using minimal stirring to reduce entrapment of oxygen.

The solutions (50 ml) were transferred immediately to the reaction vessel. The vessel was designed to reduce ingress of oxygen. The reference and auxiliary electrodes were friction fitted into the vessel lid whereas the microelectrode required a larger opening (6 mm O.D.).

Stock solutions were used immediately. When using a range of analyte concentrations a blanket of nitrogen was kept over the stock solution.

Stock solutions, under nitrogen and in the reaction vessel, were replaced every three hours to minimise analyte loss if sensitive to molecular oxygen.

The solutions in the reaction vessel were then deoxygenated with nitrogen flow of approximately one bubble per second for three minutes.

The solution was allowed to quiesce for three minutes prior to the scanning.[2] Immediately after voltammetric scans nitrogen flushing was recommenced.

(The technique of maintaining a nitrogen blanket above the solution in the reaction vessel by providing a slow nitrogen flow on the surface was not used. It was found that the flow of nitrogen generated convection within the solution causing noise on the voltammograms.)

References

1. Zoski C.G.; Bond A.M; Colyer C.L.; Myland J.C.; Oldham K.B. *Journal of Electroanalytical Chemistry* **1989,** *263*, 1-21.
2. Adams R.N. *Electrochemistry at Solid Electrodes,* ed.; Marcel Dekker: USA, 1973.

Chapter III

Fabrication

Abstract

In this chapter a method is presented to deposit an in situ pyrolysed carbon film, on a pulled quartz capillary to form disc and cylindrical electrodes, using acetylene as the hydrocarbon source. The sizes of the electrochemically active surface fabricated by this method, range from discs with nanometre radii to carbon film cylindrical electrodes 1.8 mm long.

A novel method for visualising the location of the carbon film on the quartz substrate, based on platinum plating of the carbon film is presented.

Effects of flow rate and direction of the nitrogen blanket gas on the distribution and morphology of the carbon film resulting from this method of the carbon film formation was examined using scanning electron micrographs of the platinum plated surface.

Introduction

Carbon has several allotropes, of which only graphite is electrically conductive. This conduction arises from the sp^2 hybridisation of the carbon atoms. All carbon electrodes, carbon fibre, carbon film, glassy carbon, carbon paste or highly orientated pyrolytic graphite contain the graphite crystal structure. The crystal structure, as shown in Figure III-i, consists of layers of hexagonal sp^2 hybridised carbon atoms stacked in an ABAB sequence.

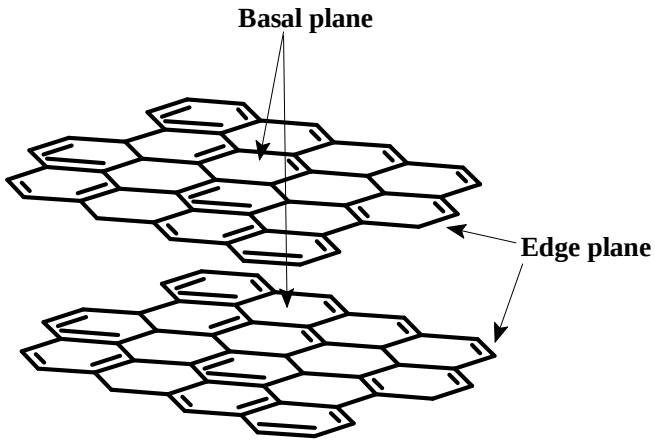

Figure III-i

Crystalline structure of graphite.

The length of the hexagonal lattice and layers of hexagonal lattices can range from 0.1 pm to 10 μm to form micro-crystallite regions.[1] This conductive region of carbon is often referred to as graphene. (In this thesis the "carbonaceous" film formed after pyrolysis of acetylene will be referred to as a carbon film. Preference is given to this term as characterisation experiments (Chapter IV) do not exhibit electron transfer characteristics similar to either edge or basal planes. This term is also in agreement with previous literature where carbonaceous films have been formed *in situ*, by polymer chain polymerisation, for electrode surfaces and resistors.[2] Carbon utilised in the construction of electrodes is derived from a range of hydrocarbon sources. Highly orientated pyrolytic graphite (HOPG) is produced from hydrocarbon gases (predominately methane) at pyrolysis temperatures above 1200 °C and up to 3800 °C. Under these conditions the basal graphite planes grow parallel to the heated substrate. If lower temperatures are used Pyrolytic Graphite (PG) is formed with reduced orientation of the graphite planes. Glassy carbon (GC) is formed by pyrolysis of polymers, such as polyacrylonitrile at 1000 °C to 3000 °C. Under these conditions interwoven ribbons of basal planes are formed.[1;3] Carbon fibres are produced from polyacrylonitrile fibres which are

heated to 3000 °C. The orientation of basal planes, within the fibre, is varied depending on method and temperature of manufacture.[1;4]

Electrodes utilising HOPG can be constructed to have either basal or edge planes exposed. With GC, carbon fibre or PG the crystal faces in contact with solution are variable and dependent on the method of fabrication of the electrode.

An alternative means of fabricating an electrode is to form the carbon surface *in situ.* That is, the carbon is formed directly onto the substrate to be used in the construction of the electrode. This method of fabrication leads to the formation of a carbon film with interesting properties when compared to the crystal surfaces of a graphite crystal.

An early example of this technique was the heating of a ceramic rod, 0.15 inch (3.8 mm diameter) in a tube furnace containing 25 % v/v methane in nitrogen to 1025 °C. After 24 hours a film $5x10^{-2}$ mm thick was formed. The carbon coated ceramic rod was then pressed into a Teflon sleeve and electrical connections made through the back of the sleeve. This surface gave similar electrochemical response to a platinum electrode for a ferrocyanide/ferricyanide system. These electrodes gave reported wave slopes of 0.059 to 0.073 V/decade. This compares with the theoretical value of 0.059 for a reversible one electron transfer.[5]

A further development of the previous method was the replacement of the ceramic rod with a 6mm diameter graphite rod, then using a pyrolysis atmosphere of 10% methane in argon for periods in excess of eight hours. The carbon film formed gave a sigmodial shaped cyclic voltammogram for dopamine in 0.01 M H_2SO_4, which after anodic oxidation became peak shaped.[6] This surface was described as a low temperature isotropic carbon. It was found to have long term stability over several months' storage, and was considered to have a surface with the character of hydrogenated carbon. The hydrogenation of the surface was attributed to

the hydrogen rich atmosphere in which the carbon film was formed.

An interesting approach to fabricating a carbon film microelectrode is the *in situ* low temperature pyrolysis of ethylene on a nickel surface within a pulled glass capillary and onto a nickel plated platinum micro disc electrode.[7] One advantage of this technique is the lower temperature used - 400-550 °C, which permits the use of glass instead of quartz. The wider transition temperature range of the liquidus phase of glass when compared to quartz enables greater reproducibility when pulling the capillaries for the electrode substrate. The carbon film formed gave similar cyclic voltammetric behaviour to that of a glassy carbon electrode for dopamine, (3,4-dihydroxyphenyl)acetic acid and 4-methylcatechol. The cyclic voltammogram of 4-methylcatechol in a buffer at pH 7.4, obtained with an electrode with a radius of 1.8 μm, was very similar in shape to that using *in situ* pyrolysis of acetylene as outlined in this thesis. The disadvantage of the above technique is its limitation to disc shaped electrodes.

A range of non-thermal techniques have been used to form carbon films, such as electron beam evaporation onto doped silica,[8] and chemical vapour deposition onto a glassy carbon electrode.[9] The carbon film produced by both these techniques yielded double layer capacitances of 15 to 25 μFcm^{-1} and 5 to 10 μFcm^{-1} respectively. These values are higher than for those formed by the pyrolysis of acetylene, 1-3 μFcm^{-1}, as outlined in this thesis work. Work on forming a carbon film by pyrolysing methane on Macor disclosed that the pyrolysis temperature greatly influenced the capacitance of the film formed.[10] At a pyrolysis temperature of 926 °C it was reported to be between 1000 and 3000 μFcm^{-1} and at 1100°C the capacitance was 315 μFcm^{-1}. Post formation heat treatment, up to 1000 °C, of a carbon film formed by electron beam evaporation did not substantially affect the capacitance.[8] From these published methods a carbon film with low capacitance appears to require a high pyrolysis temperature.

Carbon film electrodes have been known for over forty years [5] but their surface has

not been characterised in detail, certainly not to the extent of other types of carbon used in the fabrication of electrode surfaces.[1] Therefore in an attempt to understand the mechanisms which may be involved in the formation of these films, the pyrolysis variables of hydrocarbons to form graphite have been considered.

The difference between the carbon structures are due to the pyrolysis conditions; hydrocarbon pressure, temperature, residence time and occurrence of active sites on the surface.[11]

The effect of hydrocarbon source appears to have minimal influence on the nature of the carbon deposits formed as the pyrolysis products, the main factor appears to be the pyrolysis temperature rather than hydrocarbon source. Analysis of the gas formed during pyrolysis of light hydrocarbons, methane, ethene, acetylene and propane resulted in the identification of up to twenty eight different species. Ethylene and propane (propane was the hydrocarbon source) were the predominate species in the temperature range 800-900 °C, benzene from 900-1000 °C with acetylene and diacetylene between 1000-1100 °C. [11]

With this perceived independence of hydrocarbon source, for the pyrolysis pathway to graphenes, the choice of acetylene has several practical advantages.[12;13] It is stored at low pressures and is readily obtainable. (Welding grade can be purified using in-line absorbents for oxygen and acetone.)

In the simple fabrication technique outlined in this thesis work, control of temperature was achieved by using the maximum attainable stable quiet blue flame, with a micro Bunsen burner using natural gas. The temperature reached in the reaction zone was found to be 1100 °C, when measured using a thermocouple.

Using acetylene as the hydrocarbon source, at 1027 °C, five morphological types of carbonaceous deposits have reported to have been formed[14] which were dependent on the acetylene concentration (diluted with argon) and flow rate through the reactor (residence time). The carbonaceous deposits ranged from compact to “spongy”. The compact carbon was preferentially formed with a reaction mixture of 10% acetylene and a flow rate of 330 to 500

ml/min, the spongy carbon at a flow rate of 150 to 330 ml min^{-1} and a concentration of 12 to 20 %.[14] In this thesis work the acetylene concentration ranged from an initial 100 % at the tip of the pulled quartz capillary to zero on the external surface when the orifice of the pulled quartz capillary is sealed. The external surface concentration of acetylene is expected to vary depending on the nitrogen flow rate, the distance from the pulled quartz capillary orifice (dilution), the degree of turbulence (mixing), pyrolysis time (the orifice reduces in size as the pyrolysis proceeds) and post orifice sealing pyrolysis time (decarbonisation).

The residence time in the "reaction zone", is dependent on gas flow, which dictates the time available for the reactive species formed in the gas phase to react and therefore determine the rate of reaction with the quartz surface or with deposited carbon layers. At 1100 °C the reaction mechanism appears to be a mixture of molecular polymerisation and radical reaction.[15] The polymerisation of the acetylene involves the formation of polyaromatic hydrocarbons.[12] The radicals formed include C_4H_2, C_6H_2 and C_4H_4 which are initiated by hydrogen abstraction.[15] The radical pathway for formation of graphene is via the polyynes; this provides a direct radical addition to the graphene layers.[13;16]

Additional to the homogeneous reaction in the vapour phase is the heterogeneous reaction with the substrate. The reaction is heterogeneous as graphene layers grow parallel to the substrate surface and at higher temperatures conical substructures are formed.[14;17] Both of these features indicate growth emanating from a nucleation site on the surface –active sites. These nucleation sites may be initiated from a SiC interlayer. The existence of such an interlayer may explain the high degree of adhesive forces, between the substrate and graphene, which is a feature of carbon films.[8;18]

Acetylene has been reported to pyrolyse at 450 °C to form carbon fibres. [19] However attempts to fabricate a carbon film electrode at lower temperatures were unsuccessful due to failure in the adhesion between the carbon film and the quartz substrate. This was evident by visible (optical microscope 400X) aqueous solution ingress between the carbon film and

quartz capillary after several minutes immersion. This indicates that the formation of strong covalent bonds require high pyrolysis temperatures. The probable steps to the formation of these bonds are dehydration of the quartz then reduction of the silicon oxide by hydrogen radicals. The silicon radicals formed then react with carbon either as acetylene or carbon-hydrogen radicals to form a covalent bond.[8]

The initiation of these reactions, at "active sites" or their participation in the pyrolysis reaction on the substrate surface, appears to have attracted little attention.[11] This is unfortunate as the adhesion between the substrate, quartz and the carbon film is important in electrode applications. The strong adhesive properties are required for insertion into living tissue and as a detector for liquid chromatography.

In this thesis work the pyrolysis conditions required to produce an adherent carbon film with minimal decarbonisation have been utilised to form microelectrodes ranging from discs with sub nanometre radius to cylinders millimetres in length. The equipment used to fabricate these carbon film microelectrodes is relatively minimal and would be available in most laboratories.

Experimental Section

Chemicals

Acetylene and nitrogen were supplied as Instrument Grade (BOC). Hydrogen hexachloroplatinate(IV), graphite powder and sulfuric acid (A.R) were obtained from Sigma-Aldrich and all chemicals were used as received.

Pyrolysis Apparatus

The schematic diagram of the pyrolysis equipment is shown in Figure III-ii. The 1/16th inch "T" piece had the threads on one arm machined to loosely fit a quartz tube (NMR tube ~ 3 mm O.D.). On the opposite side is a standard cap with a graphite ferrule for retaining the pulled quartz capillary. Gas connections for both nitrogen and acetylene are push fit silicon tubing.

Heating was provided by a general purpose micro Bunsen burner (18 mm diameter), using natural gas with a static pressure of 25 cm water.

Alignment of the quartz tube is achieved using a two directional manipulator.

All gas pipes must be metal except the push fit silicone tubing, which was of minimal length- to reduce oxygen permeation. NOTE Copper was not used on acetylene lines as explosive copper acetylide is formed.

Procedure

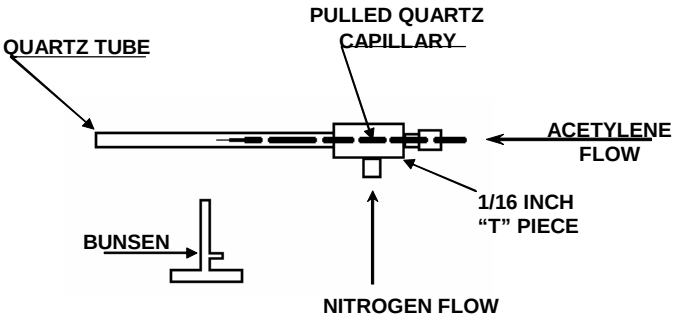

Figure III-ii

Schematic of pyrolysis equipment

The pulled quartz capillaries were formed as outlined in Chapter II.

A pulled quartz capillary was then placed in the "T" piece of the pyrolysis equipment and retained with the graphite ferrule.

The quartz tube was then placed over the pulled quartz capillary and located in contact with the "T" piece.

Nitrogen and acetylene gases were then passed through the system for 30 minutes to flush oxygen from the pipes and tubes.

Small cylindrical and disc electrodes

Acetylene pressure was set at 60 kPa and the nitrogen flow between 10 ml min^{-1} for small disc electrodes up to 1 μm radius and 40-80 ml min^{-1} for small cylinder electrodes.

Larger cylindrical microelectrodes

The nitrogen flow was reversed, entering through the open end of the quartz tube. The acetylene pressure was maintained at 60 kPa and the nitrogen flow rate set at 40 ml min^{-1} for approximately 500 μm long electrodes. Increasing the flow rate up to 80 ml min^{-1} was used to produce a carbon film along the capillary shank in excess of 1 mm.

The micro Bunsen burner was adjusted until a maximum size with a quiet steady blue flame was formed. It was then slowly moved along the quartz tube towards the tip of the pulled quartz capillary. The final position of the micro Bunsen burner was such that the tip of the blue cone of the flame was 1 mm beneath the quartz tube and 4 mm away from the tip. (The slow movement towards the pulled capillary tip was to reduce thermal shock, which will result in the tip fracturing. The pyrolysis should extend up inside the capillary from the tip to provide an electrical pathway to the powdered graphite, to be added in the next step.)

After one hundred and five seconds pyrolysis time, measured from when the tip first developed a cherry red colour, the heat is removed. After 30 seconds cooling the pyrolysed pulled quartz capillary was removed.

The open end of the pyrolysed pulled quartz capillary was then tapped into approximately 10 mm deep graphite powder. After a 5 mm deep layer had been transferred, 5 cm of tin coated copper wire (10 Amp fuse wire) was inserted into the open end pushing the powdered graphite to the tip. The fabrication of the carbon film microelectrode was now complete. If *in vivo* applications are envisaged the wire can be secured to the pulled capillary body using a neutral cure silicone or 5 minute epoxy.

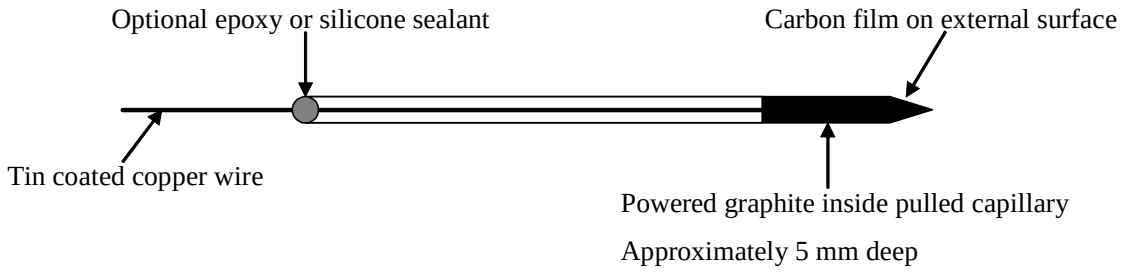

Figure III- iii

Schematic diagram of "ready to be used" carbon film microelectrode.

The electrical conduction path, in the fabricated carbon film microelectrode, as shown in Figure III-iii is as follows. The pyrolysed carbon forms a continuous deposit from the carbon film on the external surface through the sealed orifice to carbon deposited inside the pulled capillary. The graphite powder provides the electrical connect from the inside carbon deposit to the tin coated copper wire. The tin coated copper wire may be replaced with soft copper wire. The use of a "soft" metal enables a good contact for alligator type clips.

Scanning Electron Microscopy

Scanning electron microscopy was carried using a Jeol JSM 840 instrument operating at 6 kV.

Prior to attaching the microelectrode to the microscope stub the electrochemically active surface area was platinum plated using $1x10^{-3}$ M H_2PtCl_6 in 0.5 M H_2SO_4 at -0.15 V vs. Ag|AgCl for 90 seconds. After plating the electrodes were rinsed in deionised water and dried.

The microelectrodes were then shortened and mounted onto the stubs as shown in Figure III-iv. In assembling microelectrodes onto the stubs it is important that electrical continuity is maintained between the platinum plated carbon tip and the stub.

To prevent movement of the shortened electrodes during scanning electron microscopy they were restrained using electrically conductive paint and double sided adhesive as shown in Figure III-iv.

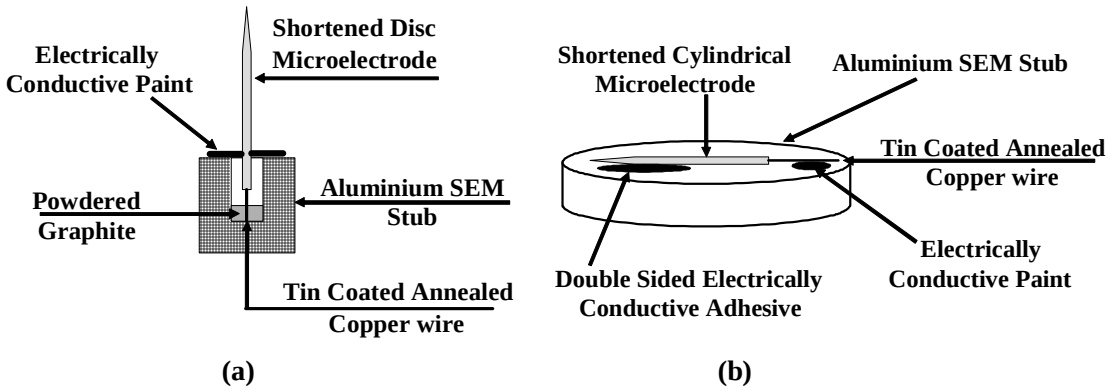

Figure III-iv

Schematic diagram for scanning electron microscope mounting configurations for platinum plated: (a) for disc and (b) for cylindrical microelectrodes.

Results and Discussion

Determination of the shape and distribution of the electrochemically active surface is of paramount importance for theoretical studies, as the limiting current can vary by a factor of two, depending on shape for a given radius of a hemispherical or disc shaped type surface (See Chapter I Limiting Current). For the application of cylindrical microelectrodes, such as for *in vivo* studies, maximisation of the analytical signal is necessary and this is achieved by matching the biological area of interest to that of the electrochemically active surface. In this thesis work the shape and location of the electrochemical active surface has been determined such that capacitance measurements and surface coverage of functional groups can be calculated and surface morphology determined.

Disc Electrodes

Previous work on examining the shape, size and morphology of microelectrodes has utilised scanning electron microscopy to define the electrochemically active surface of the microelectrode.[7;20;21] To obtain this information on the electrochemically active regions, the electrodes have been sputter coated, using either carbon or gold to form a conductive surface. The exposure surface, in a polymer matrix or free standing, provides a visual indication of the electrochemically active area by visually different fracture patterns of the materials in the exposed surface. This approach is not possible for the carbon film formed by the method outlined in this thesis work, as the surface profile of the film does not provide satisfactory relief with changes of thickness to define an edge between the quartz and carbon film.

As carbon is used to sputter coat items prior to scanning electron microscopy, to provide a conductive surface on non conductive specimens attempts were made omitting the plating step. This was unsuccessful as the contrast between the carbon film and the adjoining quartz surface was discernible. It appears that the conductivity of the *in situ* pyrolysed carbon

film is insufficient for scanning electron microscopy. Hence the need to use platinum plating to locate the carbon film on the quartz substrate. Platinum coating thickness was minimised to reduce the possibility of artefacts being generated.

An example of a scanning electron micrograph of a disc shaped electrode formed by the technique outlined in this chapter for small disc and cylinders is shown in Figure III-v together with the cyclic voltammogram obtained using 10^{-4} M hexaaammineruthenium (III) chloride. The use of hexaaammineruthenium (III) chloride as a model analyte is discussed in Chapter IV-(viii).

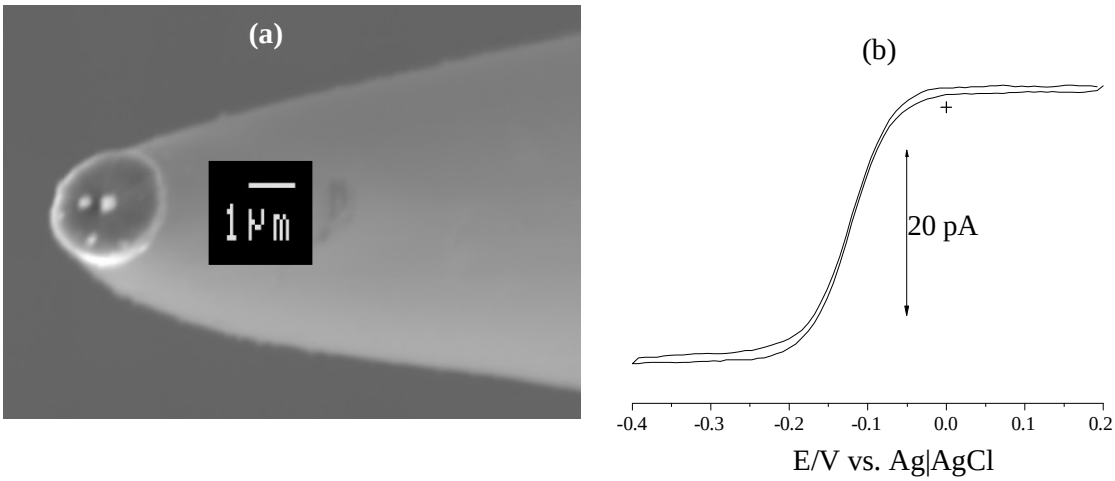

Figure III-v

Scanning electron micrograph of platinum plated disc microelectrode (a) and the cyclic voltammogram (b) in 10^{-4} M $Ru(NH_3)_6Cl_3$ with $5x10^{-2}$ M KCl supporting electrolyte. Scan rate 0.1 V s^{-1}

From the scanning electron micrograph the measured radius of the tip (after correction for tilt) was 1.6 μm and from limiting current calculations 2.2 μm (using equation (iii) Chapter I and a diffusion coefficient of $5.5x10^{-6}$ cm^2 s^{-1}.). The discrepancy is probably due to the hemispherical surface having a toroidal component to the shape. For a perfect toroidal shape the calculated radius would be 1.2 μm.[22] Considering the errors in the correction of tilt, (although the angle of tilt of the stub is obtained from the instrument, the shortened electrode is not perpendicular to the surface of the stub) and the irregular shape of the electrode surface, the difference between measured and calculated radius is small and not

significant if *in vivo* applications are considered.

Small Cylindrical Microelectrodes

During attempts to fabricate a disc microelectrode, using nitrogen flows of 80 ml min^{-1}, in the same direction as the acetylene, it was found that the carbon film extended along the shank up 50-150 μm. This feature is depicted in Figure III-vi.

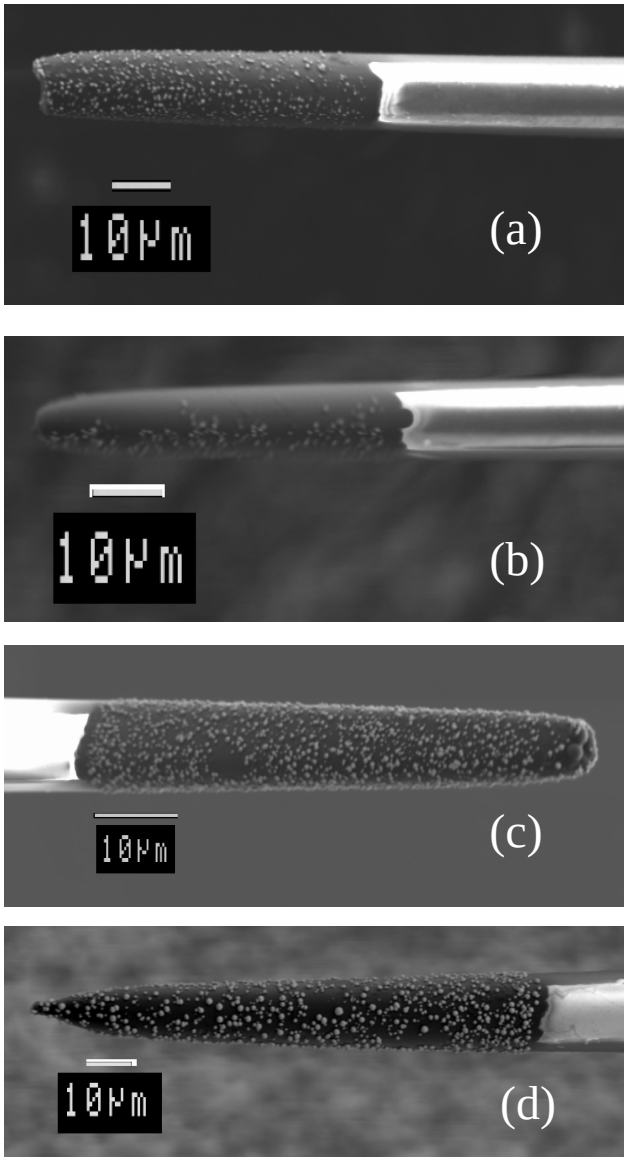

Figure III-vi

Scanning electron micrograph of cylindrical microelectrodes fabricated by acetylene/nitrogen parallel flow.

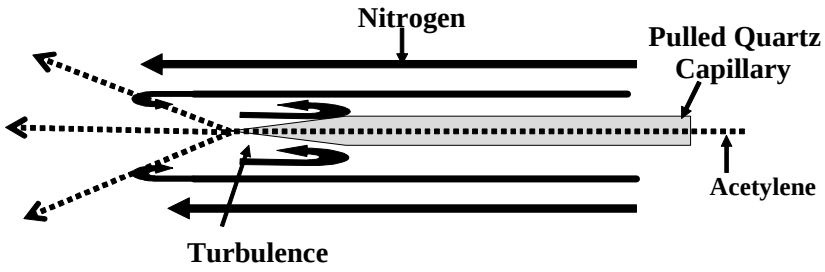

Figure III-vii

Schematic of nitrogen and acetylene gas flow at
high nitrogen flow rates

A possible explanation for extension of the carbon surface up the shank of the microelectrode is turbulence near the surface. The velocity of nitrogen flowing along the surface of the pulled quartz capillary when passing over the pulled section of the capillary generates eddies, drawing acetylene back along the microelectrode tip. The proposed nitrogen and acetylene flow paths are depicted in Figure III-vii.

The physical dimensions of the cylindrical microelectrodes shown in Figure III-v are shown in Table III-i.

Table III-i Comparison of dimensions obtained for small cylinder microelectrodes.

Electrode No	Dimensions measured from SEM's			Dimensions calculated from the Cottrell decay curve		
(Figure III-v)	Length (μm)	Radius (μm)	Area (μm^2)	Length (μm)	Radius (μm)	Area (μm^2)
(a)	53	5.5	$1.8x10^3$	60	6	$2.3x10^3$
(b)	55	5	$1.7x10^3$	65	6	$2.5x10^3$
(c)	65	5	$2.0x10^3$	78	5	$2.5x10^3$
(d)	120	7.5	$5.7x10^3$	107	10.5	$7.1x10^3$

Note. Cottrell decay curves were obtained at -0.4 V in 10^{-4} M $Ru(NH_3)_6$ (III) chloride with 0.05 M KCl

The results of the dimensions measured by both techniques in Table III-i are in satisfactory agreement for future calculations of surface properties. The slightly larger dimensions of the calculated results from the Cottrell decay curve could be attributed to the uneven surface of

the carbon film. Features, such as nodules and mud cracking visible in Figure III –x, would provide a larger electrochemical area than physical measurements.

Large Cylindrical Microelectrodes

Cylindrical electrodes can be fabricated using nitrogen flow that is either parallel or counter to that of the acetylene. With counter flow electrodes up to 1.8 mm (calculated using equation (v) Chapter I) have been made. An example of the counter flow electrode is shown in Figure III-viii. The counter flow produces a ragged edge where the carbon film terminates, probably due to slight surface irregularities disturbing gas flow up the shank. The raised uncoated section in the SEM's is an illusion caused by excessive discharge from the quartz substrate during scanning electron microscopy.

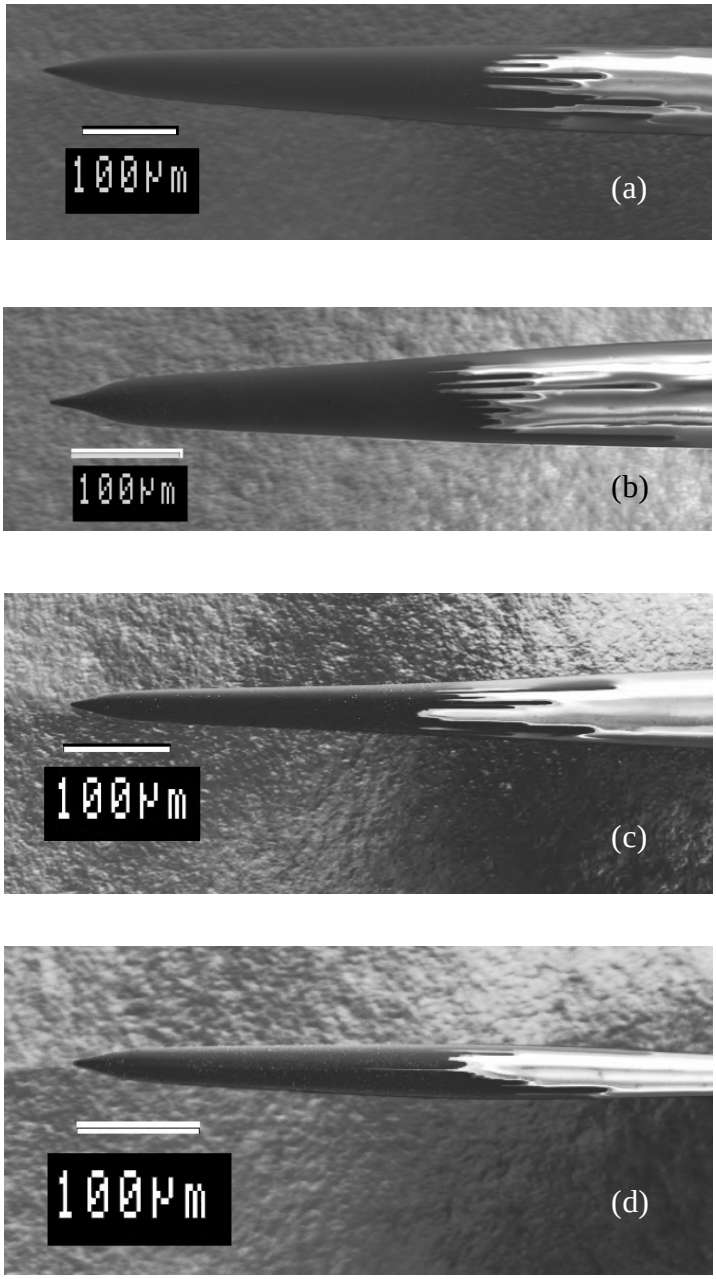

Figure III-viii

Scanning electron micrograph of large cylindrical carbon film microelectrode fabricated by acetylene with nitrogen in the counter flow direction.

Table III-ii Comparison of dimensions obtained for large cylinder microelectrodes.

Electrode No	Dimensions measured from SEM's			Dimensions calculated from the Cottrell decay curve		
(Figure III-vii)	Length (μm)	Radius (μm)	Area (μm^2)	Length (μm)	Radius (μm)	Area (μm^2)
(a)	795	21	$1.2x10^5$	550	30	$1.0x10^4$
(b)	420	31	$8.4x10^4$	510	23	$7.4x10^4$
(c)	400	20	$5.0x10^4$	300	22	$4.1x10^4$
(d)	350	20	$4.4x10^4$	460	17	$4.9x10^4$

Comparison of the Cottrell decay calculated dimensions and those obtained by scanning electron micrographs showed them to be surprisingly similar. The small cylinder electrodes in Figure III-vi (a), (b) and (c) are almost cylindrical, therefore closer agreement is expected.

The larger difference between the calculated and measured for the large cylindrical electrodes may arise from length estimations with inaccuracies due “ragged edges” and taper profile.

The correlation between calculated and measured values is considered adequate for capacitance calculations, as an error of 25 % in area for carbon film capacitance measurements translates into ±1 μF cm^{-2}. This variation is insignificant when comparing capacitance values to assign surface chemistry. (See Chapter IV-(iv))

Morphology of the Carbon Film

From the scanning electron micrograph in Figure III-v the dark region in the centre appears to be recessed (creating the toroidal shape). This recess is attributed to carbon deposits growing, on the inside walls of the pulled capillary, towards the centre. The inward growth of the carbonaceous deposits is shown in Figure III-ix.

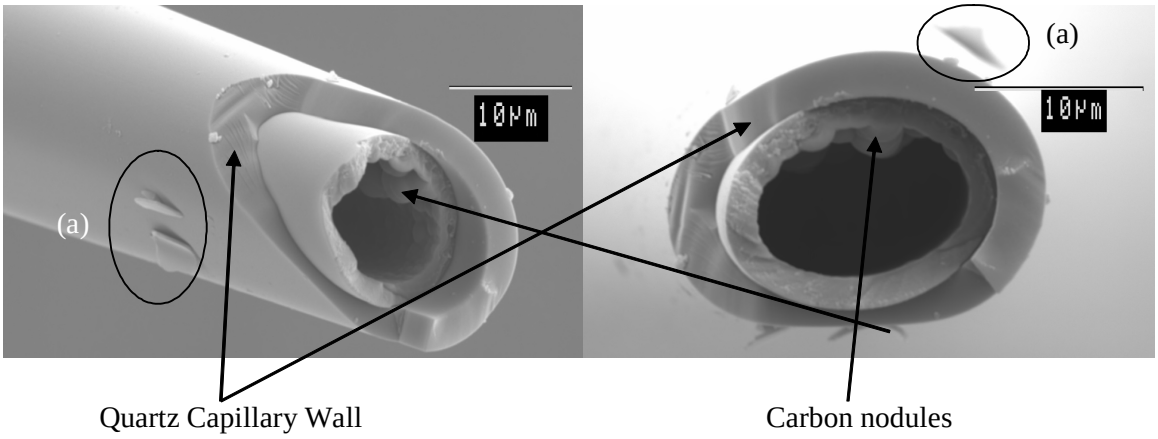

Figure III-ix

Scanning electron micrograph of carbon film microelectrode section near tip.
Circles (a) indicate possible delaminated carbon film.

It is this inward growth of carbon deposits, which restricts the acetylene flow, which is the criterion for pyrolysis time. If the carbon deposits within the capillary seal prior to the tip closing, a recessed tip will form. Using a sharp taper profile at the tip overcomes this feature and even if formed its contribution to the functionality of the electrode becomes insignificant (See Figure III-x).

The flakes in the circled area (a) in Figure III-ix are attributed to carbon film which has delaminated from the quartz substrate. (The thickness of the carbon film is discussed in Chapter IV-(iii).) During formation of the carbon film, both the quartz and carbon film have the same physical dimensions. On cooling contraction occurs resulting in the carbon film being under considerable stress. The fracturing of the electrode appears to have provided an

initiator for the delamination.

Examination of the surface close to the tip using higher magnification, after gold sputtering, provides an insight into formation of the carbon film. Examples of the carbon film surface are shown in Figure III-x. The scanning electron micrographs are of a large cylindrical electrode, which was fabricated by passing nitrogen counter to the acetylene flow. The "spongy and nodule " appearance near the orifice and the "featureless" surface 10 μm from the orifice appear to reflect the changing acetylene concentration on the morphology of the carbon film. The growth of the nodules; close to the orifice in (a), 10 μm away from the

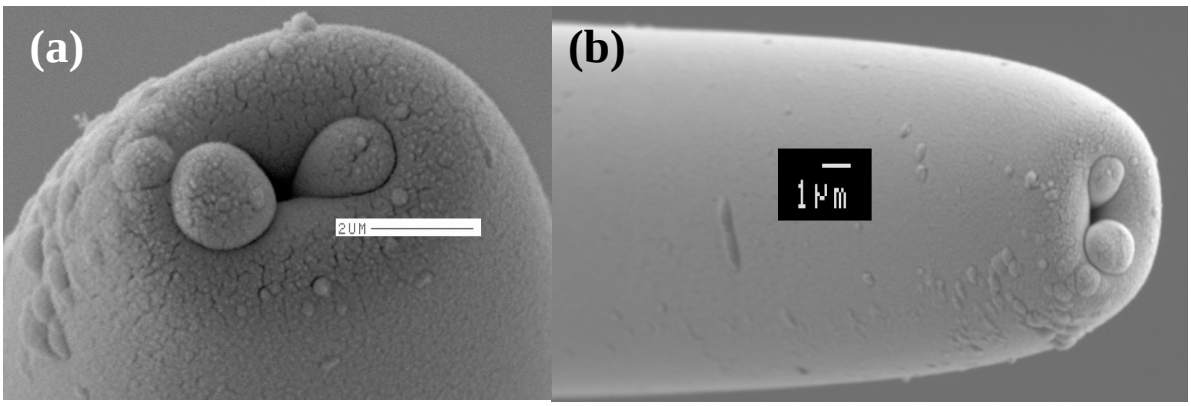

Figure III-x

High magnification scanning electron micrograph of a gold sputtered carbon film cylindrical microelectrode.
Picture (a) is of the tip of the electrode; (b) is of the tip together with a section of the electrode shank.

orifice in (b) and those on the internal surface are possibly due to "active" sites acting as nucleation points. The absence of conical structures indicates the pyrolysis temperature did not reach 1300 °C.[23] The formation of nodules appears to occur only in regions at high concentrations of acetylene. Carbon film formation is retarded due to the presence of a large concentration of hydrogen radicals.[11] It is possible these hydrogen radicals are involved in a polymerisation terminating reaction which interrupts the ordered growth of graphite formation. This may occur although the acetylene flowing through the capillary is flushing

hydrogen radicals from the reaction sites of the “reaction chamber”, which extends inside the pulled capillary 10 mm upstream from the orifice. This extension is deliberately formed during fabrication to ensure an electrically conductive pathway to the powdered graphite exists on the internal surface of the capillary. These nodules disappear when the orifice is smaller than those shown in Figure III-ix. This is illustrated in Figure III-xi.

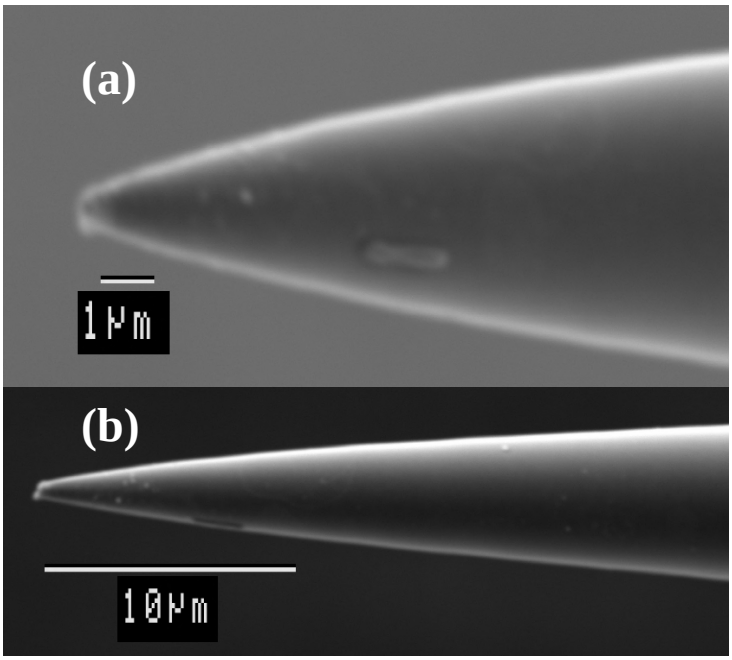

Figure III-xi

Scanning electron micrographs of a microelectrode tip with a small orifice.

In Figure III-xi(a) the orifice can be seen to be approximately 0.4 μm radius whereas the microelectrode in Figure III-x is 2.3 μm. This reduction has resulted in a lower flow rate of acetylene through the orifice (acetylene flow is controlled by pressure and maintained at 60 kPa) resulting in a lower concentration of acetylene, during pyrolysis, in the atmosphere along the shank of the electrode. This reduction in concentration results in a carbonaceous film devoid of nodules (see Figure III-xi(b)), as occurs 10 mm from the orifice in Figure III-x. From these experiments it appears that changes in orifice size, under conditions of fabrication,

and outlined in the Procedure section, result in a change to the morphology of the carbonaceous film formed. This change in surface morphology, with its consequential change in surface chemistry is expected to result in changes in electron transfer characteristics. This aspect will be discussed in Chapter IV.

Maximum and Minimum Sizes

The fabrication of very large and nanometre sized electrodes was curiosity driven. Additionally, by fabricating nanodes the crystal structure of the initial carbon layers formed may provide an indication of the presence of graphene layers.

The Largest

Using the counter flow technique “microelectrodes” up to a calculated length of 1847 μm and 24 μm radius have been fabricated. The cyclic voltammogram of this large microelectrode is shown in Figure III-xii.

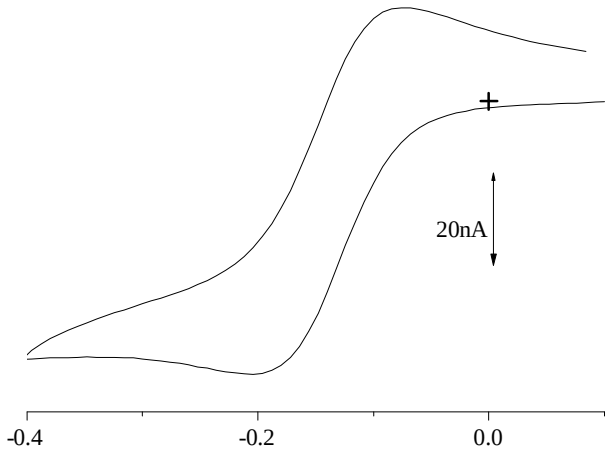

Figure III-xii

Cyclic voltammogram of 10^{-4} M $Ru(NH_3)_6Cl_3$ in 0.05 M KCl at a large carbon film cylindrical electrode. Scan rate 0.1V s^{-1}

The large electrode has an apparent peak shape, with a limiting current of 56 nA (in a 10^{-4} M $Ru(NH_3)_6Cl_3$, with $5x10^{-2}$ M KCl supporting electrolyte) which arises from the non-steady state, due to the "fast" scan rate of 0.1 V s^{-1}. For an electrode of this size a scan rate less than 0.005 V s^{-1} would be required to approach steady state.

The lack of steady state is also indicated by the difference in initial and final currents. The cyclic voltammogram does indicate a long cylindrical electrode can be simply fabricated by the procedure outlined in this chapter.

The Smallest

To produce a microelectrode smaller than 1 μm requires the quartz capillary to be drawn down to nanometre dimensions and this was achieved by increasing the heat input control on the puller. Pyrolysis was carried out using the parallel technique outlined in the Procedure section of this chapter for disc and small cylinder electrodes. Cyclic voltammetry was then undertaken on the microelectrodes in $Ru(NH_3)_6Cl_3$ with 0.05 M KCl (see Figure III-xiii) and the radii calculated using equation (iii) Chapter I.

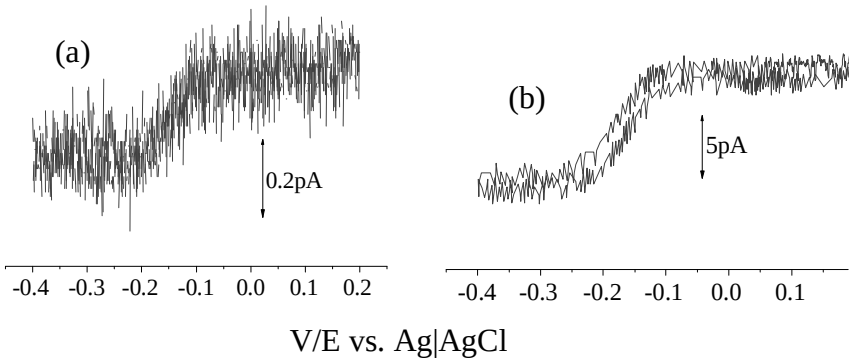

Figure III-xiii

Cyclic voltammograms of (a) $2.95x10^{-3}$ M $Ru(NH_3)_6Cl_3$ at 0.005 V s^{-1} and a step width of 200 ms, (b) $2x10^{-2}$ M $Ru(NH_3)_6Cl_3$ at 0.0001 V s^{-1} and a step width of 5 sec.
Both (a) and (b) in 0.05 M KCl supporting electrolyte.

From the limiting current of the cyclic voltammograms, shown in Figure III-xiii, the calculated radius, as disc shaped microelectrodes are; (a) 0.8 nm and (b) 1.2 nm. At these dimensions the term nanode is appropriate. The calculation of nanode radius, using microelectrode theory, has been suggested to overestimate the actual electrode size by 50-100 %![24] As these tips were beyond the resolution of the available scanning electron microscope the disc shape is only conjecture! Calculations as a disc yield the "largest" dimension. If other shapes are considered together with the possible 50-100 % overestimation of the nanodes used to generate the cyclic voltammograms in Figure III-xiii the actual size is possibly an electrically active surface consisting of only 100 atoms!

The small size of the carbon surface formed is possibly due to combination of the orifice size and the two minute pyrolysis time. (The two minute pyrolysis was used to ensure an orifice 0.5-1 μm radius sealed.)

During pyrolysis, as well as carbon formation, decarbonisation is occurring, often referred to as vaporisation which proceeds simultaneously. This latter aspect of carbon deposits formation appears to have been ignored in the literature. The decarbonisation would be expected to result in the formation of radicals, possibly different to those formed during pyrolysis, which may react to provide alternative pathways in carbon film formation.

During pyrolysis of acetylene, when using large orifice pulled quartz capillaries, carbon deposits are visible on the inside walls of the quartz tube during the initial seconds of pyrolysis. As the pyrolysis continues these deposits disappear. It therefore suggests that the very small orifice, which will seal within the first thirty seconds or less, prevents further carbon depositing on the external surface. During the remaining pyrolysis time carbon deposits already present on the shank are "vaporised" leaving a nanometre sized electrochemically active surface.

The stability of the carbon surface of nanodes is less than twenty four hours, indicating reaction with molecular oxygen. This aspect is discussed in more detail in

Chapter IV-(i).

As the critical dimension of the microelectrode becomes smaller than 50 nm, deviation from microelectrode theory occurs.[25;26] The loss of rapid attainment of steady state can be seen (Figure III-xiii) in the scanning parameters required to obtain a sigmodial voltammogram. The cyclic voltammogram of the microelectrode, shown in Figure III-(xiii)(a) scanned at the default settings, (scan rate 0.1 V s^{-1} and step width 80 ms) is shown in Figure III-xiv. Only with imagination is a sigmodial shape evident.

At concentrations required to generate a measurable Faradic current, the current density of the electrode in Figure III-(xii)(a) is 0.2 A mm^{-2}, this compares with $0.2x10^{-5}$ A mm^{-2} at a 1 μm radius microelectrode. This high current density could be the source of the unstable signal in Figure III-(xiv) due to instability of the diffusion profile at the electrode surface. The large step widths, 200-5000 milliseconds required to obtain a sigmodial shape suggest an unstable signal rather than electrical “noise”. To test this explanation would require a least a femostat, which unfortunately was not available.

Nanodes of similar dimensions to those illustrated in Figure III-(xiv) has been fabricated by electrochemically etched platinum wire coated with electrophoretic paint. The electrode is then oven dried during which paint shrinkage occurs, exposing the nanode size tip.[27] The cyclic voltammograms, used to calculate the electrode radius were obtained at 0.01V s^{-1}.

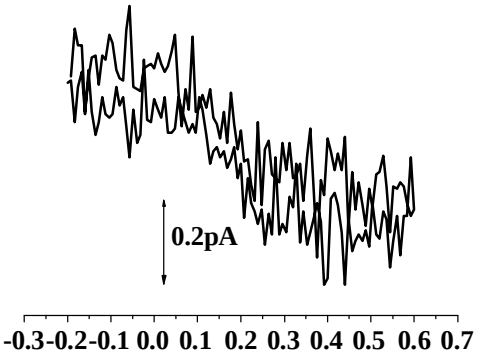

Figure III-xiv

Cyclic voltammogram of 2.95×10^{-3} M $Ru(NH_3)_6Cl_3$ in 5×10^{-2} M KCl at 0.1 V s^{-1}, step width 80 ms

Conclusion

By using very simple equipment carbon film microelectrodes ranging from less than one nanometre radius to 1800 microns in length cylindrical microelectrodes can be fabricated, by *in situ* pyrolysis of acetylene on a pulled quartz capillary. The surface morphology varies from a high concentration of "spongy" nodules near the orifice to a compact flat film 10 μm along the electrode shank, with the nodule density dependent on the orifice radius and nitrogen flow and direction.

Platinum plating of the electrochemically active surface allowed SEM visualisation of the shape and location of the carbon film. The dimensions obtained by measurement of the Cottrell decay were shown to be sufficiently accurate to calculate the microelectrode area for capacitance measurements and functional group surface concentration.

References

1. McCreery R.L. *Electroanalytical Chemistry*, Bard A.J., Ed.; Dekker: 1991.
2. Grisdale R.O.; Pfister A.C.; van Roosebreok W. *The Bell System Technical Journal* **1951,** *30*, 271-315.
3. Walker P.L.; Thrower P.A. Spain I.L., Ed..
4. Paris O.; Loidl D.; Peterlik H. *Carbon* **2002,** *40*, 551-55.
5. Beilby A.L.; Brooks W.; Lawrence G.L. *Analyical Chemistry* **1964,** *36*, 22-26.
6. Lundstrom K. 83; Vol. 146, pp. 97-108.
7. Saraceno R.A.; Engstrom C.E.; Rose M.; Ewing A.G. *Analytical Chemistry* **1989,** *61*, 560-65.
8. Blackstock J.J.; Rostami A.A.; Nowak A.M.; McCreery R.L.; Freeman M.R.; McDermott M.T. *Analytical Chemistry* **2004,** *76*, 2544-52.
9. Eriksson A.; Norekrans A.; Carlsson J. *Journal of Electroanalytical Chemistry* **1992,** *324*, 291-305.
10. McFadden C.F.; Russell L.L.; Melaragno P.R. *Analytical Chemistry* **1992,** *64*, 1521-27.
11. Oberlin A *Carbon* **2002,** *40*, 7-24.
12. Frenklach M. *Twenty Second Symposium (International) on Combustion* **1988,** 1075-82.
13. Krestinin A.V. *Kinetika i Kataliz* **2000,** *41*, 805-13.
14. Jasienko S.; Machnilowski J. *Carbon* **1981,** *19*, 199-203.
15. Kieffer J.H.; von Drasek W..A. *International Journal of Chemical Kinetics* **1990,** *22*, 747-86.
16. Krestinin A.V. *Combustion and Flame* **2000,** *120*, 513-24.
17. Hu Z. J.; Huttinger K.J. *Carbon* **2002,** *40*, 617-36.
18. *NTIS* **1990,** *DE91000357*.
19. Tesner P.A.; Robinovich E.Y.; Rafalkes I.S.; Arefieva E.F. *Carbon* **1970,** *8*, 435-42.
20. Zhao G., Giolando D.M., and Kirchoff J.R. 95; Vol. 67, pp. 2592-2598.
21. Saraceno R.A.; Ewing A.G. *Journal of Electroanalytical Chemistry* **1988,** *257*, 83-93.
22. Oldham K.B. *Journal of Electroanalytical Chemistry* **1992,** *323*, 53-76.
23. David C.; Sublet A.; Auriol A.; Rappeneau J *Carbon* **1964,** *2*, 139-48.
24. Smith C.P.; White H.S. *Analytical Chemistry* **1993,** *65*, 3343-53.

25. Zoski C.G. 2002; Vol. 14, pp. 1041-1051.

26. Conyers, Jr. J. L.; White H.S. *Analyical Chemistry* **2000,** *72*, 4441-46.

27. Watkins J.J.; Chen J.; White H.S.; Abruna H.D.; Maisonhaute E.; Amatore C. *Analyical Chemistry* **2003,** *75*, 3962-71.

Chapter IV

Characterisation of the Carbon Film Surface

Introduction

Carbon film electrodes are unique in that their deposition *in situ* is an addition reaction which forms the surface.[1-3] That is, the conductive carbon layers are deposited directly onto the electrode substrate without further treatment prior to use. Carbon films formed by non-thermal techniques, such as electron beam evaporation[4;5], radio frequency magnetron[6] and carbon inks[7] have required high temperature pyrolysis after film formation at 600-1100 °C to form a graphene network. This post-formation pyrolysis results in mass loss, with the formation of a crystalline structure similar to GC and carbon fibres. Both GC and carbon fibres are formed by the pyrolysis of polymers which results in a mixture of basal and edge planes on the electrode surface. HOPG electrodes, although formed by the same mechanism as carbon film electrodes are split along or perpendicular to the basal plane prior to use in an electrode. In the fabrication of non thermal carbon film, GC and HOPG electrodes, the final surface has active sites which will react with molecular oxygen to form a range of oxygenated functional groups.

The surface of HOPG[8], both basal and edge planes[9], GC[10] and non thermal carbon films have been well characterised using instrumental techniques such as Raman,[11] X-ray photoelectron spectroscopy,[12] Auger electron spectroscopy,[6] scanning electron microscopy[7] and model analytes.[13] Carbon films formed by direct thermal pyrolysis of carbonaceous compounds have not received such attention, with the only surface characterisation being cyclic voltammetry, using model analytes on the surface as formed and after oxidation.[14] Although the carbon film microelectrodes, as formed in this thesis work, are expected to exhibit different electron transfer characteristics to HOPG, GC and non thermally formed

carbon films, the electron transfer characteristics of GC and HOPG will be used to elucidate the surface structure of the carbon film formed by the pyrolysis of acetylene.

It is the chemical nature of the surface which determines the properties of an electrode.[15] As outlined in Chapter IV-(xiii) the surface of carbon electrodes have a large number of possible functional groups, to interact with the species undergoing redox reactions at the surface. Carbon films, formed by high temperature pyrolysis of carbonaceous gases, will have fewer "reactive sites", such as edge planes due to the large concentration of hydrogen species formed during *in situ* pyrolysis. In this Chapter the results of limited instrumental analysis (limited by the availability of equipment and size of the electrode surface) and voltammetric studies of model analytes, will be used to elucidate the surface chemistry of the carbon film formed by the pyrolysis of acetylene. The characterisation of the carbon film surface, in this work, is that formed on cylindrical microelectrodes. The cylindrical surface was chosen as the cylindrical microelectrodes (≈ 500 μm in length) will be used for *in vivo* experiments and the surface of 1μm discs are too small for instrumental analysis.

Fortuitously, the surface formed on the quartz substrate is extremely stable thereby allowing voltammetric studies before and after modification to be carried out either immediately or months after fabrication on the same electrode. This feature has been exploited by carrying out concurrent experiments on microelectrodes rather than consecutively, as is necessary with glassy carbon, edge and basal plane graphite electrodes.[16] The knowledge of surface chemistry of the carbon film obtained from characterisation experiments in this chapter is of importance for designing microelectrode surfaces for analytical specificity, the subject of Chapter IV.

As a range of techniques were used to characterise the carbon film on the microelectrodes each will be treated separately for clarity, with an introduction, experimental, results and discussion sections, together with a conclusion.

References

1. Grisdale R.O.; Pfister A.C.; van Roosebreok W. *The Bell System Technical Journal* **1951,** *30*, 271-315.

2. Blaedel W.J.; Mabbott G.A. *Analytical Chemistry* **1978,** *50*, 933-36.

3. Lundstrom K. 83; Vol. 146, pp. 97-108.

4. Schelz S.; Richmond T.; Kania P.; Oelhafen P.; Guntherodt H.J. *Surface Science* **1996,** *359*, 227-36.

5. Blackstock J.J.; Rostami A.A.; Nowak A.M.; McCreery R.L.; Freeman M.R.; McDermott M.T. *Analytical Chemistry* **2004,** *76*, 2544-52.

6. Schesinger R. ; Bruns M.; Ache H-J. *Journal of Electrochemical Society* **1997,** *144*, 6-15.

7. Ranganathan S.; McCreery R.L.; Majji S.M.; Madon M. *Journal of Electrochemical Society* **2000,** *147*, 277-82.

8. Bowling R.J.; McCreery R.L. *Analytical Chemistry* **1989,** *61*, 2763-66.

9. Ravovic L.R.; Bockrath B. *Journal of the American Chemical Society* **2005,** *127*, 5917-27.

10. McDermott M.T.; McCreery R.L. *Langmuir* **1994,** *10*, 4307-14.

11. Dillon R.O.; Woollam J.A. *Physical Review B* **1984,** *29*, 3482-88.

12. Kozlowski C.; Sherwood P.M. *Journal of the Chemical Society, Faraday Transactions* **1984,** *80*, 2099-107.

13. Fukutsuka T.; Abe T.; Inaba M.; Ogumi Z. *Journal of Electrochemical Society* **2001,** *148*, A1260-A1265.

14. McCreery R.L. *Electroanalytical Chemistry*, Bard A.J., Ed.; Dekker: 1991.

15. Chen P.; McCreery R.L. *Analytical Chemistry* **1996,** *68*, 3958-65.

16. Dekanski A.; Stevanovic J.; Stevanovic R. *Carbon* **2001,** *39*, 1207-16.

Chapter IV-(i)

Surface Stability

Abstract

In this section the long term stability of the carbon film microelectrodes was found to be up to twenty five months using dopamine as a model analyte. This property suggests the surface is similar to that of hydrogenated glassy carbon. The long term stability of the surface enables characterisation and modifications of the carbon film to be carried out even many weeks after fabrication.

Introduction

Carbon surfaces used as electrode surfaces range from edge to basal plane, if they are fabricated from pyrolysed hydrocarbon feedstock.[1;2] The edge planes, whether present as a deliberate surface of the electrode, or as a defect on a freshly cleaved basal plane, rapidly react with molecular oxygen in the atmosphere.[3] The reaction of molecular oxygen with the vacuum heat treated surface of glassy carbon changes its composition from an oxygen to carbon atomic percent of 1.5 to 5 in ten minutes.[4] The rate of change then slows with the oxygen to a carbon atomic percent of 9 being attained after 240 minutes. The oxidation products of the edge plane and molecular oxygen consist of hydroxyls, carbonyls, carboxylic acid, lactones and quinones.[4] These functional groups dramatically affect the kinetics of heterogeneous electron transfer reactions occurring at the surface.[4] Ideally the electrode surface should remain stable and reproducible, allowing sufficient time for experimentation. The reaction with molecular oxygen is reported to be retarded by hydrogenation.[5,6]The hydrogenated glassy carbon surface had oxygen to carbon atomic ratio of 0.07 after two months.[4] The lack of oxygenated functional groups after hydrogenation is attributed to the replacement of active groups on the edge plane with chemisorbed hydrogen. The effect of

hydrogenation on the stability of glassy carbon electrode was exceptional when compared to the original surface. The ΔEp values for the cyclic voltammetry of dopamine at a 1 cm^{-2} hydrogenated glassy carbon electrodes ΔEp after three months changed from 122 mV to 111 mV, whereas for the freshly polished glassy carbon electrode changed from 111 mV to 310 mV.

The long term stability of microelectrodes is a desirable property. This is particularly important for *in vivo* applications as it allows fabrication of the microelectrodes prior to either the animal or the living tissue preparation for experimentation.

As dopamine is the primary analyte of interest in this work it was used to monitor changes in cyclic voltammetric properties of the microelectrodes with time.

Experimental Section

Chemicals

Milli-Q water, dopamine (Sigma), tri-sodium phosphate dodecahydrate (Sigma), citric acid (Sigma), nitrogen (BOC Instrument Grade) and phosphoric acid (BDH Analar) were used as received.

Equipment

The three electrode system as outlined in Chapter II Electrochemical Equipment, using an Ag|AgCl (3 M KCl) reference electrode.

Electrode Fabrication

Electrodes were fabricated as outlined in Chapter III using 40 ml min^{-1} nitrogen in the parallel flow configuration.

Procedure

Cyclic voltammetry, cycling from -0.2 V to 0.9 V was carried out with 10^{-4} M dopamine in a deoxygenated citrate/phosphate buffer at pH 7.4 (Buffer composition was 46.8 gm tri-sodium phosphate dodecahydrate and 1.9 gm citric acid per litre adjusted to pH 7.4 with phosphoric acid.)

Results and Discussion

The effect of storage in a laboratory cupboard on the anodic cyclic voltammetric properties of DA, in citrate/phosphate buffer pH 7.4 with a scan rate of 0.1V s^{-1}, at a carbon film microelectrode's surface, can be seen in Table IV-(i)-i.

Table IV-(i)-i Summary of change in *E½* and waveslope with time in storage.

	Storage Time	Initial			After Storage		
Electrode	(Days)	*E½*	Waveslope	Limiting current	*E½*	Waveslope	Limiting Current
		(V)	(V/decade)	nA	(V)	(V/decade)	nA
A	750	0.262	0.085	10.5	0.288	0.111	11.4
B	360	0.330	0.184	2.2	0.310	0.151	2.1
C	140	0.237	0.097	7.8	0.271	0.103	7.9
D	80	0.291	0.144	0.63	0.232	0.129	0.7
E	70	0.232	0.096	1.2	0.212	0.098	1.3
F	50	0.255	0.140	11.8	0.278	0.122	11.7
G	20	0.229	0.098	5.8	0.219	0.086	5.8

An example of these changes can be seen in Figure IV-(i)-i for electrode A and Figure IV-(i)-ii for electrode B.

The cyclic voltammetry, for Electrode A and B indicate after storage for 750 days and 360 days respectively that the sigmodial shape has been retained. The slight changes in *E½* and waveslope are insignificant and could be considered as day to day variations. However the limiting current at Electrode A displays an increase in current with voltage. This indicates that a slight change in the surface chemistry has occurred..

The cyclic voltammogram (Figure IV-(i)-i) of Electrode A has a cathodic wave on the reverse scan between 0.15 V and -0.15 V which is absent in the cyclic voltammogram of Electrode B (Figure IV-(i)-ii). The significance of the cathodic wave is discussed in Chapter IV-(x). The reduction in size of the cathodic wave with time also indicates a change in surface chemistry. The increase in limiting current suggests a greater area of the graphene region has become

assessable. In Chapter IV-(xiii) it is postulated the surface structure of the carbon film has hydrophobic pendent groups that are in close proximity to the graphene regions. It is therefore suggested that over this very long storage time the pendent groups have been oxidised by molecular oxygen. It is proposed that the reaction with molecular oxygen has resulted in a loss of pendent groups, thus reducing the steric hindrance of dopamine to the graphene regions, thereby increasing the limiting current. These reaction products, being oxides have reduced the hydrophobic character close to the graphene region and consequently the postulated adsorption of the dopamine quinone.

The suggested reaction with molecular oxygen has resulted in similar oxide products to that obtained by electrochemically oxidising the surface. (See Chapter IV-(xi))
This reaction with molecular oxygen is also suggested by the smaller changes in the $E½$ and waveslope values of carbon film microelectrodes (Electrodes E, F and G) which have been stored for less time.

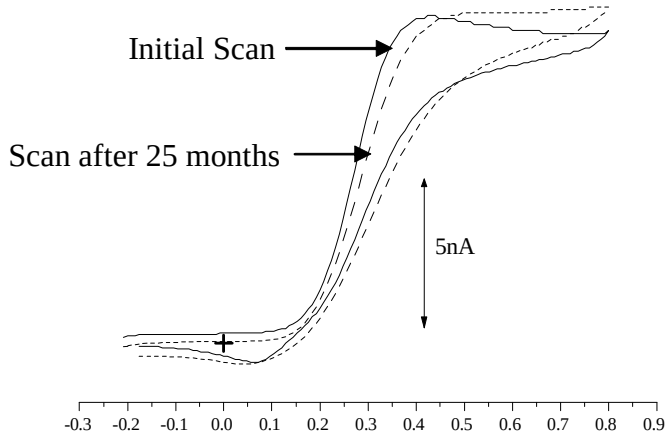

V/E vs. Ag|AgCl

Figure IV-(i)-i

Initial and after 25 months cyclic voltammogram of the oxidation of 10^{-4} M dopamine at Electrode A in citrate/phosphate buffer pH 7.4
Scan rate 0.1V s^{-1}

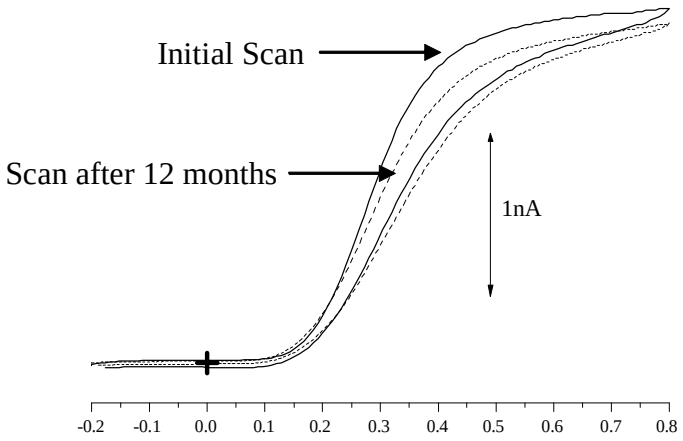

E/V vs. Ag|AgCl

Figure IV-(i)-ii

Initial and after 12 months cyclic voltammogram of the oxidation of 10^{-4} M dopamine at Electrode B in citrate/phosphate buffer pH 7.4
Scan rate 0.1 V s^{-1}

Conclusion

The long term stability of the carbon film microelectrodes, formed by *in situ* pyrolysis of acetylene, indicates the surface has similar characteristics to that of hydrogenated glassy carbon. The long term stability enables concurrent characterisation, modification and evaluation of the microelectrodes over several weeks. With unstable surfaces, such as glassy carbon, polishing, characterisation, modification and evaluations must be carried sequentially thereby eliminating errors due to oxide formation on the surface.

This long term stability has been utilised throughout this thesis as it enabled characterisations (electrochemical or instrumental) and modifications of electrode surface to be carried out immediately after fabrication or several days later. Similarly, modifications and further reactions on these modifications could be performed in batches reducing the time for experimentation.

References

1. McCreery R.L. *Electroanalytical Chemistry*, Bard A.J., Ed.; Dekker: 1991.
2. McCreery R.L. *Neuromethods Vol 27 Voltammetric Methods in Brain Systems*, Boulton A.; Baker G.Adams R.N., Eds.; Humana Press Inc: 1995.
3. Rusling J.F. *Analytical Chemistry* **1984,** *56*, 575-78.
4. Chen P.; McCreery R.L. *Analytical Chemistry* **1996,** *68*, 3958-65.
5. Chen Q.; Swain G.M. *Langmuir* **1998,** *14*, 7017-26.
6. Kuo T.C.; McCreery R.L. *Analytical Chemistry* **1999,** *71*, 1553-60.

Chapter IV-(ii)

X-ray Photoelectron Spectroscopy

Abstract

Due to the small surface area of the electrode, XPS has been limited to the detection of chemical elements within 2 nm of the surface. Using XPS for the detection of nitrogen, sulfur and chloride, after derivatisation with 2, 4-dinitrobenzenesulfenyl chloride, the presence of aliphatic double and/ or triple bonds on the electrode surface has been established. Similarly the absence of nitrogen on unmodified electrode surfaces indicates the nitrogen blanket has not formed nitrogenous products during pyrolysis of acetylene.

Introduction

XPS utilises X rays to eject a single electron from the inner orbitals of an element, the energy (binding energy) required to eject these electrons is a characteristic of the element and bond structure. As the X-rays penetrate to a depth of 0.5-2 nm, the analytical signal is not excessively diluted by the underlying structures.[1]

The bond structure of the surface requires deconvolution of the core binding energy envelope to reveal the chemical shift, or by derivatising the functional groups, with dissimilar elements to provide distinct peaks well separated from oxygen and carbon. The latter approach permits the use of equipment with reduced resolution, or non planar small surfaces, such as microelectrodes, to provide an unambiguous identification of the surface functional groups. Non-planar surfaces, such as carbon film microelectrodes produce a divergent beam of electrons, resulting in a reduced signal.

Deconvolution of the C1s envelope has been used to determine sp^2 and sp^3 compositions of amorphous and hydrogenated amorphous carbon films.[2;3] The existence of

sp^3 in a pyrolysed hydrocarbon film indicates incomplete graphitisation possibly leading to electron transfer properties similar to hydrogenated glassy carbon or boron doped diamond. The sensitivity of XPS is further illustrated using the O1s envelope of oxides on a carbon fibre, formed during anodic oxidation at a range of potentials and solution pHs. The results indicated the formation of >C-OH, >C=O, and $–CO_2H$/ester in neutral and high pH solutions at edge planes.[4]

Deconvolution of the N1s envelope has been used to determine the yield and nature of products formed during the electrochemical reduction of nitro groups after cathodically attaching a 4-nitrophenyl diazonium salt.[5] The nitro group was subsequently electrochemically reduced in HCl solution. Examination of the XPS N1s envelope showed the existence of $-NO_2$, $-NH_2$ and –NHOH, with the –NHOH group being an intermediate between $–NO_2$ and $–NH_2$. The presence of residual $–NO_2$ groups implies incomplete conversion of the $–NO_2$ group. This lack of complete conversion to the amine possibly arises from the nitro groups lacking accessibility to the graphene surface. This lack of accessibility is possibly due to steric hindrance or the nitro group being too distant from the graphene region. This lack of access to the electrochemically active surface has implications for elucidation of surface structure in Chapter IV-(vii) and surface coverage calculations in Chapters V-(i),(ii) and (iii).

Derivatisation of functional groups has been used to detect the presence of carbonyls using dinitrophenyl hydrazine[6] and pentafluorophenylhydrazine.[7] Hydroxyl groups present on the carbon surface have been confirmed using diisoprop-oxide bis(2,4-pentanedionate).[8] Derivatisation was used to detect the presence of alkynes and alkenes on the surface of the carbon film microelectrodes in this work.

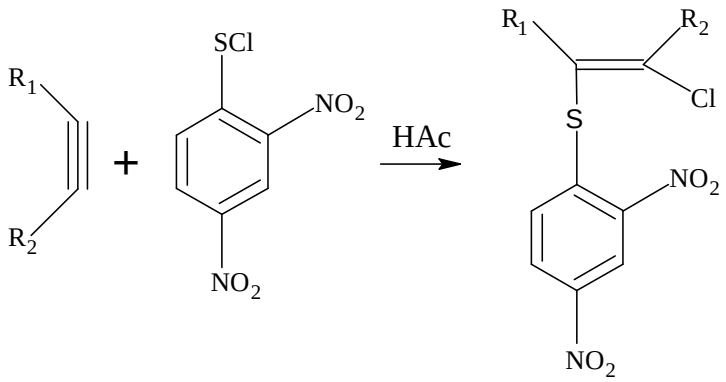

Figure IV-(ii)-i
Reaction of 2, 4-dinitrobenzenesulfenyl chloride
and an alkyne in glacial acetic acid.

The unsaturated groups are expected to form from the polyyne pathway (Chapter III Introduction) and alkene groups from the hydrogenation of alkynes. Saturated 2,4dinitrobenzenesulfenyl chloride in glacial acetic was used as the derivatising agent.[9;10] The alkyne reaction is shown in Figure IV-(ii)-i. Alkenes yield a similar product, except for the formation of a single bond in the product. The reagent was selected as the product contains three dissimilar atoms; sulfur, nitrogen and chloride. When modifying the carbon surface on the quartz substrate all reactions have to be conducted in neutral or acidic solutions, as quartz will soften or dissolve in basic solutions. The use of 2,4-dinitrobenzenesulfenyl chloride in glacial acetic satisfies both of these requirements. The use of bromine as the dissimilar atom, for example using bromine water, to differentiate between alkene and alkyne was considered. However, if intercalation occurred this would lead to erroneous conclusions.

Experimental Section

Chemicals and Reagents

2,4-dinitrobenzenesulfenyl chloride (Sigma Aldrich) and glacial acetic acid (BDH Analar) were used as received.

Equipment

XPS spectra were acquired using a Kratos XSAM800 (Kratos Analytical Instruments) with a Mg X-ray source.

Electrode Fabrication

Electrodes were fabricated as described in Chapter III using reverse nitrogen flow of 80 ml min^{-1}. With this configuration of gas flow microelectrodes with maximum length were obtained.

Surface Modification

The electrode tip was placed in a saturated glacial acetic acid solution of 2,4-dinitrobenzenesulfenyl chloride for 30 minutes. The electrode was then rinsed in glacial acetic acid for thirty seconds with gentle agitation, followed by 30 second rinse with gentle agitation in deionised water.

Results and Discussion

In this work, the XPS beam used was 700mμm diameter, the microelectrodes analysed were 300-500 μm in length and with a 20-30 mμm radius (non planar), consequently the analysis time was extremely long, requiring two hours to obtain a minimal signal count. The accumulated signal was not of sufficient magnitude to provide accurate deconvolution of XPS envelopes of the elements detected. Therefore XPS was restricted to elemental analysis and derivatisation for unambiguous identification of surface functional groups.

XPS Spectra of Unmodified Electrode

The XPS spectrum of Electrode D in Table IV-(ii)-i is shown in Figure IV-(ii)-ii.

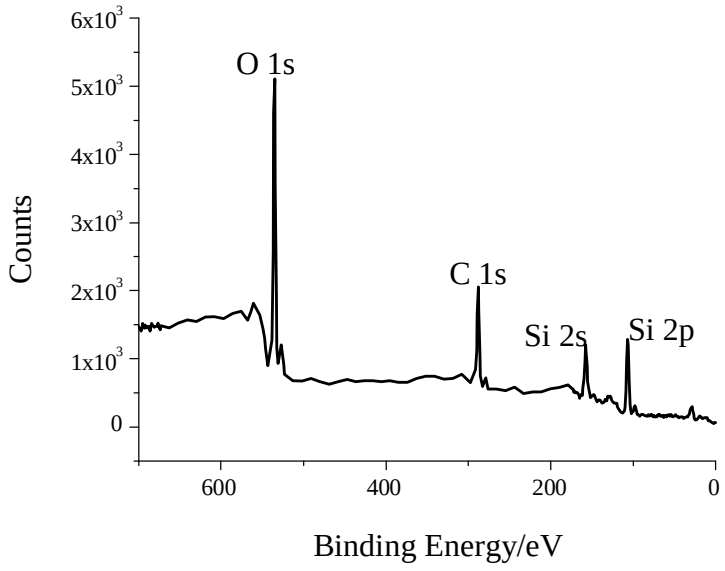

Figure IV-(ii)-ii
XPS spectrum of an unmodified carbon film electrode tip

The presence of the silicon peaks in the XPS spectra (Figure IV-(ii)-ii) is due to the XPS beam extending beyond the carbon film along the shank of the electrode.

The absence of a nitrogen peak indicates reaction with the blanket gas has not occurred. (The absence of nitrogen in all XPS spectra assists in intrepretating a sharp peak in the Raman scattering spectra of the surface. See Chapter IV-(iii))

Elemental XPS spectra analysis of this electrode and four other unmodified electrodes are given in Table IV-(ii)-i.

Table IV-(ii)-i XPS elemental composition of a carbon electrode surface

	Atomic Concentration			
Electrode	Carbon %	Oxygen %	Silicon %	Oxygen/Silicon ratio
Quartz capillary	23.3	56.9	19.8	2.9
A	23.7	54.1	22.3	2.4
B	35.8	46.3	17.9	2.6
C	36.2	44.1	20.7	2.1
D	26.7	53.6	19.7	2.7
E	62	27.3	10.7	2.6

The results of the quartz capillary (Table IV-(ii)-i), although thermally cleaned in a Bunsen flame prior to analysis, indicate the rapid absorption of contamination with carbonaceous material. (This also indicates the sensitivity of XPS as a surface analysis technique.)

The higher ratio of carbon to silicon on Electrode E (Table IV-(ii)-i) probably indicates that the carbon film extends further up the electrode shank than Electrodes A to D. The oxygen to silicon ratio ranges from 2.9 for the quartz capillary to 2.1 for Electrode C. This lower ratio for pyrolysed carbon electrodes when compared to contaminated non pyrolysed carbon on the quartz capillary possibly indicates the presence of SiC formation. (Chapter III Introduction) The ratio of 2.9 for the quartz capillary, rather than 2, as suggested by the stoichiometry of SiO_2 possibly arises from the presence of hydrogen bonded water, one water molecule per molecule of SiO_2, on the surface.

XPS Spectra of 2,4-Dinitrobenzenesulfenyl Chloride Derivatised Electrode Surface

To detect the presence of derivatising reagent on the surface required extending analysis collection time to three hours. The results of this extended collection time are shown in Figure IV-(ii)-iii.

The atomic compositions of the elements obtained from this electrode together with a second electrode are shown in Table IV-(ii)-ii.

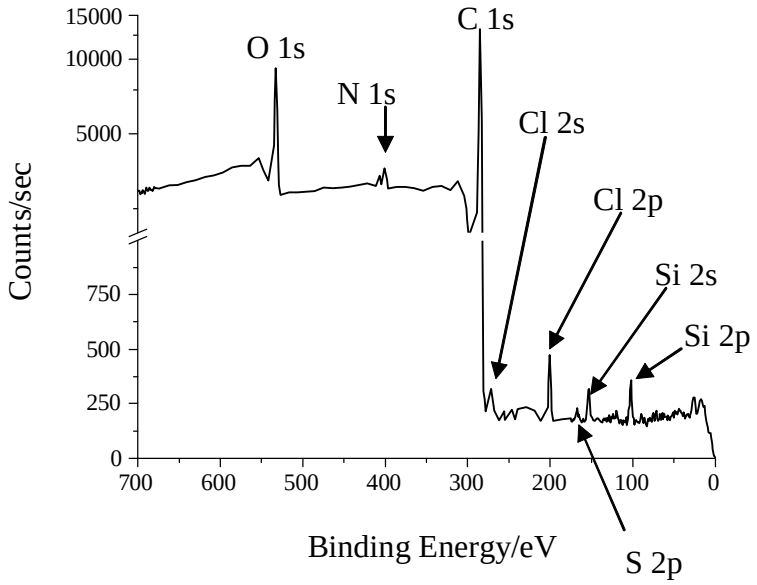

Figure IV-(ii)-iii

XPS spectra of 2,4-dinitrobenzenesulfenyl chloride derivatised electrode surface.

Table IV-(ii)-ii XPS elemental composition of a modified carbon electrode surface

	Atomic Concentration					
	Carbon	Oxygen	Silicon	Nitrogen	Sulfur	Chloride
Electrode	%	%	%	%	%	%
F	80.6	14.2	1.1	3.3	0.1	0.7
G	83.4	12.2	1.1	1.9	0.2	Not detected

The low silicon content measured on the surface of the electrodes in Table IV-ii when compared to those in Table IV-(ii)-i, implies the modified electrodes had carbon film extending further up the shank.

The stoichiometry of the 2,4-dinitrobenzenesulfenyl chloride derivative of an alkene or alkyne is expected to have an elemental ratio of N:S:Cl/2:1:1.(Figure IV-(ii)-i) However this ratio was not obtained and the lack of stoichiometry together with the absence of a chloride peak in the XPS spectra of Electrode G is attributed to the low count obtained from the small non planar surface of the electrode. The presence of unsaturated aliphatic groups is further investigated using voltammetric stripping of π bonded metal ions described in Chapter IV-(vii).

Conclusion

Although the electrode surface size restricted the analytical capabilities of XPS, its detection of chemical elements, to within 2nm of the surface, has provided information on the surface composition of the carbon film.

The XPS spectrum of an unmodified carbon film surface was found to contain only the chemical element carbon. The absence of nitrogen indicates that the nitrogen blanket neither covalently bonded nor intercalated with the carbon film.

Derivatisation of the surface with 2,4-dinitrobenzenesulfenyl chloride gave a XPS spectra containing nitrogen, sulfur and chloride. These indicated the presence of aliphatic unsaturated groups on the surface.

The presence of these unsaturated groups on the surface suggests either non aromatic ring structures or groups pendent to the surface, as 2,4-dinitrobenzenesulfenyl chloride reacts with both[9;10].

References

1. Kibel M.H. *Surface Analysis Methods in Material Science,* O'Connor D.J.; Sexton B.A.Smart R.St.C., Eds.; 1st ed.; Springer-Verlag: Germany , 1992.

2. Jackson S.T.; Nuzzo R.G *Applied Science Surfaces* **1995,** *90,* 195-203.

3. Lascovich J.C.; Giorgi R.; Scaglione S. *Applied Surface Science* **1991,** *47,* 17-21.

4. Kozlowski C.; Sherwood P.M.A *Journal of the Chemical Society. Faraday Trans* **1985,** *81,* 2745-56.

5. Ortiz B.; Saby C.; Champagne G.Y.; Belanger D. *Journal of Electroanalytical Chemistry* **1998,** *455,* 75-81.

6. Elliott C.M.; Murray R.W. **1976,** *48,* 1247-54.

7. Tougas T.P.; Collier W.G. *Analytical Chemistry* **1987,** *59,* 2269-72.

8. Collier W.G.; Tougas T.P. *Analytical Chemistry* **1987,** *59,* 396-99.

9. Kharash N.; Buess C.M. *Journal of the American Chemical Society* **1947,** *71,* 2724-28.

10. Okuyama T.; Izawa K.; Fueno T. *Journal of Organic Chemistry.* **1974,** *39,* 351-54.

Chapter IV-(iii)

Raman Spectroscopy

Abstract

Raman spectroscopy has been used to determine the crystalline nature of the carbon film deposited on the shank of the electrode. The spectra indicate the presence of small graphene (sp^2) crystallites and the absence of diamond like structures (sp^3) and edge planes. The carbon film thickness was found to decrease from the tip, along the shaft of the electrode, with a typical thickness of 25 nm. The existence of background luminescence was proposed to originate from pendent aromatic groups.

Introduction

Infrared and Raman spectroscopy both provide information about molecular vibrations. During infrared spectroscopy the absorbed photon results in the molecule being excited from the ground vibrational state to a higher vibrational state. The Raman process involves a more complex interaction in which the incident photon changes its energy by the difference in two vibrational states. This difference in vibrational energy levels between irradiated energy and emitted energy is the Raman shift. Although the energy measured in the Raman shift is extremely weak (10^{-10} of the incident energy) it has provided considerable information on crystal structure and functional groups on carbon deposits. The depth of penetration of the incident radiation depends on the frequency of the radiation and the absorption coefficient of the carbon. For HOPG, using an incident beam of 515 nm the depth is 13.5 nm and for glassy carbon with a 500 nm beam, 28.4 nm. Using a 416 nm beam the depth of penetration for glassy carbon is reduced to 24.3 nm. [1]

This “deep” penetration beneath the surface results in a greater dilution of the concentration of surface groups when compared to XPS. The dilution effect has been

overcome by using derivatives of the surface groups, which have high absorption coefficients, to analyse for the presence of carbonyl and hydroxyl groups using a fluorescein derivative[2] and the verification of the presence of edge planes, by chemisorption of dinitrophenyl hydrazine.[3]

The Raman spectra in the 1000 to 1700 cm^{-1} range provide considerable information on the crystal structure and carbon bonding. The edge plane produces a strong band at 1355 cm^{-1} [4], sp^3 bonds (diamond) a sharp peak at 1332 cm^{-1} with amorphous sp^3 giving a broad band at 1000 cm^{-1},[5] amorphous carbon has a broad band at 1500 cm^{-1}.[6] The HOPG graphene peak is very narrow occurring at 1580 cm^{-1}. This graphene peak broadens as the amount of clustering of crystals increases and disorder of the crystal regions occur.[7]
In this thesis work the Raman Scattering spectrophotometer (beam size 5 μm) was used to analyse the carbon film along the shank of the microelectrode, thereby providing a Raman "profile".

Experimental Section

Electrode fabrication

Electrodes were fabricated by the procedure outlined in Chapter III for counter flow (35 ml min^{-1}) of nitrogen.

Spectroscopy

The Raman spectra were obtained, in air, using a Renishaw Raman System 2000 with a beam size of 5 μm, radiation wavelength of 325 nm and 410 nm was used with a scan time of 2-5 minutes. The longer scan times were required to increase signal to noise ratio.

The location and focussing of the Raman beam was by visible optical microscopy prior to collection of the Raman spectra.

Results and Discussion

Scan times were limited to five minutes as prolonged exposure to the 325 nm beam produced a bluish discolouration on the surface. Maximum scan times of 500 seconds have been reported for derivatised surfaces, using a 488 nm laser to reduce irradiation damage.[8] The lower energy of the 488 nm laser beam would allow longer periods of exposure than either the 325 nm or 410 nm laser beams available for this thesis work.

Raman spectroscopy was carried out at several locations along the electrode shaft. The spectra obtained for the 410 nm laser beam are shown in Figure IV-(iii)-i and Figure IV-(iii)-ii using the 325 nm laser beam.

In both Figures IV-(iii)-i, (a), (b), (c), Figures IV-(iii)-ii (a) and (b) the Raman scattering due to the quartz substrate (Figure IV-(iii)-i, (d) and Figure IV-(iii)-ii (c)) is visible. The presence of these peaks (with a maximum intensity at 440 cm^{-1}) in the Raman scattering spectra of the carbon film indicates that the carbon film at these locations is less than 25 nm thick, the maximum penetration depth for a 410 nm laser beam. In the SEM (Figure III-ix) of the electrodes 1 μm nodules are visible near the tip therefore it appears the carbon film, along the electrode shank, can be considered to have a thickness less than 200 atoms except for close to the tip. The formation of these very thin films is due to the termination of the acetylene supply when the orifice seals. Previous techniques (Chapter III Introduction) used an externally applied methane supply to form the carbon film *in situ*. With an externally applied hydrocarbon source the pyrolysis is possible for many hours. Under these conditions final thicknesses of 50 μm are possible.

The change in the intensity ratio of peaks at 1600 cm^{-1} and 440 cm^{-1} as the beam focus moves towards the tip (Figure IV-1 (a) and (b)) increases, indicating that the carbon film thickness increases. This trend is expected as the concentration of the acetylene is highest near the orifice, decreasing with concentration (and distance) downstream from the tip. This would be expected for a reaction rate dependent on the concentration of acetylene.

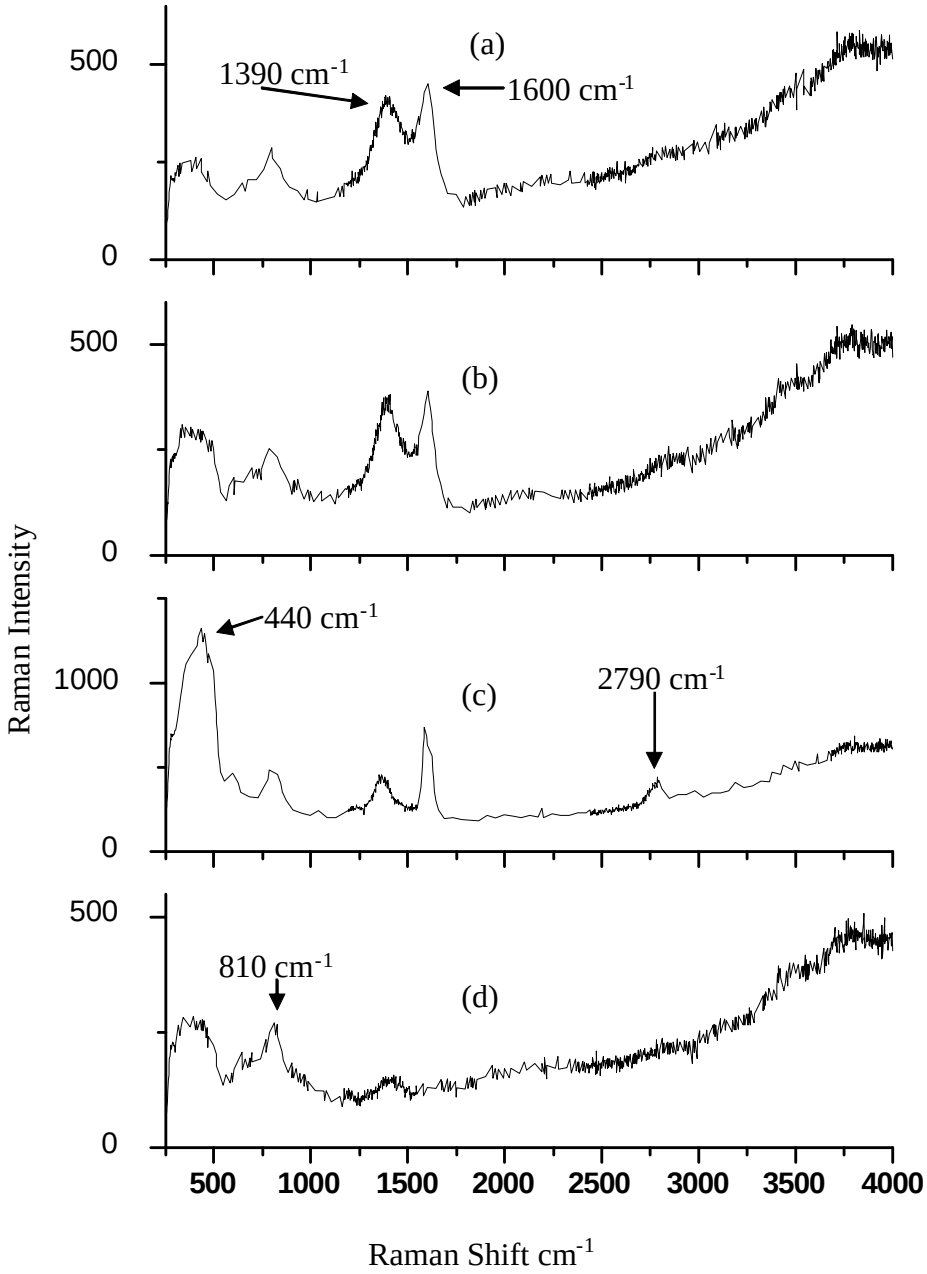

Figure IV-(iii)-i

Raman spectra of carbon film at (a) 30 μm, (b) 50 μm, (c) 1000 μm from the tip. Spectrum (d) is of the quartz capillary.
Laser beam wavelength 410 nm.

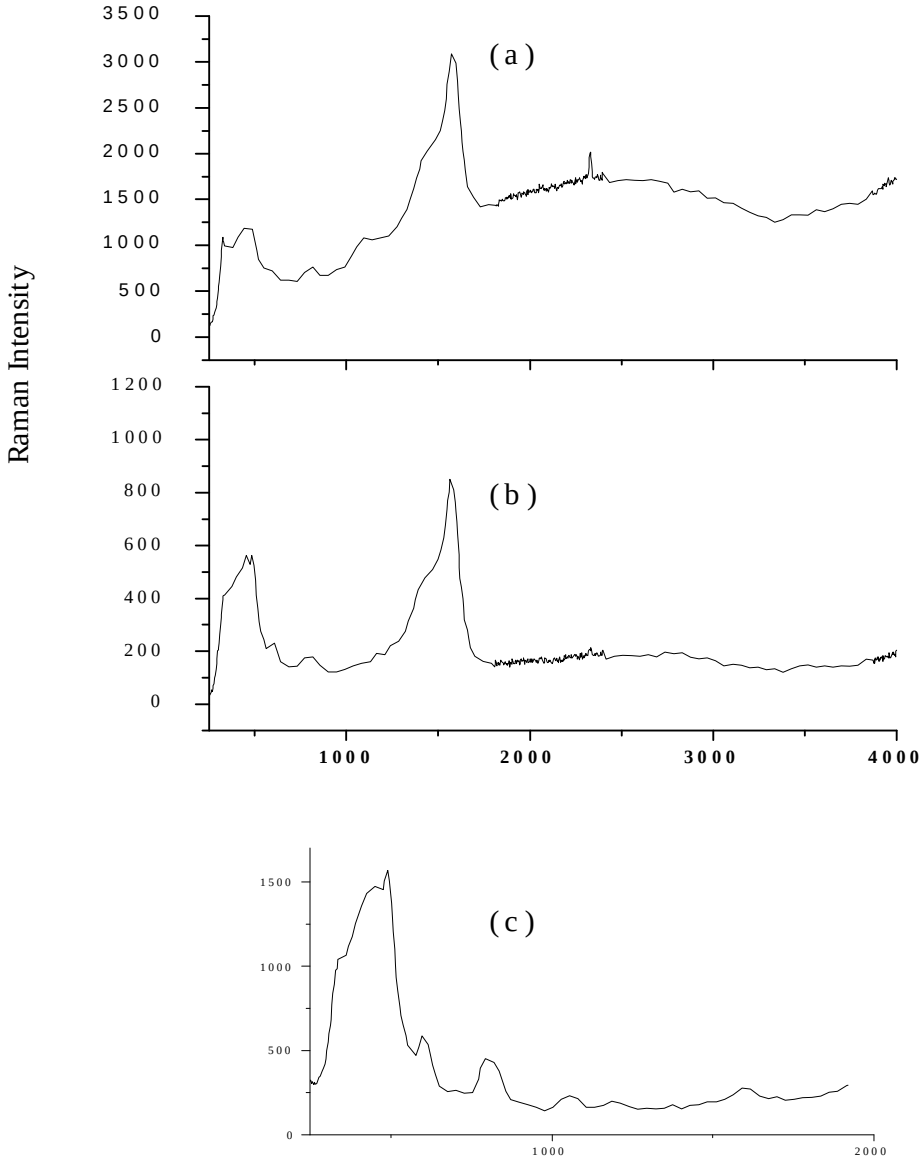

Figure IV-(iii)-ii

Raman spectra of carbon film at (a) 30 μm, (b) 50 μm, and (c) quartz capillary.
Laser beam wavelength 325 nm.

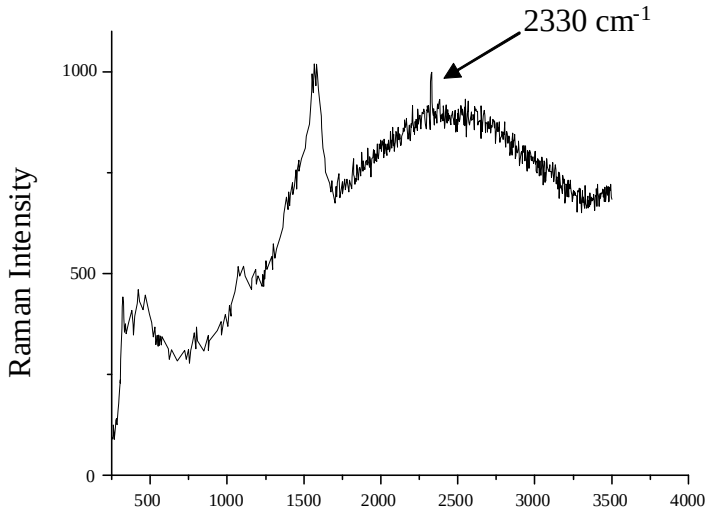

Figure IV-(iii)-iii

Raman spectra of carbon film near tip of electrode.
Laser beam wavelength 325 nm.

As well as the change in 1600 cm^{-1} to 440 cm^{-1} peak ratio the back background signal peaking at 2500 cm^{-1} also increases. This feature is more pronounced in Figure IV-(iii)-iii and was present in eighteen out of twenty three samples examined by Raman spectroscopy. This back ground signal, emitted from carbon formed by chemical vapour deposition, is attributed to luminescence.[9] Unfortunately the origin of the luminescence was not stated. Numerous other published studies of carbon surfaces analysed by Raman spectroscopy do not contain this signal.[10 3;5] By varying the deposition parameters of formation of a radio frequency magnetron spluttered carbon film it was found that luminescence increased with structural disorder.[11]

As only carbon and hydrogen are present, luminescence may arise from aromatic or conjugated alkene or alkyne groups. A literature search did not locate any luminescence arising from such conjugated structures. Therefore the disorder may arise due to the presence of pendent polycyclic aromatic compounds as they are known to exhibit luminescence.[12] Published papers, when discussing composition or chemical structure of carbon surfaces do not appear to consider pendent groups of carbon films formed *in situ*. As the carbon films,

produced by pyrolysis of acetylene and chemical vapour deposition and which possess luminescence, are formed *in situ,* the formation of polycyclic aromatic pendent groups is probable. The probability of this structure is enhanced by the presence of fused sixfold rings clusters *in* a amorphous carbon.[13] Instead of the fused sixfold rings being incorporated into the carbon film surface during graphene formation they could remain as pendent groups.

During the pyrolysis of acetylene a high initial concentration exists which could promote the formation of pendent chains as shown in Figure IV-(iii)-iv. These structures are consistent with the proposed graphite formation from pyrolysis via the polyyne pathway. (Chapter III Introduction)

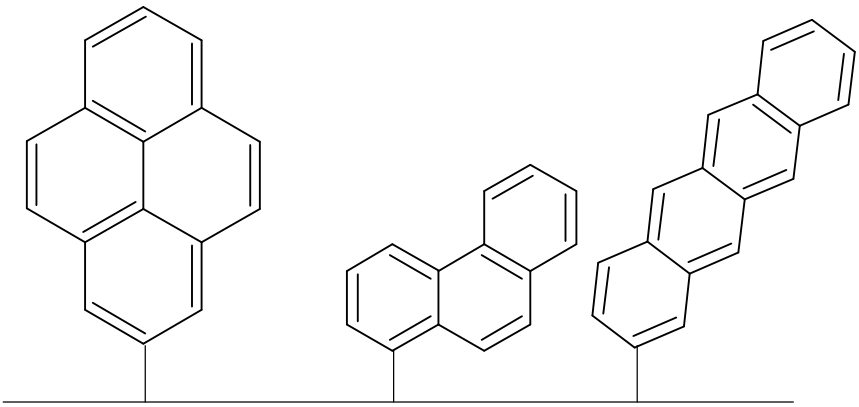

Figure IV-(iii)-iv

Schematic of possible aromatic pendent group configurations on the surface of the carbon film.

Variations in luminescence intensity, at 2500 cm^{-1}, are attributed to decarbonisation of the surface during pyrolysis. (Decarbonisation will allow removal of the more labile groups, such as pendent groups, thereby allowing organised layering of graphite crystal growth.) In Figures IV-(iii)-i, (a), (b), (c) two very strong peaks are present, 1390 and 1600 cm^{-1}. The shape and position of these peaks, obtained by Raman scattering, have been the subject of many publications. The 1390 cm^{-1} peak is referred to as the "D", disordered peak and the 1600 cm^{-1} peak, "G", for graphite.[14] The position of the "G" close to 1600 cm^{-1} indicates the presence of microcrystalline sp^2 carbon – graphite, but not necessarily six member rings.[13]

The "D" peak is forbidden in perfect graphite and reflects the degree of disorder present and is directly related to six member aromatic rings.[7] The disordering of graphene, manifested by the "D" peak, has also been attributed to the presence of sp^3 carbon.[13]

In Figure IV-(iii)-ii (a) and (b) the strong peak at 1390 cm^{-1} in Figure IV-(iii)-i (a), (b) and (c) is replaced with a shoulder at 1440 cm^{-1}. This change is directly related to the frequency of the laser for amorphous carbon. The lower energy beams provide distinct peaks, which degenerate to shoulders as the laser frequency is increased. The origin of this phenomenon was not known. Increases in intensity of the "D" are attributed to a reduction in the size of aromatic clusters. [13] The frequency and shape of the "G" and "D" peak are consistent with Raman scattering of amorphous carbon films.

In Figure IV-(iii)-i the peak at 2790 cm^{-1} has been assigned to sp^3 C-H vibrations.[15] The sample area for this peak was approximately 1000 μm from the tip and was detected optically. The region consisted of a series small isolated black spots clustered together. As the carbon film was formed using the counter flow technique these spots may have originated from hydrogenation of carbon during the initial stages of graphene formation at active sites. The presence of tetrahedral sp^3 carbon (diamondlike) in an amorphous carbon film is evident by a broad absorption band centred at 1100 cm^{-1} in the Raman scattering spectrum of polycrystalline diamond films, using a 244 nm laser.[5] The absorption at 1100 cm^{-1} for 80 % sp^3 content is approximately 50 % of the intensity of the "G" peak, while at 100 % sp^2 the peak, for an evaporated amorphous carbon film is absent. The absence of this peak in Figures IV-(iii)-i, IV-(iii)-ii and IV-(iii)-iii indicates the sp^3 content, if any is extremely small. In this reference the 100% sp^2 Raman scattering spectrum, of an evaporated amorphous carbon film using a 514nm laser contained a luminescence background. At 50 % sp^2 this signal was absent. It was also absent from spectra, using a 244 nm laser, at all sp^3 concentrations. Once again the presence of the luminescence was noted, but not the origin.

The existence of edge planes, an important feature of carbon electrodes are visible in Raman scattering at 1355 cm^{-1} and 1620 cm^{-1}.[4] The intensity of the 1355 cm^{-1} peak is similar to that of the 1600 cm^{-1} peak in polished and fractured glassy carbon.[3] The absence of these peaks infers that the carbon film has not fractured during fabrication, as any edge formed during pyrolysis will react rapidly with hydrogen radicals present.

The peak present at 2330 cm^{-1} in Figure IV-(iii)-iii and Figure IV-(iii)-ii(a) has been assigned to molecular nitrogen [16] during the characterisation of carbon surfaces.[1] The narrow peak width suggests gaseous compound. However the Raman scattering spectra obtained in this work were carried out in air. During instrumentation set up the spectra due to atmospheric gases are stored as the baseline spectrum and subtracted from each spectrum. If slight variations in path length occur due to positioning of the electrode in the beam both positive and negative peaks would be obtained. This was not the case, only positive peaks occurred. Therefore a positive assignment of this peak is not possible.

Conclusion

As Raman scattering penetrates the carbon film and the quartz substrate the Raman active groups detected are all those present in this layer. That is, they may or may not be present in the surface electrochemically active layer.

The Raman scattering does provide evidence that the carbon film layer is only several hundred carbon atoms thick and the graphene component occurs in clusters. The relative intensity of peaks in the Raman scattering spectra of the carbon film is very similar to that of an amorphous carbon film, containing predominately sp^2 carbons, formed *in situ*.

The back ground luminescence indicates the presence of a chromophore. It is proposed that luminescence originates from pendent aromatic structures on the surface, arising from branch chain formation, during the formation of the graphene.

References

1. McCreery R.L. *Electroanalytical Chemistry*, Bard A.J., Ed.; Dekker: 1991.
2. Ray K. ; McCreery R.L. *Journal of Electroanalytical Chemistry* **1999,** *469*, 150-58.
3. Ray K. ; McCreery R.L. *Analytical Chemistry* **1997,** *69*, 4680-87.
4. Katagiri G.; Ishida H.; Ishitani A. *Carbon* **1988,** *26*, 565-71.
5. Gilkes K.W.R.; Sands H.S.; Batchelder D.N.; Robertson J.; Milne W.I. *Applied Physics Letters* **1997,** *70*, 1980-82.
6. Dresselhaus M.S.; Dresselhaus G.; Pimenta M.A.; Eklund P.C. *Analytical Applications of Raman.* , Pelletier M.J.; Kaiser Optical Systems/Arbor A., Eds.; 1999.
7. Ferrari A.C. and Robertson J. *Physical Reviews* **2000**, *61*, 14096-14107.
8. Liu Y. and McCreery R.L. 95; *Journal of the American Society*, **1996**, *117*, 11254-11259.
9. Nemanich R.J.; Glass J.T.; Lucovsky G.; Shroder R.E. *Journal of Vacuum Science & Technology, A: Vacuum, Surfaces, and Films* **1988,** *6*, 1783-87.
10. Escribano R., Sloan J.J., Siddique N., Sze N., and Dudev T. *Vibrational Spectroscopy*, **2001**, *26*, 179-186.
11. Papadimitriou D.; Roupakas G.; Xue C.; Topalidou A.; Panayiotatos Y.; Dimitriadis C.A. *Thin Solid Films* **2002,** *414*, 18-24.
12. Roch T. *Analytica Chimica Acta* **1997,** *356*, 61-74.
13. Wagner J.; Ramsteiner M.; Wild Ch.; Koidl P. *Physical Review B* **1989,** *40*, 1817-23.
14. Schwan J.; Ulrich S.; Battori V.; Ehrhardt H. *Journal of Applied Physics* **1996,** *80*, 440-46.
15. Chen J.Q.; Freitas Jr. J.A.; Meeker D.L. *Diamond and Related Materials.* **2000,** *9*, 48-55.
16. Bendtsen J. *Journal of Raman Spectroscopy* ,**1974**, *2*, 133-45.

Chapter IV-(iv)

Capacitance

Abstract

Using cyclic voltammetry in 1 M KCl the double layer capacitance of the carbon film surface was found to have an average of 6.7μF cm^{-2}, with a range of 1 to 20 μF cm^{-2}. This range in capacitance implies a chemical surface structure varying between HOPG and hydrogenated glassy carbon.

Introduction

Capacitance is an important characteristic of an electrode, particularly double layer capacitance, for microelectrodes used *in vivo*. When carrying out *in vivo* experiments the Faradaic current has electrical noise (unwanted signal) imposed onto it. The electrical noise may originate from the equipment (AC hum, amplifier-Johnson noise) or electromagnetic radiation (PC monitors). The microelectrode acting as a receiving antenna adds this signal to that of the Faraday current. This electrical noise is related to capacitance.[1;2] The relationship is shown in equation (i), where i is the current generated by the voltage change E (noise signal), over time period t, R_s is the solution resistance and C_{dl} is the double layer capacitance.[3]

$$i = \frac{E}{R} e^{\frac{-t}{R_s C_{dl}}} \qquad \text{(i)}$$

The noise is greatly reduced by carrying out the experiments in a Faraday cage and using noise reducing data acquisition systems, such as signal averaging[4] and 200 Hz filters.[1] When transient *in vivo* events are being monitored the use of instrumental techniques, which either reduce the acquisition rate or filter the signal, can result in loss of signal definition.

Further reduction in noise to signal ratio can be achieved via lower electrode surface capacitance. Carbon fibres have capacitances ranging from 5-20 μF cm^{-2} [5] which is a mixture of highly orientated pyrolytic graphite (2-6 μF cm^{-2})[6;7] and edge planes (60 μF cm^{-2}) [6]. Other carbon surfaces such as hydrogenated glassy carbon are 12-20 μF cm^{-2} [8;9] carbon films- 7-20 μF cm^{-2} [10;11], boron doped diamond - 4.5 μF cm^{-2} [12] and 15-18 μF cm^{-2} for diamond coated glassy carbon.[13]. Therefore to reduce the noise originating from double layer capacitance microelectrodes with a capacitance lower than carbon fibre would be required. This suggests highly orientated pyrolytic graphite or a boron doped diamond would provide such a surface. However dopamine does not show any heterogeneous electron transfer characteristics at a highly orientated pyrolytic graphite surface.[14] Further more the electron transfer at a boron doped diamond surface is poor and variable.[15;16] The variability may be dependent on boron content.[17] The carbon film microelectrodes fabricated by the methods outlined in this work do have excellent heterogeneous electron transfer characteristics for dopamine (Chapter IV-(x)) and have low capacitance.

The large range of available capacitance values is dependent on surface chemistry, such as carbenes at edge planes.[18] It also provides an indication of the suitability for *in vivo* applications and assists in the determination of possible surface structures of the carbon film.

Experimental Section

Chemicals

Milli-Q water, potassium chloride(BDH Analar) and nitrogen (Instrument Grade) were used as received.

Equipment

The three electrode system, using an Ag|AgCl (3 M KCl) reference electrode, as outlined in Chapter II Electrochemical Equipment, was used.

Electrode Fabrication

Electrodes were fabricated as outlined in Chapter III using 40ml min^{-1} nitrogen in the parallel flow and counter flow configurations.

Procedure

Cyclic voltammetry, cycling from -0.20 V to 0.6 V in a deoxygenated 1 M KCl at scan rate between 0.1 and 0.5 V s^{-1} was carried out. The carbon film double layer capacitance is calculated using Equation (ii) this chapter, with Δi being the difference in current between the forward and reverse scan at 0.4 V.

Results and Discussion

The calculation of double layer capacitance of the microelectrodes surface was carried out using equation (ii). The selection of this equation was discussed previously in Chapter I Capacitance.

$$C_{dl} = \frac{\Delta i}{2 A \nu} \qquad \text{(ii)}$$

From equation (ii) the double layer capacitance is inversely dependent on scan rate. This effect of scan rate on Δi can be seen in Figure IV-(iv)-i.

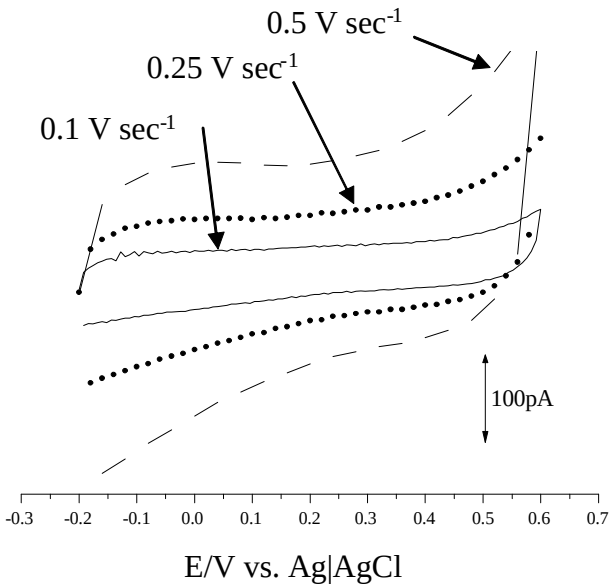

Figure IV-(iv)-i

Cyclic voltammetry of a microelectrode at various scan rates in deoxygenated 1 M KCl.

Calculating the capacitance from the cyclic voltammetric scans in Figure IV-(iv)-i gave the results shown in Figure IV-(iv)-ii. These capacitance measurements are similar to those reported for HOPG[8] except for the minium at 0.3 V. HOPG capacitance was reported to be 6 μF cm^{-2} at -0.5 V, rising slowly to 9 μF cm^{-2} at 500mV. GC and hydrogenated GC had capacitances of 30 μF cm^{-2} and 16 μF cm^{-2} respectively at -0.5 V rising to maximum of 120 % of this value at 0.15 V, then returning to the original values at 1 V.[8] Untreated and vacuum heated carbon fibres showed very little change in capacitance, 5-6 μF cm^{-2} over a similar range -0.4 V to 0.5V.[5] It therefore appears that the carbon film microelectrodes have similar characteristics to carbon fibre across a range of voltages.

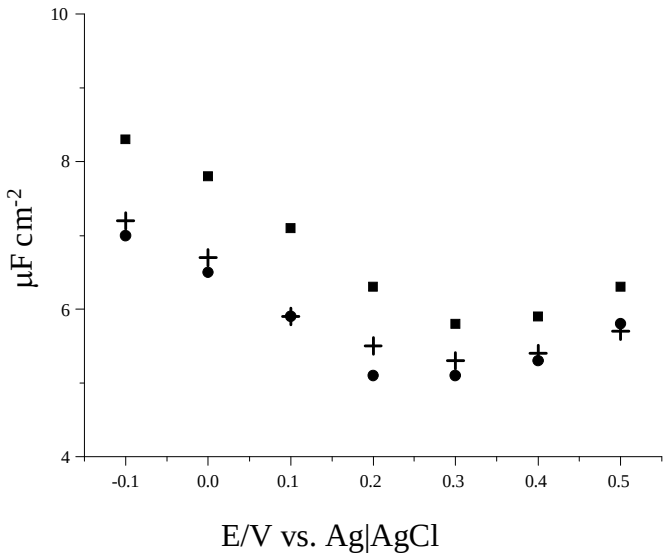

Figure IV-(iv)-ii

Double layer capacitance of a carbon film microelectrode vs. Ag|AgCl reference electrode at different scan rates. 0.5 V s^{-1} (■), 0.25 V sec^{-1} (+) and 0.1 V sec^{-1}(●)

In vivo applications involve chronocoulometric experiments, with a carbon fibre microelectrode held at a fixed potential of 0.9 V (Chapter VI Introduction). It is proposed, using carbon film microelectrodes, the fixed potential can be reduce the fixed potential to 0.4 V. (The proposed use of this lower potential is explained in Chapter VI Introduction.). Therefore when calculating the double layer capacitance of a range (n=69) of carbon film microelectrodes electrodes Δi was measured at 0.4 V with a scan rate of 0.1 V s^{-1}. The average of this sample was 6.7 μF cm^{-2}. The distribution frequency for these carbon film microelectrodes is shown in Figure IV-(iv)-iii.

From Figure IV-(iv)-iii the capacitance is evenly distributed between 1 and 11 μF cm^{-2}. Considering the possible inaccuracies in calculating the area, from Cottrell decay curves, (Chapter III Results and Discussion) the average capacitance would range from 1 to 20 μF cm^{-2}.

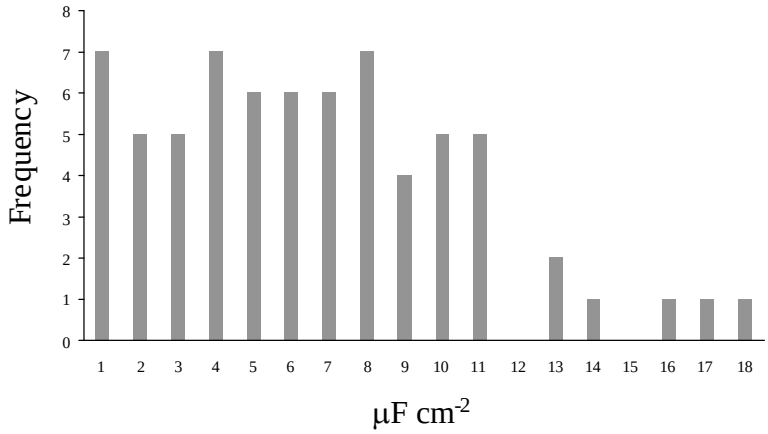

Figure IV-(v)-iii

Distribution of double layer capacitance measurements of carbon film microelectrodes

Conclusion

The possible range and even distribution in capacitance between 1 and 20 μF cm^{-2} implies a variation in surface structure between that of HOPG and hydrogenated GC. The values of 1-3 μF cm^{-2} suggest the surface here is almost a defect free graphite plane. The higher values 4-20 μF cm^{-2} suggest chemical surface structures more similar to hydrogenated GC.

The electrodes displaying mid range double layer capacitance could have surfaces which are a composite of both structures. This is suggested by the surface morphology revealed in the Figure III-v.

The low values of double layer capacitance of the carbon film indicate an absence of graphite edge planes. If present, they are a very small component of the surface structure.

References

1. Cahill P.S.; Walker Q.D.; Finnegan J.M.; Mickelson G.E.; Travis E.R.; Wightman R.M. *Analytical Chemistry* **1996,** *68*, 3180-86.

2. Venton B.J.; Wightman R.M. *Analyical Chemistry* **2003,** *1st Oct*, 414A-21A.

3. Bard A.J.; Faulkner L.R. *Electrochemical Methods. Fundamentals and Applications,* ed.; John Wiley & Sons: USA, 1980.

4. Wiedeman D.J.; Kawagoe K.T.; Kennedy R.T.; Ciolkowski E.L.; Wightman R.M. *Analyical Chemistry* **1991,** *63*, 2965-70.

5. Swain G.M.; Kuwana T. *Analytical Chemistry* **1991,** *63*, 517-19.

6. Rice R.J.; McCreery R.L. *Analytical Chemistry* **1989,** *61*, 1637-41.

7. McDermott M.T.; Kneten K.; McCreery R.L. *Journal of Physical Chemistry* **1992,** *96*, 3124-30.

8. Xu J.; Chen Q.; Swain G.M. *Analytical Chemistry* **1998,** *70*, 3146-54.

9. Chen Q.; Swain G.M. *Langmuir* **1998,** *14*, 7017-26.

10. Eriksson A.; Norekrans A.; Carlsson J. *Journal of Electroanalytical Chemistry* **1992,** *324*, 291-305.

11. Beilby A.l.; Carlsson A. *Journal of Electroanalytical Chemistry* **1988,** *248*, 283-304.

12. Swain G.M.; Ramesham R. *Analytical Chemistry* **1993,** *65*, 345-51.

13. DeClements R.; Swain G.M.; Dallas T.; Holtz M.W.; Herrick R.D.; Stickney J.L *Langmuir* **1996,** *12*, 6578-86.

14. Wightman R.M.; Palk E.C.; Borman S.; Dayton M.A. *Analytical Chemistry.* **1978,** *50*, 1410-14.

15. Alehashem S.; Chambers F.; Strojek J.W.; Swain G.M. *Analytical Chemistry* **1995,** *67*, 2812-21.

16. Strojek J.W.; Granger M.C.; Swain G.M. *Analyical Chemistry* **1996,** *68*, 2031-37.

17. Levy-Clement C.; Zenia F.; Ndao N.A.; Deneuville A. *New Diamond and Frontier Carbon Technology.* **1999,** *9*, 189-206.

18. Ravovic L.R. ; Bockrath B. *Journal of the American Chemical Society* **2005,** *127*, 5917-27.

Chapter IV-(v)

Edge Plane Concentration

Abstract

Using 9,10-anthraquinone-2,6-disulfonic acid disodium salt in perchloric acid the average edge plane concentration of the carbon film microelectrodes has been found to be less than 14 pmol cm^{-2}. At this low concentration the inferred surface structure is similar to that of a defect free HOPG, boron doped diamond or hydrogenated glassy carbon.

Introduction

The cyclic voltammetry of quinones has been used to quantify edge planes on the surface of carbon electrodes.[1] The edge plane density provides an indication of the chemical nature of the surface of an electrode. The quinones used in these studies were 9,10-anthraquinone-2,6-disulfonic acid disodium salt (AQDS) and 9,10-phenanthrenequinone (PQ).[2] The quinone surface interaction has also been investigated using scanning tunnelling microscopy[2] and an electrochemical/scanning force microscope.[3] From these studies using AQDS, the molecule was found to lie parallel to the HOPG defect free surface, whereas at defects and the adjacent stressed region the AQDS was physisorbed. It is in the physisorbed state that the redox reaction occurs. The physisorbed AQDS, when scanned by cyclic voltammetrically, produces a well defined peak with all the characteristics of a chemically attached molecule. [1;2] The electrode reaction is a two electron reduction as shown in Figure IV-(v)-i.

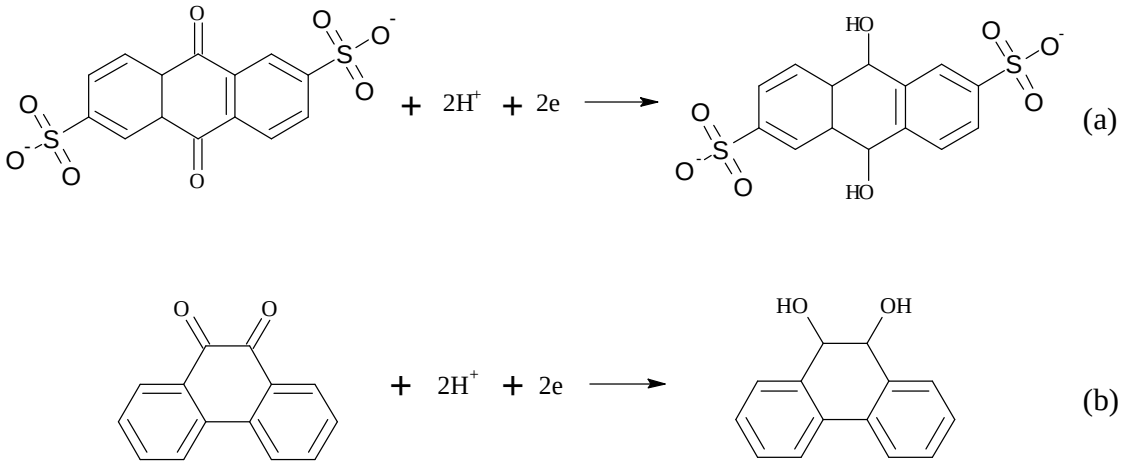

Figure IV-(v)-i

Structure and electrode reactions for (a) AQDS and (b) PQ

The preferential adsorption of PQ at an edge plane is of particular interest being the reverse reaction of the analytes of interest in this work, i.e. dopamine and ascorbic acid. The edge plane, obtained by fracturing a GC electrode, provides a lower ΔE_p for the oxidation of dopamine. The reversibility of the dione to diol reaction, at edge planes on a carbon surface, can be seen in the cyclic voltammogram of AQDS; I_p^{ox} is the same as I_p^{red} in a 10^{-5} M AQDS solution in 0.1 M $HClO_4$.[4]

The use of quinones to measure edge plane concentration, not only provides quantification of edge planes it also assists in determining possible surface electron pathways in the oxidation of dopamine and ascorbic acid at the carbon film surface.

The physisorption of the quinones follows a Langmuir isotherm, requiring only 10^{-6} M in 0.1 M $HClO_4$ to obtain full surface coverage. Under these conditions the electron transfer reaction for the solution has a low Faradaic current.[2] The absorption and electrochemical studies can therefore be carried out *in situ*.

Experimental Section

Chemicals

Milli-Q water, perchloric acid (BDH Analar), 9,10-anthraquinone-2,6-sulfonic acid disodium salt (Sigma Aldrich) and nitrogen (BOC Instrument Grade) were used as received.

Equipment

A three electrode system, using a Ag|AgCl (3 M KCl) reference electrode, was used as outlined in Chapter II Electrochemical Equipment.

Electrodes Fabrication

They were fabricated as outlined in Chapter III using 40 ml min^{-1} nitrogen in the parallel flow and counter flow configurations.

Procedure

Cyclic voltammetry was carried out cycling from 0.8 V to -0.6 V, in a deoxygenated 10^{-4} M AQDS with 0.1 M $HClO_4$ as the supporting electrolyte

Results and Discussion

In this work a solution concentration of 10^{-4} M AQDS was used. The higher concentration and wide window scanned was chosen to ensure all electrodes were "functioning" i.e. the cyclic voltammogram displayed a distinct change in reduction or oxidation current.

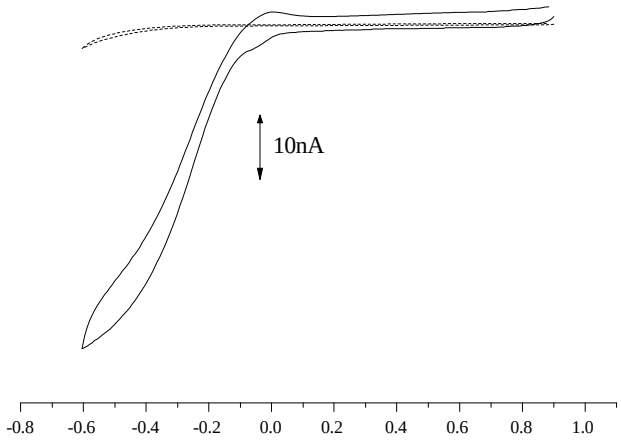

Figure IV-(v)-ii

Cyclic voltammograms of 10^{-4} M AQDS with 0.1 M $HClO_4$ as the supporting electrolyte (—) and 0.1 M $HClO_4$ (---) at a carbon film microelectrode.
Scan rate 0.1V sec^{-1}

The cyclic voltammogram of a carbon film microelectrode, in 10^{-4} M AQDS with 0.1 M $HClO_4$ as the supporting electrolyte, (length 200 μm and radius 16 μm) is depicted in Figure IV-(v)-ii. This does not display any peaks associated with an absorbed species[5] at -0.1 V.[2;6] This cyclic voltammogram is typical of the carbon film microelectrodes examined. The cyclic voltammogram shown in Figure IV-(v)-ii is visually similar to that reported for boron doped diamond and hydrogenated GC[1]. The published voltammograms of boron doped diamond and hydrogenated GC do not display a surface confined redox species. They do however display a slight redox reaction under diffusion control. The difference being that both boron doped diamond and hydrogenated GC disc electrodes display small well separated

peaks in the published voltammograms. The boron doped diamond peaks are at 0 V and -0.3 V and hydrogenated GC, 0 V and -0.1 V. Whereas, the carbon film microelectrodes has only a small shoulder at 0 V which is depicted in the cyclic voltammogram Figure IV-(v)-ii and iii. This may have the same origin as those peaks generated at the hydrogenated GC and boron doped diamond surface, i.e. a weak Faradaic oxidation and reduction peak.

Further evidence suggesting the shoulder in Figure IV-(v)-ii, is not due to adsorbed AQDS, is the width of the peak. In the published literature both the reduction and absorption

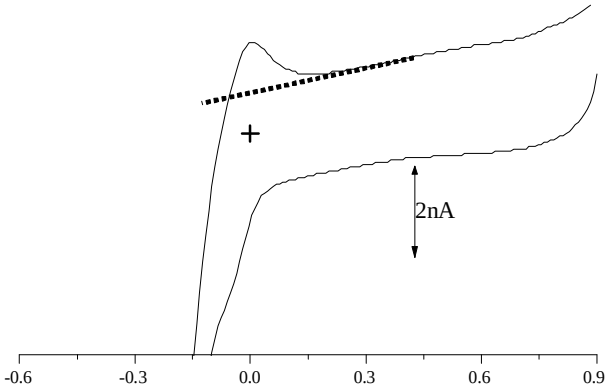

Figure IV-(v)-iii

Expanded Figure IV-(v)-i cyclic voltammogram with dotted line indicating charge integration boundaries.

peaks are approximately 0.1 V wide. In this work the anodic peaks are -0.1 V (Figure IV-(v)-iii) to 0.1 V. This wide peak is not indicative of an adsorbed species. (Figure IV-(vii)-i displays a typical adsorption peak.)

To determine if the small shoulder in Figure IV-(v)-ii is of significance (i.e. assuming it has originated from edge planes) the number of coulombs in the reduction peak was calculated. The integrated area, between the dotted line and cyclic voltammetric curve is shown in Figure IV-(v)-iii. This area is equivalent to 25 pmol/cm^2 AQDS.

From the published literature (Table IV-(v)-i) the low values obtained in this work suggests that the carbon film on the microelectrodes has a surface structure almost devoid of edge planes. The surface therefore appears to be similar to HOPG, boron doped diamond and hydrogenated GC. If the "peak" in Figure IV-(v)-iii is not due to the weak electron transfer reduction reaction of AQDS then the surface is devoid of edge planes.

Table IV-(v)-i Edge plane concentration coverage summary

Surface	AQDS Coverage (pmol cm^{-2})	Reference
GC	392±8 (Polished)	6
	166±8 (Polished)	3
	214±41 (Fractured)	3
	530±50 (Fractured)	2
Hydrogenated GC	31±5	6
HOPG	99±31	6
	45±13	2
Boron Doped Diamond	23±10	6
Carbon Film	Average 14 (n=10) Range 0.4 - 63	This work

Conclusion

Quantification of the edge plane density of the carbon film on the microelectrodes fabricated in this work suggests the surface contains very few, if any, edge planes. The electrochemistry of AQDS at a carbon film surface would therefore appear to have the similar properties to HOPG, boron doped diamond or hydrogenated glassy carbon.

References

1. Xu J.; Chen Q.; Swain G.M. *Analytical Chemistry* **1998,** *70*, 3146-54.

2. McDermott M.T.; McCreery R.L. *Langmuir* **1994,** *10*, 4307-14.

3. Ta T.C.; Kanda V.; McDermott M.T. *Journal of Physical Chemistry B* **1999,** *103*, 1295-302.

4. Rice R.J.; Pontikos N.M.; McCreery R.L. *Journal of the American Chemical Society* **1990,** *112*, 4617-22.

5. Brown A.P.; Anson F.C. *Analytical Chemistry* **1977,** *49*, 1589-95.

6. Tunon-Blanco P.; Costa-Garcia A. *The Royal Society of Chemistry(Reviews on Analytical Chemistry-Euroanalysis VIII)* **1994,** 273-90.

Chapter IV-(vi)

Potential Window

Abstract

The potential window, in 0.1 M sulfuric acid, of carbon film microelectrodes has been determined using cyclic voltammetry. It was found to range between -0.25 to 1.25 V and -0.75 to 1.25 V versus Ag|AgCl (3 M KCl) reference electrode. This wide range suggests the carbon film surface is similar to either HOPG or hydrogenated G.C.

Introduction

The first criterion to be considered when carrying out an electrochemical reaction is the potential window of the electrode, solvent and supporting electrolyte. The potential window is the electrochemical potential range which is devoid of any Faradaic currents that interfere with Faradaic currents being studied. For large disc electrodes this has been defined as the potentials when anodic and cathodic currents reach 1 μA.[1] For aqueous systems the cathodic limit is evolution of hydrogen and the anodic limit, oxygen evolution. For metals and carbon the potential window is dependent on solution pH, following the Nernst equation.[1] The potential window for carbon is also dependent on the nature of the carbon surface-crystallinity, condition and method of preparation.[2] With this reported variability cyclic voltammetry in 0.1 M sulfuric acid solution was used to assist in the characterisation of the surface of the carbon film microelectrodes.

\

Experimental Section

Chemicals

Milli-Q water, nitrogen (Instrument Grade) and sulfuric acid (BDH Analar) was used as received.

Equipment

The three electrode system, using Ag|AgCl (3 M KCl) reference electrode, was used as outlined in Chapter II Electrochemical Equipment.

Electrode Fabrication

The carbon film microelectrode were fabricated as outlined in Chapter III, using 40ml min^{-1} nitrogen in the parallel flow and counter flow configurations.

Procedure

The carbon film microelectrodes were cycled from 1.6 to -1 V in deoxygenated 0.1 M H_2SO_4.

Results and Discussion

In Figures IV-(vi)-i and IV-(vi)-ii are the extreme results (n=10) of cyclic voltammograms of carbon film microelectrodes in 0.1 M sulfuric acid. The anodic oxidation, oxygen evolution, starts ranges from 1.3 V to 1.5 V.The cathodic reduction of sulfuric acid, hydrogen evolution, varies from -0.4 V to -1 V. The carbon film microelectrode in Figure IV-(vi)-i had a double layer capacitance of 4.4 $\mu F\ cm^{-2}$, whereas the double layer capacitance of the carbon film microelectrode in Figure IV-(vi)-ii was 0.3 $\mu F\ cm^{-2}$.

The low double layer capacitance of both carbon film microelectrodes suggests a surface similar to that of HOPG. However the published anodic potential windows, in sulfuric acid, suggest a structure similar to HOPG (1.7 V) or hydrogenated GC (1.4 V).[3,4]The potential window of unmodified GC (1.2 V) is smaller than that obtained from the carbon film microelectrodes.[5]

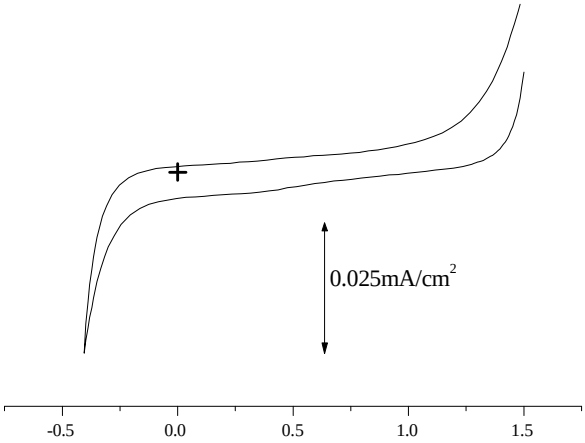

E/V vs. Ag|AgCl

Figure IV-(vi)-i

Cyclic voltammetry of a carbon film microelectrode
(C_{dl} 4.4 μF/cm^2) in 0.1 M H_2SO_4
Scan rate 100 mV/sec

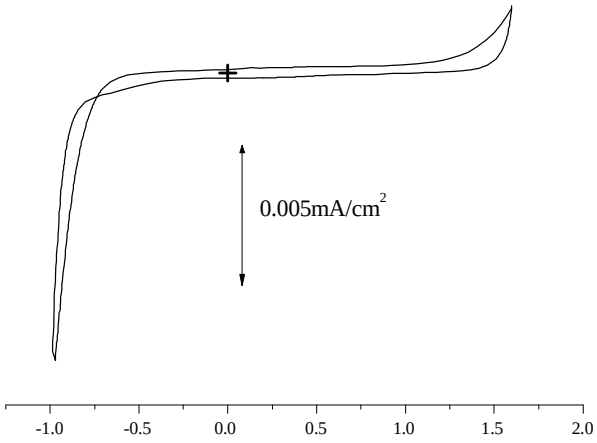

E/V vs.Ag|AgCl

Figure IV-(vi)-ii

Cyclic voltammetry of a carbon film microelectrode
(C_{dl} 0.3 μF/cm^2) in 0.1 M H_2SO_4
Scan rate 100 mV/sec

Conclusion

From cyclic voltammetry of carbon film microelectrodes in 0.1 M sulfuric acid the surface appears to be similar to that of HOPG and hydrogenated GC. From the limited number of carbon film microelectrodes used it appears the lower the capacitance the greater the potential window. It also suggests variability in the carbon film surface (See Chapter IV-(x)) with respect to electrochemistry at the surface.

References

1. Adams R.N. *Electrochemistry at Solid Electrodes,* ed.; Marcel Dekker: USA, 1973.
2. Kissinger P.T. *Carbon Electrodes*, McCreery R.L.; Cline K.K., Eds.; 2nd ed.; Marcel Dekker: USA, 1996.
3. Hathcock K.W. ; Brumfield J.C.; Goss C.A.; Irene E.A.; Murray R.W. *Analytical Chemistry* **1995,** *67*, 2201-06.
4. Chen Q.; Swain G.M. *Langmuir* **1998,** *14*, 7017-26.
5. Noel M.; Anantharaman P.N. *Surface & Coatings Technology* **1986,** *28*, 161-79.

Chapter IV-(vii)

Surface Concentration of Alkenes and Alkynes

Abstract

The concentration of alkenes and alkynes, on the surface of the carbon film, has been determined by electrochemical oxidation of Ag^{+}, Hg^{2+}, Fe^{2+}, and Ni^{2+} π-complexation bonds. The carbon film surface appears to contain predominately alkynes with a surface concentration range of $2x10^{-10}$-$5x10^{-11}$ moles cm^{-2}. The presence of these unsaturated aliphatic groups is evidence that pendent groups are present on the carbon film surface.

Using the carbon film microelectrode as a substrate it proved possible to carry out voltammetric stripping of cations to sub parts per billion levels in distilled water. This feature suggests the possible use of microelectrodes in the biological field to quantify π complexing cations.

Introduction

The proposed polyyne polymerisation pathway to the formation of carbon results in terminal alkyne groups, in particular acetylide.[1] As the formation of the carbon film, during the *in situ* pyrolysis of acetylene is occurring in a hydrogen radical rich environment, hydrogenation of the acetylide group is possible. The hydrogenation may only be thermodynamically favourable during cooling, as dehydrogenation is the preferred reaction path at higher temperatures.

Metal cations, containing *d* orbital electrons, are known to form π complexes with alkenes and alkynes.[2] The strength of these π complex bonds is such that quantitative analysis of π complexes of ethyl mercuric compounds in solution has been made by electrochemical reduction.[3] Similarly, aliphatic unsaturation in divinylbenzene styrene has been determined

using the reduction of the mercuric π complex.[4] It is therefore expected π complexes formed on the carbon film surface can undergo electrochemical redox reactions.

In this thesis work it is proposed to determine the concentration of alkenes and alkynes on the carbon film surface by immersion of the carbon film microelectrode in a solution containing the complexing cation, rinse the electrode, and then to coulometrically determine the complexed cation. Following this protocol only π-complexed cations will be present on the surface of the carbon film microelectrode, which can then be voltammetrically stripped. In considering the electrochemical methodology to determine the surface concentration of cation π complex adsorbed on the surface the following factors were considered: a single or multiple electron transfer reaction, reductive or oxidative stripping, counter anion for the π complex cation, and possible exchange of the selected cation with impurity cations from the complexing solution, rinsing solution or supporting electrolyte.

To determine the accessible aliphatic unsaturated groups present on the surface the following cations were used: Ag^{+}, Hg^{2+}, Ni^{+} and Fe^{2+}. Mercury and silver π complexes have been well reported and therefore were used initially in this work to establish the feasibility of electrochemically measuring alkene and alkyne concentration on the surface.[5;6]
Nickel cations were reported to form a weak reversible π complex only with alkyne groups.[7] Although this referenced work was carried out with nickel sulfate supported on aluminium oxide, it was considered a possible simple electrochemical means of differentiating the alkyne and alkene concentration on the carbon film surface.

Ferrous ion was included as it not only provides a surface concentration of alkenes and alkynes but also it gives a direct correlation with the carboxylic acid groups formed to provide a selective surface using ferrous sulfate (Chapter V-(i)).
The surface concentration of the cation π complexes was determined coulometrically by voltammetric stripping similar to covalently bonded nitro groups.[8] In the determination of metal ions in solution, the recommended procedure is the reduction onto the substrate

followed by anodic stripping.[9] With the cation π complex only those that are accessible will be reduced[10] and the reduced cation will be deposited onto an accessible graphene region. Voltammetric anodic stripping can then used to coulometrically determine the amount of deposited cation.

With a microelectrode this has been carried out without a supporting electrolyte.[11] In this referenced work the reduction of the cation and subsequent oxidation was carried out in the analyte solution without additional electrolyte. This may be possible with the reduction and subsequent oxidation of the cation π complex. However the counter anions stabilising effect on the cation π complex has to be considered.

The counter anion is important in both the rinse and electrolysis solution. In this work both deionised water and common anion solution have been investigated. Also it was considered important to ensure that while the electrode is transferred from the complexing solution to electrolysis solution it remains "wet" thereby reducing possible reactions due to dehydration and subsequent rehydration.

Trace impurities, in the complexing solution, rinse solution or electrolysis solution may undergo an exchange reaction with the complexed cation. This possibility was reduced by minimising immersion times in all solutions and using low concentration of the cation solution (10^{-4} M). As the complex is adsorbed on the surface quiescence time is unnecessary and voltammetric scanning was commenced immediately

Experimental

Chemicals

Nickel chloride (BDH Analar), ferrous sulfate (BDH Analar), mercuric acetate (Aldrich), Milli-Q water, potassium chloride (BDH Analar), nitrogen (BOC Instrument grade), potassium chloride (BDH Analar) and silver nitrate (BDH Analar) were used as received.

Equipment

The three electrode system, as outlined in Chapter II Electrochemical Equipment, with an Ag|AgCl (3 M KCl) reference electrode was used.

Electrode Fabrication

Electrodes were fabricated as outlined in Chapter III using 40 ml min^{-1} nitrogen in the counter flow configuration.

Procedure

Electrodes were immersed for thirty seconds in 10^{-4} M cation solution, immediately rinsed in either deionised water or a 10^{-4} M common anion solution for twenty seconds. The electrodes were then immediately placed in the nitrogen deoxygenated deionised water, a common anion or $5x10^{-2}$ M KCl solution in the three electrode cell. Electrochemical reduction and oxidation scans are commenced immediately.

The integration of the cathodic and anodic peaks were obtained using eDAQ EChem v2.0.2 software.

Results and Discussion

The cyclic voltammetry of a microelectrode in a potassium nitrate solution (Figure IV-(vii)-i) after immersion in silver nitrate solution, then rinsing in potassium nitrate, provides an excellent example of the proposed cation π complex reactions occurring.

In the cyclic voltammogram, displayed in Figure IV-(vii)-i(a), the forward scan, from 0.6 V to 0 V, indicates a noisy reduction current below 0.15 V. On the return scan, 0 V to 0.6 V, this reduction current continues up to 0.15 V. Between 0.2 V and 0.35 V a strong oxidation current occurs, with the classic shape of a redox reaction occurring with a surface adsorbed species. If the cyclic voltammetry is repeated the area of the peaks slowly decreases. The amount of decrease in the anodic peak area compared to the previous anodic peak is approximately 0.2 with each subsequent scan. If continuous scanning is stopped after two scans, recommenced after four minutes the rate of decrease between consecutive scans drops to 0.3 of the previous anodic peak. These changes in anodic peak area are shown in Figure IV-(vii)-ii.

The proposed reactions occurring at the surface are as follows. On immersion into the $AgNO_3$ solution, Ag^+ forms a π complex with the alkene and alkyne groups on the surface. The carbon film microelectrode is then rinsed in the KNO_3 solution to ensure Ag^+ /π complex contains the NO_3^- counter anion. Cyclic voltammetry is then performed, initially reducing the Ag^+ /π complex to metallic silver on the surface. This occurs between 0.15V-0 V-0.15 V. On the reverse scan above 0.2 V anodic stripping of the silver occurs. The Ag^+ diffuses away from the region of deposition to either adjacent π bonds or into solution to re-establish equilibrium between Ag^+ in solution and the π complexed Ag^+.[5;12] This loss of the π complexed Ag^+ is reflected in the 0.2 anodic area reductions of consecutive scans. If the time between consecutive scans is extended to four minutes the ratio of anodic peak area before to after decreased to 0.3. During this extended break in scanning, the Ag^+ diffuses from the electrode surface into the bulk solution.

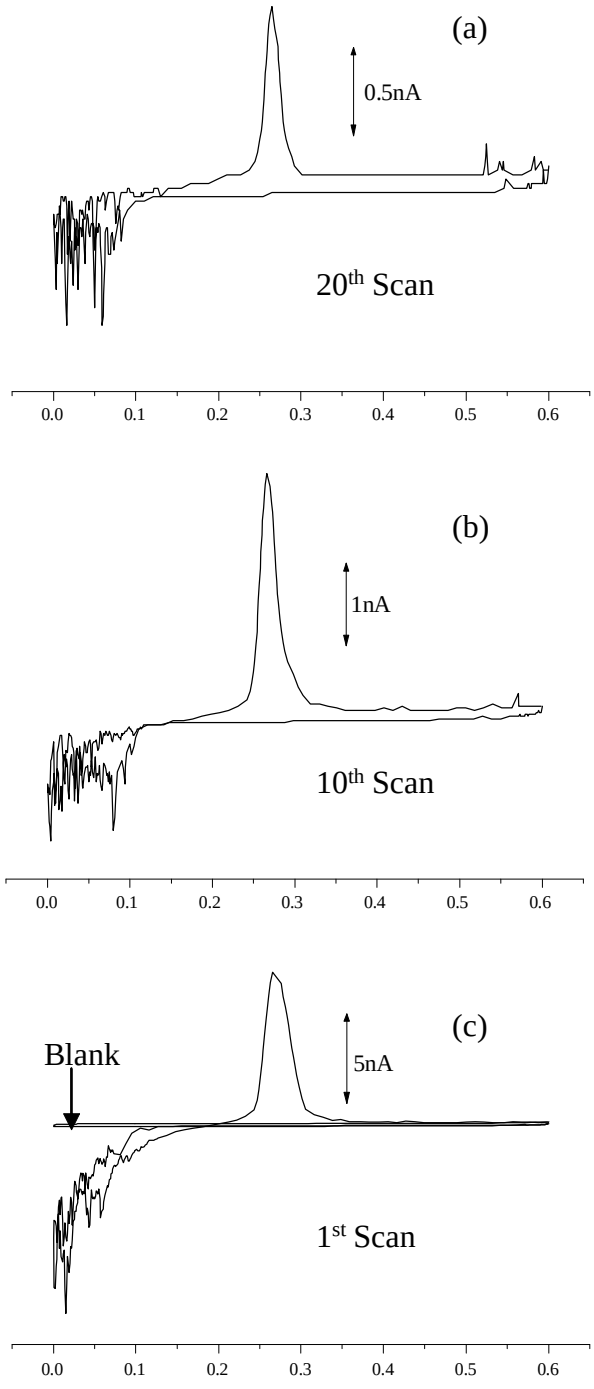

Figure IV-(vii)-i

Cyclic voltammetry of a microelectrode in 10^{-4} M KNO_3 after immersion in 10^{-4} M $AgNO_3$ and rinsing in KNO_3.

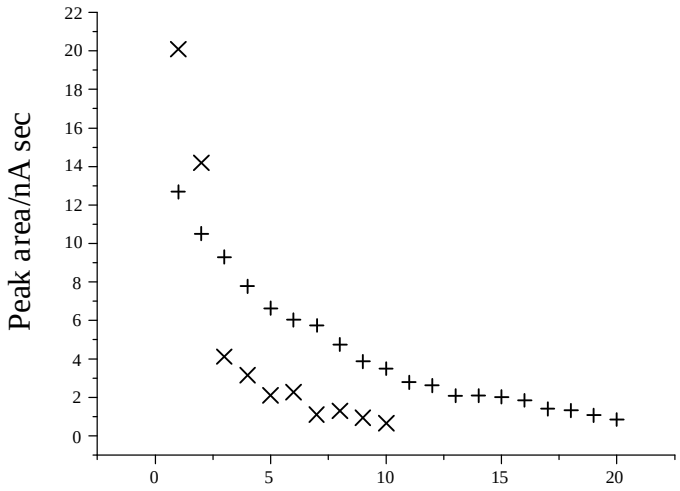

Figure IV-(vii)-ii

The anodic peak area at 0.271 V vs. Ag|AgCl during continuous (+) and discontinuous (X) scanning.

The reduction charge in the forward scan exceeded the oxidation charge for all scans due to possible inclusion of H^+ reduction to H_2 occurring simultaneously with Ag^+ to Ag. The difference in reduction and oxidation charge is more pronounced at larger currents implying dependency on current density. This relationship is shown in Figure IV-(vii)-iii.

As the blank (Figure IV-(vii)-i) does not contain any reduction current, the additional reduction current to Ag^+ implies the H^+/H_2 reduction pathway has been catalysed during the reduction of Ag^+.

.

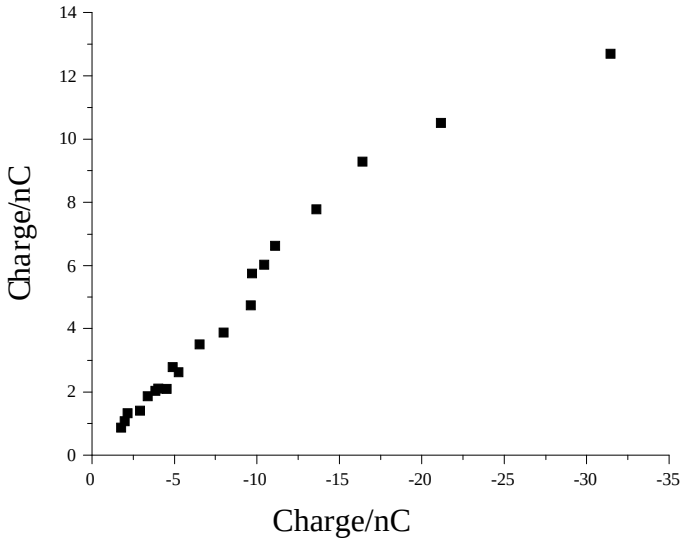

Figure IV-(vii)-iii

Ag^+/Ag versus Ag/Ag^+ during continuous cyclic voltammetry.

Mercury π Complex

Mercuric acetate has been reported to form a π complex with styrene,[13] a possible surface structure on carbon film microelectrodes. To maintain a common anion, acetic acid was initially investigated; however use of acetic acid resulted in multiple peaks during linear anodic scans (Figure IV-(vii)-iv). This was attributed to π complexing cations present in the acetic acid. As mercuric hydroxide is insoluble, use of alkali or alkali earth acetates are precluded. Ammonium acetate was not considered due to the possible formation of mercuric ammonium complexes; therefore chloride ions (10^{-4} M KCl) in both the rinse solution and supporting electrolyte were used. Although π complexing cations are present, as shown in Figure IV-(vii)-v, their anodic peaks only became significant after extended immersion times.

During the reduction scan and prior to anodic stripping of the mercury film possible amalgam formation may occur with the impurities in the supporting electrolyte. These amalgamate impurities during anodic stripping of the mercury film may interfere, therefore only linear voltammetry (-0.5 V to 0.6 V) was used. This also reduced possible contact time with the supporting electrolyte impurities. The scan time spent in the cathodic region was sufficient to reduce complexed Hg^{2+}. The effect of long contact time is shown in Figure IV-(vii)-v hence the need to minimise contact time during rinsing and voltammetry.

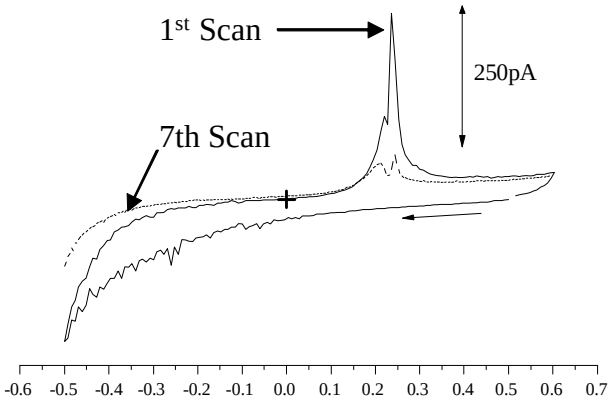

Figure IV-(vii)-iv

Cyclic (1st Scan) and linear (7th Scan) voltammetry, at 0.1 V s^{-1}, of surface complexed impurities from 10^{-4} M acetic acid.

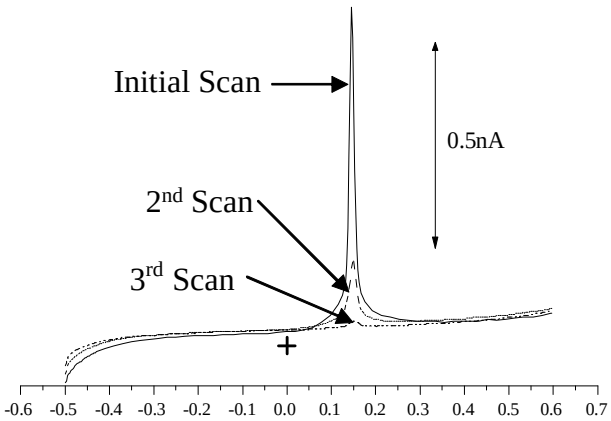

Figure IV-(vii)-v

Linear voltammetry scans at 0.1 V s^{-1} of surface complexed impurities after three minutes immersion in 10^{-4} M KCl.

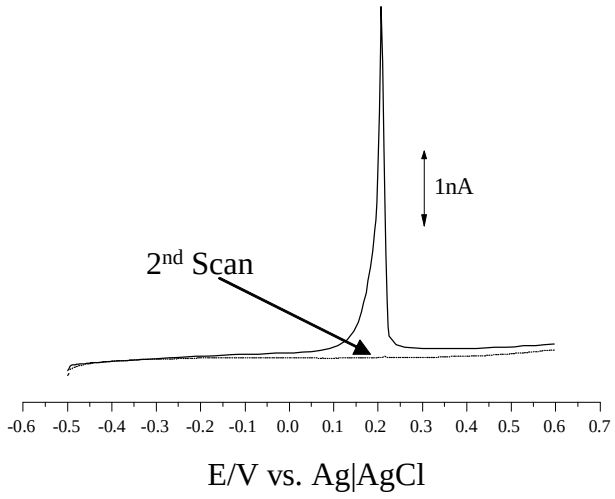

Figure IV-(vii)-vi

Linear scan (-0.5 V to 0.6 V at 0.1 V s^{-1}) of a microelectrode in 10^{-4} M KCl after immersion in mercuric acetate and rinsing in 10^{-4} M KCl

In Figure IV-(vii)-vi the second scan was devoid of a mercury anodic peak. This contrasts with the silver π complex, shown in Figure IV-(vii)-i, where twenty scans were required to eliminate the anodic peak. A possible explanation for this feature is oxidation of the π mercury complex during anodic stripping. It has been reported that mercuric π complex when electrochemically oxidised in the presence of perchloric acid at 2.4 V yields carboxylic acids.[14] Although this voltage is considerably higher than that used in this work, the presence of adjacent or conjugated unsaturation groups may promote the formation of carboxylic acid at lower voltages. Chemical reaction during anodic oxidation of the mercury π complex is indicated by zero or very small anodic current after re-immersion in the mercury acetate solution. (n= 5)

Ferrous π Complex

Stable and isolatable ferrous chloride ethylene complexes have been have been reported.[15] It is therefore probable ferrous π complexes will be formed on the surface of the electrode and that oxidation is possible during linear voltammetry. The ferrous complex was

formed by immersion of the microelectrode in a 10^{-4} M FeSO4 solution, rinsed in a 10^{-4} M KCl and anodically scanned in 10^{-4} M KCl solution. As the chloride counter anion stabilised Hg its use was extended to that of the Fe^{2+} π complex.

During the anodic linear scan ferrous species will not undergo reduction, only the oxidation to ferric. An example of the anodic oxidation of ferrous π complex during linear scanning is shown in Figure IV-(vii)-vii.

In Figure IV-(vii)-vii, the first scan after immersion gave a charge of 0.088 nC. When the voltammetric scan was repeated the charge decreased to 0.010 nC. The third scan was after re-immersion in 10^{-4} M ferrous sulfate. A charge of 0.181 nC was obtained which decreased to 0.016 nC (fourth scan). A fifth scan i.e. the electrode after the second immersion was scanned three times and gave a charge of 0.003 nC. This rapid depletion of the accessible ferrous π complex bonds indicates the possible loss of ferrous ions from solution due to the formation of ferric hydroxide or ferric ions which do not form π complexes. The latter could be due to the ferric ion having an oxidation state of three and therefore could not be complexed. Repeating the re-immersion, on a second electrode, a slight decrease, from 0.340 nC to 0.220nC was measured. The similarity of the anodic charges on re-immersion indicates that the π bonds are not altered by the oxidation of the complexed ferrous ion.

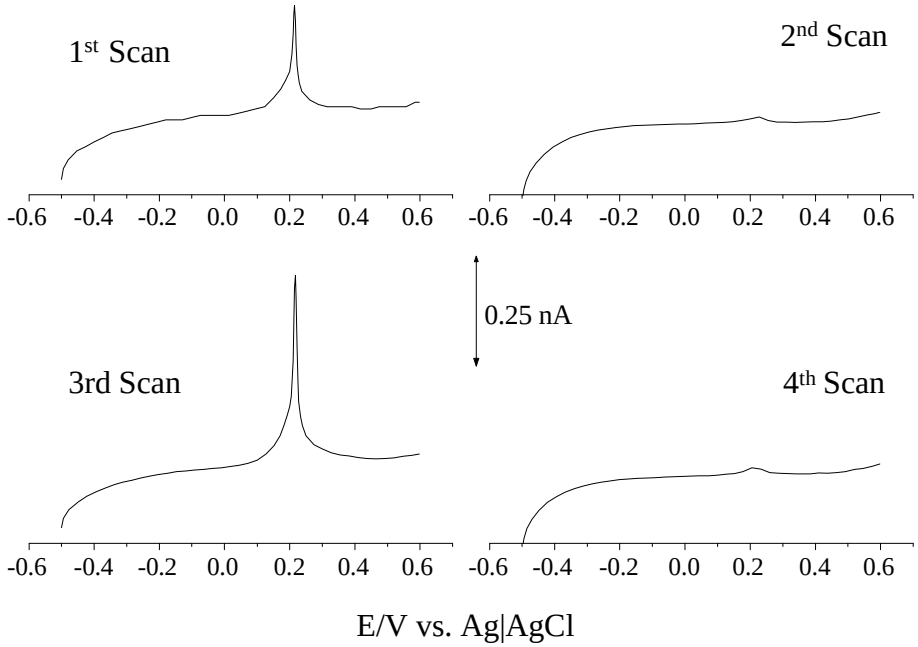

Figure IV-(vii)-vii

Linear scan at 0.1 V s^{-1} in 10^{-4} M KCl.
1st & 3rd scan immediately after immersion in 10^{-4} M $FeSO_4$,
2nd & 4th repeat scans after 1st & 3rd.

Nickel π Complex

To determine the alkyne surface concentration on the surface of the carbon film microelectrode using nickel a simple immersion into a 10^{-4} M nickel chloride solution was used. The carbon film microelectrode was then rinsed in 10^{-4} M potassium chloride. Linear scanning was then carried out between -0.5 V to 0.8 V. An example of the linear anodic oxidation of a microelectrode, using nickel is shown in Figure IV-(vii)-viii. The scan (a) was after immersion and rinsing, scan (b), immediately after scan (a). This was repeated in scans (c) to (f). The second (c) and third scan (e) are after re-immersion. (Peak areas were (a) 0.182 nC, scan (c) 0.207 nC and (e) 0.183 nC.) The presence of an anodic oxidation peak in the

second scan (Figure IV-(viii)-v (c) and (e)) indicates the alkyne group has not changed during oxidation. The absence of a residual anodic oxidation peak in Figure IV-(vii)-v (b), (d) and (f) indicates the dissociation constant for the nickel -π complex is large, larger than that for silver. A small disassociation constant would favour the reformation of the nickel π alkyne complex.

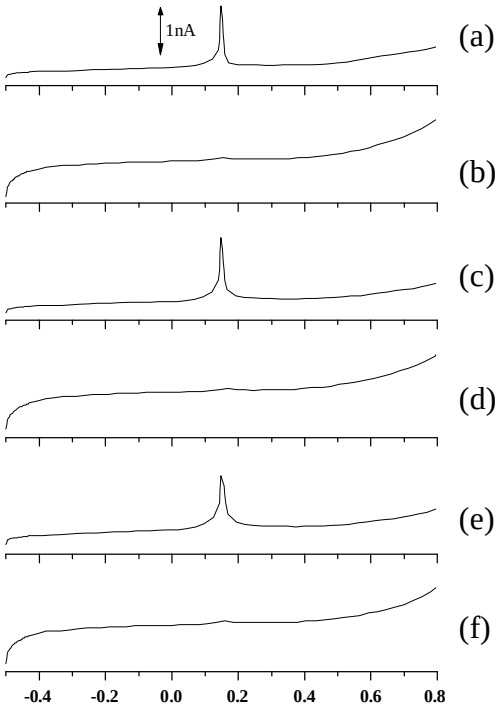

Figure IV-(vii)-viii

Linear scans at 100 mV/sec of a microelectrode after immersion in 10^{-4} M $NiCl_2$ and rinsing in 10^{-4} M KCl. Scan (a) and (b) after first immersion. Scan (c) and (d) after the second immersion. Scan (e) and (f) after the third immersion

The summary of surface concentrations of unsaturated aliphatic groups obtained by anodic stripping of the cation π-complexes of Ag^{+}, Hg^{2+}, Fe^{2+} and Ni^{2+} are listed in Table IV-(vii)-i.

Table IV-(vii)-i Summary of unsaturated aliphatic group concentrations

Cation	Average Cation Surface Concentration (Moles.cm^{-2})	Cation Surface Concentration Range (Moles.cm^{-2})	Average E at i_{max} (V)	Standard Deviation of i_{max} (V)
Ag^{+}	2.0×10^{-10}	1.6×10^{-12} - 1.7×10^{-9}	0.24	0.023
Hg^{++}	2.2×10^{-11}	4.8×10^{-13} - 8.6×10^{-11}	0.19	0.014
Fe^{2+}	2.1×10^{-11}	9.2×10^{-12} - 3.5×10^{-11}	0.22	0.003
Ni^{2+}	5.4×10^{-11}	5.2×10^{-12} - 1.0×10^{-10}	0.15	0.007

Note

1) Sample sizes: Ag^{+} n=12, Hg^{2+} n=13, Fe^{2+} n=3 and Ni^{2+} n=9.

2) Samples below detection levels were not included in the calculation of average cation surface concentration

3) The proposed electrochemical reactions are listed as follows:

$$Fe^{2+}(\pi\text{-complex}) \rightleftharpoons Fe^{3+}(\text{solution}) + e$$

$$Ag^{+}(\pi\text{-complex}) + e \rightleftharpoons Ag(\text{carbon film surface}) \rightleftharpoons Ag^{+}(\text{solution}) + e$$

$$Hg^{2+}(\pi\text{-complex}) + 2e \rightleftharpoons Hg(\text{carbon film surface}) \rightleftharpoons Hg^{2+}(\text{solution}) + 2e$$

$$Ni^{2+}(\pi\text{-complex}) + 2e \rightleftharpoons Ni(\text{carbon film surface}) \rightleftharpoons Ni^{2+}(\text{solution}) + 2e$$

The results in Table IV-(vii)-i indicate similar results are obtained irrespective of the π complexing cation. The results for the Ni^{2+} complex are between that of Ag^{2+} and Fe^{2+} indicating that the most probable unsaturated aliphatic group on the surface of the carbon film are alkynes. This suggests that not only is acetylene the predominant species in the thermal

pyrolysis of hydrocarbons, acetylides are also the most stable non-graphene species formed on the surface.

The cation π-complexation bonds when anodically oxidised exhibited different pathways. The Hg^{2+}, when undergoing anodic oxidation modified the alkyne groups such that further complexation did not occur. Ag^{+}, Fe^{2+} and Ni^{2+} cations when oxidised or reduced did not modify the alkyne groups. The strong complexation of Ag^{+} with the unsaturated aliphatic groups[2], when compared to Ni^{2+}, was demonstrated by the "slow release" of the Ag^{+} ions into the bulk solution. The "slow release" of Ag^{+} indicates the rapid reforming of the π complex compared to the precipitation as the chloride. The lack of modification of the alkyne groups, when the Fe^{2+} π-complex was anodically oxidised eliminates this pathway in the formation of carboxylic acids using $FeSO_4$ (Chapter V-(i)).

Trace analysis of Cations using π Complexation

The formation of a π complex provides a site for adsorptive stripping voltammetry capable of detecting cations at low concentration as evidenced in Figure IV-(vii)-iv and v. A further example of adsorption voltammetric stripping is shown in Figure IV-(viii)-ix. In this example the microelectrode was allowed to stand in Milli-Q water for six minutes prior to scanning. The first scan appears to contain three peaks: a shoulder at 0.24 V, the main peak at 0.278 V and shoulder at 0.288 V. The total peak area of the first scan is 1 nC and the seventh is 0.02nA sec. Assuming the π complexing cation is copper (copper is known to occur at 1-5 ppm in reticulated tap water and therefore possible traces in de ionised water) the concentration of the complexed cation is 0.01 ppm. The peak in the seventh scan is equivalent to 0.0002 ppm copper.

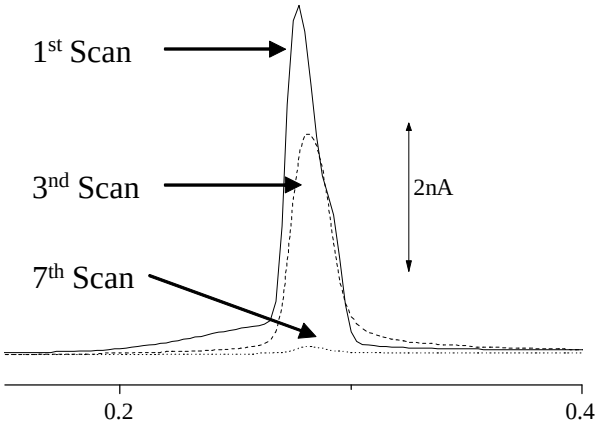

Figure IV-(viii)-ix

Linear scans of a carbon film microelectrode, at 0.1 V/sec, after standing in Milli Q water for 6 minutes.

Thus the microelectrodes containing alkene and/or alkynes are capable of selective adsorption of π complexing cations with quantification to less than 1ppb. As the degree of π complexing, with cations, is in equilibrium with the cations in solution these microelectrodes may be of value in measuring speciated π complexing cations in natural waters or biological systems.

A similarly facile adsorption technique has been reported for Pb^{2+} on GC and carbon fibre.[16] In this example, carboxylate groups formed by the oxidation of edge planes provide the surface bonding. The maximum coverage obtained was $2.5x10^{-10}$ moles cm^{-2} for GC and $1.3x10^{-7}$ moles cm^{-2} on carbon fibre. This high surface concentration for carboxylic acids on edge planes and carbon fibre surfaces, when compared to a carbon film, suggests that the alkene/alkyne groups on the carbon film are well separated.

Conclusion

The different rate of decrease in anodic peak areas at different potentials confirms the existence of a cation surface interaction. This cation surface interaction is ascribed to the presence of π complexes. The surface concentration of a ferrous π complex, assuming maximum packing density, is $3x10^{-8}$ moles cm^{-2}. This is a geometrical calculation based on the complex being parallel to the surface, carbon to carbon bond length of 140 pm and carbon to ferrous 110 pm.

The average surface concentration of alkene or alkyne groups which are accessible to the graphene surface, measured coulometrically, ranged from 1 % to 0.1 % of the theoretical maximum. The nickel complex surface concentration being similar to that of silver, ferrous and mercury implies that most of the unsaturated aliphatic bonds are alkyne. This assumes that the nickel ion in solution has the same affinity to acetylides as nickel ions on aluminium oxide.[7]

The presence of detectable alkenes or alkynes confirms the presence on the surface of pendent groups, as postulated in Chapter III Introduction arising from residual acetylide groups on the surface.

A change in anodic peak size, after re-immersion, indicates that both a reaction has occurred during anodic oxidation and also the strength of the cation π-complex that had formed.

The ability to quantify π complexing cations on a rigid microelectrode suggests applications in the biological field for *in situ* trace metal analysis.

References

1. Krestinin A.V. *Combustion and Flame* **2000,** *120*, 513-24.
2. Yang R.T.; Kikkinidis E.S *AIChE Journal* **1995,** *41*, 509-17.
3. Tanase I.; Ionegi I.; Luca G. *Revue Roumaine de Chimie* **1985,** *30*, 851-58.
4. Novak V.; Forst V. *Chemicky Prumysl* **1972,** *22*, 569-72.
5. Brandt P. *Acta Chemica Scandinavica* **1959,** *13*, 1639-52.
6. Chatt J. *Chemical Society Reviews.* **1951,** *48*, 7-43.
7. Yang R.T.; Foldes R. *Industrial Engineering Chemical Research* **1996,** *35*, 1006-11.
8. Brooksby P.A.; Downard A.J. *Langmuir* **2004,** *20*, 5038-45.
9. Adams R.N. *Electrochemistry at Solid Electrodes,* ed.; Marcel Dekker: USA, 1973.
10. Ortiz B.; Saby C.; Champagne G.Y.; Belanger D. *Journal of Electroanalytical Chemistry* **1998,** *455*, 75-81.
11. da Silva S.M. *Electroanalysis* **1998,** *10*, 722-25.
12. Hartley F.R. *Chemical Reviews* **1973,** *73*, 163-90.
13. Dlask V. *Reaction Kinetics and Catalysis Letters* **1991,** *47*, 87-91.
14. Fleischmann M.; Pletcher D.; Race G.M. *Journal of the Chemical Society (B)* **1970,** 1746-49
15. Herberhold M. *Metal π Complexes,* ed.; Elservier Publishing Co: Netherlands, 1972.
16. Bartlett P.N.; Denuault G.; Sousa M.F.B. *Analyst* **2000,** *125*, 1135-38.

Chapter IV-(viii)

Outer Sphere Electron Transfer using Hexaaminеruthenium (III) Chloride

Abstract

The waveslope for the reduction of hexaaminеruthenium (III) chloride at the carbon film surface has been measured. The results, 0.060 ±0.0024 V/decade, imply an almost ideal single heterogeneous electron transfer is occurring at the carbon film surface. This almost theoretical value suggests a unique carbon surface structure. This unique carbon structure possibly arises from the presence of the postulated electron rich pendent groups.

The change in the reduction limiting current, of hexaaminеruthenium (III) chloride with scan rate, was proposed to originate from the presence of a planar diffusion current in the total liming current. It is also proposed that the radial and planar diffusion currents can be linearly combined.

Introduction

Hexaaminеruthenium (III) chloride ($Ru(NH_3)_6^{3+/2+}$) was selected as the initial model analyte to assist in the characterisation of the carbon film on the microelectrode as it is has been reported to be insensitive to oxides present on the surface.[1] Earlier work suggests that only when thick oxide layers are formed does interference with the electron transfer occurs during reduction of hexaaminеruthenium (III) chloride.[2-4] As the carbon film formed on the microelectrodes was not expected to be heavily oxidised, interference was not anticipated.

The relative insensitivity of the carbon surface chemistry to electron transfer reactions, with $Ru(NH_3)_6^{3+}$, is attributed to outer sphere electron transfer taking place during cathodic reduction.[5] The single electron reduction occurring at the carbon film microelectrode surface is shown in the equation below.

$$Ru(NH_3)_6^{3+} + e \rightleftharpoons Ru(NH_3)_6^{2+}$$

$Ru(NH_3)_6^{3+}$is therefore an ideal model analyte to elucidate both surface chemistry and the electrode physical shape. Information on the surface chemistry of carbon electrodes has been obtained by measuring the heterogeneous electron transfer rate constant for the reduction of $Ru(NH_3)_6^{3+}$.[6-8] Unfortunately the heterogeneous electron transfer rate constant could not be measured with these carbon film microelectrodes (Chapter I Heterogeneous Electron Transfer Rate). However many publications have tabulated ΔE_p for the reduction of hexaaminеruthenium (III) chloride for large disc electrodes at a range of carbon surfaces. (The fabrication of microelectrodes of known carbon surface chemistry, such as basal or edge plane HOPG would be difficult!)

The ΔE_p obtained from the cyclic voltammogram, for the larger electrodes, has been used to calculate the stoichiometric number of electrons.

$$\Delta E_p \approx \frac{0.059}{n} \qquad \text{(i)}$$

The relationship in equation IV-(viii)-i can be directly compared to the waveslope. (Chapter I Waveslope) Using this comparison the surface electrochemistry of the carbon film microelectrodes can be related to the electrochemistry of other carbon structures.

Experimental Section

Chemicals

Milli-Q water, potassium chloride (BDH Analar), hexaaminеruthenium (III) chloride (Strem Chemicals) and nitrogen (Instrument Grade) were used as received.

Equipment

The three electrode system, using Ag|AgCl (3 M KCl) reference, as outlined in Chapter II Electrochemical Equipment, was used.

Electrode Fabrication

The carbon film microelectrodes were fabricated as outlined in Chapter III using 40 ml min^{-1} nitrogen in both the parallel flow and counter flow configurations.

Procedure

The carbon film microelectrodes were voltammetrically cycled from 0.1 V to -0.4 V in deoxygenated 10^{-4} M hexaaminеruthenium (III) chloride with 0.05 M KCl as the supporting electrolyte.

Results and Discussion

Cyclic voltammetry was carried using 0.05 M KCl as the supporting electrolyte. Although supporting electrolytes are unnecessary with microelectrodes, they were employed to ensure only Faradaic currents were measured, particularly with the larger cylindrical microelectrodes.

The cyclic voltammograms of 10^{-4} M $Ru(NH_3)_6^{3+/2+}$ display almost perfect sigmodial response (Chapter I The Sigmodial Shape) at slow scan rates. This is shown in an example of a carbon film micro electrode, with a calculated length and radius of 93 μm and 7 μm respectively, in Figure IV-(viii)-i at a range of scan rates. In Figure IV-(viii)-i, the effect of double layer capacitive charging, at scan rates above 0.05 V s^{-1}, is seen between 0.1 V and -0.4 V.

Under quasi steady state, at 0.1 V s^{-1} an average waveslope of 0.060 V/decade (n=29) was derived with a standard deviation of 0.024. The average $E½$ for this sample was 0.137 V with a standard deviation of 0.0082 V. The narrow distribution of wave slope as a function of electrode size (limiting current), as shown in Figure IV-(viii) ii, indicates that the chemistry of the carbon film surface is consistent for an electrochemically reversible outer sphere electron transfer. The average waveslope of 0.060 V/decade is very close to the theoretical value of 0.059 V/decade for a single electron transfer.

By plotting limiting current versus the square of scan rate (Figure IV-(viii)-iii) the linearity of the plot indicates that the heterogeneous electron transfer is under diffusion control, as expected from an outer sphere electron transfer at a graphene surface.
The almost theoretical waveslope of 0.060 V/decade for the single electron reduction of $Ru(NH_3)_6^{3+}$, at the carbon film surface is low when compared to ΔE_p for other carbon surfaces (See Table IV-(viii)-i). The heavily oxidised GC and boron doped diamond (boron in sp^3 matrix) are the only surfaces reported which indicate a ΔE_p close to that of a single electron transfer. As the carbon film does not contain either an oxidised surface or sp^3 carbon these

results imply unique carbon structures present on the surface, which does not hinder the heterogeneous electron transfer during reduction reactions of outer sphere electron transfer analytes.

A consequence of an almost theoretical sigmodial cyclic voltammogram of $Ru(NH_3)_6^{3+/2+}$ is the symmetrical response to differential pulse voltammetry (Figure IV-(viii)-iv). This enables a low detection limit; $5x10^{-7}$ M with linearity to 10^{-4} M, almost 3 decades. This linearity ($R^2 = 0.999$) with respect to concentration is shown in Figure IV-(viii)-v.

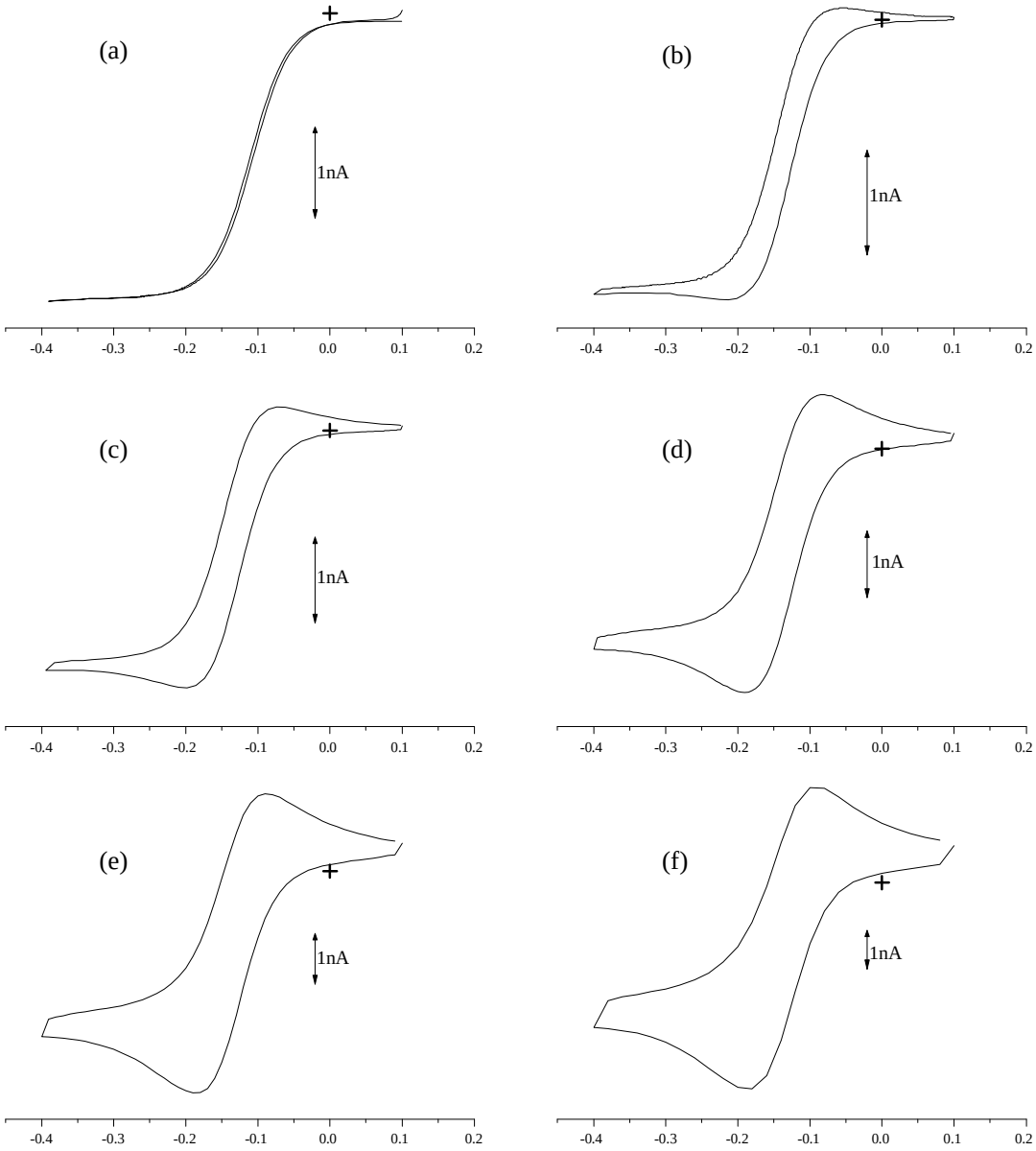

Figure IV-(viii)-i

Cyclic voltammograms of a carbon film microelectrode of 10^{-4} M $Ru(NH_3)_6Cl_3$ in 0.05 M KCl, with a scan rate of (a) 0.005 V s^{-1}, (b) 0.05 V s^{-1}, (c) 0.1 V s^{-1}, (d) 0.25 V s^{-1}, (e) 0.5 V s^{-1} and (f) 1 V sec^{-1}.

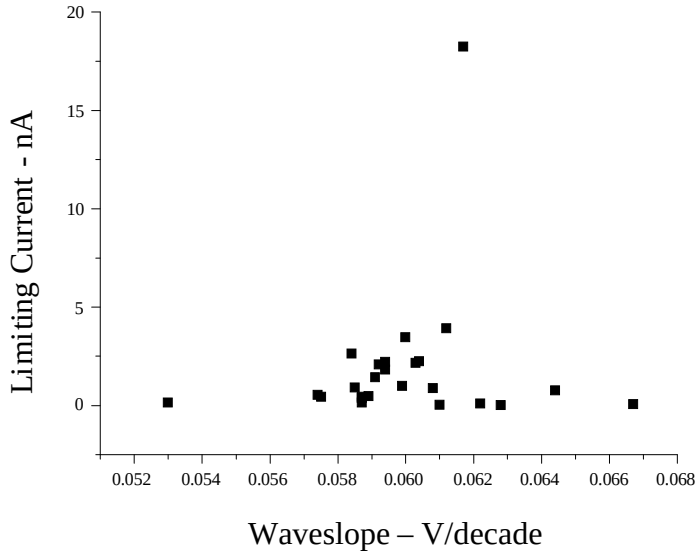

Figure IV-(viii)-ii

Waveslope versus limiting current for carbon film microelectrodes in 10^{-4} M $Ru(NH_3)_6Cl_3$ with a supporting electrolyte of 0.05 M KCl.

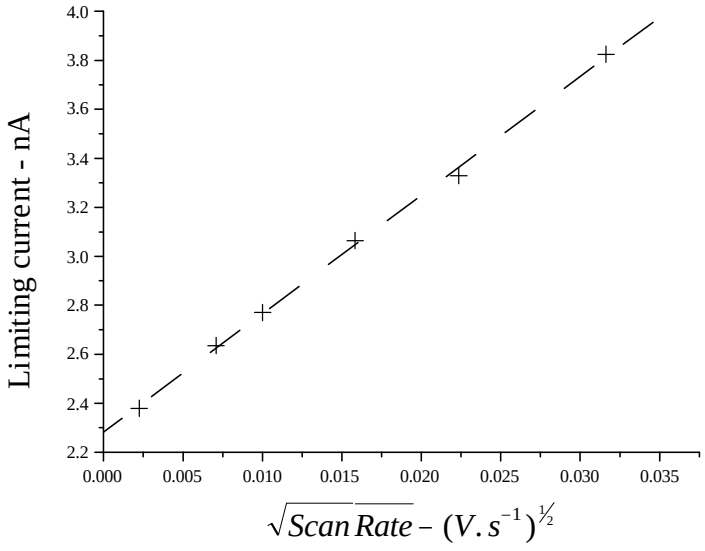

Figure IV-(viii)-iii

Limiting current versus the square of the scan rate for a carbon film microelectrode in 10^{-4} M $Ru(NH_3)_6Cl_3$ with a supporting electrolyte of 0.05 M KCl.

The graph, shown in Figure IV-(viii)-iii, displays a positive limiting current at zero scan rate. This non-zero current is attributed to the radial diffusion component of the limiting current measured at the cylindrical microelectrode used in this experiment. As the cylindrical microelectrode's radius is of a greater dimension than that of the critical dimension for a perfect microelectrode the diffusion current has both radial and planar components.[16] This is expressed in Equation (ix) where i_t is the total diffusion current, i_r the radial diffusion current and i_p the planar diffusion current.

$$i_t = i_r + i_p \qquad \text{(ix)}$$

The radial component i_r being equivalent i_{qss} in equation (iv) Chapter I. The planar component i_p will be proportional to the square root of the scan rate, as in the Randles-Sevcik equation for peak current at an electrode controlled by planar diffusion. The planar diffusion current component of these "larger" cylindrical microelectrodes will be used to establish the presence or absence of adsorbed species on the carbon microelectrodes surface during anodic oxidation of catecholamines in Chapter IV-(x).

Table IV-(viii)-i Comparison of ΔE_p and waveslope at different carbon surfaces.

Carbon Type	Modification	ΔE_p (V)	Reference
GC	Freshly polished	0.076±0.007	1
	Polished and oxidised in air	0.123	1
	Oxygen/Carbon 14:1 (XPS)		
	Vacuum heat treated	0.115	1
	Polished	0.082±0.008	9
	Oxidised at 1.8V in H_2SO_4 for 90 sec	0.065±0.003	9
	Hydrogenated	0.094±0.003	10
	Hydrogenated	0.097	11
	Diamond coated	0.145	11
HOPG		0.285	12
Diamond	Boron doped	0.07	13
		0.074	14
		Waveslope (V/decade)	
Pyrolysed Photoresist Film		0.125±0.005	8
Carbon Film		0.060±0.0024	This work

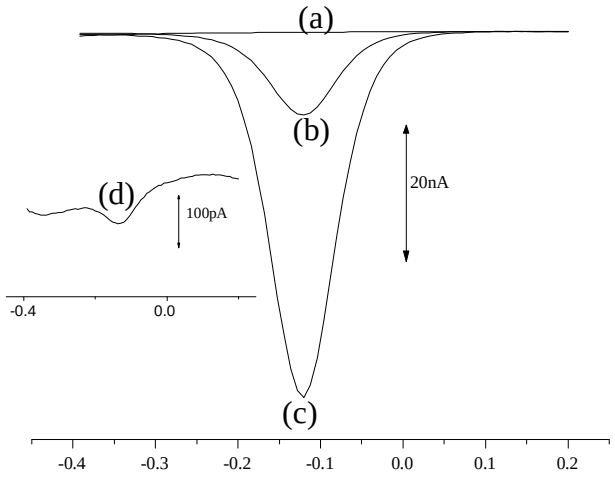

Figure IV-(viii)-iv

Differential pulse voltammetry of a carbon film microelectrode of (a) 0.05 M KCl together with $Ru(NH_3)_6Cl_3$, (b) $5x10^{-5}$ M, (c) 10^{-4} M and inset (d) $5x10^{-7}$ M.

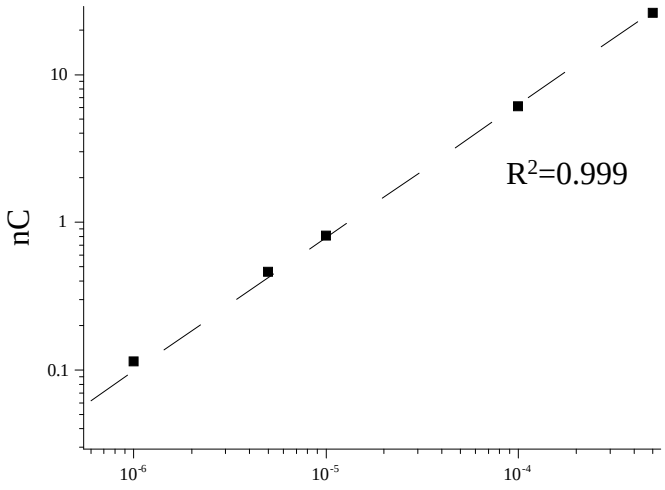

Figure IV-(viii)-v

Differential pulse peak area versus concentration of $Ru(NH_3)_6Cl_3$ in 0.05 M KCl

Conclusion

The reduction of $Ru(NH_3)_6^{3+/2+}$ during voltammetry at a carbon film microelectrode indicates the surface does not contain any hydrophobic functional or steric groups hindering the reversibility of the outer sphere electron transfer[15]. The independence of electrode size and waveslope together with the small standard deviation of the waveslope suggests, that for an outer sphere electron transfer, such as with $Ru(NH_3)_6^{3+/2+}$, the surface is homogeneous. The waveslope, 0.06 V/decade indicates a carbon film surface with unique features. From the published ΔE_p results only the vigorously oxidised glassy carbon surface approaches the carbon film of this work. As the carbon film does not contain an oxidised surface (see Chapter IV-(xi) for the effect of surface oxides on the cyclic voltammetry of DA.) another heterogeneous electron transfer pathway is suggested. It was postulated from Raman spectroscopy and stripping voltammetry of surface bound cations that surface contains electron rich pendent groups. It is these groups which may explain the excellent heterogeneous electron transfer for the reduction of $Ru(NH_3)_6^{3+}$, leading to the almost theoretical sigmodial cyclic voltammograms.

The deviation from theoretical sigmodial cyclic voltammogram shape was proposed to originate from the planar component of the total limiting diffusion current. It was also proposed that the radial and planar components are additive.

References

1. Chen P.; McCreery R.L. *Analytical Chemistry* **1996,** *68*, 3958-65.
2. Kovach P.M. *Journal of the Electrochemical Society.* **1985,** *Reviews and News,* 243C-5C.
3. Kovach P.M.; Deakin M.R.; Wightman R.M. *Journal of Physical Chemistry* **1986,** *90,* 4612-17.
4. Jaworski R.K. ; McCreery R.L. *Journal of Electroanalytical Chemistry* **1994,** *369*, 175-81.

5. Segre E. *Electron Exchange Reactions*, Sutin N, Ed.; 1962 ed.; George Banta: USA, 1962.

6. Chen P.; Fryling M.A.; McCreery R.L. *Analytical Chemistry* **1995,** *67*, 3115-22.

7. DeClements R.; Swain M.W.; Dallas T.; Holtz M.W.; Herrick R.D.; Stickney J.L *Langmuir* **1996,** *12*, 6578-86.

8. Ranganathan S.; McCreery R.L. *Analytical Chemistry* **2001,** *73*, 893-900.

9. Kiema G.K.; Fitzpatrick G.; McDermott M.T. *Analytical Chemistry* **1999,** *71*, 4306-12.

10. Chen Q.; Swain G.M. *Langmuir* **1998,** *14*, 7017-26.

11. DeClements R.; Swain G.M.; Dallas T.; Holtz M.W.; Herrick R.D.; Stickney J.L *Langmuir* **1996,** *12*, 6578-86.

12. Cline K.K.; McDermott M.T.; McCreery R.L. *Journal of Physical Chemistry* **1994,** *98*, 5314-19.

13. Granger M.C.; Swain G.M. *Journal of the Electrochemical Society* **1999,** *146*, 4551-58.

14. Granger M.C.; Witek M.; Xu J.; Wang J.; Hupert M.; Hanks A.; Koppang M.D.; Butler J.E.; Lucazeau G.; Mermoux M.; Stropek J.W.; Swain G.M. *Analytical Chemistry* **2000,** *72*, 3793-804.

15. Saby C.; Ortiz B.; Champagne G.Y.; Belanger D. Langmuir **1997**, *13*, 6805-6813.

16. Wang J.; Analytical *Electrochemistry*, 2nd Ed, Wiley-VCH, 2000

Chapter IV-(ix)

Reduction of Potassium Hexacyanoferrate (III)

Abstract

The waveslope of $Fe(CN)_6^{3-}$ at the surface of carbon film microelectrodes in 1 M KCl has been found to be highly variable. The measured range was from 0.170 to 0 300 V/decade (n=5). A similar number had waveslopes too high to measure. These variable and high values suggest the surface behaves electrochemically as that of HOPG.

Measurement of the waveslope of sub micron "disc" electrodes is similar to that of an edge plane which implies the graphene layers are formed parallel to the inside quartz surface.

Introduction

The reduction of potassium hexacyanoferrate (III) to potassium hexacyanoferrate (II) ($Fe(CN)_6^{3-/4-}$) has been used extensively to characterise the surface of carbon electrodes.[1] The lack of published literature using microelectrodes, with basic carbon crystal structures, necessitates the comparisons of ΔE_p values obtained from large disc electrodes with the waveslopes obtained in this work. This is similar to the approach used in Chapter IV-(viii) using $Ru(NH_3)_6^{3+/2+}$. An additional comparison may be made with carbon film formed from pyrolysed methane under a nitrogen blanket.[2;3] Direct comparison of the pyrolysed methane carbon film electrodes is not possible due to slightly different pyrolysis techniques.
The reduction reaction of $Fe(CN)_6^{3-}$ is reported to be surface sensitive but independent of oxides.[4;5] The surface sensitivity appears to be dependent on carbon crystal orientation and surface preparation.[1;6] Freshly fractured surfaces of GC gave ΔE_p values of 75 mV, polished GC 357 mV and laser activation after polishing 75 mV.[6] With this differentiation between polished and fractured surfaces and particularly the low value ΔE_p of the fractured GC,

$Fe(CN)_6^{3-/4-}$ was used to provide an additional means of detecting the presence of surface edge planes. This cyclic voltammetric difference between the basal plane and edge plane is such that it can be seen visually in the referenced cyclic voltammograms.[7]

The small ΔE_p for the reduction of $Fe(CN)_6^{3-}$ also provides a means of establishing if the initial deposit of graphene is a layered structure. During the pyrolysis of acetylene it is expected that the initial layers are parallel to the substrate (Chapter III Introduction). Therefore, with submicron "disc" electrodes these layers will terminate at the orifice with a predominance of edge planes. If cyclic voltammetry, using $Fe(CN)_6^{3-}$, is carried out on freshly fabricated carbon film microelectrodes, thereby limiting the extent of oxidation in air, the waveslope should be close to 0.059 V/decade. Such a low value will indicate the presence of edge planes. (The use of AQDS (Chapter IV-(v)), to detect edge planes on a sub micron disc electrode, was not possible because the limiting current will be below the detection level of the Picostat used in this work.)

Experimental Section

Chemicals

Milli-Q water, potassium hexacyanoferrate (III) (BDH Analar), potassium chloride (Analar), and nitrogen (Instrument Grade) were used as received.

Equipment

The three electrode system, using Ag|AgCl (3 M KCl) reference, as outlined in Chapter II Electrochemical Equipment, was used.

Electrodes Fabrication

The carbon film microelectrodes were fabricated as outlined in Chapter III, using 40 ml min^{-1} nitrogen in both the parallel flow and counter flow configurations.

Procedure

The carbon film microelectrodes were voltammetrically cycled from -0.5 V to 0.4 V in deoxygenated 10^{-4} M $K_3Fe(CN)_6$ with 0.5 M KCl as the supporting electrolyte.

Results and Discussion

The cyclic voltammetry of $Fe(CN)_6^{3-/4-}$ produced variable results at both cylindrical and small "disc" electrode surfaces. This variability, of a cylindrical electrode, is depicted in Figure IV-(ix)-i.

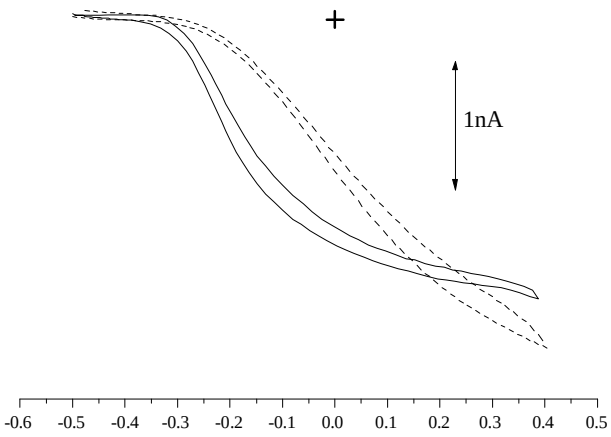

Figure IV-(ix)-i

Cyclic voltammogram at two carbon film microelectrodes of 10^{-4} M $K_3Fe(CN)_6$ in supporting electrolyte 0.5 M KCl
Scan rate 0.05 V sec^{-1}

In Figure IV-(ix)-i the solid line cyclic voltammogram (waveslope 0.170 V/decade) is a typical shape of an irreversible electron transfer.[8] The irreversibility is indicated by a difference between *E¾-E¼* of 0.170 V. This is greater than the Tomeš criteria of 0.0565 V for a reversible one electron transfer.[8] The use of the Tomeš criteria provides a simple means of establishing reversibility, as is the case of the dotted line chromatogram in Figure IV-(ix)-I, which has an almost unmeasurable waveslope of 0.3 V/decade.

A summary of published ΔE_p and waveslopes for the reduction of $Fe(CN)_6^{3-}$ and those obtained in this work is given in Table IV-(viii)-i. The range given for the carbon

film (this work) was for only five samples, a further eight samples having indeterminate limiting currents. The large waveslope values and range suggests the surface of the cylindrical carbon film electrodes is similar to that of HOPG.

The pyrolytic carbon film, in Table IV-(iv)-i was formed *in situ* by the pyrolysis of methane. During pyrolysis sand was present in a rotating pyrolysis chamber. The sand was used to provide an even coating thickness.[9] Under these conditions it would be expected that the surface, as it is being formed, is mechanically damaged. This damage will manifest itself as edge planes. As a consequence an electrochemically active surface similar to that of a freshly fracture GC surface, will be formed. This is reflected in similar values of waveslope and ΔE_p for these electrodes.

When considering sub micron "disc" electrodes the waveslope values are consistently lower than that of the cylindrical electrodes. The lowest waveslope measured was 0.071 V/decade. The cyclic voltammogram of this electrode is shown in Figure IV-(ix)-ii

Table IV-(ix)-i. Comparison of ΔE_p and waveslope with types of carbon surfaces.

Carbon Type	Surface	ΔE_p (V)	Reference
GC	Fractured	0.075±0.006 (1 M KCl)	6
	Polished	0.357±0.049 (1 M KCl)	6
		0.135±0.007 (1 M KCl)	10
	Polished and Laser Etched	0.075±0.004 (1 M KCl)	6
	Hydrogenated	0.119±0.005 (1 M KCl)	10
		0.080 (1 M KCl)	11
HOPG		0.7-1.5 (1 M KCl)	12
		0.7-1.37 (1 M KCl)	13
Pyrolysed Photoresist Film		0.265±0.017 (1 M KCl) on Si	14
		0.140±0.009 (1 M KCl) on GC	14
Diamond	Boron Doped	0.443 (1 M KCl) 2000ppm	15
		0.094 (1 M KCl) 14000ppm	
Pyrolytic Carbon Film		0.080 (2 M KCl)	2
		Waveslope (mV/decade)	
Pyrolytic Carbon Film		0.059-0.073 (0.5 M KCl)	3
Carbon Film	Cylindrical	0.17-0.3 (1 M KCl)*	This work
	Small Disc	0.071-0.22 (1 M KCl)**	This work

Note * (n=5), **(n=6)

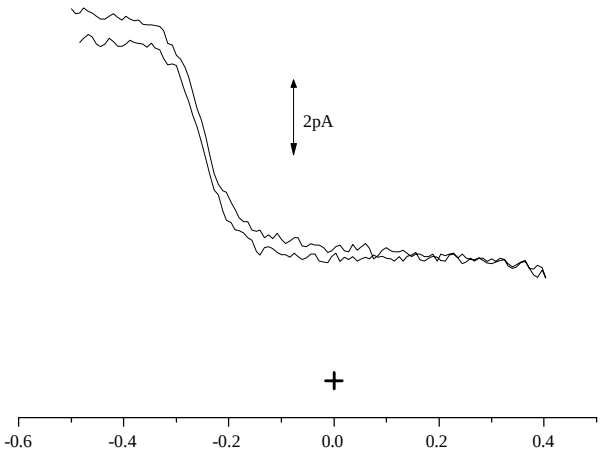

Figure IV-(ix)-ii

Cyclic voltammogram of 10^{-4} M $K_3Fe(CN)_6$, at a carbon film "disc" electrode in 1 M KCl supporting electrolyte. Scan rate 0.1 V s^{-1}

The waveslope for the electrode depicted in Figure IV-(ix)-ii is almost that expected for a reversible electron transfer reaction. The Tomeš criterion is almost achieved with a *E¾-E¼* of 0.064 V for this 0.2 μm radius "disc" electrode.

The waveslopes for these small "disc" electrodes suggest that the graphene has an edge plane characteristic when the surface is terminated at the orifice rather than on the shank of the electrode, as with cylindrical electrodes.

Conclusion

The waveslopes obtained from the cyclic voltammetry, of the reduction of $Fe(CN)_6^{3-}$ in 1 M KCl, indicate that the carbon formed on the shank of the cylindrical electrodes is similar to a basal plane whereas the carbon deposit at a sub micron diameter pulled quartz capillary has edge plane.

The HOPG in the referenced work in Table IV-(ix)-i was a validated basal plane. The formation of basal like characteristics on the surface of the electrodes shank is consistent with graphene layers growing parallel with the substrate, during *in situ* pyrolysis. The presence of

edge plane carbon at the orifice is similarly obtained by graphene growth parallel to the inside surface of the quartz.

From the SEMs (Chapter III Results and Discussion, Small Cylindrical Microelectrodes) the surface does not contain sharp features, but rounded profiles. It is therefore suggested that any edge planes that may form are due to decarbonisation in the later stages of pyrolysis. As the internal diameter at the tip was not accurately measurable with an optical microscope, therefore to ensure recessed tips were not formed, a standard two minutes pyrolysis time was used for all microelectrodes. Electrodes with small orifices will undergo a degree of decarbonisation and exposing the carbon edge plane.

References

1. McCreery R.L. *Electroanalytical Chemistry*, Bard A.J., Ed.; Dekker: 1991.
2. Lundstrom K. *Analytica Chimica Acta*, **1983**; **146**, 97-108.
3. Beilby A.L.; Brooks W.; Lawrence G.L. *Analytical Chemistry* **1964,** *36*, 22-26.
4. Chen P.; McCreery R.L. *Analytical Chemistry* **1996,** *68*, 3958-65.
5. Goss C.A; Brumfield J.C.; Irene E.A.; Murray R.W. *Analytical Chemistry* **1993,** *65*, 1378-89.
6. Rice R.J.; Pontikos N.M.; McCreery R.L. *Journal of the American Chemical Society* **1990,** *112*, 4617-22.
7. Bowling R.J.; Packard R.T.; McCreery R.L. *Journal of the American Chemical Society* **1989,** *111*, 1217-23.
8. Oldham K.B.; Myland J.C. *Fundermentals of Electrochemical Science,* ed.; Academic Press: UK, 1994.
9. Grisdale R.O.; Pfister A.C.; van Roosebreok W. *The Bell System Technical Journal* **1951,** *30*, 271-315.
10. Kuo T.C.; McCreery R.L. *Analytical Chemistry* **1999,** *71*, 1553-60.
11. DeClements R.; Swain G.M.; Dallas T.; Holtz M.W.; Herrick R.D.; Stickney J.L *Langmuir* **1996,** *12*, 6578-86.
12. Cline K.K.; McDermott M.T.; McCreery R.L. *Journal of Physical Chemistry* **1994,** *98*, 5314-19.
13. Kneten K.R.; McCreery R.L. *Analytical Chemistry* **1992,** *64*, 2518-24.
14. Ranganathan S.; McCreery R.L. *Analytical Chemistry* **2001,** *73*, 893-900.
15. Levy-Clement C.; Zenia F.; Ndao N.A.; Deneuville A. *New Diamond and Frontier Carbon Technology*. **1999,** *9*, 189-206.

Chapter IV-(x)

Anodic Oxidation - Diol to Dione

Dopamine and Ascorbic Acid

Abstract

Using cyclic voltammetry of dopamine and ascorbic acid, the carbon film microelectrode's electrochemical properties were found to vary with electrochemically active surface area. For small area microelectrodes the heterogeneous electron transfer was similar to HOPG. For the large area microelectrodes the heterogeneous transfer approximated hydrogenated GC. These changes were attributed to increased film thickness as the area increased, the thicker film deposit having an increased concentration of pendent alkene, alkyne and aromatic groups.

Using the cathodic wave formed during the reverse cyclic voltammetric scan of dopamine and catechol at pH 7.4, the surface area of the adsorbed species, on the carbon film, was calculated to be at least 50% of the electrochemically active surface area.

A limited study of the adsorption and catalysis of dopamine during anodic oxidation, on the carbon film surface, suggests that that the initial step is the deprotonation of the hydroxyl groups. From cyclic voltammetry at different pH's and scanning rates the adsorbed species appears to have minimal influence on the heterogeneous electron transfer.

The adsorption species in the anodic oxidation of dopamine has been reported to be dopamine quinone, with the adsorption at the surface of carbon fibre microelectrode, occurring through the amine group of catecholamines. Cyclic voltammetry of norepinephrine and catechol yielded a distinct cathodic wave on the reverse scan, which indicates that the carbonyl group is the determinant in the adsorption pathway during anodic oxidation at the surface of a carbon film microelectrode.

Introduction

4-(2-aminoethyl)benzene-1,2-diol (dopamine, 3-hydroxytyramine or DA) is the target neurotransmitter in this work and 2-oxo-L-threo-hexono-1,4-lactone-2,3-enediol (Vitamin C, ascorbic acid or AA) is a major interfering compound for applications of the carbon film microelectrodes in the extracellular fluid in the brain. Both DA and AA are 1,2-diols, which under anodic potential oxidise electrochemically and irreversibly to 1,2-diones (Figure IV-(x)-i). It is this reaction which is used to measure the concentration of DA during *in vivo* studies. (At physiological pH 7.4 DA is protonated.)

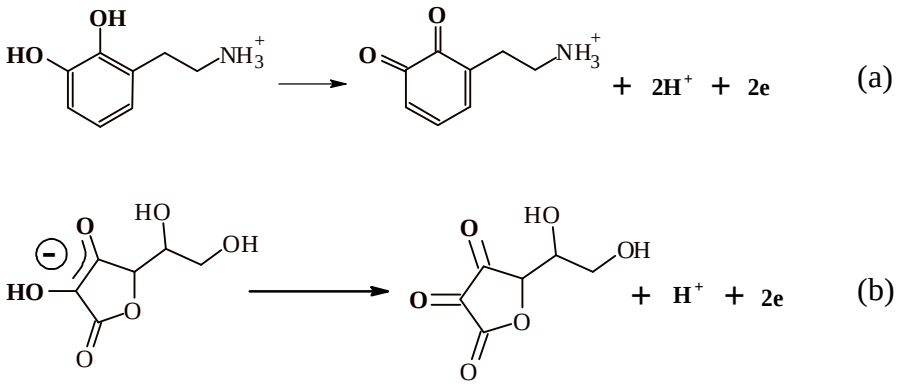

Figure IV-(x)-i
Anodic oxidation of DA (a) and AA (b) at a carbon electrode surface in pH 7.4 buffer.

Due to their common structure and electrochemical oxidation pathway both will be considered together in this chapter. Since, there is more published literature for DA in this context than that for AA, most of the discussion on surface interaction will involve DA chemistry. This literature reporting disparities probably arises from the need to maximise the DA signal from micromolar concentrations present in the extracellular fluid, whereas AA occurs in millimolar concentrations and its suppression is the subject of many papers. Perhaps

a study of the AA heterogeneous pathway mechanism may provide an insight into alternate approaches to reduce electron transfer rather than the current method of anionic barriers. The use of carbon, as the electrochemically active surface for the both *in vivo* and *in vitro* detection of DA and AA, has resulted in reporting of electron transfer mechanisms at varying carbon surface structures. Therefore, in this chapter it is the electron transfer rate of DA and AA which will be used to assist in the characterisation of the carbon film surface.

The proposed reaction pathway, at a carbon fibre surface and at pH 7.2 is adsorption of DA[1;2] onto the surface, followed by sequential loss of an electron, proton, electron and a proton.[3] This sequence is different from another publication, which purports the loss of a proton, electron, proton and electron with electron transfer as the rate determining step.[4] This latter publication however suggests that AA^- follows the previous proposed sequence as it is independent of pH.

The initial adsorption of DA onto the carbon fibre surface is the heterogeneous rate determining step, reported to involve the protonated amine group.[1] This was proposed from the waveform shape obtained during fast scanning cyclic voltammetry. The heterogeneous transfer rate of DA has also been reported to be catalysed by physisorbed DA itself on a GC surface.[5] The mechanism for DA heterogeneous electron transfer at a pyrolysed polymer surface (GC or carbon fibre) appears to be adsorption of protonated amine, oxidation of the adsorbed DA then homogeneous electron transfer between dopamine quinone and DA in solution.

At both GC and carbon fibre surfaces the cyclic voltammograms of DA showed well defined features. Freshly fractured GC had a ΔE_p 0.087 V [6] and the carbon fibre sigmodial curves were visually assessed.[7, 5] For AA at freshly fractured GC the ΔE_p was 0.356 V which increased to 0.392 V on standing in air for 10 hours. The large ΔE_p value for AA indicates a lack of self catalytic processes.

Hydrogenating the GC, which is carried out using a microwave generated plasma in a hydrogen atmosdphere,[8] produces a surface that not only has a low ΔE_p value of 0.091 V for DA but remained low, 0.097 V after 10 hours in air.[6] The ΔE_p for AA under the same conditions was 0.335 V and 0.347 V respectively. These low ΔE_p values for DA, at carbon surface containing edge planes, which have been hydrogenated, would be expected to have minimal physisorption. The heterogeneous electron transfer pathway for such a hydrophobic surface suggests a mechanism in which the hydrophobic groups on the analyte should be considered.

The HOPG the surface has an extremely slow heterogeneous electron transfer rate for DA, which yields poorly defined cyclic voltammograms.[9-11] To achieve well defined peaks the HOPG required anodic oxidation,[12] (creation of a hydrophilic surface) or laser treatment[11] (formation of edge planes).

The heterogeneous electron transfer at boron doped diamond films has also been studied. On hydrogen plasma treated surfaces the ΔE_p for DA was 0.480 V and AA 0.780 V.[13] These ΔE_p values for boron doped diamond films are considerably higher than that of hydrogen terminated glassy carbon. For boron doped diamond film "as grown" the ΔE_p for DA was 0.9 V.[14] The boron concentration in the doped diamond was $\approx 5 \times 10^{19}$ atoms cm^{-3} in both references. The low heterogeneous electron transfer rate at boron doped diamond surfaces has been attributed to the lack of adsorption of DA.[13]

From published work there is a large variation in heterogeneous electron transfer rates, for both DA and AA, and the rate is highly dependent on the chemistry of the carbon surface. DA and AA as well as being analytes of interest in the application these carbon film microelectrodes, the variations in $E½$ and waveslope may provide a means of characterising the carbon film.

Experimental Section

Chemicals

Ascorbic acid (BDH), dopamine (Aldrich), catechol (Aldrich), norepinephrine (Aldrich) potassium phosphate decahydrate (Aldrich), phosphoric acid (BDH), citric acid (Aldrich) and nitrogen (BOC Instrument Grade) were used as received.

Equipment

The three electrode system, with a Ag|AgCl (3 M KCl) reference electrode, was used as outlined in Chapter II Electrochemical Equipment.

Electrodes Fabrication

The microelectrodes were fabricated as outlined in Chapter III, using 40 ml min^{-1} nitrogen in both the parallel flow and counter flow configurations.

Procedure

Cyclic voltammetry was carried out cycling the carbon film microelectrode from -0.2 V to 0.8 V in deoxygenated 10^{-4} M solutions of DA and AA in citrate/phosphate buffer at pH 7.4. Buffer composition, 46.8 gm tri-sodium phosphate dodecahydrate and 1.9 gm citric acid per litre adjusted to pH 7.4 with phosphoric acid. All solutions were prepared daily using deoxygenated buffer. Ascorbic acid, norepinephrine and dopamine standard solutions were replaced every three hours.

Aqueous solutions were prepared using Milli-Q water (Milli-Q Reagent Water System).

Results and Discussion

Dependence of Heterogenous Electron Transfer of DA and AA as a Function of Electrode Size

The cyclic voltammograms obtained for the carbon film microelectrodes for DA and AA appear to be dependent on the quartz capillary orifice dimension. Carbon film microelectrodes with small limiting current <1 nA for 10^{-4} M DA (limiting current is indicative of electrode size) tend to display cyclic voltammograms without a waveslope. Examples of a cyclic voltammogram of DA and AA at small electrodes are shown in Figure IV-(x)-ii and Figure IV-(x)-iii.

The lack of waveslope for both DA and AA at small carbon film microelectrodes implies a carbon surface with HOPG heterogeneous electron transfer characteristics.

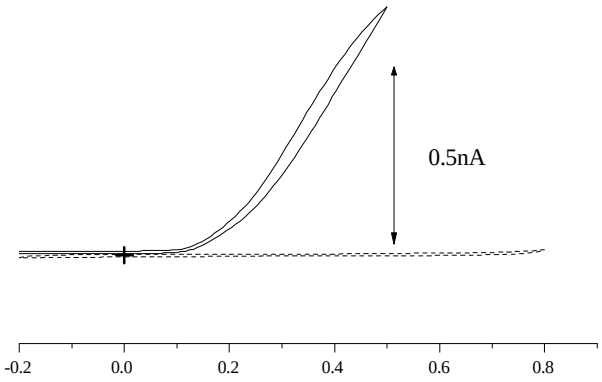

Figure IV-(x)-ii

Cyclic voltammogram of 10^{-4} M DA (—) in citrate/phosphate buffer pH 7.4 and buffer only (---) at a "small" carbon film microelectrode
Scan rate 0.1 V s^{-1}

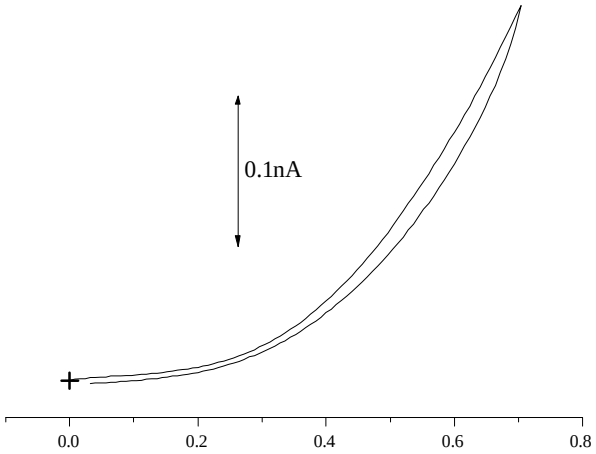

Figure IV-(x)-iii

Cyclic voltammogram of 10^{-4} M AA in
citrate/phosphate buffer pH 7.4, at a "small" carbon
film microelectrode
Scan rate 100 mV/sec

Both Figures IV-(x)-ii and iii are cyclic voltammograms obtained using the same electrode. The larger "waveslope" for AA is consistent for "medium" (up to a limiting current up 5 nA) and small electrodes.

Electrodes in the "medium" range gave very good sigmodial cyclic voltammograms for DA (Figure IV-(ix)-iv). The shape of the DA cyclic voltammogram is typical of an irreversible oxidation reaction, whereas the AA cyclic voltammogram has displayed a lack of heterogeneous electron transfer. These features of DA and AA are displayed in Figure IV-(x)-iv. The waveslope for DA in Figure IV-(x)-iv is 0.126 V/decade. Carbon surfaces with waveslopes approaching the DA value are hydrogenated GC and freshly fractured GC. The lack of a definable waveslope of AA still suggests a surface chemically similar to HOPG.

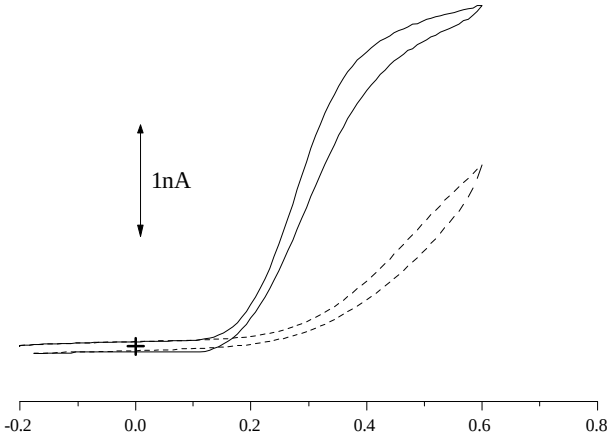

Figure IV-(x)-iv

Cyclic voltammograms of 10^{-4} M DA (—) and 10^{-4} M AA (---) in citrate/phosphate buffer pH 7.4, at a "medium" size carbon film microelectrode. Scan rate 0.1 V s^{-1}

When chronoamperometrically monitoring DA i*n vivo* the potential is fixed at 0.9 V with respect to the reference Ag|AgCl electrode.The existence of a large Faradaic current difference (approximately 50%) between AA and DA at 0.9 V indicates that these electrodes have potential for *in vivo* applications. However to monitor the small *in vivo* currents, in the picoamp range, the size of the electrodes is maximised for the specific dopagenic region of the brain. The optimum size is between 250 and 500 μm in length. (For *in vito* experiments this approximates to a limiting curent between 16 to 32 nA for a carbon film microelectrode in 10^{-4} M DA.)

To consistently fabricate the required length for *in vivo* applications requires the quartz capillary to have an orifice between 0.5 and 1 μm radius. With this orifice radius and using counter gas flow during pyrolysis, microelectrodes fabrication efficiency was 75% for microelectrodes with a length between 250 and 500 μm.

Microelectrodes of this size did not retain the Faradaic difference at 0.9 V as for the "medium" sized carbon film microelectrodes. This further change in heterogeneous electron transfer properties as the electrochemical area increases is shown in Figure IV-(x)-v.

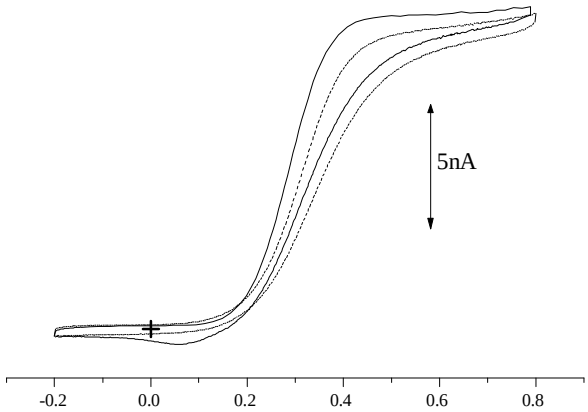

Figure IV-(x)-v

Cyclic voltammograms of 10^{-4} M DA (—) and 10^{-4} M AA (---) in a citrate/phosphate buffer pH 7.4 at a large carbon film microelectrode. Scan rate 0.1 V sec^{-1}

The cyclic voltammograms in Figure IV-(x)-v are very good examples of irreversible heterogeneous electron transfers at a microelectrode. In Figure IV-(x)-v the waveslope of DA is 0.117 V/decade and AA 0.131 V/decade. The average waveslope for "medium" to "large" carbon film microelectrodes was 0.124 V/decade, with a standard deviation of 24.0 for n=36. An average waveslope for AA for the same size range was not possible due to the number of carbon film microelectrodes having an undefined limiting current.

The almost parallel voltammetry of DA and AA at carbon film microelectrodes, of the size required for *in vivo* applications necessitates surface treatment to suppress the AA Faradaic current. With the Faradaic AA current suppressed, all changes in Faradaic current can be attributed to other oxidisable species. This is the subject of the work in Chapter V.

The heterogeneous electron transfer for DA and AA at larger microelectrodes indicates the carbon film surface is similar to that displayed by GC and hydrogenated GC. The variation in `heterogeneous electron transfer rate with microelectrode size indicates chemistry of the surface is changing.

These changes in heterogeneous electron transfer rate of DA and AA together with surface morphology differences, due to size (See Chapter III Fabrication), are probably directly related to film thickness. For small carbon film cylindrical microelectrodes the surface would have the initial layers composed almost entirely of graphene layers parallel to the quartz substrate. Such a surface would be expected to display HOPG heterogeneous electron transfer characteristics, i.e. cyclic voltammograms similar to Figures IV-(x)-ii and iii. Increasing the surface area with commensurate increase in carbon film thickness changes the surface chemistry. This is suggested by changes in Raman shift spectroscopy (Chapter IV-(iii)). This change in surface chemistry appears to shift towards a hydrogenated carbon surface chemistry. The possibility of edge planes on the carbon film surface has been eliminated, using cyclic voltammetry of AQDS (Chapter IV-(v)), $Fe(CN)_6^{3-/4-}$ (Chapter IV-(ix)), capacitance (Chapter IV-(v)) measurements and Raman shift spectroscopy. Pyrolysis of acetylene to form the carbon film is expected to form a surface containing alkyne, alkane (Chapter IV-(vii)) and aromatic pendent groups (Chapter IV-(iii)). Such a surface rich in pendent electron polarisable groups, alkenes, alkynes, aromatic chains, and probable conjugation between all, could provide an environment promoting hydrophobic segments of molecules favourable to adsorption/orientation near the graphene regions. Charged ions, such as AA would not be favoured for heterogeneous electron transfer.

Cathodic Wave

Examination of the cyclic voltammogram of DA between 0.2 and -0.2 V on the reverse scan (Figure IV-(x)-v) reveals a slight cathodic wave. This is not present in the cyclic voltammogram of AA on the same carbon film microelectrode. The proposal that DA is

adsorbed on the surface of the electrode, via the amine group is the rate determining step,[1] with the adsorbed DA providing catalysis for the heterogeneous electron transfer[5] may explain this wave.

The anodic oxidation of DA is electrochemically irreversible, therefore only if the dopamine quinone, formed by oxidation of DA, remains adsorbed on the surface is cathodic reduction possible. The lack of this wave in the cyclic voltammograms of AA suggests that adsorption is not involved in the heterogeneous reaction pathway AA oxidation.

To elucidate this further catechol and norepinephrine were examined using cyclic voltammetry. The electrode reaction is the same as DA and AA, i.e. a two electron transfer during the oxidation of a 1,2-diol to a 1,2-dione at pH 7.4. This is shown in Figure IV-(x)-vi. The cyclic voltammograms of catechol and norepinephrine are shown in Figure IV-(x)-vii. Also included are the cyclic voltammograms of DA and AA, together with insets showing the cathodic wave regions.

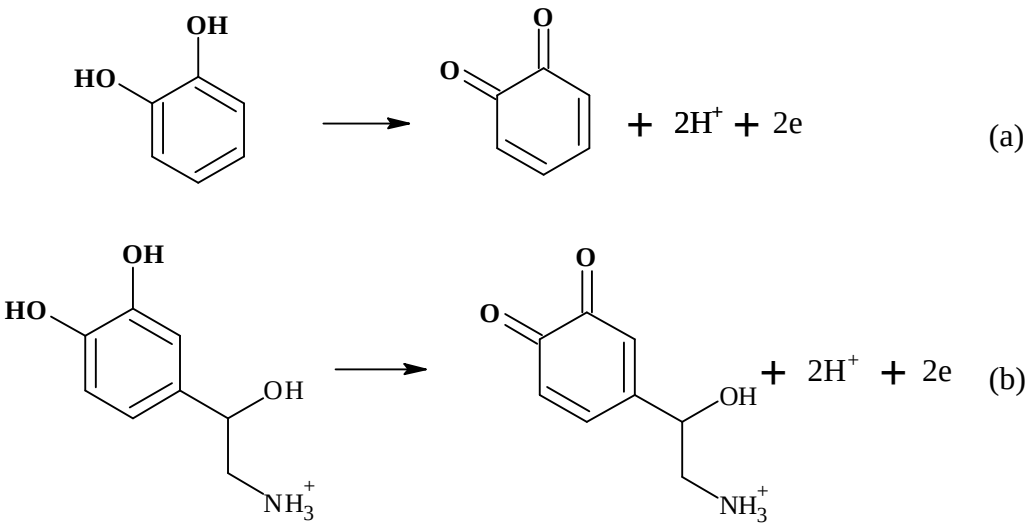

Figure IV-(x)-vi

Anodic oxidation of catechol (a) and norepinephrine (b) at a carbon electrode

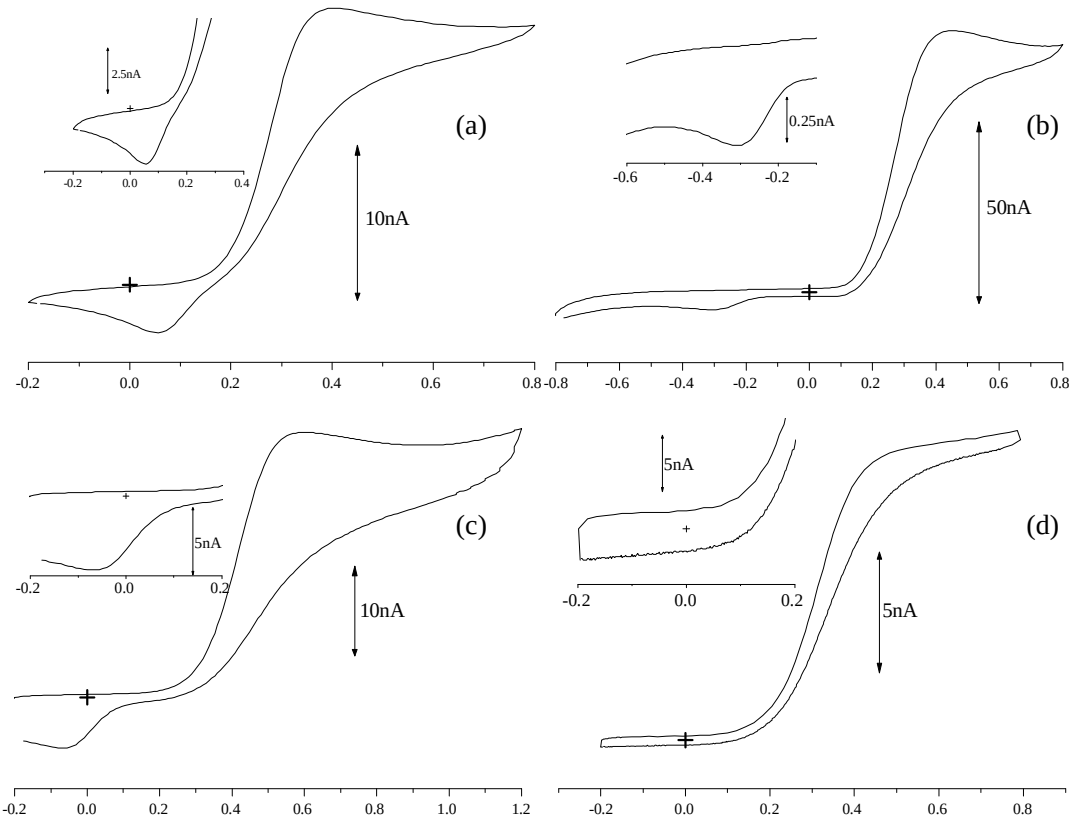

Figure IV-(x)-vii

Cyclic voltammograms of 10^{-4} M solutions of DA (a), norepinephrine (b), catechol (c) and AA (d) in citrate/phosphate buffer pH 7.4
Insets are cyclic voltammograms between -0.2 V and 0.2 V.
Scan rate 0.1 V s^{-1}

The cathodic waves in the cyclic voltammograms of catechol and norepinephrine occur at a lower potential than the commencement of the escarpment of the anodic scan. This is evidence that the cathodic wave is not an artefact of non-steady state voltammetry. The potential of the cathodic wave varies (up to 0.2 V) relative to the escarpment, indicating variability in surface chemistry. The cathodic wave of catechol indicates that the amine group on a catecholamine is not implicated in the adsorption step on carbon films, as fabricated in this work.

Verification of the origin of the cathodic wave was investigated by restricting the anodic scan range of norepinephrine to -0.8 V to 0 V. Norepinephrine was selected as the cathodic wave is well separated from the oxidation escarpment. This is shown in Figure IV-(x)-viii.

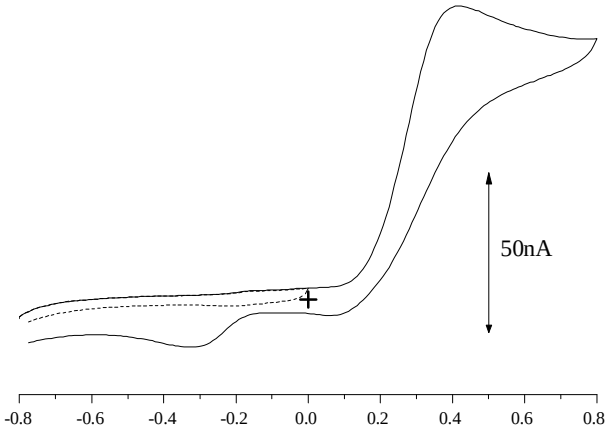

Figure IV-(x)-viii

Cyclic voltammograms of 10^{-4} M norepinephrine in citrate/phosphate buffer at pH 7.4. The potential range is (—) -0.8 V to 0.8 V and (---) -0.8 V to 0 V. Scan rate 0.25 V s^{-1}

The absence of the cathodic wave, in the restricted potential cyclic voltammogram indicates that the species undergoing reduction indicated by the cathodic wave was generated during oxidation. This result supports the proposal that a quinone is adsorbed on the surface during anodic oxidation. At a carbon fibre surface it is proposed that DA adsorbs onto the surface, which then undergoes a two electron oxidation to form the quinone, the quinone then desorbs.[2]

Effect of Adsorbed Species on Heterogeneous Electron Transfer Rate

To determine if the rate limiting step in the heterogeneous electron transfer of catechols is catalysed by adsorption the limiting current as a function of scan rate was measured. These results are presented in Table IV-(x)-i.

Table IV-(x)-i. Changes in heterogeneous electron transfer control with scan rate and electron transfer area (expressed as moles/cm^2) calculated from cathodic wave.

Catechols	Electrode	Heterogeneous Electron Transfer Control	Scan Rate Range ($V\ s^{-1}$)	Cathodic Wave Area Average moles cm^{-2} (Range)
Norepinephrine	A	Diffusion	0.05-0.25	$1.1x10^{-11}$ ($0.8\text{-}1.3x10^{-11}$)
	B	Adsorption	0.05-5	$3.5x10^{-12}$ ($0.9x10^{-12}$-$1.1x10^{-11}$)
		Diffusion	0.5-5	
	C	In determinant	0.1-5	$3x10^{-12}$ ($3x10^{-13}$-$1.9x10^{-11}$)
Catechol	A	Adsorption	0.025-0.5	$2.0x10^{-11}$ ($1.4\text{-}3.6x10^{-11}$)
	B	Diffusion	0.1-5	$1.0x10^{-10}$ ($4.5x10^{-11}$-$3.6x10^{-10}$)
	C	Diffusion	0.025-5	$2.8x10^{-11}$ ($1.2\text{-}4.6x10^{-11}$)
DA	D	Diffusion	0.1-1	$1.4x10^{-11}$ ($0.7\text{-}2.0x10^{-11}$)
	E	Inconclusive	0.1-2	$1.6x10^{-11}$ ($0.6\text{-}1.8x10^{-11}$)
	F	Inconclusive	0.25-2	$1.5x10^{-11}$ ($0.9\text{-}2.4x10^{-11}$)

The heterogeneous electron transfer control was determined by selecting the correlation coefficient closest to one. However the difference (R^2) between diffusion control and adsorption was very small. In two of the examples in Table IV-(x)-i the difference was considered in determinant. An example of the closeness of the regression analysis is shown in Figure IV-(x)-ix.

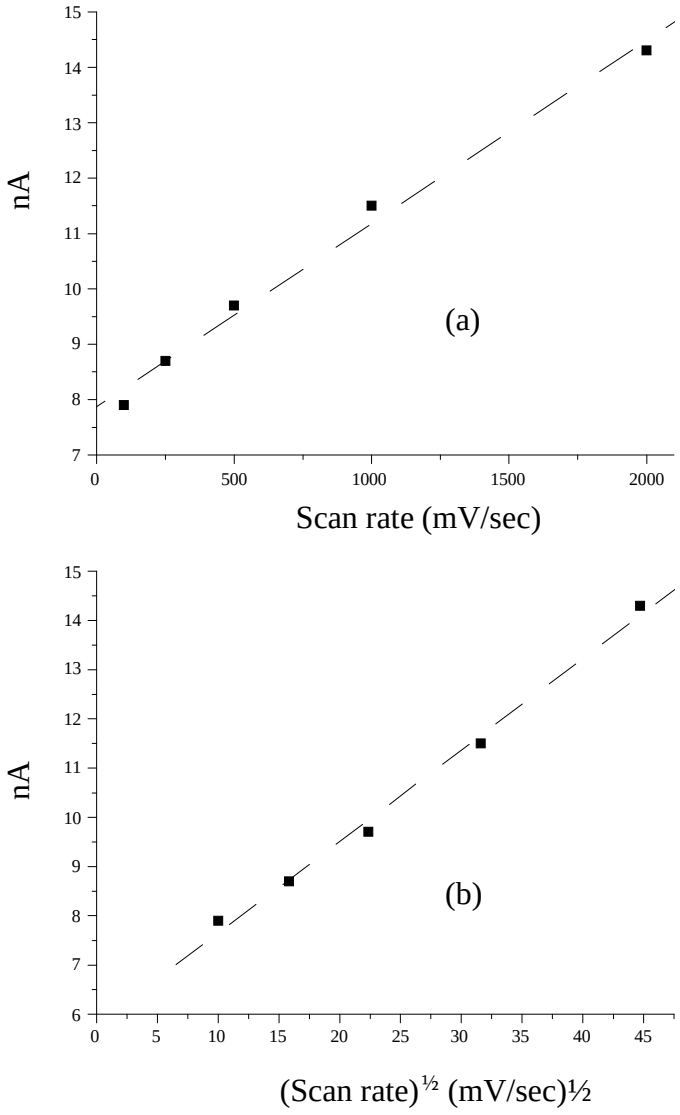

Figure IV-(x)-ix

Comparison of linear regression analyses of the limiting current and linear (a) and square (b) of the scan rate.

In Figure IV-(x)-ix (Electrode E Table IV-(x)-i) the correlation coefficient for the linear plot of limiting current versus the scan rate gave a R^2 value of 0.995; for the square of scan rate it was 0.996. It therefore appears that the adsorbed species control over the heterogeneous electron transfer is minimal.

Calculation of the Surface Area of the Adsorbed Species

The cathodic wave provides a means of estimating the area covered by the adsorbed species, which will provide a further insight into the nature of the carbon film on the microelectrode. Using the current at the lowest potential of the reverse scan as the baseline for scan rates at 0.1 V s^{-1}, the area occupied by the adsorbed species, during DA cyclic voltammetry was found to have an average $0.7x10^{-11}$ moles cm^{-2} with a range between 0.2-$1.3x10^{-11}$ moles cm^{-2} for n=10.

Assuming adsorption of catechol (being the simplest analyte used to calculate molecular area) is parallel to the carbon film surface, the maximum surface concentration would be $0.15x10^{-10}$ moles cm^{-2}. (Catechol length 420 pm and width 280 pm) It therefore appears that the adsorbed species occupies approximately 50% of the electrochemically active surface as measured using the Cottrell decay. (Chapter III Results and Discussion Small Cylindrical Microelectrodes)

As the cathodic wave for DA, catechol and norepinephrine was not visible at low scan rates, the cathodic wave area was measured at faster rates to determine if the area was scan rate dependent. The cathodic wave area was found not to be scan rate dependent. The average and range of results of this investigation are presented in Table IV-(x)-i. These results indicate that the catechol cathodic wave appears slightly larger for dopamine, with norepinephrine the smallest. The smaller cathodic wave size of norepinephrine does appear to be a real feature, as only the “large” electrodes displayed a cathodic wave. Examination of cathodic waves for dopamine and catechol from the same carbon film microelectrodes indicate that they have the same propensity to form an adsorbed species. The results of cathodic wave area measurements are shown in Table IV-(x)-ii.

The surface coverage of the adsorbed species on several carbon film microelectrodes, derived from results from cathodic wave measurements has exceeded the theoretical coverage of $0.15x10^{-11}$ moles cm^{-2} for DA. Therefore when considering these measurements, the

accuracy of the microelectrode dimensions calculated from the Cottrell decay and defining the cathodic wave area should be considered. With both of these considerations the adsorbed species probably has coverage of at least 50% of electrochemically active area. The mix of adsorbed and "free" areas may explain the variable heterogeneous electron transfer control determined by scan rate. The lower than theoretical coverage suggests the adsorbed species are parallel to the graphene region.

Table IV-(x)-ii. Comparison of adsorbed species coverage on the same carbon film microelectrodes`

	Catechol	Dopamine
Electrode	Moles cm^{-2}	Moles cm^{-2}
G	$2.1x10^{-11}$	$2.1x10^{-11}$
H	$2.6x10^{-11}$	$1.6x10^{-11}$
I	$3.4x10^{-11}$	$0.6x10^{-10}$

From these results it is proposed that the aromatic component of the catechols provide the interface for the initial contact with the carbon film surface. The presence of electrically conductive surface adjacent to the graphene region provides the surface for the heterogeneous electron transfer. If this adjacent conductive surface is not present then a heterogeneous electron transfer similar to an atomically flat basal plane of HOPG will occur, i.e. an insignificant electron transfer rate.

Heterogeneous Electron Transfer Pathway for the Oxidation of Dopamine at a Carbon Film Surface

The published heterogeneous electron transfer pathways for the anodic oxidation of catechols[3;4] are based on the "square" or "nine member box" system of Laviron for 1,4-benzoquinone/hydroquinone at a platinum electrode.[15] This is shown in Figure IV-(x)-x.

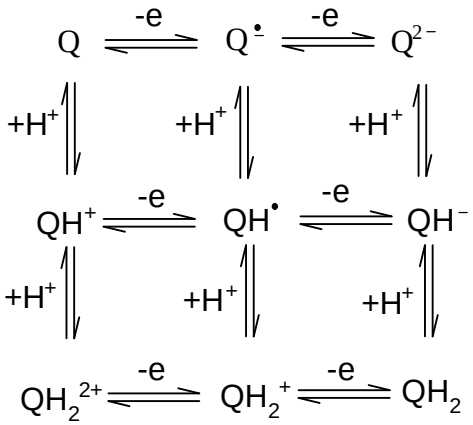

Figure IV-(x)-x

Heterogeneous electron transfer pathway
for 1,4-benzoquinone/1.4-hydroquinone**.**

:

At neutral pH the following pathway has been proposed for catechol anodic oxidation at carbon paste electrodes:[4]

$$QH_2 \overset{-H^+}{\rightleftharpoons} QH^- \overset{-e}{\rightleftharpoons} QH\bullet \overset{-H^+}{\rightleftharpoons} Q\bullet^- \overset{-e}{\rightleftharpoons} Q \qquad \text{(i)}$$

In this pathway (equation (i)) the initial step is the loss of a proton, suggesting a greater pH dependency for the anodic to the cathodic pathway.

An alternative pathway for an adsorbed species is outlined in equation (ii).[3]

$$QH_2 \overset{-e}{\rightleftharpoons} QH_2^+ \overset{-H^+}{\rightleftharpoons} QH\bullet \overset{-e}{\rightleftharpoons} QH^+ \overset{-H^+}{\rightleftharpoons} Q \qquad \text{(ii)}$$

In equation (ii) the initial step in this pathway is the loss of an electron and the formation of positively charged intermediate. The presence of a positively charged intermediate suggests the possibility of nucleophilic attack by hydroxide ions. Such a reaction has been reported to occur during the oxidation of phenol.

During the anodic oxidation of phenol, in 0.09 M H_2SO_4 at a GC electrode (Figure IV-(x)-xi), nucleophilic addition of hydroxide ions occurred to yield 1,4-benzoquinone and 1,2-benzoquinone.[16] The proposed mechanism was the initial loss of an electron and a proton to form the phenoxy radical. The phenoxy radical loses a further electron, to form phenoxonium

ion, which then undergoes nucleophilic addition, with a hydroxide ion, at the 2 or 4 position. Both of the hydroxy groups then under go anodic oxidation, losing two electrons and two protons. This reaction pathway yields a stoichiometric total of three electrons for the anodic oxidation of phenol.

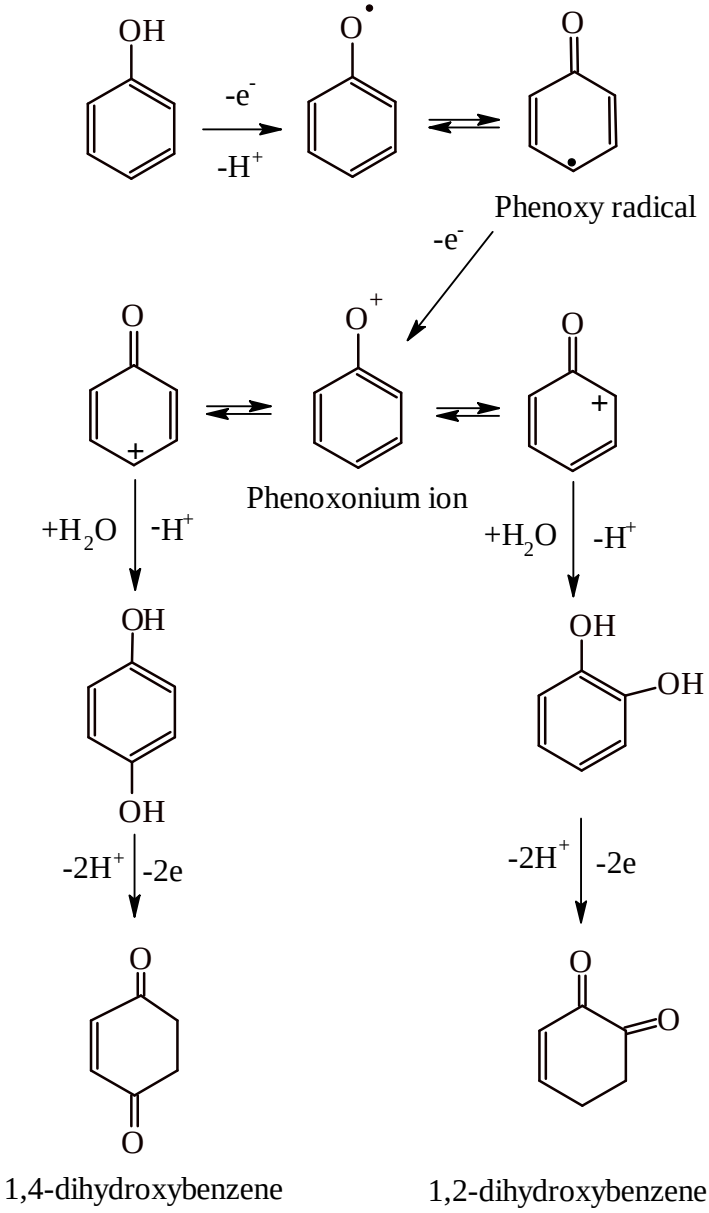

Figure IV-(x)-xi

Anodic oxidation pathway of phenol in 0.09 M H_2SO_4 at a GC electrode.[8]

If, during the anodic oxidation of DA, catechol or norepinephrine nucleophilic addition of a hydroxide ion occurred the electrochemical oxidation stoichiometry would be in excess of two electrons per mole of catechol unless the second hydroxy group in the 1,2-diol configuration of the catechols completely deactivates the ortho and para directing effect of the first hydroxy group. Such an explanation would be necessary for a reaction pathway for the anodic oxidation of a catechol, which includes a positively charged species.

If the anodic oxidation reaction pathway proposed in equation (i) is occurring then E½ may be related to the pK_a of the catechols. The pK_a of the catechols used in this thesis work are listed in Table IV-(x)-iii.

Table IV-(x)-iii. pK_a values of catechols

Catechols	pK_1	pK_2	pK_3
DA	8.96	10.5	11.2
Catechol	9.3	13.0	
Norepinephrine	8.57	9.53	11.1

The closeness of the pK_a values for the catechols in Table IV-(x)-iii precludes the possibility of variations in *E½* providing an indication of the possible anodic oxidation pathways.

If Equation (i) is the heterogeneous electron transfer pathway, at a carbon film surface, a shift in *E½* will reflect changes in the pH of the supporting electrolyte. If Equation (ii) is the pathway then independence of pH will exist as the adsorption of DA is suggested to be a precursor and rate limiting step to the heterogeneous electron transfer. This dependency on rate of adsorption was detected by a decrease in limiting current during rapid scanning cyclic voltammetry.[1]

To establish the most probable heterogeneous electron transfer pathway for the anodic oxidation of DA, cyclic voltammetry of DA was carried out in supporting electrolytes at three

different pHs, 2.1, 7.4 and 10.1. The cyclic voltammetry at pH 2.1 (citric acid) is shown in Figure IV-(x)-xii.

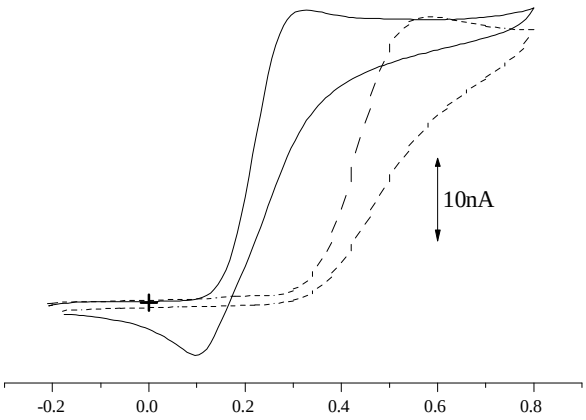

Figure IV-(x)-xii

Cyclic voltammograms of 10^{-4} M DA in citrate/phosphate buffer pH 7.4 (—) and $2x10^{-3}$ M citric acid (---)
Scan rate 0.1 V s^{-1}

The effect of acidifying the solution has resulted in the loss of the cathodic wave at -0.2 V to 0.2 V and *E½* has shifted 0.2 V (n=7) to a higher potential. The shift in *E½*, over the pH range 7.4 to 2.1, is approximately is 0.05 V/pH. This pH dependency, of *E½*, is half that reported for carbon fibre over this range. [3]

The shift in *E½*, in acidic solutions of DA, results in the heterogeneous electron transfer being hindered by protonation. This shift in *E½* is probably due to either a reduction in the concentration of DA^- or desorption of the adsorbed species at low pH.

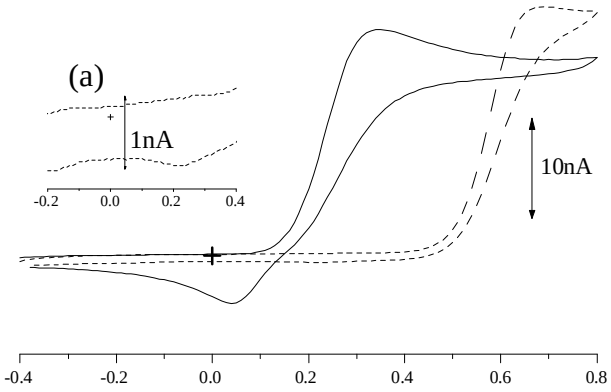

Figure IV-(x)-xiii

Cyclic voltammograms of 10^{-4} M catechol in citrate/phosphate buffer pH 7.4 (—) and $2x10^{-3}$ M citric acid, pH 2.1 (---)
Scan rate 0.1 V s^{-1}
Inset is a section of the cyclic voltammogram of catechol in citric acid between -0.2 V to 0.4 V.

The cyclic voltammogram of catechol (Figure IV-(x)-xiii), pH 2.1 citric acid displays a similar effect of reducing the pH as that with dopamine. The $E½$ is shifted to a more anodic potential at pH 2.1 ($\Delta E½$ 0.3 V (n=10)), however the cathodic wave size has been reduced. The residual cathodic wave of catechol has shifted anodically from 0.05 V to 0.2 V. This similarity between DA and catechol verifies the participation of the hydroxy groups as the adsorbed species on a carbon film surface.

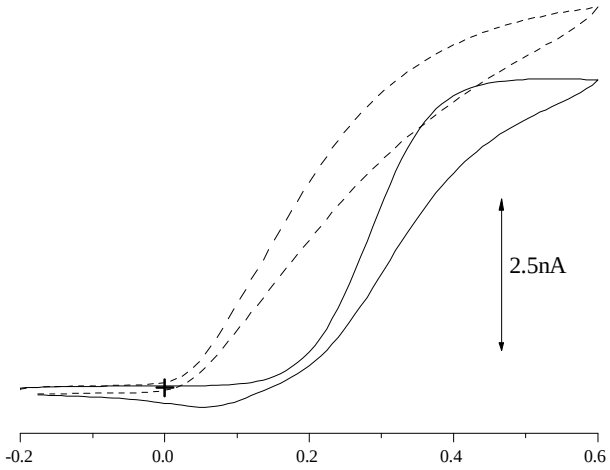

Figure IV-(x)-xiv

Cyclic voltammograms of 10^{-4} M DA in citrate/phosphate buffer pH 7.4 (—) and phosphate buffer pH 10.1 (---) Scan rate 0.1 V/sec

When the anodic oxidation of DA is carried out in a phosphate buffer at pH 10.1, (Figure IV-(x)-xiv the oxidation is shifted 0.2 V to a lower potential, when compared to pH 7.4 (0.08 V/pH). At this higher pH the waveslope is similar, however the limiting current has increased and the cathodic wave has disappeared. The increase in limiting current is probably due to an increase in diffusion coefficient, as the DA is no longer positively charged. The disappearance of the cathodic wave maybe attributed to amalgamation into the reverse scan escarpment. This possibility is based on the cathodic wave minimum potential appearing to be independent of the $E½$ of the anodic oxidation of the catechol.

This feature is shown in Figure IV-(x)-xv of the anodic oxidation of catechol at pH 10.1. As an adsorbed species its interaction with the carbon film is expected to be independent of the heterogeneous electron transfer reaction occurring.

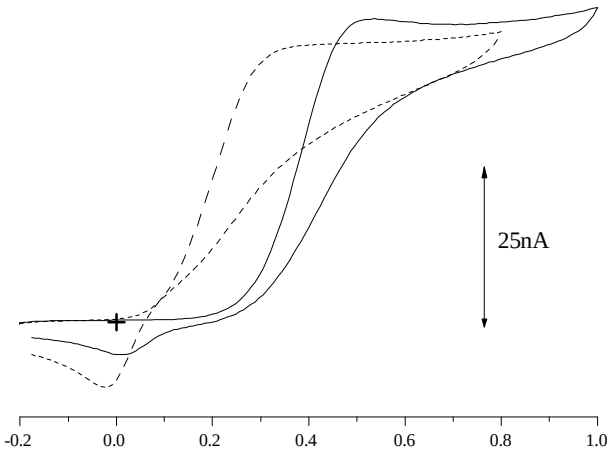

Figure IV-(x)-xv

Cyclic voltammograms of 10^{-4} M catechol in
citrate/phosphate buffer pH 7.4 (—) and phosphate buffer
pH 10.1 (---)
Scan rate 0.1 V s^{-1}

The cyclic voltammogram of catechol shown in Figure IV-(x)-xv depicts an unchanged limiting current and cathodic wave with a cathodic shift in $E_{½}$ of 0.2 V. The basic environment appears to catalyse the heterogeneous electron transfer.

From this thesis work the heterogeneous electron transfer for a catechol at a carbon film microelectrode is pH dependent. Increasing the pH catalyses the heterogeneous electron transfer, suggesting deprotonation of the hydroxyl group is a critical step in the heterogeneous pathway. The decrease in the cathodic wave size, with increasing or decreasing pH and the lack of consistency in the determination of diffusion or adsorption control using changes in scanning rate, indicates that adsorption of either the dopamine quinone or an intermediate are not critical in heterogeneous electron transfer during the anodic oxidation of DA. The lack of similar changes in cyclic voltammetric shapes, with higher pH, when comparing catechol and DA, (Figures IV-(x)-xiv and xv) indicates that the amine group on the DA may be influencing

the heterogeneous electron transfer. This suggests that Equation (i) probably best describes the anodic oxidation pathway of DA at a carbon film microelectrode.

Conclusion

Cyclic voltammetry of DA and AA has provided an indication into the varying chemistry of carbon film microelectrode surface as the electrochemically active area changes. Using the published heterogeneous electron transfer characteristics of carbon electrodes these changes appear to be directly related to the presence of hydrophobic, aromatic and/or aliphatic groups on the surface. The surface concentrations of these groups increase with film thickness. The "small" carbon film microelectrodes with a thin carbon coating displayed a surface similar to HOPG. As the coating thickness increased (with surface area) the carbon film had the characteristics of a hydrogenated carbon surface, with respect to the heterogeneous electron transfer of DA and AA.

The cathodic wave occurring during the cyclic voltammetry of DA and catechol at pH 7.4 provided a unique opportunity to measure the area of the graphene regions. This adsorption of a catechol together with excellent heterogeneous electron transfer properties of the carbon film indicates the unique nature of the structures present on the surface.
From this limited work, the catalysis of dopamine on the carbon film surface was attributed to the adsorption of the aromatic component of the catecholamine. Using this hypothesis the difference in $E½$ of catechols is attributed to the pK_a of the hydroxyl groups undergoing anodic oxidation. It is proposed that it is the uncharged moiety which undergoes anodic oxidation. The self catalysis of dopamine in neutral and basic solutions, during cyclic voltammetry, at high scan rates was attributed to the adsorption of dopamine quinone.

References

1. Bath B.D.; Michael D.J.; Trafton B.J.; Joseph J.D.; Runnels P.L.; Wightman R.M. *Analytical Chemistry* **2000,** *72*, 5994-6002.
2. Bath B.D., Martin H.B., Wightman R.M., and Anderson M.R. *Langmuir* **2001**, *17*, 7032-7039.
3. Runnels P.L., Joseph J.D., Logman M.J., and Wightman R.M. *Analytical Chemistry*, **1999**, *71*, 2782-2789.
4. Deakin M.R.; Kovach P.M.; Stutts K.J.; Wightman R.M. *Analytical Chemistry* **1986,** *58*, 1474-80.
5. DuVall S.H. and McCreery R.L. *Journal of the Chemical American Society*, **2000**, **122**, 6759-6764.
6. Kuo T.C.; McCreery R.L. *Analytical Chemistry* **1999,** *71*, 1553-60.
7. Dayton M.A.; Ewing A.G.; Wightman R.M. *Analytical Chemistry* **1980,** *52*, 2392-96.
8. DeClements R. ; Swain G.M.; Dallas T.; Holtz M.W.; Herrick R.D.; Stickney J.L *Langmuir* **1996,** *12*, 6578-86.
9. Kneten K.R.; McCreery R.L. *Analytical Chemistry* **1992,** *64*, 2518-24.
10. Swain G.M.; Kuwana T. *Analytical Chemistry* **1991,** *63*, 517-19.
11. Bowling R.J. ; Packard R.T.; McCreery R.L. *Journal of the American Chemical Society* **1989,** *111*, 1217-23.
12. Wightman R.M.; Palk E.C.; Borman S.; Dayton M.A. *Analytical Chemistry.* **1978,** *50*, 1410-14.
13. Granger M.C.; Witek M.; Xu J.; Wang J.; Hupert M.; Hanks A.; Koppang M.D.; Butler J.E.; Lucazeau G.; Mermoux M.; Stropek J.W.; Swain G.M. *Analytical Chemistry* **2000,** *72*, 3793-804.
14. Alehashem S.; Chambers F.; Strojek J.W.; Swain G.M. *Analytical Chemistry* **1995,** *67*, 2812-21.
15. Laviron E. *Journal of Electroanalytical Chemistry* **1984,** *164*, 213-27.
16. Gattrell M.; Kirk D.W. *Canadian Journal of Chemical Engineering* **1990,** *68*, 997-1003.

Chapter IV-(xi)

Surface Oxidation

Abstract

The carbon film microelectrodes were oxidised in citrate/phosphate buffer pH 7.4 for 60 and 100 seconds to determine the location of sites undergoing electrochemical oxidation. Under these conditions the E½ and waveslope of DA and AA were reduced. The capacitance and limiting current were unaffected. This suggests the oxidation is not occurring at the graphene regions. It is proposed that pendent groups are being oxidised and catalysing the heterogeneous electrode transfer.

The anodic oxidation, in citrate/phosphate buffer reduced the inherent selectivity of DA in the presence of AA when compared to the non-oxidised carbon film.

Introduction

Simple electrochemical oxidation of carbon electrodes was an early technique used to improve the heterogeneous electron transfer of DA and provide selectivity in the presence of AA.[1] The published electrochemical conditions applied to oxidise the surface varied in rigour, ranging from 7 V to -5 V cycle at 0.1 V s^{-1} in a phosphate buffer pH 7.4 for several minutes[2] to 0 V to 3 V cycling for 20 seconds followed by 1.5 V for twenty seconds in a saline solution.[1] It was reported that the most vigorous conditions provided discrimination of AA and DA using differential pulse voltammetry. Although an electrochemically oxidised surface is a simple approach to improve selectivity of DA from AA, it is prone to fouling when used *in vivo*.[3] As both selectivity and fouling are of interest in this work the use of electrochemical oxidation of the carbon film surface was investigated. Additionally, the electrochemical nature of the oxidised surface may provide additional information on the chemical structure of the surface as formed.

Electrochemical oxidation of carbon fibre (in deoxygenated solutions) is reported to form a range of oxides, with intercalation occurring in acid solutions at high potentials.[4] At neutral pH and lower voltages (1.75 V for 5 minutes in 0.1 M KNO_3 then 1 minute at -1 V, vs. SCE) surface oxides were also produced on GC without a change in surface area.[5]
The surface oxides, from X-ray and elemental analysis, suggested a range of oxygenated functional groups. The high oxygen content suggested the presence of both carbonyl and hydroxyl groups.[6] These surface oxides increased the wettability of the GC surface resulting in a change in contact angle from 72° to 54°, (using sessile drop method with 0.1 M KNO_3). Such a large contact angle change would result in a hydrophilic surface. The hydrophilic surface would be expected to promote heterogeneous electron transfer during oxidation of DA and AA without adsorption.

The anodic oxidation of HOPG surface (cycling between 0.136 V to 1.63 V vs. SCE for 2 – 5 cycles) in 1 M KNO_3, acetate buffer pH 5.2 and 1 M H_2SO_4 resulted in intercalation of the anions leading to the formation of blistering of the surface.[7;8] The blisters formed were 20 to 1000 nm in height and 0.5 to 50 μm at the base. With phosphate anions, as the supporting electrolyte, etching occurred along the "grain boundaries".[8] The use of phosphate anions produced minimal damage to the HOPG surface, therefore in this thesis work the citrate/phosphate buffer pH 7.4 was adopted as the supporting electrolyte during the anodic oxidation of the carbon film on the microelectrodes. The reported etching along the grain boundaries suggests the exposure of edge planes with the consequential increase in capacitance.

If, therefore the carbon film microelectrode can be anodically oxidised, without a change in graphene area, but with changes in $E½$ or waveslope, this would imply that oxidisable and surface assessable structures are present, such as pendent groups, since edge planes are absent from the carbon film surface. An increase in capacitance together with a

decrease in $E_{1/2}$ and waveslope would indicate a surface which was predominantly HOPG in nature.

Experimental Section

Chemicals

Ascorbic acid (BDH), dopamine (Sigma Aldrich), potassium phosphate decahydrate (Sigma Aldrich), phosphoric acid (BDH), citric acid (Sigma Aldrich) and nitrogen (BOC Instrument Grade) were all used as received . All solutions were prepared daily, ascorbic acid and dopamine solutions were replaced every three hours. Aqueous solutions were prepared using Milli-Q water (Milli-Q Reagent Water System).

Equipment

The three electrode system, using Ag|AgCl (3 M KCl) reference, as outlined in Chapter II Electrochemical Equipment, was used.

Electrodes Fabrication

The carbon film microelectrodes were fabricated as outlined in Chapter III using 40 ml min^{-1} nitrogen in both the parallel flow and counter flow configurations.

Procedure

Cyclic voltammetry, cycling from -0.2 V to 0.8 V was carried out in 10^{-4} M solutions of DA and AA in a deoxygenated citrate/phosphate buffer at pH 7.4 (Buffer composition, 46.8 gm tri-sodium phosphate dodecahydrate and 1.9 gm citric acid per litre adjusted to pH 7.4 with phosphoric acid.)

Chronopotentiometric anodic oxidation, in citrate/phosphate buffer, was carried out at 1.5 V for 60 and 100 seconds using eDAQ Scope software.

Results and Discussion

A typical chronoamperometric response for the oxidation of a carbon film microelectrode at 1.5V for sixty seconds in citrate/phosphate buffer is shown in Figure IV-(xi)-i.

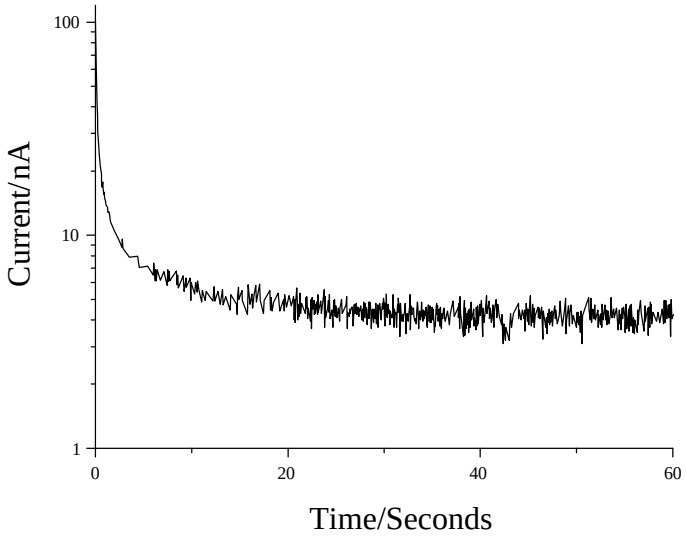

Figure IV-(xi)-i

Chronoamperometry of a carbon film microelectrode
at 1.5 V in citrate/phosphate buffer

The chronoamperometric trace, of a $3x10^{-4}$ cm^2 microelectrode, indicates approximately twenty seconds' stabilisation time followed by a steady 14 $\mu A\ cm^{-2}$ anodic current. The noise on the trace is attributed to oxygen gas evolution at the surface.[5]

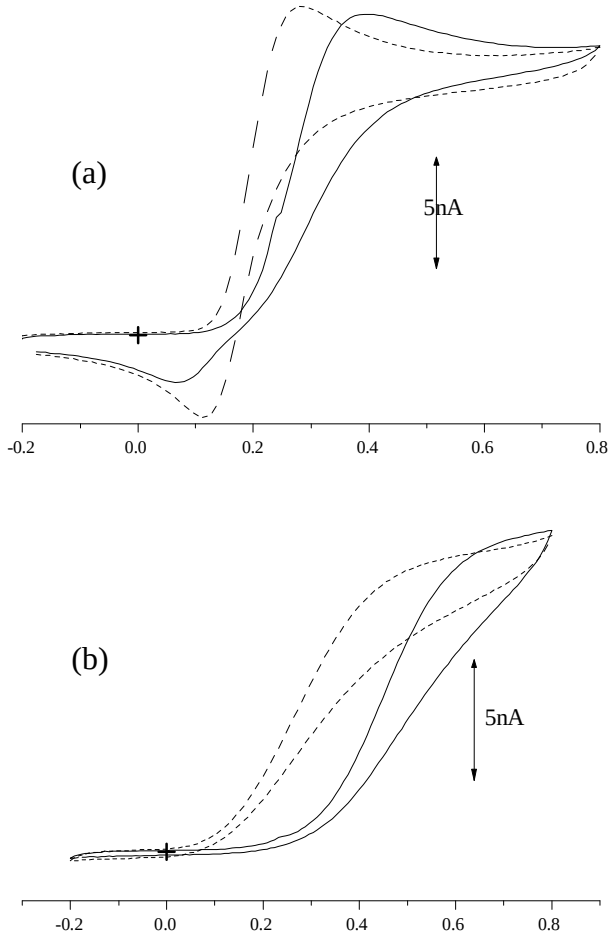

Figure IV-(xi)-ii

Cyclic voltammograms of 10^{-4} M DA (a), (—) before and after (---); 10^{-4} M AA (b), (—) before and (---) after anodic oxidation in citrate\phosphate buffer pH 7.4 at a carbon film microelectrode.
Scan rate 0.1 V sec^{-1}

The effect of this mild anodic oxidation on the carbon film can be seen in the changes in the cyclic voltammetry of DA and AA as shown in Figure IV-(xi)-ii. The anodic oxidation of the carbon film on the microelectrode resulted in the shift of the *E½* of DA to a lower potential with a smaller waveslope. Figure IV-(xi)-ii (a) the *E½* shift was 0.272 V to 0.199 V, the waveslope decreased from 0.094 to 0.057 V/decade. The limiting current for DA

decreased slightly from 13.1 nA to 12.5 nA. However for a range of samples (n=9) the average limiting current increased 5% (standard deviation 8.4%). The average waveslope decreased from 0.123 V/decade to 0.066 V/decade and $E½$ decreased from 0.290 V to 0.198 V. The lack of change in capacitance can be seen in the non Faradaic region (-0.1 V to -0.2 V) of the cyclic voltammogram.

Qualitative measurements for AA changes were not possible as the limiting current in the original (before) scan, could not be defined. Visually, the $E½$ of AA has shifted to a lower potential with negligible change in waveslope.

The change in waveslope and $E½$ for DA under mild anodic oxidation has significantly changed the heterogenous electron transfer at the carbon film surface without a significant change in the limiting current or capacitance.

The formation of oxides, particularly hydroxyl groups would promote surface adsorption of dopamine and/or dopamine semi quinone via hydrogen bonding thereby providing a hydrophilic interaction. The mildly anodically oxidised surface therefore provides two possible reaction pathways for heterogeneous electron transfer: (a) the original adsorption orientation interaction, (b) the hydrophilic orientation interaction with the oxides. The retention of the original pathway is evident by the retention of the cathodic wave. This combination of pathways would explain the significant changes in $E½$ and waveslope.
The lack of change in limiting current and capacitance, together with the retention of the cathodic wave, indicates that the graphene regions were not attacked during anodic oxidation. Therefore to achieve major changes in heterogeneous electron transfer without chemically modifying the graphene region suggests that pendent groups are present and oxidation of these groups occurred close to the graphene regions.

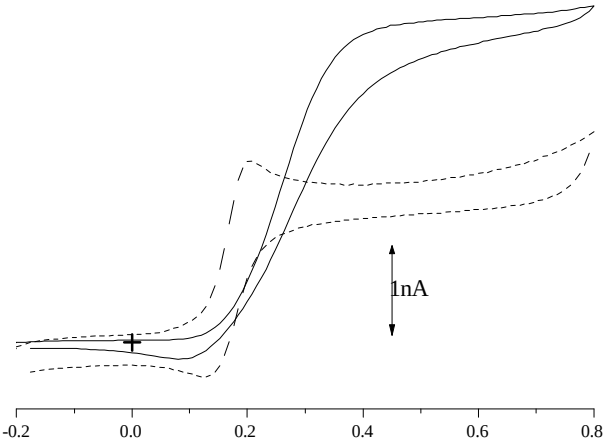

Figure IV-(xi)-iii

Cyclic voltammograms of 10^{-4} M DA (—) before and after (---) anodic oxidation, in citrate/phosphate buffer pH 7.4, at a carbon film microelectrode. Scan rate 0.1 V sec^{-1}

To further investigate the effect of anodic oxidation on the carbon film the oxidation time was extended to 100 seconds. The cyclic voltammetry of DA after this extended time can be seen in Figure IV-(xi) iii.

The limiting current decreased by 50% and the capacitance increased fourfold, the waveslope and E½ decreased by 60% (n=2). To account for these changes in E½ and waveslope it is proposed that oxidation of the graphene region has occurred. The loss of the cathodic wave indicates that possibly all the sites providing DA adsorption have now been destroyed. The heterogeneous electron transfer, at the carbon film surface after 100 seconds anodic oxidation, is thus completely under hydrophilic interaction control.

Conclusion

Anodic oxidation of carbon film microelectrodes catalysed the heterogeneous electron transfer for both DA and AA. Under mild anodic oxidation conditions, limiting current and DA adsorption was not affected, suggesting that the oxidation had not occurred in the graphene region. It is proposed that the oxidation occurred at pendent groups close to the

surface. After this mild oxidation the heterogeneous electron transfer of DA occurs through both an adsorption interaction and hydrophilic/interaction.

Under more vigorous anodic oxidation the formation of oxides or the loss of graphene carbon severely reduces the effective electrochemically active surface. This additional oxidation appears to have oxidised the hydrophobic interaction sites resulting in solely hydrophilic interaction.

The mild anodic oxidation of the carbon film reduced differentiation between DA and AA, which was the opposite of that reported for graphite electrodes.[2]

The reduction in the electrochemically active area resulting from increased anodic oxidation time is unacceptable for *in vivo* applications, as responses in the picoampere range are frequently measured.

References

1. Gonon F..; Fombarlet C.M.; Buda M.J.; Pujol J.F. *Analytical Chemistry* **1981,** *53*, 1386-89.
2. Falat L. *Analytical Chemistry* **1982,** *54*, 2108-11.
3. Suand-Chagny M.F.; Cespuglio R.; Rivot J.P.; Buda M.; Gonon F. *Journal of Neuroscience Methods* **1993,** *48*, 241-50.
4. McCreery R.L. *Electroanalytical Chemistry*, Bard A.J., Ed.; Dekker: 1991.
5. Engstrom R.C.; Strasser V.A. *Analytical Chemistry* **1984,** *56*, 136-41.
6. Kepley L.J.; Bard A.J *Analytical Chemistry* **1988,** *60*, 1459-67.
7. Wightman R.M.; Palk E.C.; Borman S.; Dayton M.A. *Analytical Chemistry.* **1978,** *50*, 1410-14.
8. Hathcock K.W. ; Brumfield J.C.; Goss C.A.; Irene E.A.; Murray R.W. *Analytical Chemistry* **1995,** *67*, 2201-06.

Chapter IV-(xii)

Ferrocene in a Non Aqueous Solvent

Abstract

` *The waveslope for the oxidation of ferrocene in acetonitrile, with $5x10^{-2}$ M tetraethylammonium hexafluorophosphate was found to have an average value of 0.048 V/decade. This very low value suggests a unique carbon surface which assists the heterogeneous electron transfer. It is proposed that the pendent groups on the surface participate in the heterogeneous electron transfer.*

Introduction

All previous surface characterisation cyclic voltammetric studies in this thesis have been carried out using supporting electrolytes in water. In this sub-chapter the cyclic voltammetry the oxidation of ferrocene (bis(cyclopentadienyl) iron) of in acetonitrile was studied. Although the oxidation of ferrocene has been studied in other solvent systems (chloroform,[1] polyethylene glycol[2]) acetonitrile was chosen as its heterogeneous electron transfer has been reported for a range of carbon surfaces. The cyclic voltammetry of the oxidation of ferrocene in acetonitrile therefore provides another insight into the possible surface structures present on the surface of the carbon film.

The oxidation of ferrocene to ferricinium ion (Equation (i)) is a single reversible electron transfer in non-aqueous solvents[3] with the heterogeneous electron transfer being diffusion controlled for all carbon surfaces.[4-6]

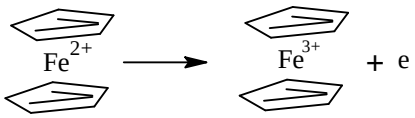

(i)

In this sub chapter cyclic voltammetry has been used to measure the waveslope of the oxidation of ferrocene in acetonitrile, using tetraethylammonium hexafluorophosphate (TEAHFP) as the supporting electrolyte, as this allows comparisons with published ΔE_p values and assign possibly surface structure to the carbon film.

Experimental Section

Chemicals

Ferrocene (Aldrich), acetonitrile (Aldrich) and tetraethylammonium hexafluorophosphate (Aldrich) were used as received.

Equipment

The three electrode system, using pseudo platinum reference, as outlined in Chapter II Electrochemical Equipment, was used.

Electrode Fabrication

The carbon film microelectrodes were fabricated as outlined in Chapter III using 40 ml min^{-1} nitrogen in both the parallel flow and counter flow configurations.

Procedure

Safety

The appropriate care should be taken when handling acetonitrile. Cyclic voltammetry has to be carried out with adequate ventilation.

Cyclic voltammetry

The carbon film microelectrode was cycled from 0 V to 0.9 V in deoxygenated $5x10^{-2}$ M tetraethylammonium hexafluorophosphate acetonitrile solution containing 10^{-4} M ferrocene at scan rates from 0.005 V s^{-1} to 10 V s^{-1}.

Results and Discussion

The cyclic voltammograms of the oxidation of ferrocene at the carbon film microelectrode gave an almost perfect sigmodial response at scan rates above 0.05 V s^{-1} (Figure XII-(xii)-i).

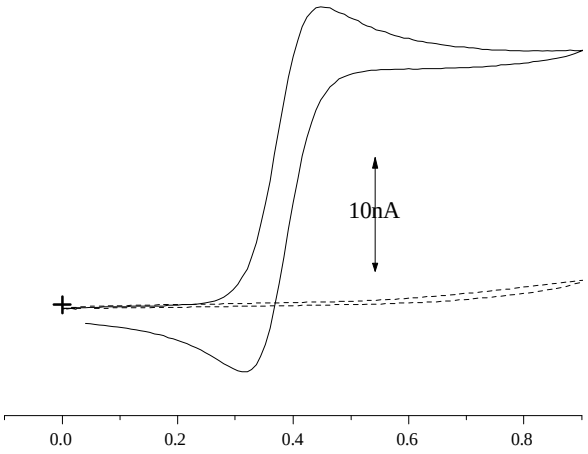

Figure IV-(xii)-i

Cyclic voltammograms of 10^{-4} M ferrocene (—) in $5x10^{-2}$ M TEAHFP acetonitrile and $5x10^{-2}$ M TEAHFP acetonitrile (---) at a carbon film microelectrode.
Scan rate 0.1 V s^{-1}

The waveslope for the oxidation of ferrocene at carbon film electrodes was 0.048 V/decade with a range between 0.068 and 0.038 V/decade (n=11). The wide range of results is attributed to convectional currents in the solvent. Acetonitrile has a lower viscosity than water and would be prone to differential temperature convection currents. This feature is (See Figure IV-(xii)-ii) evident at scan rates less than 0.05 V s^{-1} where current instability is prominent in the Faradaic region.

Although the waveslope range was very high, the values obtained are in reasonable agreement with that of a single electron transfer (0.059 V/decade).

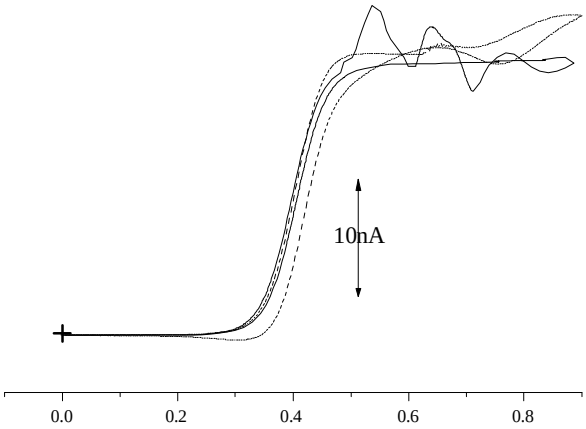

E/V vs. pseudo Pt reference

Figure IV-(xii)-ii

Cyclic voltammogram of 10^{-4} M ferrocene in $5x10^{-2}$ M TEAHFP acetonitrile at a carbon film microelectrode with a scan rate of 0.025 V s^{-1} (---) and 0.005 V s^{-1} (—).

The heterogeneous electron transfer rate for the oxidation of ferrocene at a carbon film electrode was found to be diffusion controlled from 0.25 V s^{-1} to 10 V s^{-1}. This is illustrated in Figure IV-(xii)-iii. Below 0.25 V s^{-1} the heterogeneous electron transfer rate appears to be independent of diffusion.

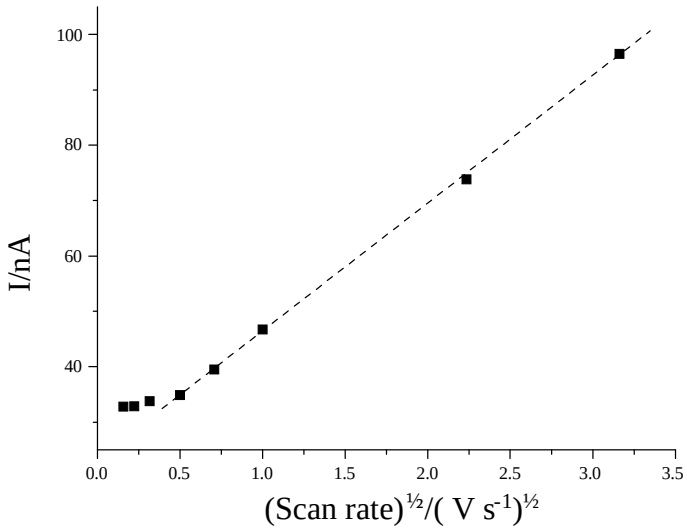

Figure IV-(xii)-iii

Limiting current of the oxidation of 10^{-4} M ferrocene in $5x10^{-2}$ M TEAHFP acetonitrile at a carbon film electrode versus the square root of the scan rate

The apparent deviation of the heterogeneous electron transfer rate from diffusion control is probably due to thermal convection currents. This is particularly evident at scan rates below 0.1 V s^{-1} and is illustrated in Table IV-(xii)-i, where the limiting current at 0.005 V s^{-1} has exceeded that of faster scan rates.

Table IV-(xii)-i. Effect of scan rates below 0.1 V s^{-1} on limiting current

	Scan Rate (V s^{-1})			
	0.1	0.05	0.025	0.005
Electrode	Limiting Current (nA)			
A	11.92	11.69	11.62	11.65
B	18.25	18.28	18.28	19.23
C	10.70	10.35	10.47	11.35
D	15.00	14.85	14.60	14.70
E	15.80	14.85	14.20	14.55

As with aqueous systems, to ascertain the nature of the surface of the carbon film microelectrode waveslope values have be compared to published ΔE_p values which are tabulated in Table IV-(xii)-ii.

Table IV-(xii)-ii. Effect of carbon surface on waveslope and ΔE_p

Carbon Surface	ΔE_p (V)	Reference
GC	0.063-0.075	4
HOPG - Edge Plane	0.087	5
Basal Plane	0.115	6
Diamond Film	0.074	7
	Waveslope (mV/decade)	
Carbon Film	0.038-0.068	This work

From the published values in Table IV-(xi)-ii the carbon film has a heterogeneous electron transfer similar to all electrodes listed except electrodes fabricated from basal plane HOPG. Previous surface characterisation experiments, in this work, have strongly suggested the absence of edge planes and sp^3 (diamond) structure, it therefore appears that the carbon film has a unique structure. The uniqueness of the surface, probably due to the presence of

pendent groups, provides a heterogeneous electron transfer pathway similar to the anodic oxidation of DA.

Conclusion

From the waveslope measurements of the oxidation of ferrocene in acetonitrile at a carbon film microelectrode, the carbon film appears to have unique carbon surface functionalities. The low values when compared to HOPG, suggest an additional heterogeneous electron transfer pathway to that occurring at an atomically flat graphene surface. From previous chapters in this work surface structures, such as pendent groups, are providing the electron transfer pathways similar to a graphite edge plane.

References

1. Pantano P.; Kuhr W.G. *Analytical Chemistry* **1993,** *65*, 2452-58.
2. Zhou H.; Dong S. *Electrochimica Acta* **1997,** *42*, 1801-07.
3. Bond A.M.; McLennan E.A.; Stojanovic R.S.; Thomas F.G. *Analytical Chemistry* **1987,** *59*, 2853-60.
4. Fann Y-C.; Hao H-S.; Kapoor R.C. *Journal of the Chinese Chemical Society (Taipei)* **1989,** *36*, 21-24.
5. Britton W.; Assubaie F. *Journal of Electroanalytical Chemistry* **1984,** *178*, 153-63.
6. Liu Y.; Freund M.S. *Langmuir* **2000,** *16*, 283-86.
7. Haymond S.; Babcock G.T.; Swain G.M. *Electroanalysis*, 2003**,** *15*, 249-53.

Chapter IV-(xiii)

Conclusion

In this Conclusion to Chapter IV "Characterisation of the Carbon Film Surface" the previous sub-chapters proposals have been correlated to postulate a surface chemistry for the carbon film formed by *in situ* pyrolysis of acetylene on a pulled quartz capillary.

The structures proposed in each sub chapter are listed in Table IV-(xiii)-i.

Table IV-(xiii)-i Summary of sub chapter surface properties.

Sub Chapter	Surface Properties
(i) Surface Stability	Surface similar to hydrogenated GC
(ii) XPS	Double and/or triple aliphatic bonds present Nitrogen bonding absent
(iii) Raman	Film thickness less than 100 carbon atoms thick Small graphene crystal clusters Film thickness decreases with distance from orifice Possible aromatic pendent groups
(iv) Capacitance	Average 6.7 $\mu F\ cm^{-2}$. Between HOPG and hydrogenated GC
(v) Edge Plane Concentration	Less than $14x10^{-12}$ mole cm^{-2}. Devoid of edge planes
(vi) Potential Window	Between -0.75 V and 1.25 V. Similar to HOPG or hydrogenated GC
(vii) Alkene and Alkyne Surface Concentration	Between $2x10^{-10}$ and $5x10^{-11}$ moles cm^{-2} Aproximately 5 to 10% of the surface. Predominately alkynes
(viii) Outer Sphere Electron Transfer $Ru(NH_3)_6^{2+/3+}$	Unique, unlike any unmodified reported carbon surface based on reported waveslope values.
(ix) $Fe(CN)_6^{3-/4-}$	Waveslope similar to HOPG Initial graphene layers parallel to the quartz substrate
(x) Diol Oxidation to a Dione DA & AA	Heterogeneous electron transfer dependent carbon film thickness Changing from HOPG to hydrogenated GC as thickness increases Cathodic wave suggests the graphene area to be greater than 50%
(xi) Electrochemically Oxidised Surface	Presence of electrochemically oxidisable pendent groups close to the graphene regions.
(xii) Ferrocene	Unique, unlike any unmodified reported carbon surface based on reported waveslope values.

To unify the required structures requires the incorporation of the following features:-

(a) Graphene network extending from the surface to the graphite powder inside the pulled quartz capillary.

(b) At least 50% of the graphene surface areas to be free from steric hindrance to molecules the size of dopamine.

(c) The surface to be free from edge planes. This implies that the uneven morphological features are achieved by limited sp^3 (-C-C-) bonding.

(d) Pendent alkene/alkyne groups accessible to the graphene regions. Such groups also require sp^3 (-C-C-) bonding to the graphene areas.

(e) Electrically conductive structures adjacent to or within the graphene region to provide a non-atomically flat electron transfer zone.

(f) Aromatic groups sufficiently isolated from the conjugated π electrons of the graphene to form fluorophores.

The requirement for a sp^3 structures and the absence of sp^3 diamond peak in the Raman spectrogram is possibly due to the spatial extent of the bonding. The sp^3 diamond peak arises from a three dimensional structure, whereas the sp^3 carbon carbon bonds on the carbon film surface are discontinuous three dimensional bonds. The low concentration of the sp^3 bonds in the surface layers, penetrated by the laser, and the small extinction coefficient of the –C-C- bond would account for the lack of a visible Raman peak. The electron rich surface is attributed to the presence of unsaturated pendent groups, aliphatic or aromatic attached to the graphene.

A diagrammatic representation of these proposed chemical structures are shown in Figure IV-(xiii)-i.

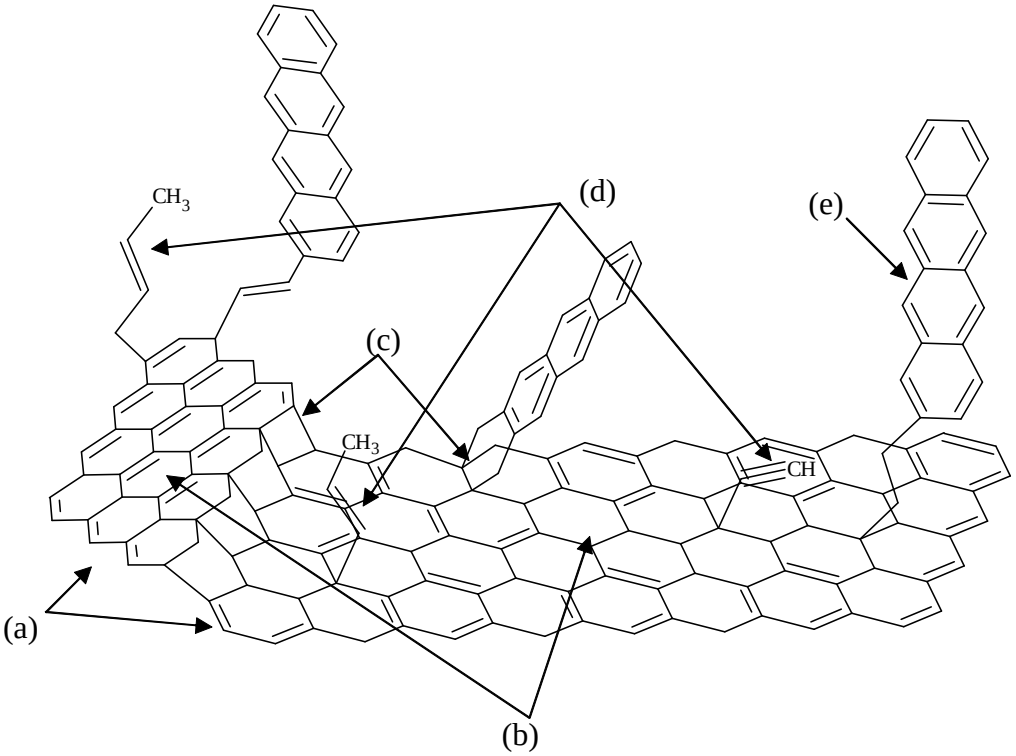

Figure IV-(xiii)-i

Diagrammatic representation of the proposed carbon film surface
An extensive graphene network featuring:
(a) Accessible graphene regions
(b) sp^3 bonding
(c) Electrically conductive structures in the graphene zones.
(d) Pendent alkyne/alkene groups
(e) Isolated fluorophores

In Figure IV-(xiii)-i the electrically conductive structures in the graphene zones could include the conjugated π electron systems (d) with the sp^3 bonds (c) linking graphene zones. The rapid oxidation of polyacetylene groups precludes their inclusion in the proposed surface structure.

The experiments carried out in this chapter to characterise the carbon film, formed by *in situ* pyrolysis of acetylene on the quartz substrate, indicate a unique surface with electrochemical properties representing all forms of carbon electrodes.

In Chapter V the chemical structures proposed on the carbon film surface will be utilised to provide selectivity for DA in an AA containing matrix.

Chapter V

Selectivity

Introduction

The *in vivo* electrochemical quantitative measurement of DA in the presence of AA has plagued neuroscientists since carbon fibre chronopotentiometric techniques were first used to monitor DA release in 1978.[1] The difficulty arises from the similarity in oxidation potentials and the differences in basal concentration between DA (50 nM) and AA (100 μM) in the extracellular fluid.[2] Initially separation was achieved using normal pulse techniques on untreated [1] and electrochemically oxidised surfaces,[3;4] however temporal resolution was limited by the scan rate. Biological events, such as dopamine release after electrical stimulation, occurring in milliseconds were not detected. An alternative approach is the coating of the electrode with anionic membranes such as perfluorosulfonated polymer (Nafion)[5], poly(aminobenzoic acid)[6], N,N-dimethylaniline[7] and poly(ester sulfonic acid)[8]. Using an anionic membrane excludes AA, which is in the anionic form at physiological pH 7.4. In contrast dopamine, at pH 7.4 is in the cationic form as the amine is protonated and therefore can permeate the film. An example of the use of anionic membrane (Nafion, a copolymer with an approximate molecular weight of 10^5-10^6 Da) coating on a carbon film microelectrode electrode is shown in Figure V-i together with the structure of the Nafion (Figure V-i (inset)).

The cyclic voltammogram of AA, prior to coating (see Chapter VI, Experimental), displays a typical irreversible oxidation shape at a carbon film microelectrode. After coating the carbon film microelectrode with Nafion the cyclic voltammetric response to AA was greatly reduced. The Nafion coating, in Figure V-i does not completely suppress the AA Faradaic current. As the ascorbate anion is in dynamic equilibrium with the non ionised form, diffusion through the membrane of this small fraction of non ionised AA will be sufficient to

provide a background current comparable with that produced by the expected concentration of DA.

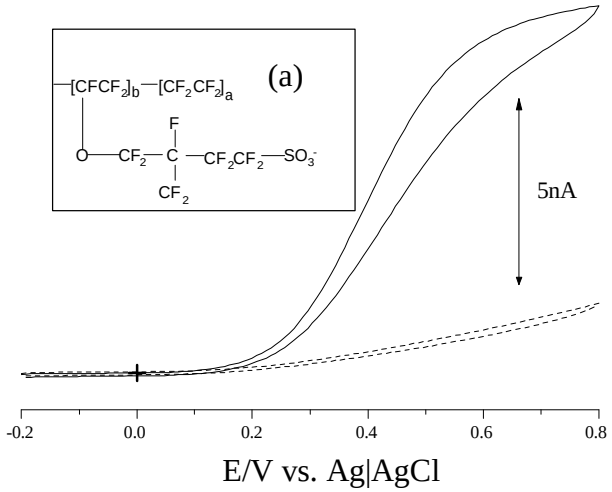

Figure V-i

Cyclic voltammogram of 10^{-4} M AA in citrate/phosphate buffer pH 7.4 at a carbon film microelectrode (—) and Nafion coated carbon film microelectrode (---). Scan rate 0.1V s^{-1} .Inset (a) is the structure of the Nafion. Monomer compositions (a) and (b) are dependent on polymerisation conditions.

The selectivity and sensitivity of Nafion has been further enhanced by the addition of an ionophore, the crown ether, dibenzo-18crown-6.[9] Sensitivity increase, with the use of an anionic membrane, is attributed to the accumulation of hydrophobic endogenous cationic neurotransmitters in preference to the smaller hydrophilic cations.[2]

Another modification of Nafion was the addition of the synthetic clay laponite. Laponite has a high cation exchange capacity which appears to accumulate DA resulting in an enhanced chronoamperometric signal of some five fold.[10]

The suppression of AA signal has also been reported using a coating of conductive polymers, such as a bilayer of poly(3-methylthiophene)/polypyrrole[11] and a monolayer of

overoxidised poly(N-acetylaniline).[11] The selectivity between DA and AA was reported to involve an interaction between the cationic sites and AA in the conductive polymer. Another approach, using a polymer coating to reduce the Faradaic response of AA, was the use of permselectivity of a polymer instead of ion exchange.[12] In this approach L-β-3,4-dihydroxyphenylaniline (L Dopa) is electrochemically polymerised on the electrode surface to form a melanin type polymer.

Polymer coatings are simple to apply, provide selectivity and increased sensitivity however they are inherently slow to react to rapid concentration changes (milliseconds) due to diffusion through the polymer film.[13] Although the Nafion film thickness is only 200-500 nm[14] the diffusion distorts the temporal response.[13] This distortion can be minimised using deconvolution techniques.[14]

A simpler approach to deconvolution of a DA signal is the minimisation of the AA barrier by forming a monolayer. This has been reported to be achieved by covalently attaching carboxylic groups to the electrode surface electrochemically.
Covalently attaching *p*-phenyl acetate via a diazonium salt to GC and carbon fibre disc electrodes was reported to reduce the response of AA to 0.43% with respect to the unmodified electrode.[15] Amino acids, glycine,[16] and alanine[17] have been attached to GC by anodic oxidation in acetonitrile to form amine links to the carbon surface. The amino acids, glycine and alanine covalently bonded to GC electrodes were reported to provide good discrimination when used in the differential pulse mode. Chemical attachment of the amino acid, glutamic acid, to an anodised GC surface in an aqueous solution at 60°C, was reported to have produced selectivity between AA and DA using differential pulse techniques.[18] The nature of the bonds formed was not stated.

Another technique found to provide selectivity was fast scan cyclic voltammetry.[19] By carrying out cyclic voltammetry at 300 V s^{-1} "finger print" cyclic voltammograms are obtained with a slight loss of temporal resolution.[20] (At 300 V s^{-1} the cyclic voltammogram

scan takes only 100 ms.) The quantitative results of fast scan cyclic voltammetry are comparable with microdialysis/HPLC when measuring the uptake kinetics of DA *in vivo*.[21] Fast scan cyclic voltammetry therefore not only provides qualitative information but also quantitative data. The "finger print" obtained by fast scan cyclic voltammetry, after background subtraction, is sufficiently reproducible to permit principal component regression analysis to identify neurotransmitters having overlapping cyclic voltammograms.[22]

A recently published means of achieving DA selective detection in the presence of AA is the differential pulse voltammetry and square wave voltammetry at a liquid/liquid (water/1,2-dichloroethane) interface.[23] The preferential transfer of dopamine across the interface (1.13 cm^2) was achieved using dibenzo-18-crown-6. Under these conditions the lowest detectable level of DA was 2 μM using differential pulse and square wave voltammetry. In the presence of $25x10^{-3}$ M AA the detection level increased to 10 μM DA. This interesting approach, with its high selectivity, may have applications for *in vivo* monitoring of the basal levels of DA. Under these conditions the effects of the slow diffusion of DA, in the dichloroethane, will be minimal.

In this chapter three modifications of the carbon film will be described with the principal aim of achieving selectivity. The secondary aspect was to exploit anti-fouling properties which are discussed in Chapter VI.

The first modification utilises the unsaturated groups, detected by metal π complexes outlined in Chapter IV-(vii), to form an anionic barrier. It is proposed that this barrier consists of carboxylic acid groups. The second modification is also the proposed formation of carboxylic acid on the surface, utilising the anodic oxidation of ethanol on the surface of the carbon film. The anodic oxidation of ethanol was expected to be an addition reaction locating the carboxylic group on the carbon film surface; whereas the proposed carboxylic acid groups formed using the metal π complex was on the pendent groups, consequentially in this latter case the carboxylic acid groups extended beyond the graphene surface. The last modifying

approach to achieve selectivity was to assess the anodic barrier properties of nitro groups by covalently attaching dinitroaniline and dinitrodiphenyl amine to the carbon film surface via anodic oxidation in dichloromethane. Although the anodic membrane properties would be weaker than a carboxylic acid they may improve suppression of the AA Faradaic current, if the surface coverage is high. This latter technique together with the nitro groups possible antifouling properties made this an interesting surface modification study.

The above three surface modifications, hopefully to provide selectivity to the carbon film microelectrodes are treated individually in separate sub-chapters with an introduction, experimental results and discussion sections.

References

1. Ponchon J.; Cespuglio R.; Gonon F.; Jouvet M.; Pujol J. *Analytical Chemistry* **1979,** *51*, 1483-86.
2. Clark R.A.; Zerby S.E.; Ewing A.G. *Electroanalytical Chemistry,* Bard A.J.; Rubinstein I., Eds.; Marcel Dekker. Inc.: U.S.A., 1998.
3. Suand-Chagny M.F.; Cespuglio R.; Rivot J.P.; Buda M.; Gonon F. *Journal of Neuroscience Methods* **1993,** *48,* 241-50.
4. Gonon F..; Fombarlet C.M.; Buda M.J.; Pujol J.F. *Analytical Chemistry* **1981,** *53*, 1386-89.
5. Gerhardt G.A. , Oke A.F., Nagy G., Moghaddam B., and Adams R.N. *Brain Research* **1984**; *290*, 390-395.
6. Xu F.; Gao M.; Wang L.; Shi G.; Zhang W.; Jin L.; Jin J. *Talanta* **2001,** *55*, 329-36.
7. Roy P.R.; Saha M.S.; Okajima T.; Park S-G; Fujishima A.; Ohsaka T. *Electroanalysis (New York)* **2004,** *16*, 1777-84.
8. Lau Y.Y.; Chein J.B.; Wong D.K.Y.; Ewing A.G. *Electroanalysis* **1991,** *3*, 87-95.
9. Crespi F.; Mobius C. *Journal of Neuroscience Methods* **1992,** *42*, 149-61.
10. Lacroix M.; Bianco P.; Lojou E. *Electroanalysis* **1999,** *11*, 1068-74.
11. Xu H.X., Kitamura F., Ohsaka T., and Tokuda K. *Analytical Sciences*, **1994**; *10*, 399-404.

12. Rubianes M.D.; Rivas G.A. *Analytical Letters* **2003,** *36*, 329-45.

13. Stuart J.N.; Hummon A.B.; Sweedler J.V. *Analytical Chemistry* **2004,** *April*, 122A.

14. Garris P.A.; Wightman R.M. *Neuromethods Vol 27. Voltammetric Methods in Brain Systems*, Boulton A.; Baker G.Adams R.N., Eds.; Humana Press Inc: 1995.

15. Downard A.J.; Roddick A.D.; Bond A.M. *Analytica Chimica Acta* **1995,** *317*, 303-10.

16. Zhang L.; Lin X. *Fresenius' Journal of Analytical Chemistry* **2001,** *370*, 956-62.

17. Zhang L.; Sun Y. *Analytical Sciences* **2001,** *17*, 939-43.

18. Lin X.; Zhang L. *Analytical Letters* **2001,** *34*, 1585-601.

19. Millar J.; Stamford J.A.; Kruk Z.L.; Wightman R.M. *European Journal of Pharmacology* **1985,** *109*, 341-48.

20. Michael D.J.; Wightman R.M. *Journal of Pharmaceutical and Biomedical Analysis* **1999,** *19*, 33-46.

21. Budygin E.A.; Kilpatrick M.R.; Gainetdinov R.R.; Wightman R.M. *Neuroscience Letters* **2000,** *281*, 9-12.

22. Heien M.L.A.V.; Johnson M.A.; Wightman R.M. *Analytical Chemistry* **2004,** *76*, 5697-704.

23. Beni V.; Ghita M.; Arrigan D.W.M. *Biosensors & Bioelectronics* **2005,** *20*, 2097-103.

Chapter V-(i)

Formation of Carboxylic Acid Groups on a Carbon Film Surface by Ferrous Complex Oxidation

Abstract

The unsaturated alkyl pendent chains on the surface of the carbon film microelectrode are utilised to form an anionic barrier to ascorbic acid. This was achieved by immersion in a ferrous sulfate solution, followed by storage in air overnight. The anionic barrier was identified as consisting of carboxylic acid groups and their surface concentration was found to be $3x10^{-11}$ mole cm^{-2}.

The ease of hydrolysis of the 1,2-diaminopropane derivative of the carboxylic acid groups on the surface of the carbon film microelectrode, using citric acid, was demonstrated.

Introduction

The presence of alkene and or alkyne pendent groups postulated in Chapter IV-(vii) provides an opportunity to form an anionic barrier without reducing the electrochemically active regions. Any chemical modification reacting with the electrochemically active region of the carbon film microelectrode will decrease the limiting current. *In vivo* chronoamperometric changes in DA levels are measured in the pA range, therefore conservation of the electrochemically active area to maintain the maximum limiting current is of paramount importance. Therefore a reaction converting the proposed alkene/alkyne pendent groups to carboxylic acids would provide an anionic barrier and leave the electrochemically active (graphene) region unaffected.

A possible approach was the oxidation of the unsaturated aliphatic groups with ferrous sulfate. It had been noted after linear voltammetric oxidation of the ferrous π complex (Chapter IV-(vii)), that the Faradaic region of the cyclic voltammograms of AA had been

suppressed. Adsorption of ferrous ions onto the carbon film microelectrodes immediately prior to cyclic voltammetry did not result in suppression of the Faradaic current. The suppression of the AA Faradaic current was found to be time dependent, requiring overnight storage before full suppression was developed. This suppression of the Faradaic current for AA, together with only a slight change in the voltammogram obtained from the oxidation of DA suggested the presence of an anionic barrier, such as that provided by carboxylic acid groups.

A possible explanation for the formation of carboxylic acids is a reaction pathway similar to that of ferric nitrate reaction with alkenes. The reaction of ferric nitrate nonahydrate and oxygen, in direct contact with styrene has been reported to yield benzaldehyde and benzoic acid with an eighty percent yield at 80°C.[1] As aldehydes are unstable in air the benzaldehyde probably forms benzoic acid, after reaction with oxygen. The oxidation mechanism in the presence of iron nitrate was suggested to proceed via an olefin/nitrate complex which inserted an oxygen atom of the coordinated nitrate into the alkene. The iron nitrosyl intermediate then recombines with dioxygen in the atmosphere. The publication suggested that the ferrous state would enhance the oxidising capacity of the metal nitrate salt. The apparent long reaction time is probably a function of the evaporation rate of water prior to dioxygen oxidation of ferrous to ferric. The requirement for iron to be in the ferric state is dependent on the presence of water of hydration. In the anhydrous state ferric is the preferred oxidation state.[1]

To verify the proposed carboxylic acid reaction product of ferrous sulfate, on the carbon film surface, it was first derivatised to form an amide (equation (ii)) via the acid chloride (equation (i)).[2] (R= Carbon film electrode surface)

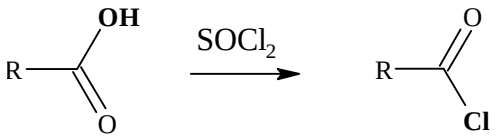

(i)

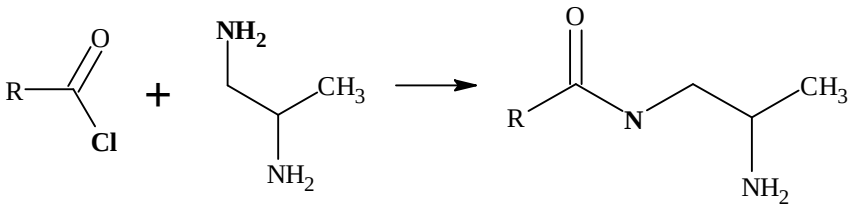

(ii)

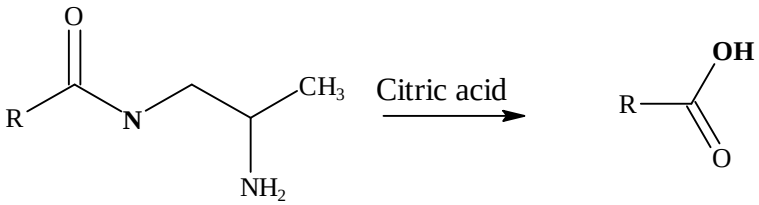

(iii)

The amide was then hydrolysed back to the carboxylic acid (equation (iii)). These reaction steps were verified using cyclic voltammetry of 10^{-4} M AA.

The formation of the amide will convert the anionic barrier into a cationic barrier at pH 7.4. With a cationic barrier the Faradaic oxidation current of AA then becomes evident. To ensure complete removal of all anionic barrier properties the reaction with the acid chloride was carried out with a diamine (1.2-diaminopropane). The 1,2-diamine ensured a cationic barrier close to the graphene region, due to the presence of the unreacted amine group being protonated at pH 7.4.

Amide formation was preferred to esterification due to the possible hydrolysis of the ester groups at pH 7.4. However it was found serendipitously that a 0.0 1M citric acid

solution hydrolysed the proposed amide groups to the carboxylic acid. This was fortuitous as the same carbon film microelectrodes could then be used for carboxylic acid surface coverage determination.

To determine the surface coverage of the proposed carboxylic acids cyclic voltammetric reduction of the dinitrobenzyl chloride derivative was carried out.
The cyclic voltammetric reduction of the nitro group in 1 M HCl has been reported to be a six electron transfer as shown in equation (iv).[3]

$$\begin{aligned} R\text{-}NO_2 + 4H^+ + 4e &\longleftrightarrow R\text{-}NHOH + H_2O \\ R\text{-}NHOH + 2H^+ + 2e &\longleftrightarrow R\text{-}NH_2 \end{aligned} \qquad \text{(iv)}$$

It was also reported that XPS analysis of the surface detected unreduced nitro groups. This implies only nitro groups accessible to the conductive region of the GC electrode surface have been reduced. The lack of surface morphology homogeneity is probably due to the method of electrode preparation prior to modification. The GC electrode had been polished with 0.05 μm alumina slurry; this would have created irregular features of micron dimensions. Atomically this is very large; consequently the nitro groups being anchored covalently to the surface are restricted in accessibility to adjacent graphene regions. Nitro groups, which are not sterically accessible to the graphene region, cannot be reduced. The coulometric determination therefore represents a minimum surface concentration.

Capacitance measurements were made on the carbon film microelectrode, after modification with ferrous sulfate, to ascertain if any changes in the graphene region had occurred and to ensure their use *in vivo* was not impaired.

Experimental

Chemicals and Reagents

Dopamine (Aldrich), ascorbic acid (BDH), potassium phosphate decahydrate (Aldrich), phosphoric acid (BDH Analar), ferrous sulphate (BDH Analar), thionyl chloride (Aldrich), 1,2-diaminopropane (Aldrich), 1,2-diaminoethane (Aldrich), citric acid (Aldrich), pyridine (Aldrich), 3,5-dinitrobenzyl chloride (Aldrich) and high purity nitrogen (BOC) (Instrument Grade) were used as received. All solutions were prepared daily. Aqueous solutions were prepared using Milli-Q water (Milli-Q Reagent Water System).

Equipment

The three electrode system, with an Ag|AgCl (3 M KCl) as outlined in Chapter II Electrochemical Equipment, was used.

Electrode Fabrication

The carbon film microelectrodes were fabricated as outlined in Chapter III using 40 ml min^{-1} nitrogen in the counter flow configuration.

Procedure

Cyclic Voltammetry

Surface Characterisation using DA, AA and norepinephrine

The carbon film microelectrodes, unmodified and modified, were cycled from -0.2 V to 0.8 V at 0.1 V s^{-1} in deoxygenated 10^{-4} M DA and AA citrate/phosphate buffer solutions (pH 7.4). Buffer composition, 46.8 gm tri-sodium phosphate dodecahydrate and 1.9 gm citric acid per litre and adjusted to pH 7.4 with phosphoric acid. All solutions were prepared daily using deoxygenated buffer. Ascorbic acid, norepinephrine and dopamine standard solutions were replaced every three hours

Reduction of 3,5-dinitro adduct in 0.1 M HCl

The modified carbon film microelectrode was cathodically scanned cyclic voltammetrically from 0.8 V to -0.8 V at 0.1 V s^{-1} in deoxygenated 0.1 M HCl. The cathodic wave area was determined using eDAQ EChem software.

Ferrous sulfate modification of carbon film microelectrodes

The electrodes were immersed in a solution of 0.01 M ferrous sulfate, with gently agitation, for 20 seconds then rinsed for 20 seconds, with gentle agitation, in deionized water and allowed to stand in air overnight.

1,2-diaminopropane modification of carbon film microelectrodes

The modification of carbon film microelectrodes were carried out in a fume cupboard. The electrodes were oven dried for 15 minutes at 80°C then immersed in thionyl chloride and gently agitated for 20 seconds, followed immediately with 20 seconds immersion, with gentle agitation, in 1,2-diaminopropane. The electrode was then rinsed in ethanol with gentle agitation for 20 seconds and finally rinsed in deionised water for 20 seconds with gentle agitation.

3,5-dinitrobenzyl chloride modification of the carbon film electrode surface

The modification of carbon film microelectrodes were carried out in a fume cupboard. The electrodes were dried in an oven at 80°C for 15 minutes. The electrodes were then immersed in thionyl chloride for 20 seconds, with gentle agitation, then immediately in 1,2-diaminoethane for 20 seconds with gentle agitation. The electrodes were then immediately immersed in 0.01 M 3,5-dinitrobenzyl chloride in pyridine for 20 seconds with gentle agitation. After this final reaction the electrodes were rinsed in ethanol and deionised water for 20 seconds with gentle agitation.

Results and Discussion

Heterogeneous electron transfer of AA and DA after chemical modification with ferrous sulfate

To evaluate the efficiency of ferrous chloride immersion to form an anionic barrier, cyclic voltammetry of 10^{-4} M AA (n=14) was carried out. The results are shown in Figure V-(i)-i

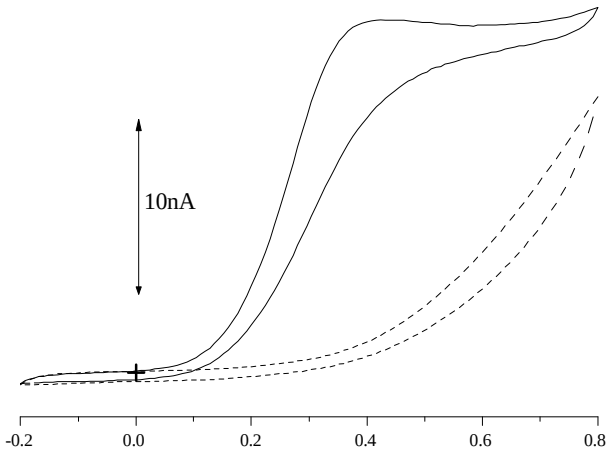

Figure V-(i)-i

Cyclic voltammetry of 10^{-4} M AA at a carbon film microelectrode in citrate/phosphate buffer pH 7.4, (—) before ferrous sulfate immersion and after (---)
Scan rate 0.1V s^{-1}

The cyclic voltammogram, prior to ferrous sulfate modification, displays an excellent sigmodial shape for the electrochemically irreversible anodic oxidation of AA. However, for the carbon film microelectrodes after ferrous sulfate modification the Faradaic current (0.3 V to 0.8 V) was suppressed, indicating that an anionic barrier was formed on the surface.

The effect on the heterogeneous electron transfer of DA after ferrous sulfate modification is shown in Figure V-(i)-ii.

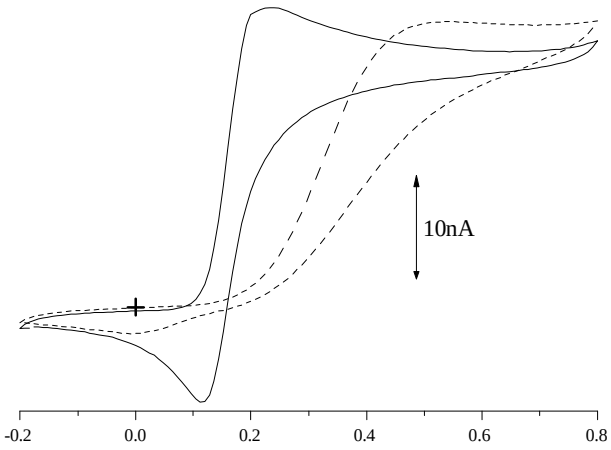

Figure V-(i)-ii

Cyclic voltammetry of 10^{-4} M DA at a carbon film microelectrode in citrate/phosphate buffer pH 7.4, (—) before ferrous sulfate immersion and after (---) Scan rate 0.1V sec^{-1}

The cyclic voltammogram of DA (Figure V-(i)-ii), after ferrous sulfate modification, indicates that the surface functional groups formed have a similar effect as the cyclic voltammetry of DA in citric acid (Figure IV-(x)-vii). The *E½* was shifted 0.2 V to a higher potential with a loss of the cathodic wave. The loss of the cathodic wave is visibly apparent when the forward and reverse scans are averaged. This is shown in Figure V-(i)-iii. If, as proposed, carboxylic acid moieties are formed after ferrous sulfate modification,

the environment near the surface will be acidic, hence the similar cyclic voltammetry as in citric acid solution.

The DA limiting current at 10^{-4} M showed an increase of 6.9%, in a range of 2% to 13% (n=6). The slight increase indicates that the graphene regions have not been reduced suggesting only pendent groups are involved in the reaction with ferrous sulphate. The increase could be due to the removal of steric hindrance. The formation of carboxylic acids at unsaturated locations in the pendent chain will undergo chain scission, removing bulky pendent groups, thereby providing less steric hindrance to DA diffusing towards the surface.

A further indication of retention of the graphene area is the low capacitance, with an average 3.5 μF cm^{-2} (n=4) of the carbon film after ferrous chloride modification.

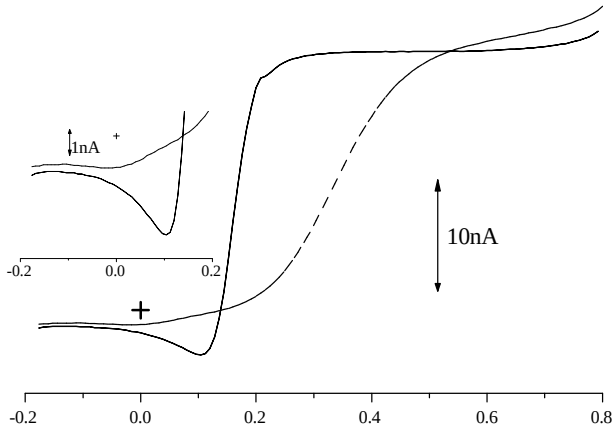

Figure V-(i)-iii

The average forward and reverse cyclic voltammograms of 10^{-4} M DA at a carbon film microelectrode in citrate/phosphate buffer pH 7.4, (—) before ferrous sulfate modification and after (---). The inset is the rescaled -0.2 V to 0.2 V section.
Scan rate 0.1 V s^{-1}

Deductive verification of the presence of carboxylic acids, formed after ferrous sulfate modification, using cyclic voltammetry of AA.

A batch (n=5) of carbon film microelectrodes were characterised using cyclic voltammetry of DA and AA, modified with ferrous sulfate, reacted with thionyl chloride, 1,2-diaminopropane and rinsed in citric acid. Each step of the reaction sequence was followed using cyclic voltammetry of 10^{-4} M AA in a citrate/phosphate buffer pH 7.4. These cyclic voltammograms are shown in Figure V-(i)-iv together with proposed reactions occurring with the surface bound functional groups.

The original surface, (Figure V-(i)-iv(a)) containing the proposed unsaturated groups, yielded a typical cyclic voltammogram for the anodic oxidation of a irreversible electrochemical reaction. The shape is typical for AA at the carbon film microelectrode fabricated in this thesis work.

After carrying out the chemical modification with ferrous sulfate, as outlined in the Experimental Section of this sub chapter, the cyclic voltammogram shown in Figure V-(i)-iv(b) was obtained. The Faradaic current of AA was significantly reduced. If, as proposed the surface unsaturated groups have been oxidised to carboxylic acids, an anionic barrier has formed.

If the anionic barrier containing carboxylic acids was converted to a positive (cationic barrier) such as a protonated amine the original AA oxidation Faradaic current would be restored. The cyclic voltammogram of AA, after reaction with thionyl chloride to form an acid chloride, then a diamine to form an amide is shown in Figure V-(i)-iv(c). The lack of return to the original cyclic voltammogram (Figure V-(i)-iv(a)) could be due to incomplete conversion of the amide to the carboxylic acid.

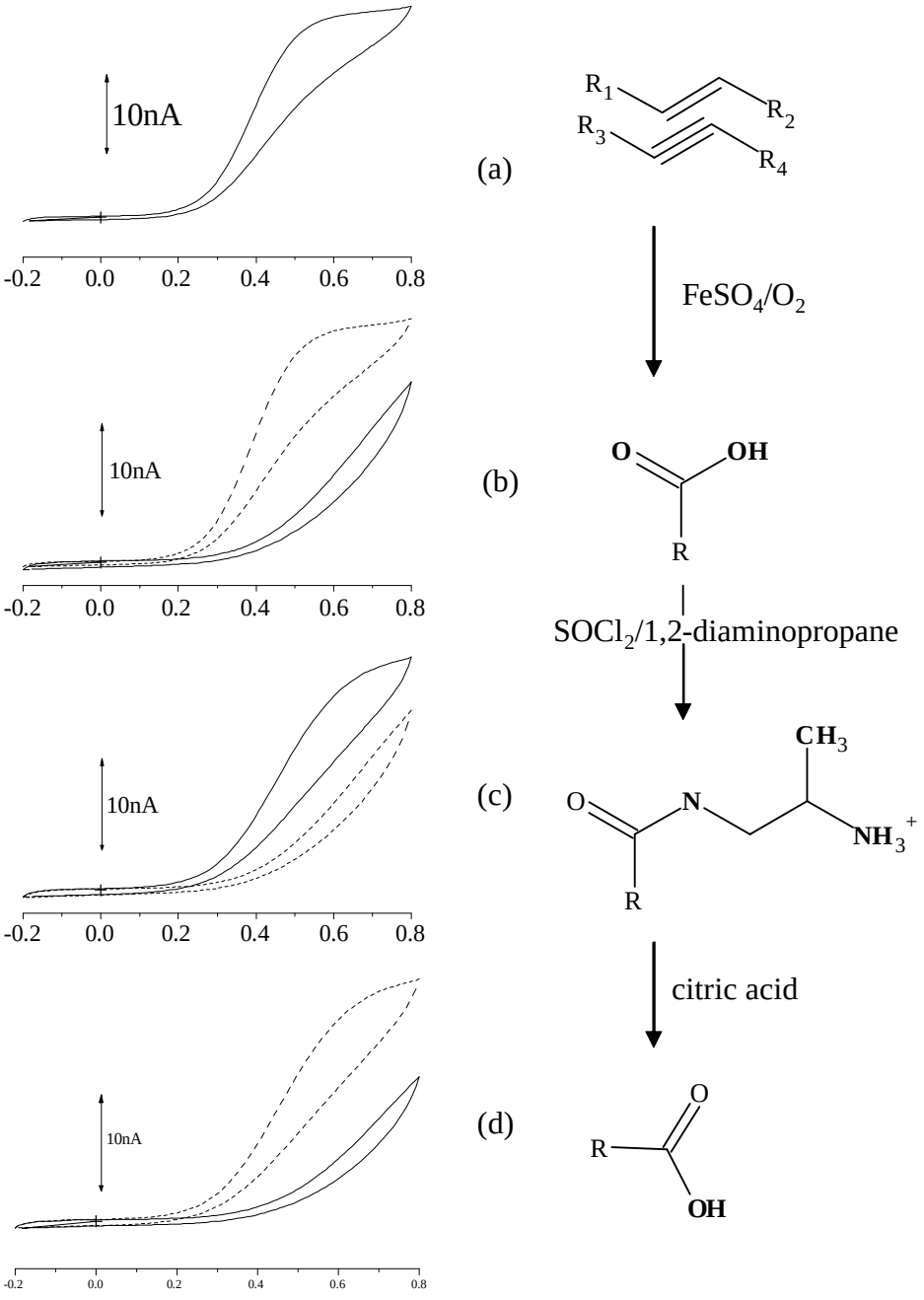

Figure V-(i)-iv

Cyclic voltammograms of 10^{-4} M AA in citrate/phosphate buffer pH 7.4 at a carbon film microelectrode and proposed surface functional groups (a), after reaction with $FeSO_4$ (b), after reaction with 1,2-diaminopropane (c) and after reaction with citric acid (d). (—) is the cyclic voltammogram after the indicated reaction and (---) that of the preceding surface.
Scan rate 0.1 V s^{-1}

In Figure V-(i)-iv(d) the cyclic voltammogram, after rinsing in citric acid, the suppression of the AA Faradaic current indicates an that anionic barrier has been created. It is proposed that the amide group has been hydrolysed. As simple amides are stable in mild acid and alkali aqueous solutions the use of a 1,2-diamine appears to have facilitated hydrolysis. A possible mechanism for the hydrolysis of the 1,2-diamine adduct is as follows. Under acidic conditions the amine adjacent to the amide is protonated. To maintain electro neutrality the local hydroxide concentration will be high, thereby promoting basic hydrolysis of the amide via nucleophilic addition of the hydroxide.

From the changes in AA cyclic voltammetry, as depicted in Figure V-(i)-iv, the formation of carboxylic acid groups on the surface of the carbon film microelectrode is indicated after immersion in a solution of ferrous sulfate.

Determination of carboxylic acid surface concentration following the ferrous sulfate modification

The carbon film microelectrodes after rinsing in citric acid were modified with 3,5-dinitrobenzyl chloride as outlined in the Experimental Section. After modification the carbon film microelectrodes was cathodically reduced in 0.1 M hydrochloric acid. The cyclic voltammogram of the reduction is shown in Figure V-(i)-v.

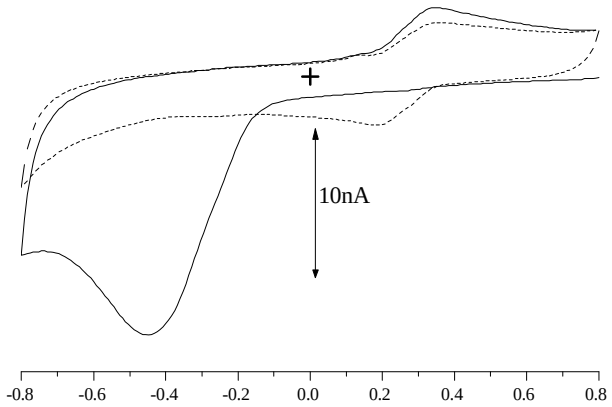

Figure V-(i)-v

Cyclic voltammograms of 3,5-dinitrobenzyl chloride derivatised surface of ferrous sulfate modified carbon film microelectrode in 0.1 M HCl (—) is the first and (---) is the second scan. Scan rate 0.1V s^{-1}

The large irreversible wave between -0.2 V to -0.7 V, in the first scan, is attributed to the reduction of the dinitro groups.[3] In the following scan this wave is absent, however a reversible wave is present at 0.18 V on the forward scan and 0.35 V on the reverse scan. These reversible waves are attributed to partially reduced nitro groups, hydroxyaminophenyl groups (Ar-NHOH) oxidising to the nitrosophenyl (Ar-NO).[3]

Blanks (n=8) were carried out by repeating all steps except the ferrous chloride modification. An example of these cyclic voltammogram scans are shown in Figure V-(i)-vi.

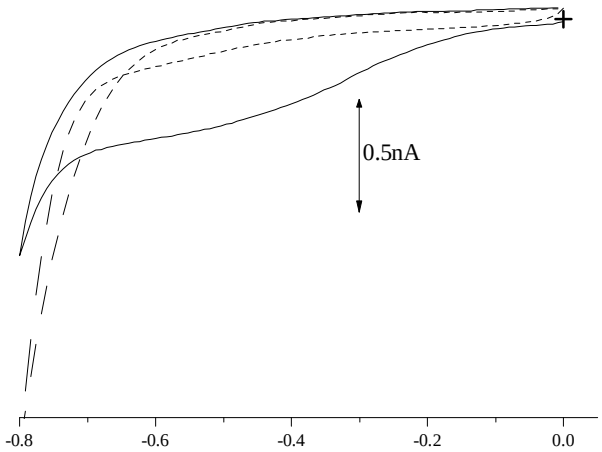

Figure V-(i)-vi

Blank cyclic voltammograms of carbon film microelectrodes after $SOCl_2$ treatment and reaction with 3,5-dinitrobenzyl chloride in 0.1 M HCl, (—) is the first and (---) is the second scan.
Scan rate 0.1 V s^{-1}

The cyclic voltammogram (Figure V-(i)-vi) displays irreversible reduction of a functional group between -0.1 V and -0.7 V on the surface of the carbon film microelectrode during the first scan. The second scan displays only a background current similar to that shown in Figure V-(i)-vii.

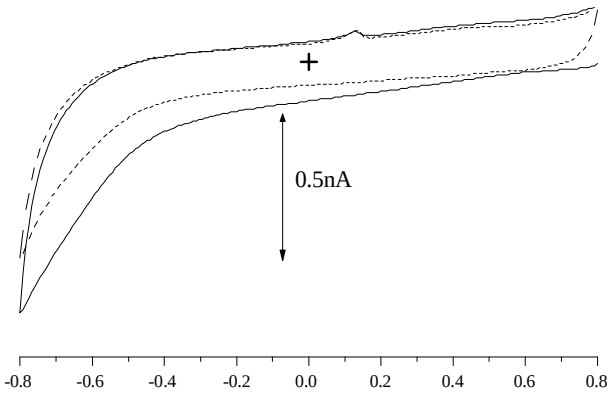

Figure V-(i)-vii

Cyclic voltammogram of an unmodified carbon film microelectrode in 1 M HCl, (—) is the first and (---) is the fourth scan. Scan rate 0.1 V s^{-1}

To investigate the occurrence of this cathodic wave unmodified microelectrodes (n=5) were cathodically reduced in 0.1 M HCl. The results are shown in Figure V-(i)-vii. The slight difference between the first and fourth scan is probably due to steady state being established at the "larger" cylindrical microelectrode. This cyclic voltammogram indicates that a Faradaic current is absent. Comparing this Figure with Figure V-(i)-vii suggests that an absorbed species is present. The functional group or groups are unknown; however interference with the determination of the nitro group coverage is minimal. To reduce possible ambiguity the coulombic measurement of the cathodic wave was only considered when the distinctive wave was present. Measurement of the coulombic size of the cathodic wave was obtained using the integration function of the eDAQ acquisition software.

The carbon film microelectrodes used in the above identification, together with an additional three microelectrodes gave an average surface coverage of $3x10^{-11}$ mole cm^{-2} in a range of $2x10^{-13}$ to $2x10^{-10}$ moles cm^{-2}. The surface concentration, of the dinitrobenzyl chloride derivatised ferrous sulfate modified carbon film, measured was similar to the surface

concentration obtained using cation π complexes (Chapter IV-(vii)). As both methods measure the alkyl unsaturation concentration a slightly higher coverage would be expected using the dinitrobenzyl derivative, due to its larger molecular size, i.e. greater accessibility is expected to the graphene surface.

Conclusion

Using a facile modification of the carbon film surface, which only involved the immersion in a ferrous sulfate solution, suppression of the AA Faradaic current was obtained. The cyclic voltammogram of DA, after ferrous sulfate treatment, *E½* had shifted anodically 0.2 V; however the limiting current remained unchanged. The lack of change in the limiting current suggests that the graphene area has not been reduced; therefore all chemical reactions occurring have taken place on the pendent groups. Using cyclic voltammetry of AA, after derivatisation by ferrous sulfate, the modified surface anionic barrier was identified as carboxylic acid groups. The surface coverage of the carboxylic groups was quantified via the dinitrobenzyl derivative. The carboxylic acid surface concentration was found to have an average concentration greater than 3.1×10^{-11} moles cm^{-2}.

The ease of hydrolysis of 1,2-diamine suggests the use of this functional group as a means regeneration of electrode surfaces used for complexing sensors.

References

1. Pillai U.R.; Sahle-Demessie E.; Namboodiri V.V.; Varma R.S. *Green Chemistry* **2002,** *4*, 495-97.
2. Watkins B.F.; Behling J.R.; Kariv E.; Miller L.L. *Journal of the American Chemical Society* **1975,** *97*, 3549-50.
3. Ortiz B.; Saby C.; Champagne G.Y.; Belanger D. *Journal of Electroanalytical Chemistry* **1998,** *455*, 75-81.

Chapter V-(ii)

Ethanol Modified Carbon Film Surface

Abstract

Anodic oxidation of ethanol, in the presence of 1,8-diazabicyclo[5.4.0]undec-7-ene , was used to form an anionic barrier to ascorbic acid on the surface of a carbon film microelectrode. The anionic barrier, using a 3,5-dinitrobenzyl derivative was identified as carboxylic acid groups with a surface coverage of $5x10^{-11}$ moles cm^{-2}.

A reaction pathway for the formation of carboxylic groups from the anodic oxidation of ethanol is proposed involving carbocations.

Introduction

Modification of GC electrodes by anodic oxidation of alcohols; 1-octanol (1 M H_2SO_4)[1] and 1,ω-alkanediols (0.1 M H_2SO_4)[2] has been reported to form an ether linkage to the surface of the GC electrode. The surface bound groups displayed barrier properties to AA and $Fe(CN)_6^{3-}$ and exhibited a resistance to fouling by the protein bovine serum albumin.[3;4] Both properties, barrier to AA and resistance to fouling by proteins, are of interest for the *in vivo* application of the cylindrical carbon film microelectrodes fabricated in this thesis work. The suppression of the Faradaic current of AA after anodic oxidation of 1,ω-alkanediols (0.1 M H_2SO_4) was attributed to oxidation of the terminal hydroxy groups to carboxylic acids (the other hydroxyl group providing the ether linkage to the carbon surface.). The carboxylic acid's presence on the attached diol was deduced from the similar suppression of the AA Faradaic current by anionic barriers formed by Nafion, stearic acid in a modified carbon paste electrode and ω-thiol carboxylic acids. The cyclic voltammetry of DA, after 1,ω-alkanediols modification of a GC surface, showed a significant maximum oxidation peak current reduction and a doubling of capacitance. The reduction in peak maxima indicates loss of

graphene region. The increase in capacitance indicates the modification of the graphene region.

The surface attachment of 1-octanol via the ether linkage was characterised using cyclic voltammetry of catechol and $Fe(CN)_6^{3-}$. When compared to the unmodified surface the catechol oxidation and reduction peaks decreased slightly in area. However the cyclic voltammogram of $Fe(CN)_6^{3-}$ after anodic oxidation of 1-octanol was devoid of a Faradaic current. The Faradaic current returned after the addition of trimethyldodecylammonium chloride. This cyclic voltammetric behaviour of catechol and $Fe(CN)_6^{3-}$ was suggested to be similar to that of a gold electrode modified with a self assembling monolayer of a long chain aliphatic thiol.

An alternative explanation to the long chain thiol effect is the anodic oxidation of 1-octanol onto the glassy carbon surface forming an anionic barrier due to the presence of carboxylic groups. The formation of such a barrier would explain the lack of Faradaic current for the reduction of $Fe(CN)_6^{3-}$. The addition of trimethyldodecylammonium chloride to the $Fe(CN)_6^{3-}$ solution would form a quaternary salt with the carboxylic acid nullifying the anionic carboxylic acid charge. With the removal of the anionic barrier access to the graphene area of the glassy carbon surface for $Fe(CN)_6^{3-}$ is restored, enabling the previously measured Faradaic current to return. The reduction of the catechol Faradaic oxidation peak after anodic oxidation of 1-octanol is probably due to steric interference (by the attached 1-octanol) or loss of graphene regions.

The proposed ether linkages, of alcohols to the GC surface after anodic oxidation, may have arisen in a similar manner as the reported formation of 1,1-diethoxyethane after anodic oxidation of ethanol, at a platinum electrode.[5]

In this sub chapter the monohydric alcohol, ethanol will be attached, via anodic oxidation, to the carbon film surface to form an anionic barrier. It is proposed that the anionic barrier consists of carboxylic acid groups (formed by the oxidation of the hydroxyl group) and

the attachment to the carbon film is via a carbon-carbon bond. It is also proposed that the carbon-carbon bond is the reaction product of a carbocation, formed during the anodic oxidation of the alcohol. (A carbocation has been postulated as an intermediate in the oxidation of ethanol, to acetaldehyde, at a platinum electrode.[5]) Verification and determination of the concentration of carboxylic acid groups on the surface of the carbon film microelectrode was made by the reduction of a 3,5-dinitrobenzyl derivative.

It is proposed attached ethanol is oxidised to an aldehyde, either electrochemically or by reaction with a carbocation. The aldehyde formed reacts with molecular oxygen, on exposure to the atmosphere, to form an attached carboxylic acid. To elucidate the proposed oxidation pathway of the attached ethanol, anodic oxidation of ethanal and ethanoic acid was carried out as both were reported as products of the electrochemical oxidation of ethanol at platinum and gold electrodes and are therefore possible reaction intermediates.[6;7]

Methanol was anodically oxidised at the surface of the carbon film microelectrode to determine if the carbon carbon bond formed was located at the α and/or β carbon of ethanol. The formation of a anionic barrier using methanol indicates that the carbon carbon bond occurs at the α position on ethanol. If an anionic barrier did not form then the carbon carbon bond would occur through the β position.

Experimental Section

Chemicals

Dopamine (Aldrich), ascorbic acid (BDH), potassium phosphate decahydrate (Aldrich), phosphoric acid (BDH Analar), thionyl chloride (Aldrich), 1,2-diaminoethane (Aldrich), pyridine (Aldrich), 3,5-dinitrobenzyl chloride (Aldrich), ethanol (Shell Chemical), methanol (BDH), ethanal (Aldrich), glacial ethanoic acid (BDH), potassium chloride (BDH), 1,8-diazabicyclo[5.4.0]undec-7-ene (Aldrich), dichloromethane (BDH) and nitrogen (BOC) (Instrument Grade) were all used as received. All solutions were prepared daily. Aqueous solutions were prepared using Milli-Q water (Milli-Q Reagent Water System).

Equipment

The three electrode system, as outlined in Chapter II Electrochemical Equipment, was used with a platinum pseudo reference electrode for non–aqueous solutions and an Ag|AgCl (3 M KCl) reference electrode for aqueous solutions

Electrode Fabrication

The carbon film microelectrodes were fabricated as outlined in Chapter III using 40 ml min^{-1} nitrogen in the counter flow configuration.

Procedure

Surface Modification

The anodic oxidation of ethanol, ethanal, ethanoic acid and methanol with 10^{-4} M 1,8-diazabicyclo[5.4.0]undec-7-ene (DBU) at a carbon film microelectrode was carried out by scanning from 0.3 V to 1.6 V, twenty times at 0.1 V s^{-1} in deoxygenated solutions.

3,5-dinitrobenzyl chloride reaction with the modified carbon film electrode surface.

The reaction on the carbon film microelectrodes were carried out in a fume cupboard. The electrodes were dried in an oven at 80°C for 15 minutes. The electrodes were then immersed in thionyl chloride for 20 seconds, with gentle agitation, then immediately in 1,2-diaminoethane for 20 seconds with gentle agitation. The electrodes were then immediately immersed in 0.01 M 3,5-dinitrobenzyl chloride in pyridine for 20 seconds with gentle agitation. After this final reaction the electrodes were rinsed in ethanol and deionised water for 20 seconds each with gentle agitation.

Capacitance measurement

See Chapter IV-(iv) for cyclic voltammetric method to measure capacitance.

Results and Discussion

The anodic oxidation of ethanol at a carbon film microelectrode (Figure V-(ii)-i) shows only a slight change in the Faradaic current after twenty scans, when compared to that reported for anodic oxidation of 1-octanol.[1] As the carbon film electrodes are microelectrodes, a supporting electrolyte, such as sulfuric acid, was not used. This eliminated the need to investigate the effect of the supporting electrolyte.[1]

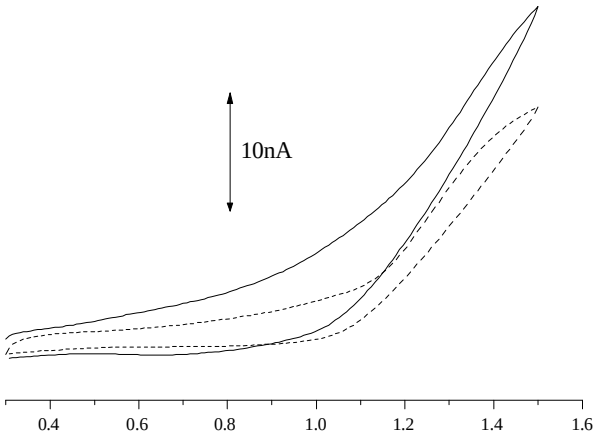

Figure V-(ii)-i

Cyclic voltammetry of the anodic oxidation of ethanol at a carbon film microelectrode, (—) first scan and (---) twentieth scan.
Scan rate 0.1 V s^{-1}

After anodic oxidation in ethanol the anionic barrier formed was evaluated using cyclic voltammetry of AA at pH 7.4. This is shown in Figure V-(ii)-ii.

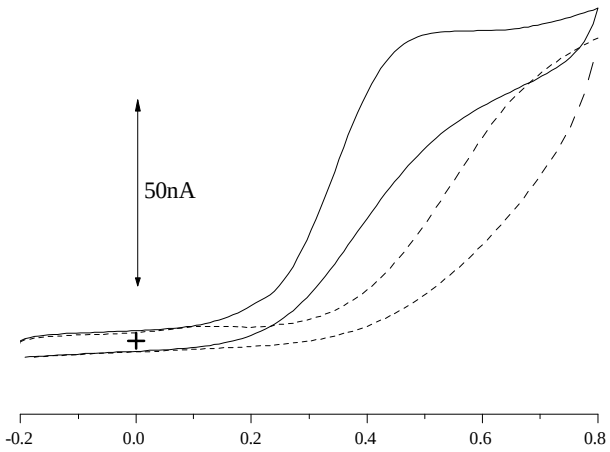

Figure V-(ii)-ii

Cyclic voltammograms of 10^{-4} M AA in citrate/phosphate buffer pH 7.4 at a carbon film microelectrodes before (—) anodic and (---) after oxidation in ethanol.
Scan rate 0.1 V s^{-1}

The cyclic voltammograms (Figure V-(ii)-ii) (n=4) of AA before and after anodic oxidation in ethanol shows suppression of the Faradaic current after anodic oxidation. Capacitance measurements (n=3) of the carbon film microelectrode gave an average of 6 μF cm^{-2}. This result is very close to the average value (6.7 μF cm^{-2}) obtained at unmodified carbon film microelectrodes. (Chapter IV-(iv) Results and Discussion) This lack of change in capacitance can be seen in the non Faradaic region, -0.2 V to 0.1 V and indicates that the graphene region has not been modified.

If as postulated a carbocation is formed, the addition of a strong base, 1,8-diazabicyclo[5.4.0]undec-7-ene (DBU), a hindered amine to ethanol would stabilise the carbocation increasing the possibility of additional surface modification. The effect of the addition of 10^{-4} M DBU to ethanol during anodic oxidation on the cyclic voltammetry of AA is shown in Figure V-(ii)-iii.

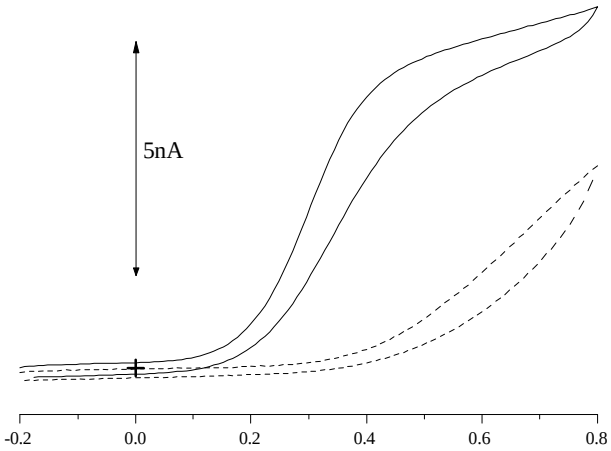

Figure V-(ii)-iii

Cyclic voltammograms of 10^{-4} M AA in citrate/phosphate buffer pH 7.4 at a carbon film microelectrodes (—) before anodic oxidation and (---) after in ethanol and 10^{-4} M DBU. Scan rate 0.1V s^{-1}

The cyclic voltammogram of AA after the addition of 10^{-4} M DBU (n=7) displays a greater suppression of the AA oxidation Faradaic current of approximately 50% at 0.8 V. This indicates that the stabilisation of a positively charged intermediate species, such as a carbocation, has promoted the attachment of ethanol to the surface of the carbon film. The capacitance did not change after the addition of DBU in ethanol. This is visually indicated by the lack of change between the forward and reverse scans in the non Faradaic region, –0.2 V to 0.1 V, in Figure V-(ii)-iii.

During the cyclic voltammetric anodic oxidation of ethanol at the carbon film microelectrode surface, in the presence of 10^{-4} M DBU (shown in Figure V-(ii)-iv), a greater change in anodic current occurred when compared to ethanol only (Figure V-(ii)-i).

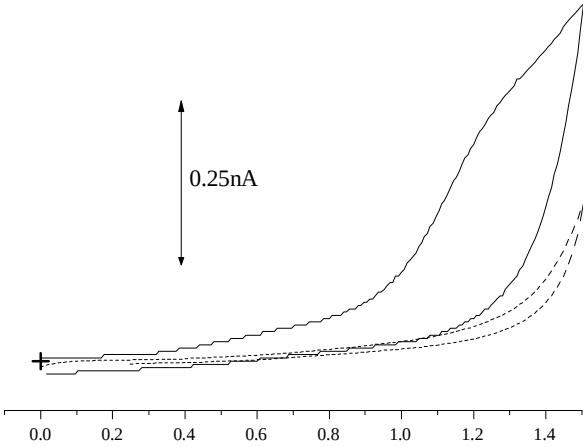

Figure V-(ii)-iv

Cyclic voltammetry of the anodic oxidation of ethanol and 10^{-4} M DBU at a carbon film microelectrode, (—) first scan and (---) twentieth scan.
Scan rate 0.1V s^{-1}

This additional change in the anodic oxidation peak suggests that the DBU has modified the carbon film surface on the microelectrode. To investigate if DBU has contributed to the additional suppression of the AA current in the Faradaic region anodic oxidation of the carbon film microelectrode was carried out with 10^{-4} M DBU in dichloromethane (DCM). DCM was used as the solvent due to the lack anodic oxidation occurring in the potential window used in this work. This is shown in Figure V-(ii)-v. The cyclic voltammograms of the anodic oxidation of 10^{-4} M DBU in DCM are also shown in Figure V-(ii)-v.

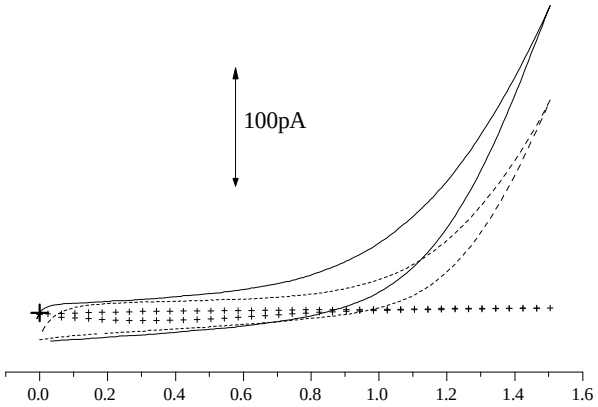

Figure V-(ii)-v

Cyclic voltammetry of the anodic oxidation of 10^{-4} M DBU in DCM at a carbon film microelectrode, (+++) DCM only, (—) first scan and (---) twentieth scan. Scan rate 0.1 V s^{-1}

The cyclic voltammograms of the anodic oxidation of 10^{-4} M DBU in DCM appears to be that of capacitance only without a Faradaic current component. This lack of a Faradaic current suggests surface modification has not occurred, which is shown in the resultant cyclic voltammograms of the oxidation of AA before and after anodic oxidation of 10^{-4} M DBU in DCM (n=3) retaining their sigmodial shape. (Figure V-(ii)-vi.).

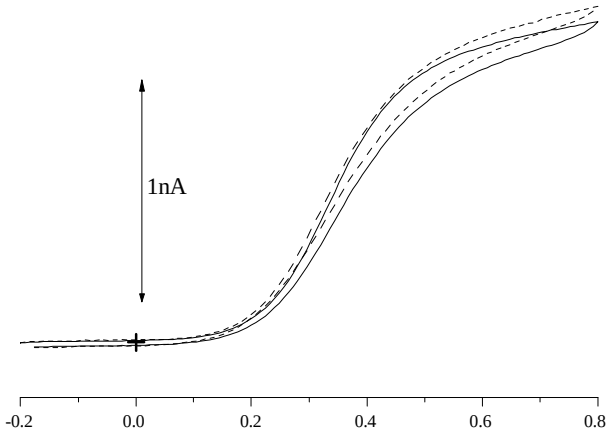

Figure V-(ii)-vi

Cyclic voltammograms of 10^{-4}M AA in citrate/phosphate buffer pH 7.4 at carbon film microelectrodes (—) before and (---) after anodic oxidation of 10^{-4} M DBU in DCM. Scan rate 0.1 V sec^{-1}

This indicates anodic oxidation of DBU in DCM has not contributed to the anionic barrier formed by the anodic oxidation of ethanol. The capacitance of the carbon film after anodic oxidation was 4 μF cm^{-2} (n=3). As this is within the range of unmodified carbon film capacitance measurements (Chapter IV-(iv) Results and Discussion), this indicates if the anodic oxidation of 10^{-4} M DBU in DCM has resulted in attachment of any species, it has not occurred in the graphene regions. This is also indicated by the similar limiting current before and after modification.

As the addition of DBU has enhanced the formation of the anionic barrier all subsequent anodic oxidations employ DBU. This ensured maximum surface coverage of all proposed carbocation additions to the carbon film surface and provides an unambiguous comparison to the results shown in Figure V-(ii)-iii.

To verify the presence and quantify the surface coverage derivatisation of the carbon film microelectrode surface was carried with 3,5-dinitrobenzyl chloride after amidisation. The dinitrobenzyl groups were then reduced electrochemically in 0.1 M HCl (See Chapter V-(i)

Results and Discussion). The average (n=5) carboxylic acid surface coverage was found to be $5x10^{-11}$ moles cm^{-2}.

The previously reported electrochemical oxidation product of ethanol, ethanal, was anodically oxidised by cyclic voltammetry at the carbon film microelectrode in a DCM solution of 10^{-4} M ethanal and 10^{-4} M DBU. The cyclic voltammogram of the anodic oxidation is shown in Figure V-(ii)-vii.

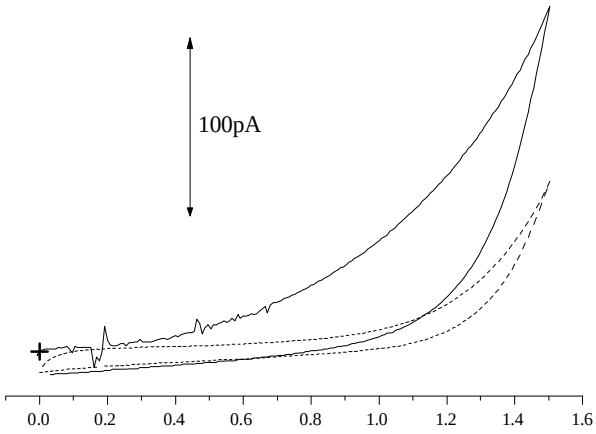

Figure V-(ii)-vii

Cyclic voltammograms of the anodic oxidation of 10^{-4} M ethanal and 10^{-4} M DBU in DCM, at a carbon film microelectrode, (—) first scan and (---) twentieth. Scan rate 0.1 V s^{-1}

The cyclic voltammogram shown in Figure V-(ii)-vii is similar to Figure V-(ii)-iv in shape change in peak current after twenty anodic scans. From the qualitative change in the cyclic voltammogram envelope it appears the surface has been modified. The effect on this change is shown in the cyclic voltammogram of the oxidation of AA, which is shown in Figure V-(ii)-viii.

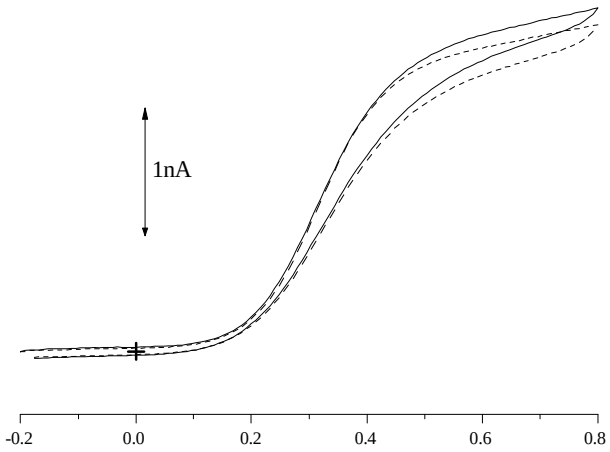

Figure V-(ii)-viii

Cyclic voltammograms of 10^{-4} M AA in citrate/phosphate buffer pH 7.4 at a carbon film microelectrode (—) before and (---) after anodic oxidation of 10^{-4} M ethanal and 10^{-4} M DBU in DCM.
Scan rate 0.1 V s^{-1}

Although the anodic oxidation of ethanal and DBU in DCM displayed a large change in the maximum oxidation current the change in the limiting Faradaic current during the oxidation of AA (n=4) was insignificant. This indicates that the anionic barrier formed during anodic oxidation of ethanol is not the result of anodic oxidation of ethanal. It also verifies that DCM or DBU are not contributing to the anionic barrier.

The cyclic voltammogram of the anodic oxidation of 10^{-4} M ethanoic acid, another reported oxidation product, together with 10^{-4} M DBU in DCM (n=4) at a carbon film microelectrode is shown in Figure V-(ii)-ix. The cyclic voltammogram of AA (n=2) resulting from the anodic oxidation of ethanoic acid and DBU is shown in Figure V-(ii)-x.

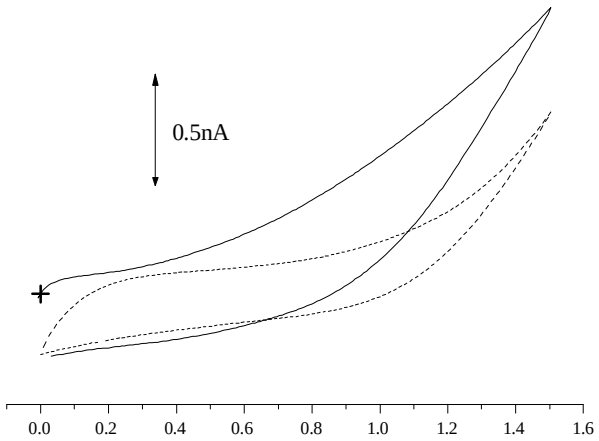

E/V vs. Pt pseudo reference

Figure V-(ii)-ix

Cyclic voltammograms of the anodic oxidation of 10^{-4} M ethanoic acid and 10^{-4} M DBU in DCM, at a carbon film microelectrode, (—) first and (---) twentieth scan. Scan rate 0.1 V s^{-1}

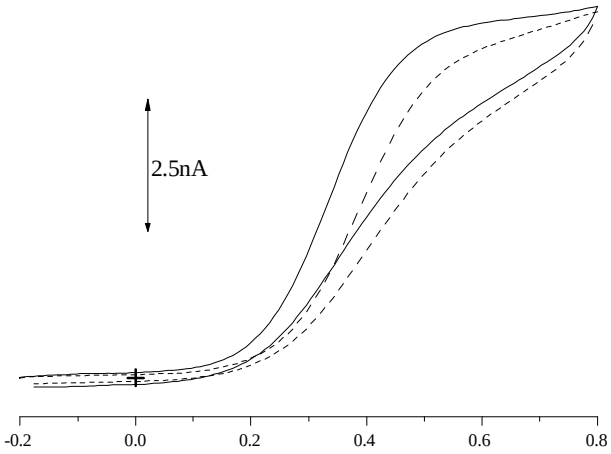

E/V vs. Ag|AgCl

Figure V-(ii)-x

Cyclic voltammograms of 10^{-4} M AA in citrate/phosphate buffer pH 7.4 at a carbon film microelectrode (—) before and (---) after anodic oxidation of 10^{-4} M ethanoic acid and 10^{-4} M DBU in DCM.

The anodic oxidation of ethanoic acid and DBU in DCM shows a slower rate of change in current than DBU in ethanol (Figure V-(ii)-iv), DBU in DCM (Figure V-(ii)-vi) and DBU in

ethanal (Figure V-(ii)-vii). This is possibly due to the partial neutralisation of DBU with ethanoic acid. It is expected that the concentration of DBU would be in excess of that of ethanoic acid. The higher concentration of ethanoic acid used during anodic oxidation was to ensure concentration was not limiting the rate of surface modification.

The cyclic voltammograms of the oxidation of AA (Figure V-(ii)-x) before and after anodic oxidation of ethanoic acid and DBU do not show any significant change in either the limiting current or the waveslope. The lack of change in the cyclic voltammograms of AA after anodic oxidation in DCM solutions containing ethanal or ethanoic acid suggests that they do not participate in the formation of the carboxylic acid groups on the surface of the carbon film microelectrode.

To locate the position of carbon carbon bond on ethanol the cyclic voltammetric anodic oxidation of methanol was carried out. This is shown in Figure V-(ii)-xi.

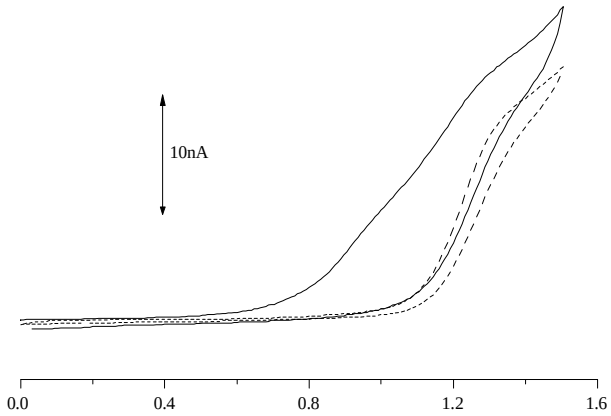

E/V vs. Pt pseudo reference

Figure V-(ii)-xi

Cyclic voltammograms of the anodic oxidation of methanol and 10^{-4} M DBU, at a carbon film microelectrode, (—) first scan and (---) twentieth. Scan rate 0.1V s^{-1}

The change in the cyclic voltammetric envelope during the anodic oxidation of methanol is similar to that of the anodic oxidation of ethanol. (Figure V-(ii)-iv). The effect of this change on the oxidation of AA can be seen in Figure V-(ii)-xii.

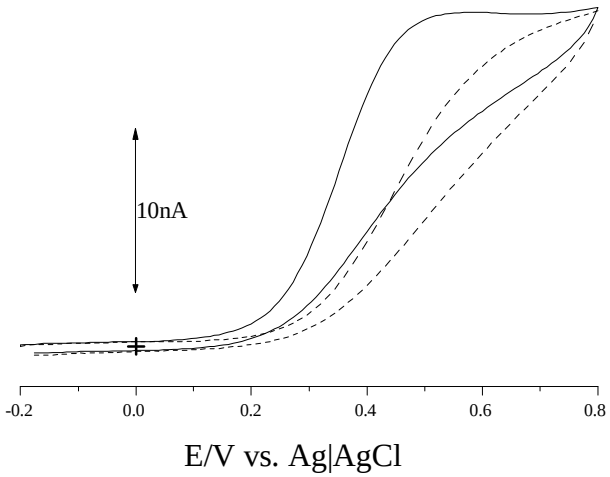

Figure V-(ii)-xii

Cyclic voltammograms of 10^{-4} M AA in citrate/phosphate buffer pH 7.4 at a carbon film microelectrodes (—) before and (---) after anodic oxidation of methanol and 10^{-4} M DBU in DCM. Scan rate 0.1V s^{-1}

The cyclic voltammogram of the oxidation of AA before and after anodic oxidation of methanol (Figure V-(ii)-xii) indicates a slight change in wave slope, the limiting current at 0.8 V remained the same and suppression of Faradaic current is minimal when compared to the ethanol anodic oxidised surface (Figure V-(ii)-iii). It therefore appears the preferred location of the carbon carbon bond linking ethanol to the carbon film surface is via the β carbon.

The proposed carbocation, being an electrophile could form an addition product with either or any of the unsaturated aliphatic pendent groups, the proposed aromatic structure or the graphene area of the carbon film. If the graphene region has undergone electrophilic reaction, the Faradaic limiting current will be reduced. To determine if the graphene area has been reduced, due to anodic oxidation of ethanol, containing DBU, cyclic voltammetry was carried out using DA. These results are shown in Figure V-(ii)-xiii.

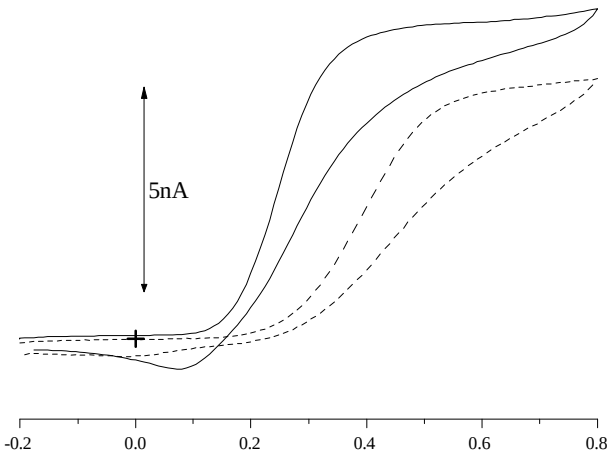

Figure V-(ii)-xiii

Cyclic voltammograms of 10^{-4} M DA at a carbon film microelectrodes in citrate/phosphate buffer pH 7.4 (—) before and (---) after anodic oxidation in ethanol and 10^{-4} M DBU. Scan rate 0.1 V s^{-1}

The cyclic voltammograms (Figure V-(ii)-xiii) (n=3) show a significant loss in limiting current and cathodic wave at 0.1V, after surface modification. The decrease in magnitude of these features indicates a loss in, or access to, the heterogeneous electron transfer surface suggesting that electrophilic addition has occurred here.

The proposed reaction pathway for the formation of carboxylic acid on the carbon film surface of the microelectrode after anodic oxidation of ethanol is shown in Figure V-(ii)-xiv.

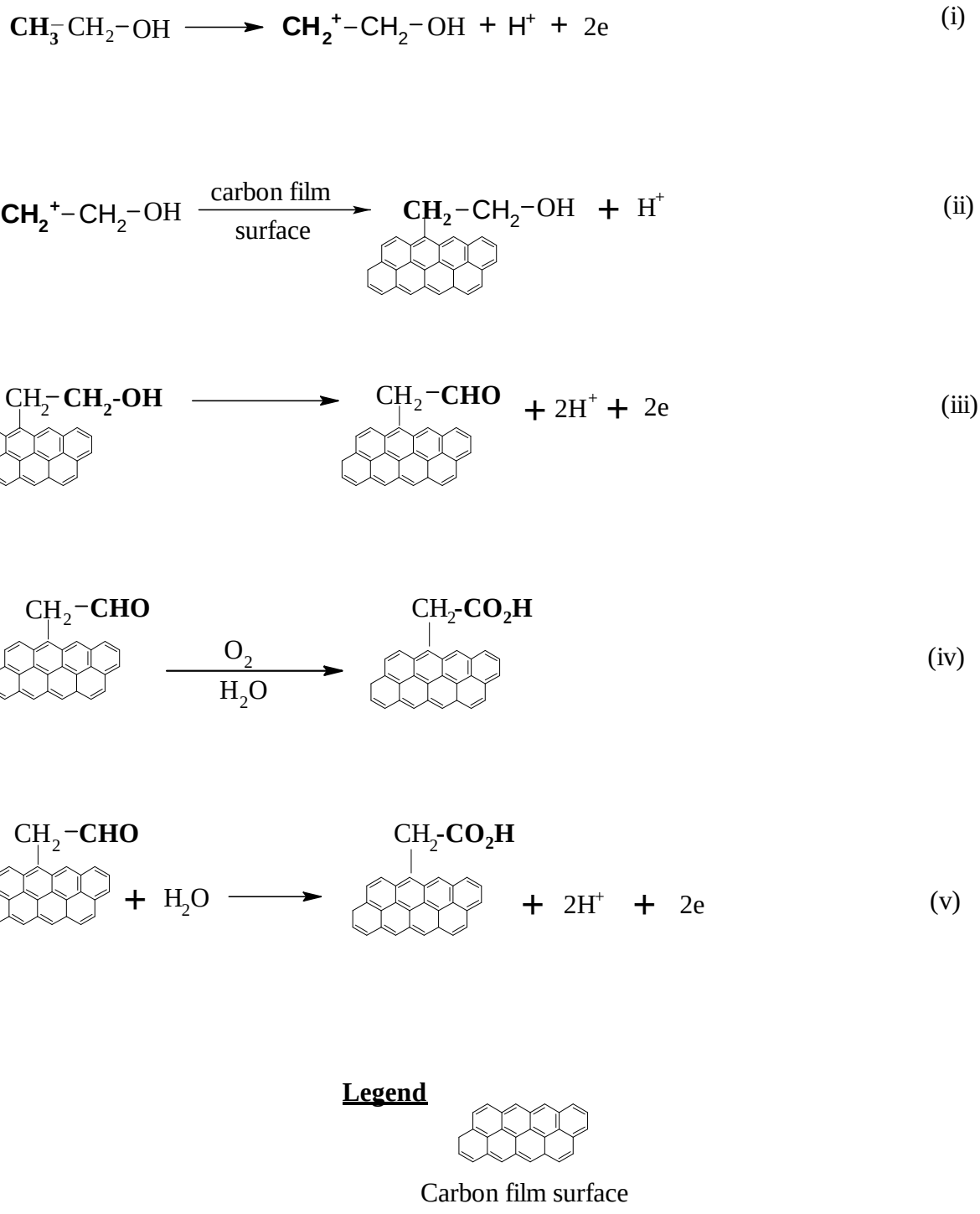

Figure V-(ii)-xiv

The proposed reaction pathway for the formation of carboxylic acid groups, on the surface of a carbon film microelectrode after anodic oxidation in ethanol containing DBU.

The initial step (equation (i)) is the oxidation of ethanol to form the carbocation.[5] The carbocation is preferentially located on the β carbon, possibly due to the electron withdrawing properties of the hydroxyl group on the α carbon.

The second step is the reaction of the ethanol carbocation with the carbon film surface (equation (ii)). The carbocation can either undergo an electrophilic addition or substitution. The substitution reaction (equation (ii)) would be energetically preferred, as the aromatic structure is retained. An addition reaction would destroy the aromaticity and therefore provide a simple explanation for the loss in limiting current. The lost of limiting current could also be explained by the presence of sterically hindering groups, such as carboxylic acid. This steric hindrance would explain the loss in limiting current for the energetically favoured substitution reaction. The substitution reaction is therefore the most probable mechanism for the attachment of the carbocation to the carbon film surface.

The anodic oxidation of ethanol is reported to yield both ethanal[5] and carboxylic acid.[7] However, as the major product is ethanal it is proposed the pathway from ethanol to carboxylic acid is via ethanal (equation (iii)). The attached ethanal is oxidised either by molecular oxygen (in air) (equation (iv)) or by electrochemical oxidation (equation (v)). As ethanoic acid was not the major product of the anodic oxidation of ethanol[8], ethanoic acid via electrochemical oxidation of ethanal is not expected to be the preferred pathway. Therefore it is proposed that the conversion of ethanal to ethanoic acid is probably via oxidation in air.

Conclusion

The anodic oxidation of ethanol, in the presence of DBU, at the surface of the carbon film microelectrodes provided a modified surface which reduced the heterogeneous electron transfer rate for AA. This modified surface also resulted in the reduction in the limiting current and a positive shift in $E_{½}$ of 0.2 V of DA during cyclic voltammetry. The reduction in limiting current suggests that the ethanol attachment was in the graphene region of the carbon

film. It is proposed that this selectivity, obtained towards AA, was due to the electrostatic repulsion of carboxylic groups on the carbon film surface. The presence of carboxylic acid groups on the surface of a carbon film microelectrode, after anodic oxidation of ethanol in the presence of DBU, was verified and quantified using a 3,5-dinitrobenzyl derivative. Using cyclic voltammetry of the oxidation of AA after anodic oxidation of reported reaction products, ethanal and ethanoic acid, the following reaction pathway was proposed. The initial product is the formation of an adduct, between a β carbocation and the graphene region of the carbon film surface. This adduct is then electrochemically oxidised to the aldehyde, which oxidised in air to the carboxylic acid.

References

1. Maeda H.; Yamauchi Y.; Hosoe M.; Li T.; Yamaguchi E. *Chemical and Pharmaceutical Bulletin* **1994,** *42*, 1870-73.
2. Maeda H.; Yamauchi Y.; Yoshida M.; Ohmori H. *Analytical Sciences* **1995,** *11*, 947-52.
3. Maeda H., Itami M., Katayama K., Yamauchi Y., and Ohmori H. **1997**; *Analytical Sciences, 13*, 721-727.
4. Guo B.; Anzai J.; Osa T. *Chemical and Pharmaceutical Bulletin* **1996,** *44*, 860-62.
5. Sundholm G *Journal of Electroanalytical Chemistry* **1971,** *31*, 265-67.
6. Betowska-Brzezinska M.; Uczak T. *Journal of Applied Electrochemistry* **1997,** *27*, 999-1011.
7. Souza J.P.I.; Queiroz S.L.; Bergamaski K.; Gonzalez E.R.; Nart F.C. *Journal of Physical Chemistry B* **2002,** *106*, 9825-30.
8. Iwasita T.; Rasch B.; Cattaneo E.; Vielstich W. *Electrochimica Acta* **1989,** *34*, 1073-79.

Chapter V-(iii)

Modification of Carbon Film Microelectrode Surface using Aromatic Amines

Abstract

Dinitroanilines and dinitrodiphenyl amine has been attached to the pendent groups on the surface of carbon film microelectrodes by anodic oxidation. The average surface coverage of 2,4-dinitroaniline was determined to be $1.1x10^{-10}$ moles cm^{-2}. These groups provided limited suppression of the Faradaic oxidation current of ascorbic acid.

Introduction

The traditional barriers to AA signal have been anionic, based on acid groups, either carboxylic or sulfonic (See Chapter V Introduction). In this sub chapter the nitro group was investigated as a possible anionic barrier. Although the nitro group is less electro negative than a carboxylic acid group, it has a strong dipole (3.46 D)[1]). With this strong dipole the nitro group may provide sufficient barrier to reduce the Faradaic current of AA at potentials used to chronoamperometrically follow the DA efflux. The possible antifouling properties of the nitro group were also considered of interest as no published references pertaining to the fouling properties of nitro groups could be found.

To form a nitro barrier requires anodic oxidation of a functional group to react with the surface, as cathodic attachment could result in reduction of the nitro group. The slight reduction of the nitro group during anodic attachment, via the diazonium salt, of 4-nitrophenyl radical was reported.[2] The amine group formed would then require chemical or electrochemical oxidation to reform the nitro group. To attach the nitro groups to the surface nitrated aromatic amines were selected. The >N-H bond is resistant to hydrolysis and facile

methods of bonding to GC have been reported.[3] Aromatic amines were selected due to the reported higher surface coverage, $7.3x10^{-10}$ moles cm^{-2} [3], than aliphatic amines.[4] The facile method used for the surface modification of a carbon fibre electrode was the chronopotentiometric anodic oxidation of $6x10^{-4}$ M 4-nitrobenzylamine, in acetonitrile, with 0.1 M tetrabutylammonium tetrafluoroborate as the supporting electrolyte, at 1.6 V (versus SCE.) for 90 seconds. The published proposed reaction pathway is shown in Figure V-(iii)-i.[3]

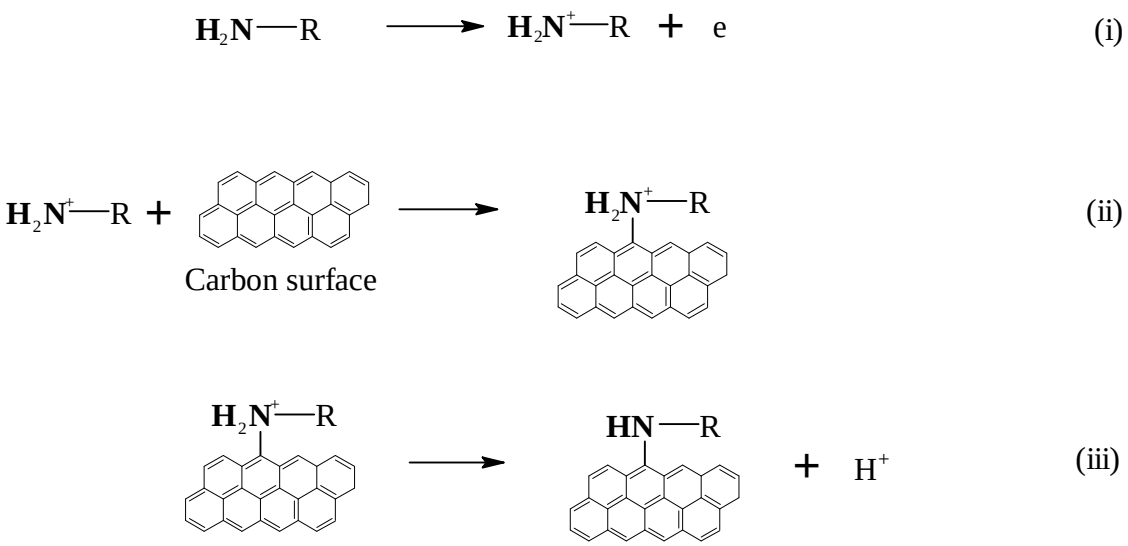

Figure V-(iii)-i

Anodic oxidation pathway for the attachment of amines to a carbon fibre surface

The attachment of the amine to the carbon film surface is similar to that proposed for the attachment of ethanol (Chapter V-(ii)). As in the case of ethanol attachment, the nitrogen cation reaction with the carbon film surface could be either a substitution or elimination reaction. To maximise the effect of the nitro group, in forming an anionic barrier, disubstituted aniline was used as the aromatic amine. To increase the surface concentration of the dinitro groups 1,8-diazabicyclo[5.4.0]undec-7-ene (DBU) was added to stabilise the

nitrogen cation formed. The success of DBU in stabilising the carbocation on ethanol (Chapter V-(ii)) was expected to be repeated with the nitrogen cation.

The effect of substitution position was also investigated using three commercially available disubstituted anilines: 2,4-dinitroaniline, 2,6-dinitroaniline and 3,5-dinitroaniline. 2,6-dinitrodiphenyl amine was also included as the additional aromatic group was considered as a possible source of the inherent supression of AA for “medium size” carbon film microelectrodes (Chapter IV-(x) Results and Discussion).

To evaluate the barrier properties to AA, after modification of the carbon film microelectrode surface, cyclic voltammetry was carried out in citrate/phosphate buffer at pH 7.4. To determine the surface coverage of the disubstituted nitro anilines cathodic reduction using cyclic voltammetry was carried out in 0.1 M HCl.

Experimental Section

Chemicals

Dopamine (Aldrich), ascorbic acid (BDH), potassium phosphate decahydrate (Aldrich), phosphoric acid (BDH Analar), 2,4-dinitroaniline (Aldrich), 2,6-dinitroaniline (Aldrich), 3,5-dinitroaniline (Aldrich), 2,4-dinitrodiphenyl amine (BDH), dichloromethane (BDH), 1,8-diazabicyclo[5.4.0]undec-7-ene (Aldrich), hydrochloric acid (BDH) and nitrogen (BOC) (Instrument Grade) were all used as received. All solutions were prepared daily. Aqueous solutions were prepared using Milli-Q water (Milli-Q Reagent Water System).

Equipment

The three electrode system was used, as outlined in Chapter II Electrochemical Equipment. Two reference electrodes were used: an Ag|AgCl (3 M KCl) reference in aqueous solutions and a pseudo platinum electrode in non-aqueous solvents.

Electrode Fabrication

The microelectrodes were fabricated as outlined in Chapter III, using 40 ml min^{-1} nitrogen in the counter flow configurations.

Procedure

Modification of the electrode surface

The carbon film microelectrode was cycled ten times between 0.5 V to 2.0 V versus a pseudo platinum reference electrode at 0.1 V s^{-1} in a dichloromethane (DCM) solution containing 10^{-4} M aniline and 10^{-4} M 1,8-diazabicyclo[5.4.0]undec-7-ene (DBU). The carbon film microelectrodes were then rinsed in DCM for 10 seconds with gentle agitation, followed by 10 seconds gentle agitation in ethanol and ten seconds gentle agitation in deionised water.

Cyclic voltammetry of AA and DA

See Chapter IV-(x) Dopamine and Ascorbic acid - Experimental section.

Determination of the nitro group surface concentration

See Chapter V (i) Experimental section.

Results and Discussion

The cyclic voltammograms of the anodic oxidation of the dinitroanilines and dinitrodiphenyl amine together with their corresponding oxidation of AA are shown in Figure V-(iii)-ii. The cyclic voltammograms (a)(n=8), (c)(n=9), (e)(n=6) and (g)(n=10) are nondescript when compared to that of carbon fibre[3] and GC[5]. This difference is proposed to be dependent on the chemical groups which are reacting with the cation formed during anodic oxidation. GC and carbon both contain the reactive edge planes. The anodic oxidative attachment of ethanol (Chapter V-(ii)) produced an anodic wave which decreased with repetitive scanning whereas the anodic oxidation wave and subsequent scans of the amines did not change. This implies the graphene region of the carbon film microelectrodes are undergoing modification.

The cyclic voltammograms of the resultant surface modification (b), (d), (f) and (h) show a degree of suppression of the AA Faradaic current. From these results the location of the nitro groups on the benzene ring does not appear to influence the degree of suppression of the AA Faradaic current. The inclusion of the additional phenyl ring appears to have mitigated the dinitro suppression of the AA Faradaic current. This reduction in AA barrier could be attributed to the second phenyl group sterically limiting access to reactive sites.

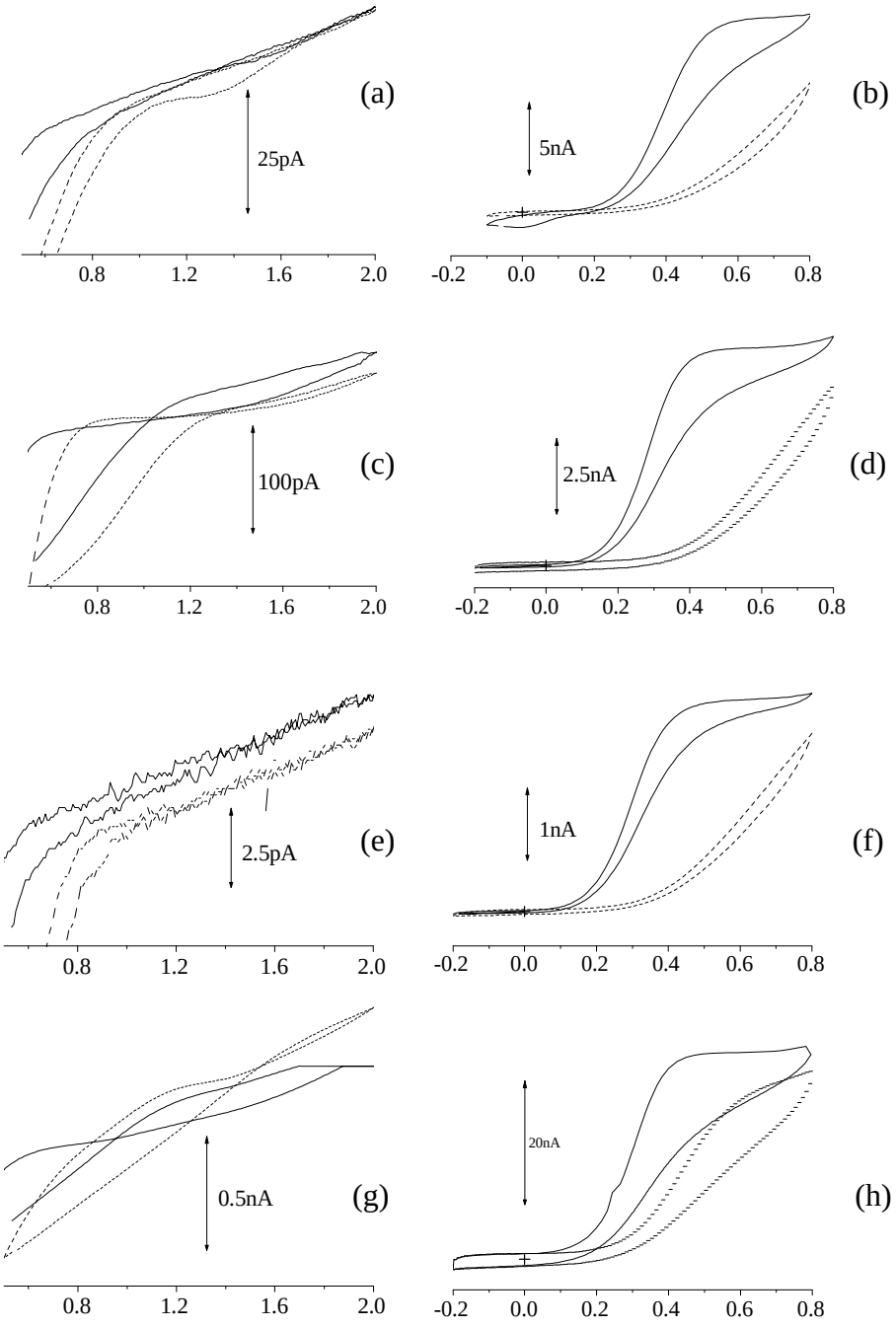

Figure V-(iii)-ii

Cyclic voltammograms (first scan (—) and 10^{th} (---)) of the anodic oxidation of 10^{-4}M (a) 2,4-dinitroaniline, (c) 2,6-dinitroaniline, (e) 3,5-dinitroaniline and (g) 2,6-dinitrodiphenyl amine and 10^{-4} M DBU in DCM at a carbon film microelectrode. Cyclic voltammograms (b), (d), (f) and (h) are the corresponding oxidation of 10^{-4} M AA in pH 7.4 buffer, before (—) and (---) after surface modification by anodic oxidation of the anilines at the same carbon film microelectrode. Scan rate 0.1 V s^{-1}

The location of the attached dinitro groups, on the pendent chain, is indicated by the lack of change in the limiting current of DA (n=12). This is shown in Figure V-(iii)-iii. This contrasts with the ethanol attachment which reduced the graphene region. This difference in attachment location, although both reactive species appear to be cations, is ascribed to a difference in the electrical potential of the cation. An example of this is the cation reaction on basal graphite which requires the use of nitrophenyl radicals generated from the diazo salt to form a covalent bond.[6] As the graphene region of the carbon film is the same structure as a basal plane, the cation formed by anodic oxidation of ethanol may have cation radical characteristics. The positively charged amine species is therefore probably closer in characteristics to that of a cation than a radical cation, hence the lack of attachment in the graphene region.

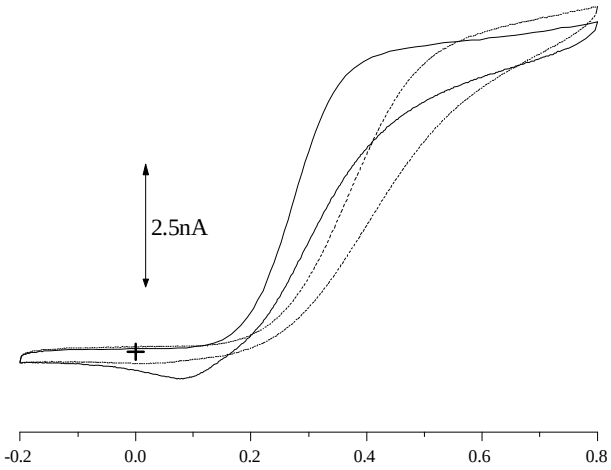

Figure V-(iii)-iii

Cyclic voltammograms of the anodic oxidation of 10^{-4} M DA in citrate/phosphate buffer pH 7.4, at a carbon film microelectrode, before (—) and after (---) modification with 2, 6-dinitroaniline. Scan rate 0.1 V s^{-1}

An indication of the location of the amine reaction is the loss of the cathodic wave (0 V to 0.2 V Figure (iii)-iii). The loss of the cathodic wave indicates that the amine reaction site is close to the graphene region. This loss of cathodic wave together with the anodic shift in E½ indicates the catalytic effect the graphene neighbouring groups possess in the anodic oxidation of DA.

The average surface coverage of nitro groups was $1.1x10^{-10}$ moles cm^{-2} (n=4) for 2,4-dinitroaniline. (Time constraints precluded other groups being measured.) The 2,4-dinitroaniline samples ranged from $1.3x10^{-11}$ to $2x10^{-10}$ moles cm^{-2}.

These results are similar to those obtained for unsaturated aliphatic groups (Chapter IV-(vii)) implying concentration of the aromatic groups adjacent to the graphene region.

Conclusion

Dinitro groups were found to produce a limited barrier to Faradaic oxidation of AA in citrate/phosphate buffer solutions at pH 7.4 at an average surface coverage of $1.1x10^{-10}$ moles cm^{-2}.

The amine linkage has occurred on adjacent aromatic pendent groups (indicated by the reduction in the cathodic wave) to the graphene region, leaving the electrochemically active surface area undiminished. This is additional evidence of the presence of surface pendent chains.

References

1. McMurry John *Organic Chemistry*, ed.; Brooks/Cole: U.S.A., 1999.
2. Allongue P., Delamar M., Desbat B., Fagebaume O., Hitmi R., Pinson J., and Saveant J.M. *Journal of the American Chemical Society*, **1997**, *119*, 201-207.
3. Barbier B.; Pinson J.; Desarmot G.; Sanchez M. *Journal of Electrochemical Society* **1990,** *137*, 1757-64.
4. Deinhammer R.S.; Ho M.; Anderegg J.W.; Porter M.D. *Langmuir* **1994,** *10*, 1306-13.
5. Downard A.J. and Mohamed A. *Electroanalysis*, **1999**, *11*, 418-423.

6. Liu Y.; McCreery R.L. *Journal of the American Chemical Society* **1995,** *117*, 11254-59.

Chapter V-(iv)

Modification of Carbon Film Surfaces to form a Dual Functional Ascorbic Acid Barrier

Abstract

The unique surface of the carbon film microelectrode has been modified by two facile anodic oxidation procedures. The first anodic oxidation modification of the surface pendent groups was with dinitroanilines, the second was the formation of carboxylic acid, on the graphene surface, via the anodic oxidation of ethanol. From coverage measurements of the nitro groups (10^{-11} moles cm^{-2}) the dinitroanilines did not undergo a substitution reaction during anodic oxidation of ethanol. The barrier properties of each modification appears to be additive with respect to the suppression of the Faradaic oxidation current of ascorbic acid and changes to the limiting current of DA.

Introduction

In the previous sub-chapters of Chapter V the carbon film surface has been modified by forming adducts with either the pendent groups or graphene regions. Previously published work on electrode surface modification has resulted in the formation of mono-functional surface adducts.[1] In this sub chapter a dual functionality will be formed on the microelectrode surface utilising the unique different reactive sites of the carbon film surface.

The initial modification will be the attachment of 2,4-dinitroaniline to the pendent aromatic groups (Chapter V-(iii)). The second modification was the attachment of carboxylic acid groups to the graphene region (Chapter V-(ii)).

To obtain the dual functionality on the carbon film microelectrode surface nitro groups were attached using dinitroanilines followed by carboxylic acids via anodic oxidation of ethanol

The dual functionality is to provide anti fouling properties from the nitro groups and an anionic barrier to AA using carboxylic acid groups.

Experimental Section

Chemicals

As outlined in Experimental section of Chapter V-(ii) and (iii).

Equipment

As outlined in Experimental section of Chapter V-(ii) and (iii).

Electrode Fabrication

As outlined in Experimental section of Chapter V-(ii)

Surface Modification

The carbon film microelectrodes were modified by the procedure outlined in Chapter V-(ii) and Chapter V-(iii) Experimental Section.

Cyclic Voltammetry

The carbon film microelectrodes were evaluated using cyclic voltammetry of AA and DA. (Chapter IV-(x))

Determination of dinitro group concentration on the surface.

The procedure is outlined in Chapter V-(i).

Results and Discussion

The two facile anodic oxidation steps form a bifunctional surface group modification which is additive in suppression of the AA oxidation Faradaic current. The additive suppression of the AA Faradaic currents are shown in the cyclic voltammograms in Figure V-(iv)-i.

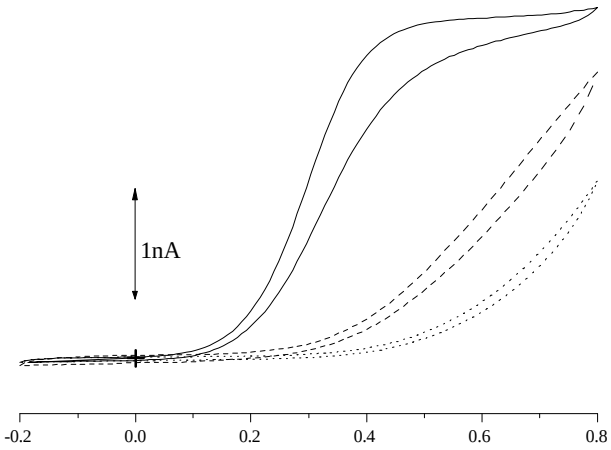

Figure V-(iv)-i

Cyclic voltammograms of 10^{-4} M AA in citrate/phosphate buffer pH 7.4 before (—), (---) after anodic oxidation in 10^{-4} M 3,5-dinitroaniline and 10^{-4} M DBU and (···) after anodic oxidation of ethanol containing 10^{-4} M DBU.
Scan rate 0.1 V s^{-1}

The cyclic voltammogram of the oxidation of AA in citrate/phosphate buffer - pH 7.4, at a carbon film microelectrode, prior to modification displayed a well defined sigmodial shape. The cyclic voltammogram of the oxidation of AA, after the carbon film surface was anodically oxidised in the presence 2,4-dinitroaniline (n=7) or dinitrodiphenyl amine (n=4) and DBU indicates an anionic barrier was formed on the surface. The degree of suppression of the AA oxidation Faradaic current was similar to that reported in Chapter V-(iii).

After anodic oxidation in ethanol, containing DBU, the barrier properties to the Faradaic oxidation of AA was further enhanced. The cyclic voltammogram now has a similar shape to those presented the ethanol modified surface in Chapter V-(ii).

Cyclic voltammetry using DA shows a similar additive trend with regard to loss of sigmodial shape, limiting current and loss of cathodic wave. This is shown in Figure V-(iv)-ii.

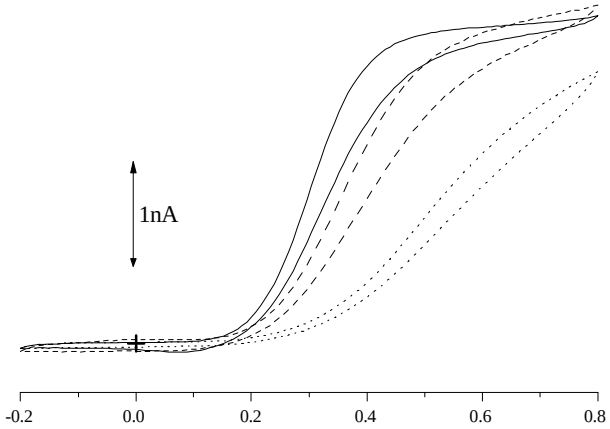

Figure V-(iv)-ii

Cyclic voltammograms of 10^{-4} M DA in citrate/phosphate buffer pH 7.4 before (—), (---) after anodic oxidation in 10^{-4} M 3,5-dinitroaniline and 10^{-4} M DBU and (···) after anodic oxidation of ethanol containing 10^{-4} M DBU.
Scan rate 0.1 V s^{-1}

The cyclic voltammogram of DA, for the same electrode as in Figure V-(iv)-i displays a loss in the cathodic wave with retention of the limiting current after modification with the 3,5-dinitroaniline. After anodic oxidation in ethanol and DBU, the $E½$ shifted to a higher potential with a loss of limiting current. These changes occurred to a lesser degree without DBU, during anodic oxidation of ethanol (Chapter V-(ii) results and Discussion) indicating additivity of changes in the cyclic voltammetry of DA.

The nitro group coverage was found to range between $5x10^{-12}$ and $2x10^{-11}$ moles cm^{-2} (n=2) after 2,4-dinitroaniline and ethanol modification. This range of results is similar to that obtained for the single step attachment of dinitroanilines reported in Chapter V-(iii). These results indicate the proposed carbocations formed during the anodic oxidation of ethanol have not replaced the nitro groups previously attached to the surface.

Conclusion

The unique surface chemistry of the carbon film surface has been modified using electrochemically generated cations, carbon and nitrogen, to form adducts at the different reactive sites. The change in suppression of the Faradaic current to anodic oxidation of AA appears to be additive, as are the changes to the anodic oxidation of DA.

The ability to attach different functional groups independently to the surface of a microelectrode presents opportunities for simultaneous analytical analyses.

References

1.Downard A.J. *Electroanalysis* **2000,** *12*, 1085-96.

Chapter VI

In Vivo Anti-Fouling Properties of Surface Modified Carbon Film Microelectrodes

Abstract

The anti-fouling properties of carbon film microelectrodes, modified by the anodic oxidation of 2,4-dinitroaniline in dichloromethane, have been evaluated in vivo for four hours, in the extracellular fluid of an anaesthetised rat brain. After this period in vivo, the modified carbon film microelectrode did not display any signs of fouling, when measured using in vitro cyclic voltammetry of dopamine.

Introduction

In the previous chapters of this thesis electrochemical experimentation has been *in vitro.* In this chapter the carbon film microelectrodes are evaluated *in vivo,* for fouling in the extracellular fluid of the central nervous system, using anaesthetised rats. Fouling in this environment typically causes a 40% decrease in sensitivity[1] during DA efflux measurements, using a carbon fibre microelectrode. In this thesis work *in vivo* evaluation of fouling of carbon film microelectrodes was carried out as an adjunct to experiments being conducted in the Department of Psychology, Macquarie University. These experiments complied with the Australian Code of Practice for use of animals in scientific experiments and were approved by the Macquarie University Animal Ethics Committee.

To measure the efflux of DA experimentation was carried out using fixed potential (0.8 to 0.9 V vs. Ag|AgCl) chronoamperometric monitoring in the nucleus accumbens, after electrical stimulation in the laterodorsal tegmental area (LDT) of the hindbrain.[2] This region of the brain has the cholinergic and glutamatergic neuronal cells. These cells contain the excitatory transmitters acetylcholine and glutamate. These neurons are connected to the DA

neuronal cells in the ventral tegmentum, which in turn are connected to the dopaminergic neurons in the nucleus accumbens. The electrical stimulation when applied to the cholinergic and glutamatergic neurons in the laterodorsal tegmental area evokes the release of acetylcholine and glutamate. This activates the dopaminergic cells in the ventral tegmentum to release DA in the nucleus accumbens. It is this evoked release of DA in the nucleus accumbens, which is monitored by fixed potential chronoamperometry, with carbon microelectrodes. The schematic of the three electrode configuration for fixed potential chronoamperometry is shown in Figure VI-i.

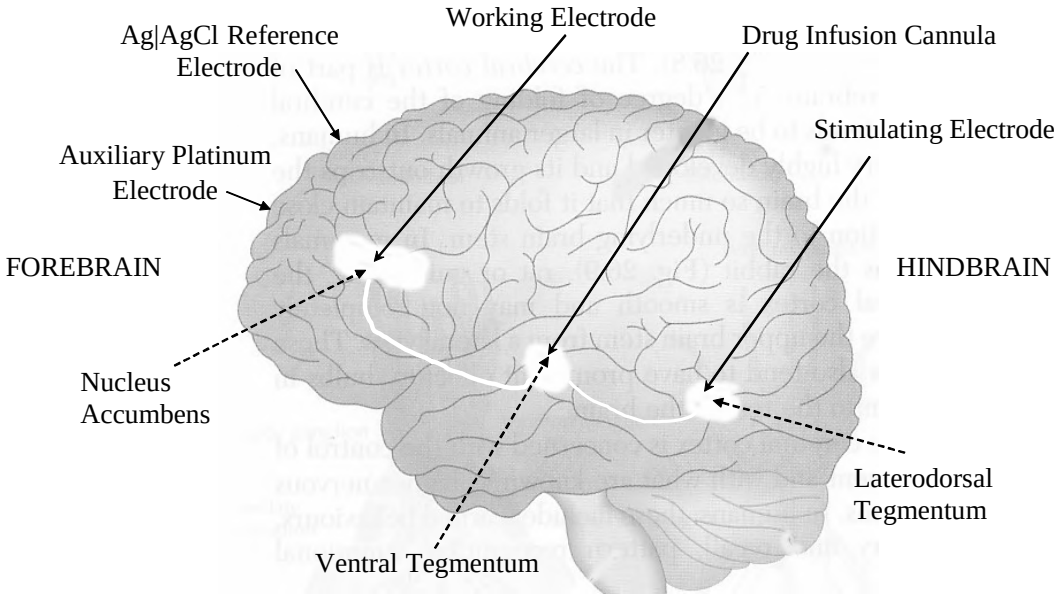

Figure VI-i

Schematic of electrodes implanted in an anaesthetised rat's brain.

The DA is released from vesicles in the neuron into the synaptic cleft, an extracellular region between neurons measuring between 30- 50 nm in the mammalian brain. It is the release into extracellular fluid which provides the opportunity to monitor DA. The electrode tip, which is considerably larger than the synapsis, is forced into these synapses which

number in the ten thousands, however each has many vesicles, (the sites which release DA into the synapse) which when combined produce a detectable and quantifiable amount of DA. [3]

The DA released into the synaptic cleft interacts with receptors on both sides of the cleft, pre and post synaptic sides, with the remaining or "efflux" DA reaching the carbon microelectrode surface as it diffuses into the extracellular space.

To evoke the DA efflux a train of electrical pulses was applied to the cholinergic and glutamatergic cells in the laterodorsal tegmentum. In a typical experiment the electrical stimulation consists of a train of eleven to fifteen monophasic pulses of 800 μA at 35-50 Hz. This is repeated after thirty seconds, thus preventing depletion of DA in the terminal vesicles.[2] An example of this type of amperometric response, obtained during this thesis work, is shown in Figure V-ii. The DA efflux measured in this example is equivalent to 10^{-11} moles of DA being released for each burst of 15 pulses.

The fixed potential chronoamperometric trace, shown in Figure V-ii, illustrates the excellent temporal resolution obtained by carbon film microelectrodes. In the inset of Figure V-ii the pulses are 20 milliseconds apart, which with the high data acquisition rate of 10,000 data points per second provide a detailed tracking of the concentration changes of DA during exocytosis. The rising section of this trace corresponds to the DA efflux during electrical stimulation. Approximately 60 milliseconds after the last electrical stimulation pulse the current reaches a maximum of 400 pA before decaying to the pre-stimulation level. This decay in concentration of DA in the synapsis is the result of uptake by pre and post synaptic receptors and diffusion into the extracellular fluid.

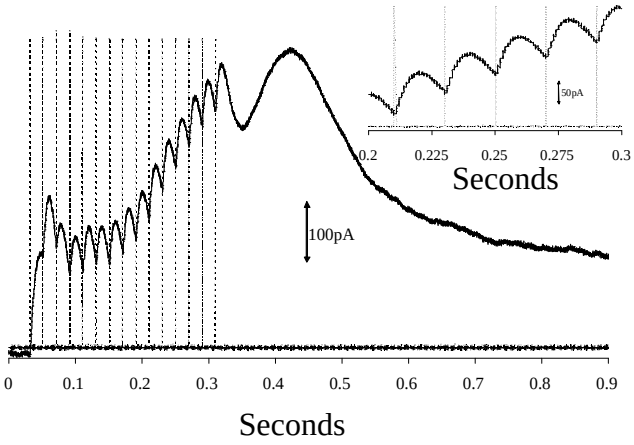

Figure VI-ii

Fixed potential (0.9 V vs. Ag|AgCl) chronoamperometric trace of DA efflux, in the nucleus accumbens of an anaesthetised rat during and after 15 pulses at 50 Hz (---). The inset shows the peak details with the overlay of the electrical pulses (---) at 20 millisecond intervals (50 Hz).

The sensitivity of microelectrodes during *in vivo* applications has been illustrated using an isolated neuron from the retina of a mouse. A 5 μm diameter carbon fibre disc electrode monitoring chemically evoked DA efflux, measured an average of $52x10^{-21}$ moles of DA released.[4] The DA concentration within the vesicles, prior to exocytotic release was calculated to be 0.8 M. The concentration in the vesicles was estimated using concentration changes with time and applying Fick's Laws of Diffusion. This high concentration ensures that the DA receptors, across the synapse, receive DA at a sufficient concentration to relay the neurological signal.

Using *in vivo* fixed potential microelectrodes, chronoamperometric changes in the pattern of DA efflux have been used to assist in the understanding the dopamine function within the central nervous system,[5-7] that include neurological and psychiatric disorders, such as Parkinson's and Schizophrenia. [8] Recently studies on the effects of "drugs of abuse", morphine, cocaine,[9] anti-depressants,[10] and methamphetamines[11] have utilised *in vivo* chronoamperometry of DA to understand the addictive processes.

Typically for *in vivo* experiments the microelectrodes are implanted in the brain tissue for at least one hour[2] to six hours. This results in loss of 40-60% in sensitivity and temporal response of the carbon fibre electrode.[1] To conduct experiments over two weeks, in freely moving mice, requires the use of removable microelectrodes.[12] This degradation in response has been attributed to interference (fouling) of the electrode surface by adsorption of proteins from the extracellular fluid of both live animals[7] and brain slices.[13]

The extracellular fluid not only contains electrochemical interfering molecules (ascorbic acid) but also other biologically active molecules. The insertion of a microelectrode into a living tissue is an invasion by a foreign body which invokes an immediate response by the immune system. Damage to the central nervous system results in gliosis,[12] a neuron protection system in which astrocytes engulf intruders to prevent further damage to the neural network. This process is relatively slow whereas it is possible that proteins, derived from the disruption of the cells during insertion of the microelectrode participate in the fouling of the electrode surface during the 1 to six hour experiments.[14] Various strategies have been used to overcome *in vivo* fouling, including surface modification, hydrogels and topography changes.[14] These surface modifications have been evaluated *in vitro* using non-living tissue, such as fibrinogen,[15] mouse fibroblasts and macrophages.[16] Earlier work had used bovine and human serum albumin for anti-fouling evaluation.[17-19]

In this thesis work surface modified carbon film microelectrodes were evaluated *in vivo*, thus enabling several possible mechanisms of fouling to occur, particularly protein interactions with the carbon surface of the electrode. Changes in the cyclic voltammograms of DA and AA before and after *in vivo* application were used to assess the extent of fouling.

Experimental Section

Chemicals

Nafion solution (5% in lower aliphatic alcohols and water) (Aldrich), dopamine (Aldrich), ascorbic acid (Aldrich), potassium phosphate decahydrate (Aldrich), phosphoric acid (BDH), citric acid (Aldrich), nitrogen (BOC Instrument Grade), urethane (Sigma) and nomifensine maleate salt (Sigma) were used as received.

Equipment

In Vivo

Kopf stereotaxic frame, concentric bipolar stimulating electrode (O.D. 100 μm; tip length 250 μm SNE-100, David Kopf Instruments, Tujunga CA, USA), Ag|AgCl reference electrode, platinum auxiliary electrode and data acquisition system (e-corder and picostat-eDAQ Australia).

In vitro

As outlined in Chapter II Electrochemical Equipment.

In Vivo Electrochemistry

Preparation of animals

Male Hooded Wistar rats, weighing 255-370 g, were obtained from the Animal Resources Centre, Adelaide (SA, Australia). Rats were housed in pairs in plastic and steel cages and maintained at a constant temperature (22 ± 0.5 °C) with a 12:12 h light-dark cycle, with lights on at 08.00 am. Food pellets and water were available ad libitum.

Surgery

Animals were anaesthetised with urethane (1.8 g/kg intraperitoneal) supplemented 30 min later with 0.3 g/kg urethane. Animals were placed in a Kopf stereotaxic frame in which the skull was secured by a nose clamp, incisor bar, and earbars. Constant body temperature

(37^{o}C) was maintained with a temperature regulated heating pad (TC-831, CWE Inc., NY, USA). An incision extending approximately 3 cm was made along the midline of the scalp to expose the cranial landmark of bregma. Holes were drilled in the skull to enable electrode and cannula placement over the left ventral tegmental area, left nucleus accumbens and left laterodorsal tengmentum. A subsequent hole was drilled on the right, enabling placement of a Ag/AgCl reference and stainless-steel auxiliary electrode combination onto cortical tissue. A concentric bipolar stimulating electrode (O.D. 100 μm; tip length 250 μm) (SNE-100, David Kopf Instruments, Tujunga CA, USA) was implanted in the left laterodorsal tegmentum through the cerebellum at 23° vertical angle along the AP plane (interaurel coordinates AP +1.8 mm, ML +0.6 mm and DV +3.6 mm.[20] The reference/auxiliary electrode combination was placed so that the tip of this electrode pair just made contact with contralateral cortical tissue. A 31g stainless-steel guide cannula was inserted above the ventral tegmental area (interaural co-ordinates: anterior posterior –1.5 mm, medial lateral plane + 0.8 mm, and dorsal ventral + 3.3 mm)[20].

Preliminary recording commenced prior to recording electrode placement, allowing precise determination of the point at which the electrode tip made contact with the brain surface, indicated by an increase in oxidation current. The electrode was then lowered to its final position in the nucleus accumbens (anterior posterior +1.7 mm from bregma, medial lateral plane +1.2 mm, and dorsal ventral -7.5 mm[20]

Fixed Potential Chronoamperometry

Intra-ventral tegmental area drug-induced changes in left laterodorsal tegmentum electrical stimulation-evoked (5-15 pulses, 50 Hz) nucleus accumbens dopamine release were monitored in the nucleus accumbens using fixed potential chronoamperometry (10 K samples s^{-1}). All recordings were performed in a Faraday cage (80 cm x 86 cm x 80 cm) to prevent interference from external line-voltage noise.

Monophasic constant current square wave pulses (600-1000 μA) were applied to the stimulating electrode in the laterodorsal tegmentum via an optical isolator through a programmable pulse generator (Iso-Flex/Master-8; AMPI, Israel). This varied between animals, but remained constant over the duration of the experiment. In the experiments, 5 to 15 monophasic pulses (0.5 millisecond duration) were delivered at 50 Hz`.

Oxidation current was continuously monitored by applying a fixed potential of 0.9 V to the recording electrode via an electrometer (Powerlab system, eDAQ Australia.).

In Vitro Electrochemistry

Electrode Fabrication

Carbon Fibre Electrodes

Carbon fibre microelectrodes were fashioned by threading a single carbon fibre (10 μm O.D.) through a borosilicate capillary tube. The tube was then heated and pulled (Sutter Puller), to form a tip through which the carbon fibre protruded. The carbon fibre inside the capillary is then permanently located with cyanoacrylate adhesive and allowed to cross link overnight. Graphite powder was tamped into the bore of the electrode and a copper wire inserted into the graphite powder. The copper wire was secured in place with cyanoacrylate adhesive. The carbon fibre was cut to approximately 500 μm, in length. Before placement in the brain, the carbon fibre electrode was immersed in concentrated nitric acid (40% w/w) for 20 seconds with gentle agitation. The carbon fibre electrode was rinsed in hot water for 10 seconds, with gentle agitation.

Carbon Film Microelectrodes

As outlined in Chapter III, with a nitrogen 40 ml min^{-1} counter flow configuration was used.

Surface Modification

Nafion Coating

Carbon film microelectrodes were immersed in the Nafion solution, as received, for ten seconds, on removal inverted, flicked (a quick wrist action to reduce dry coating thickness near tip) then allowed to air dry at room temperature for five minutes. The Nafion coated carbon film microelectrodes were then oven dried at 80°C for ten minutes. The Nafion coating procedure was then repeated twice.

Ferrous Sulfate Modification

As outlined in Chapter V-(i) Experimental

Ethanol Modification

As outlined in Chapter V-(ii) Experimental

2,4-Dinitroaniline Modification

As outlined in Chapter V-(iii) Experimental

Dual Functionality Modification

As outlined in Chapter V-(iv) Experimental

Cyclic Voltammetry of DA and AA

Cyclic voltammetric conditions as outlined in Chapter IV-(x) Experimental

Electrode Cleaning after in vivo use

The electrodes where removed from the rat's brain after *in vivo* studies and gently rinsed in warm water to remove any weakly adhering brain tissue. The removal of weakly adhering brain tissue was to prevent any physical interference to diffusion of DA and AA, during subsequent *in vitro* evaluation.

The evaluation prior to *in vivo* work and after was carried out using the solutions and procedure outlined in Chapter IV-(x) Experimental.

Results and Discussion

After conclusion of the neurochemical experiments, the carbon fibre microelectrode was removed and the carbon film microelectrode inserted into the nucleus accumbens. The reinsertion of a microelectrode may cause "leakage" (lack of intimate contact between the neurons in nucleus accumbens and the microelectrode), which will affect the quality of the chronoamperometric trace but will not influence the extent of fouling. Using carbon film microelectrodes in this way, as an adjunct to existing neurochemical studies, animal usage was minimised without jeopardising the integrity of the fouling studies.

A typical pre *in vivo* cyclic voltammogram of DA and AA, both at 10^{-4} M obtained at a carbon fibre microelectrode, (O.D. 10 μm and length 500 μm) is shown in Figure VI-iii.

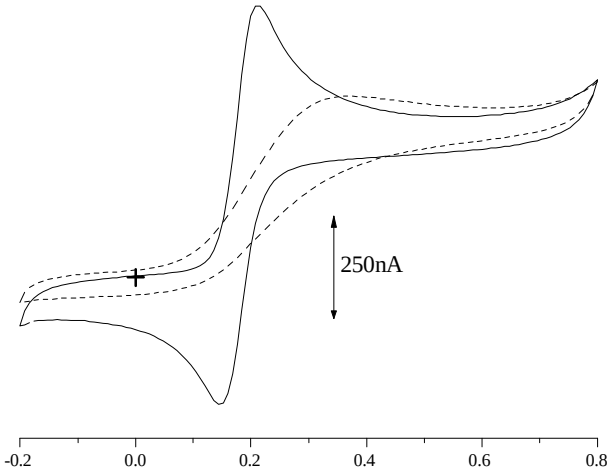

Figure VI-iii

Cyclic voltammogram of 10^{-4} M DA (—) and 10^{-4} M AA (---), in citrate phosphate buffer pH 7.4, at a carbon fibre microelectrode.
Scan rate 0.1 V s^{-1}

The cyclic voltammograms of DA and AA, as shown in Figure VI-iii, display a typical sigmodial response at a carbon fibre microelectrode. The large cathodic, at 0.2 V, and anodic peak at 0.15 V, for DA indicate lack of steady state due to the large size of the electrode. Although the optically measured O.D. is 10 μm, the rough surface of the carbon fibre can

effectively increase the O.D. eight fold. (Measured in this thesis work using the Cottrell decay during the reduction of $Ru(NH_3)_6^{3+}$)

When used *in vivo* a carbon fibre microelectrode produced the fixed potential chronoamperometric trace shown in Figure VI-iv.

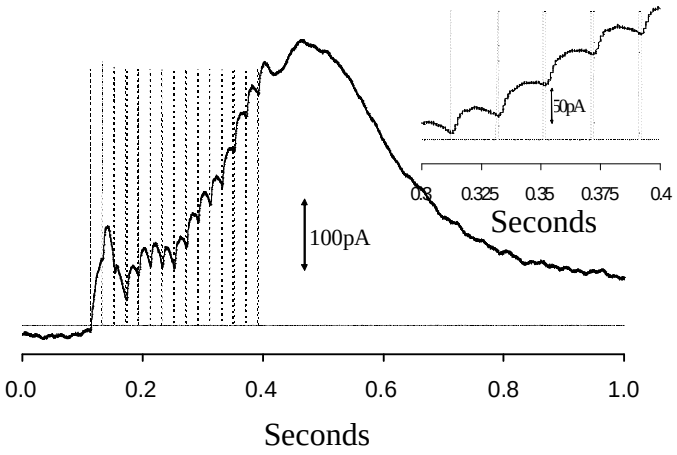

Figure VI-iv

Fixed potential (0.8 V vs. Ag|AgCl) amperometric trace of DA efflux in the nucleus accumbens of an anaesthetised rat, during 15 pulses at 50 Hz (---), at a carbon fibre microelectrode. The inset shows the peak details with the overlay of the electrical pulses (---).

The fixed potential chronoamperometric trace in Figure VI-iv shows close tracking of the DA efflux, with inset showing the resolution between the simulating pulses, which occurred at 20 millisecond intervals.

The effect of fouling by the brain extracellular fluid on a carbon fibre microelectrode after two hours *in vivo*, can be seen in Figure VI-v.

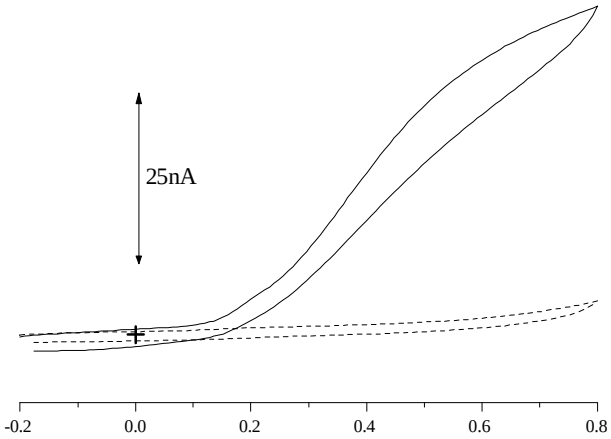

Figure VI-v

Cyclic voltammograms of 10^{-4} M DA (—) and 10^{-4} M AA (---) at a carbon fibre microelectrode in citrate/phosphate buffer pH 7.4, after 2hrs *in vivo*.
Scan rate 0.1 V s^{-1}

The changes to the shape of the cyclic voltammograms of DA and AA, post *in vivo* application (n=5), can be seen by comparing Figure VI-iii and VI-v. The lack of sigmodial response for both DA and AA indicates that the heterogeneous electron transfer has been modified. This reduction of heterogeneous electron transfer of DA and AA is symptomatic of *in vivo* fouling. The reduction in heterogeneous electron transfer rate of DA, at the carbon fibre microelectrode surface post *in vivo* suggests the formation of a Donnan type membrane. The almost complete suppression of the heterogeneous electron transfer of AA at the carbon fibre microelectrode surface suggests a membrane with predominately anionic properties. The predominant anionic properties are indicated by the selectivity indicated from the differences in the cyclic voltammetry of the 10^{-4} M solutions of DA and AA. Proteins, containing external negative charges, attached to the carbon fibre surface would explain the observed selectivity of the fouling barrier.

The reduction in amperometric current occurs during implantation[21] suggesting the majority of fouling of carbon fibre microelectrodes occurs during the initial thirty minutes of

in vivo exposure. To overcome this initial decay in response sensitivity, a stabilisation protocol of typically one hour *in vivo* exposure prior to commencement of experimentation is followed. After the initial loss in sensitivity the response for DA remains constant for two hours.[22] Hence the need to post calibrate after *in vivo* experiments.[1]

To investigate the susceptibility to fouling of modified carbon film microelectrodes the following carbon film modifications were selected for *in vivo* evaluation: ferrous sulfate (Chapter V-(i)), anodic oxidation of 2,4-dinitroaniline in DCM (Chapter V-(iii)), bifunctional modification using the anodic oxidation of 2,4-dinotroaniline in DCM followed by anodic oxidation of ethanol with DBU (Chapter V-(vi)) and Nafion coated.

Ferrous sulfate modified surface

The ferrous sulfate modification was chosen as it was the most labile method of creating a hydrophilic surface (carboxylic acids). The result (n=1) after 45 minutes *in vivo* is shown in Figure VI-vi. The fouling after this limited time *in vivo* is similar to that of the untreated carbon fibre after two hours. The sigmodial shape of DA, together with the cathodic wave has disappeared. The limiting current at 0.9 V has decreased to half the original value. From this result the hydrophilic surface has not retarded the formation of protein films on the surface, possibly due to the external negative charge of proteins.

Although fouling has taken place on the surface of the ferrous sulfate modified carbon film microelectrodes the tracking of the DA efflux is unimpaired. This can be seen in Figure VI-vi (b) where the DA efflux follows the electrical stimulation pulses.

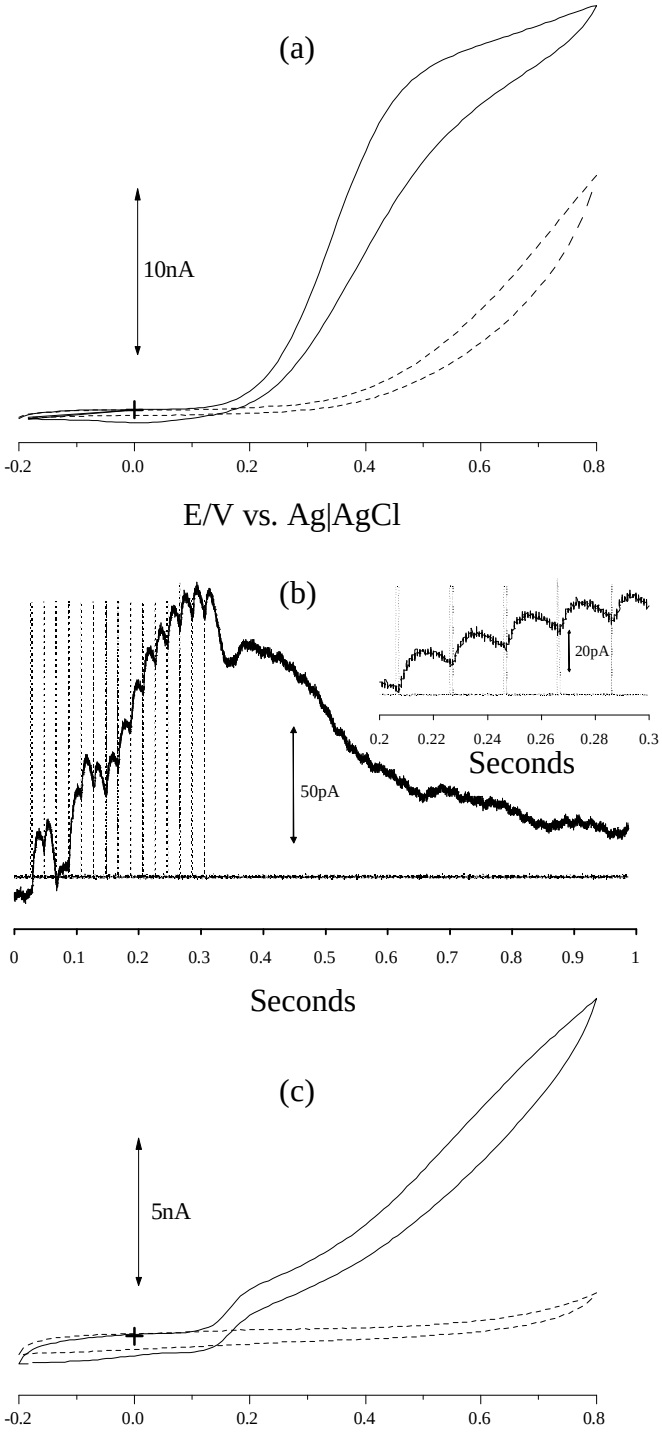

Figure VI-vi

Cyclic voltammograms of 10^{-4} M DA (—) and 10^{-4} M AA (---) at a ferrous sulfate modified carbon film microelectrode, in citrate/phosphate buffer pH 7.4, with (a) before and (c) after *in vivo* use.
Scan rate 0.1 V s^{-1}
(b) Inset, the DA efflux recorded during a 15 pulse electrical stimulation using a ferrous sulfate modified carbon film microelectrode.

2,4-Dinitroaniline modified surface

A short term (45 minutes) *in vivo* evaluation of a 2,4-dinitroaniline modified carbon film microelectrode surface retained the DA sigmodial response and the cyclic voltammetric shape of AA. This is shown in Figure VI-vii. Although only *in vivo* for 45 minutes the lack of fouling is in contrast with the heavy fouling of the ferrous sulfate modified carbon film microelectrode (Figure VI-vi) shown after the same time interval.

The fixed potential chronoamperometric traces (Figure VI-viii (b) and (c)) showed similar responses to the evoked DA efflux, with possible finer detail obtained from the 2,4-dinitroaniline modified carbon film microelectrode than the carbon fibre. This increase in detail is probably attributable to the lack of a protein membrane on the surface of the microelectrode. The presence of any membrane will restrict the diffusion rate of DA to the surface, thus tracking of the DA efflux maxima will be reduced, return to basal levels extended and small rapid changes in concentration will not be detectable.

On extending the time *in vivo* to four hours the 2,4-dinitroaniline modified carbon film microelectrodes (Figure VI-viii) continued to display retention of the DA sigmodial shape. (n=5 with *in vivo* time 2-4 hours). The retention of the sigmodial shape for DA indicates fouling has not occurred.

The constancy of the anodic current at fixed potential chronoamperometry during *in vivo* evaluation (Figure VI-viii (a) and (b)), confirms the lack of long term fouling occurring at 0.9 V.

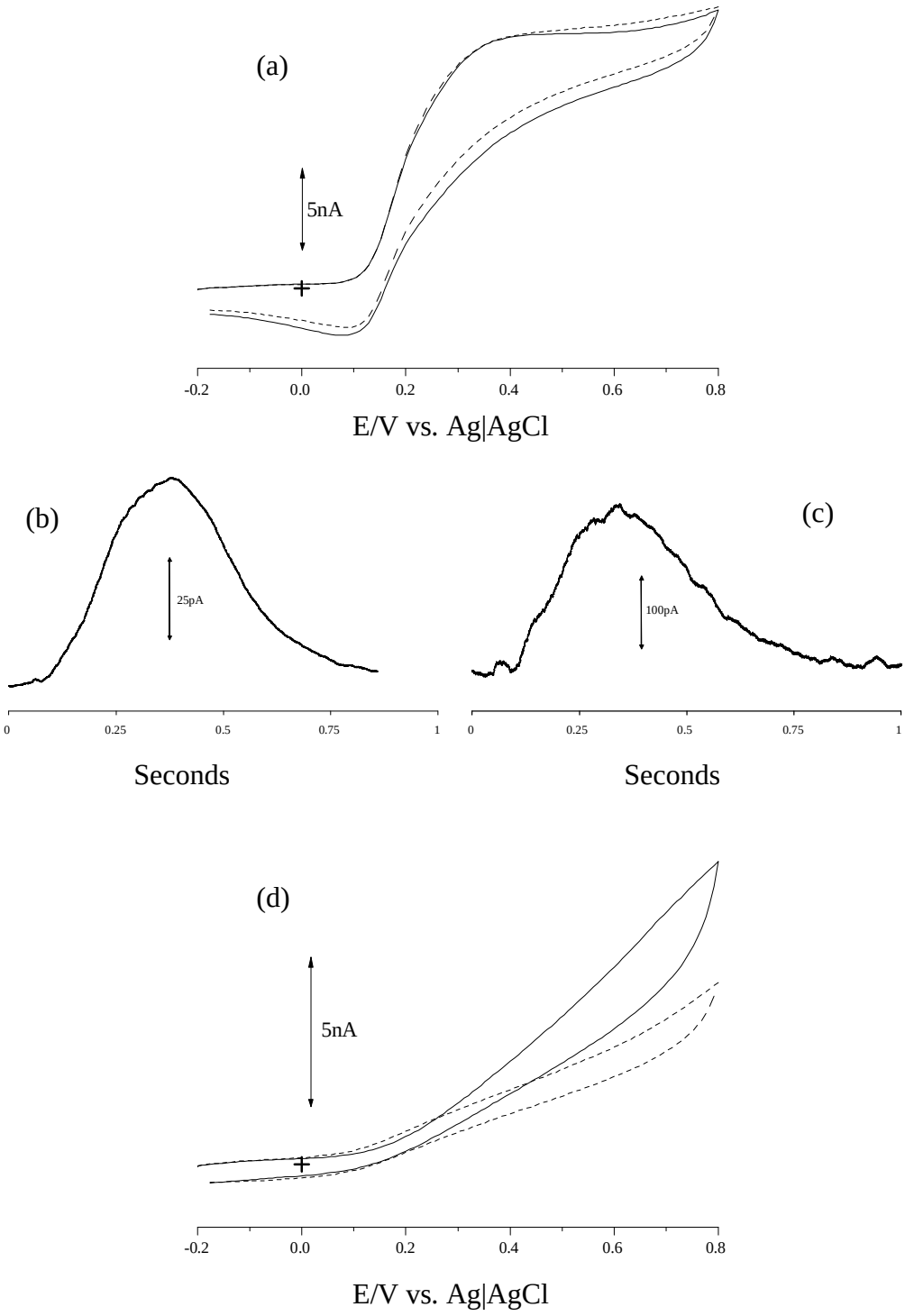

Figure VI-vii

Cyclic voltammograms of 10^{-4} M DA (a) and 10^{-4} M AA (d) in a citrate/phosphate buffer pH 7.4, before (—) and after (---) 45 minutes *in vivo*. Scan rate 0.1 V s^{-1}
Fixed potential chronoamperometric recordings of DA efflux, during 15 pulses at 50 Hz, at a carbon fibre electrode (b) and a 2,4-dinitroaniline modified carbon film microelectrode (c).

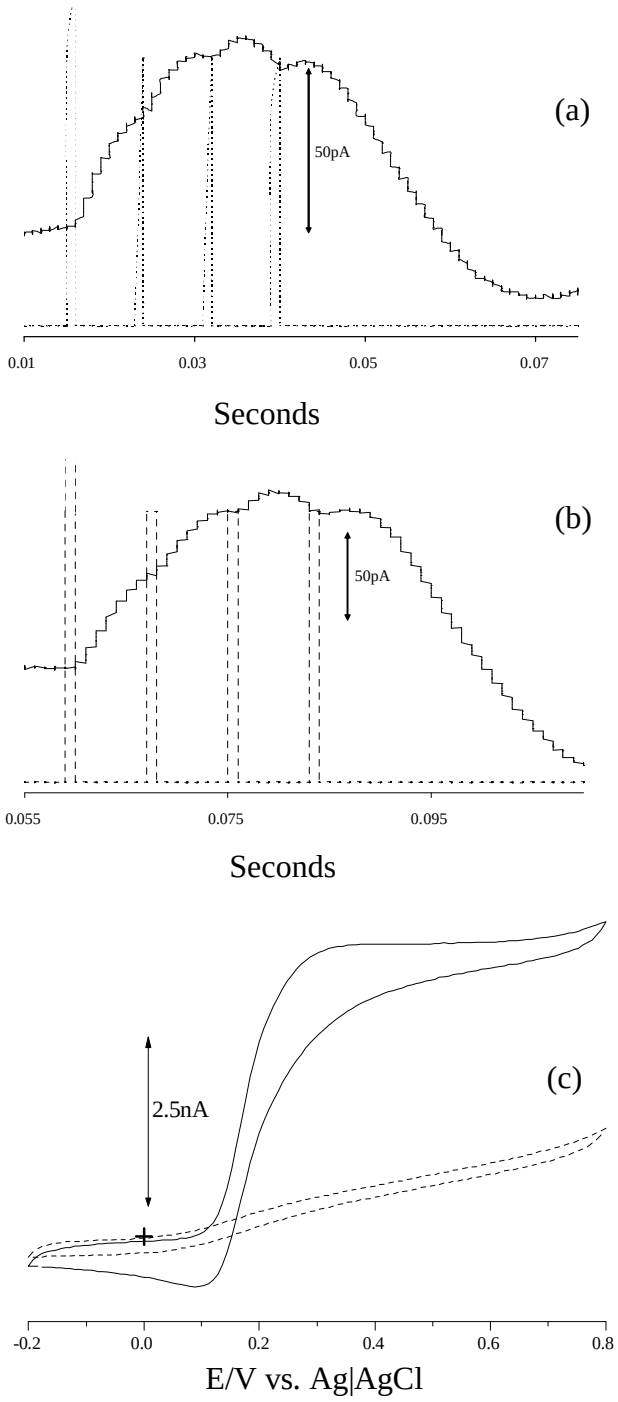

Figure VI-viii

Fixed potential chronoamperometric *in vivo* recordings at a 2,4-dinitroaniline modified carbon film microelectrode of DA efflux after 2minutes (a) and four hours (b) during the application of four pulses at 100 Hz.
The cyclic voltammograms (c) of 10^{-4} M DA (—) and 10^{-4} M AA (---) in a citrate/phosphate buffer (pH 7.4) after 4 hours *in vivo.*
Scan rate of 0.1 V s^{-1}

Dual functional modified surface

The selectivity for DA with respect to AA, when using 2,4-dinitroaniline modified carbon film surfaces was enhanced when further modified by the addition of carboxylic acid groups during the anodic oxidation of ethanol in the presence of DBU(Chapter V-(iv)). This dual functional surface modification appears to possess the ideal surface for the *in vivo* monitoring of evoked DA efflux. The results of the *in vivo* application of one of these dual functionally modified carbon film microelectrode is shown in Figure VI-ix.

Comparison of the cyclic voltammograms of DA and AA pre and post *in vivo*, (Figure Vi-ix (a) and (c)) show a retarding of the heterogeneous electron transfer rate. This retardation of heterogeneous electron transfer indicates that fouling of the surface has occurred. The extent of fouling, indicated by the change in heterogeneous electron transfer, is similar to that of carbon fibre and ferrous sulfate modified carbon film surface. It therefore appears either the surface concentration of the nitro groups is too low or carboxylic acid groups being closer to the graphene region aid in protein attachment.

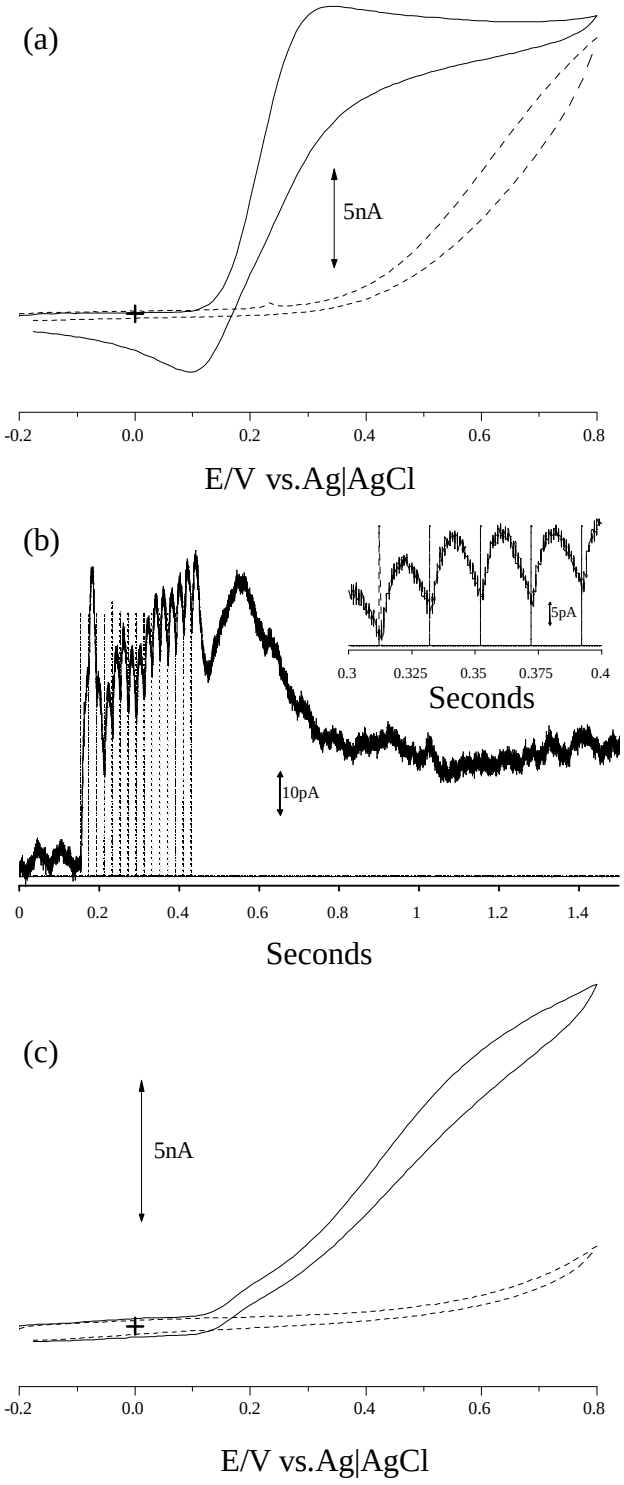

Figure VI-ix

Cyclic voltammograms of 10^{-4} M DA (—) and 10^{-4} M AA (---) at a 2,4-dinitroaniline and ethanol/DBU modified carbon film microelectrode in citrate/phosphate buffer pH 7.4, with (a) before and (c) after *in vivo,* Scan rate 0.1 V s^{-1}
(b) DA efflux, after a 15 pulse 50 Hz electrical stimulation, with a 2,4-dinitroaniline, ethanol and DBU modified carbon film microelectrode.

Nafion

A selective anionic membrane, such as Nafion, has been reported to minimise fouling.[23] For a limited comparative study (n=2) carbon film microelectrodes were coated with Nafion and then implanted *in vivo* for thirty minutes. The post cyclic *in vivo* voltammograms of DA and AA are shown in Figure VI-x (a) and (b).

Pre and post *in vivo* cyclic voltammograms of AA both display only a small heterogeneous electron transfer. The pre and post voltammograms of DA did exhibit a minor change in heterogeneous electron transfer. This slight change after only 30 minutes may be an indicator of additional modification of the surface with extended time *in vivo*. Had time and more animals been available *in vivo* times of four hours would have been investigated. This would have enabled a direct comparison of the effects of fouling with 2,4-dinitroaniline modified carbon film microelectrodes.

The fixed potential chronoamperometric recording of the evoked DA efflux (Figure VI-x (b)) indicates the Nafion coated microelectrode tracks the DA efflux similar to uncoated carbon fibre and modified carbon film microelectrodes. All microelectrodes had a current maxima delay of 0.1 second after the stimulating pulse. This indicates coatings, either intentional, as with Nafion or unintentional in the case of *in situ* fouling, the diffusion time through the coating, for fixed potential chronoamperometric investigations, as used in this thesis work, are insignificant.

Comparison of short exposure *in vivo* of 2,4-dinitroaniline modified carbon film or Nafion coated carbon film microelectrode indicates the former is less prone to fouling.

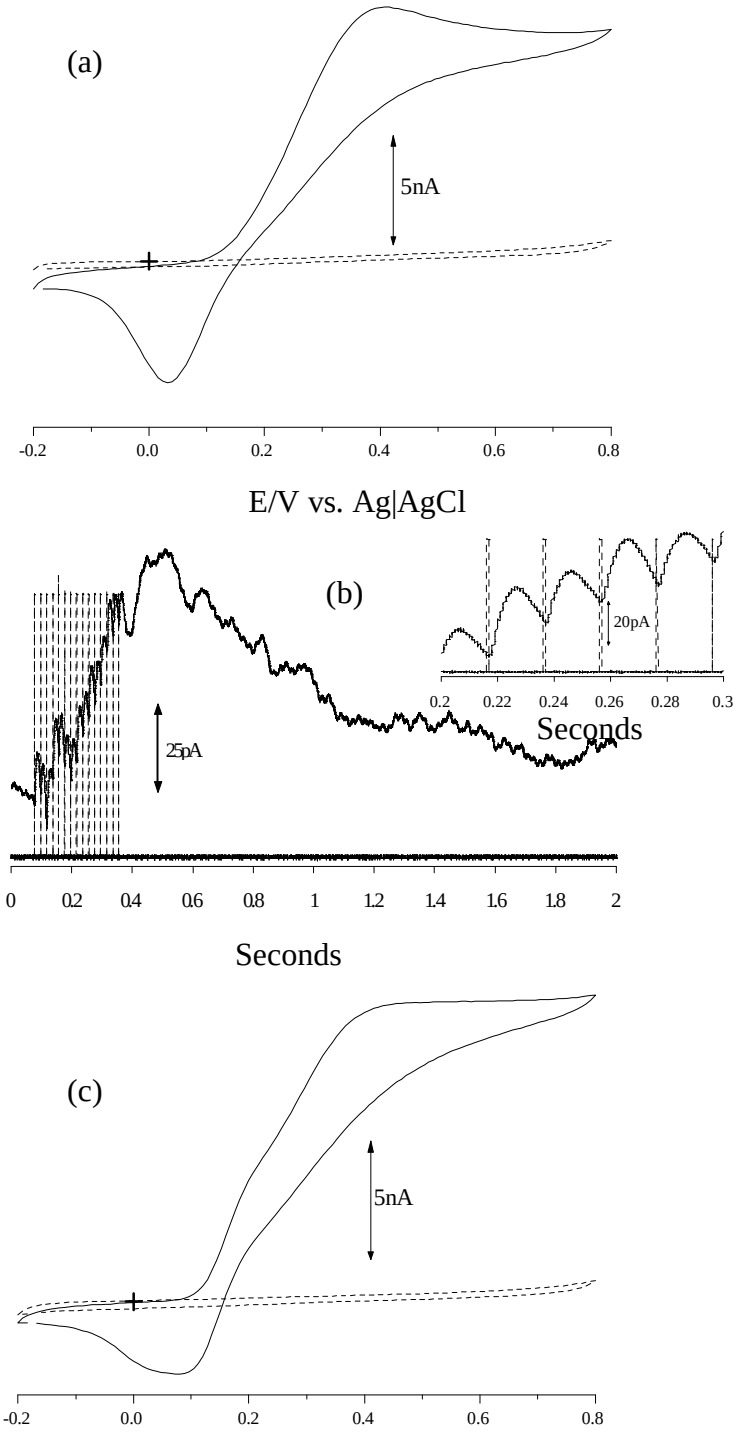

Figure VI-x

Cyclic voltammograms of 10^{-4} M DA (—) and 10^{-4} M AA (---) at a Nafion modified carbon film microelectrode in citrate/phosphate buffer pH 7.4, before (a) and (c) after 30 minutes *in vivo.*
Scan rate 0.1 V s^{-1}
(b) DA efflux, after a 15 pulse electrical stimulation, with a Nafion modified carbon film microelectrode.

Conclusion

The anodic oxidation of 2,4-dinitroaniline at a carbon film microelectrode has resulted in the formation of a surface resistant to fouling when used to monitor the efflux of DA in the extracellular fluid of a rat's brain. The slight selectivity, with regards to the suppression of the Faradaic current of AA is also maintained during *in vivo* studies. However the conversion of the 2,4-dinitroaniline modified surface to a bifunctional surface containing carboxylic acids, to obtain greater selectivity, compromised the anti-fouling properties of the 2,4-dinitroaniline groups.

The possible application of 2,4-dinitroaniline modified carbon film microelectrodes will be in long term *in vivo* chronoamperometry and fast scan cyclic voltammetry. The latter, by utilising the low capacitance and anti-fouling properties of the 2,4-dinitroaniline modified carbon film, is expected to provide a readily recognisable finger print cyclic voltammogram of neurotransmitters over extended periods *in vivo.* The retention of the DA sigmodial shape, for extended *in vivo* fixed potential chronoamperometry recording should enable lower fixed potentials to be applied. It is expected that this may reduce the propensity to foul whilst still providing a degree of selectivity with respect to AA.

References

1. Kawagoe K.T.; Zimmerman J.B.; Wightman R.M. *Journal of Neuroscience Methods.* **1993,** *48*, 225-40.
2. Foster G.L.; Blaha C.D. *European Journal of Neuroscience* **2003,** *17*, 751-62.
3. Venton B.J.; Wightman R.M. *Analytical Chemistry* **2003,** *1st Oct*, 414A-21A.
4. Hochsteltler S.E.; Puopolo M.; Gustincich S.; Raviola E.; Wightman R.M. *Analytical Chemistry* **2000,** *72*, 489-96.
5. Benoit-Marand M.; Borrelli E.; Gonon F. *Journal of Neuroscience* **2001,** *21*, 9134-41.
6. Baufreton J.; Garret M.; Rivera A.; de la Calle A.; Gonon F.; Dufy B.; Bioulac B.; Taupignon A. *Journal of Neuroscience* **2003,** *23*, 816-25.
7. Miller A. D.; Blaha C. D. *European Journal of Neuroscience*, **2005,** *21*, 1837-46.

8. Nieoullin A *Progress in Neurobiology* **2002,** *67*, 53-83.

9. Rouge-Pont F.; Usiello A.; Benoit-Marand M.; Gonon.F.; Piazza P.V.; Borrelli E. *Journal of Neuroscience* **2002,** *22*, 3293-301.

10. Zhou F-M.; Liang Y.; Salas R.; Zhang L.; Biassi M.B.; Dani J.A. *Neuron* **2005,** *46*, 65-74.

11. Davidson C.; Lee T.H.; Ellinwood E.H. *Neurochemistry International*, **2005,** *46*, 189-203.

12. Yavich L.; Tiihonen J. *Journal of Neuroscience Methods* **2000,** *104*, 55-63.

13. Stamford J. S.; Justice J. B. Jr. *Analytical Chemistry News & Features*, **1996, 359A**-63A.

14. Wisniewski N.; Moussy F.; Reichert W.M. *Fresenius' Journal of Analytical Chemistry* **2000,** *366*, 611-21.

15. Sharma S.; Johnson R.W.; Desai T.A. *Biosensors and Bioelectronics* **2004,** *20*, 227-39.

16. Lan S.; Veiseh M.; Zhang M. **2005,** *20*, 1697-708.

17. Guo B.; Anzai J.; Osa T. *Chemical and Pharmaceutical Bulletin* **1996,** *44*, 860-62.

18. Downard A.; Roddick A.D. *Electroanalysis* **1995,** *7*, 376-78.

19. Blaha C.D. *Biosensors and Bioelectronics* **1996,** *11*, 63-79.

20. Paxinos; Watson C. *The Rat Brain in Sterotaxic Coordinates,* ed.; Academic Press: New York, 1997.

21. Cahill P.S.; Walker Q.D.; Finnegan J.M.; Mickelson G.E.; Travis E.R.; Wightman R.M. *Analytical Chemistry* **1996,** *68*, 3180-86.

22. Ewing A.G.; Bigelow J.C.; Wightman R.M. *Science* **1983,** *221*, 169-71.

23. Kawagoe K.T.; Wightman R.M. *Talanta* **1994,** *41*, 865-74.

Chapter VII

Conclusion

In this work, a method to fabricate a carbon film microelectrode with anti-fouling and selectivity suitable for *in vivo* monitoring, of DA efflux in a rats brain, has been detailed. These carbon film microelectrodes were successfully utilised to monitor the efflux of DA, using constant potential chronoamperometry, for four hours *in vivo.*

The fabrication of the carbon film microelectrode is based on the pyrolysis of acetylene flowing from a pulled quartz capillary into a nitrogen atmosphere. The carbon film is formed on the surface adjacent to the acetylene exit orifice of the pulled capillary. By varying the direction and flow rate of the nitrogen atmosphere, carbon film microelectrodes ranging from nanometre discs to cylindrical microelectrodes 1.8mm in length were fabricated. The location of the electrochemically active surface, being only several hundred atoms thick, was not possible using standard SEM techniques as the relief between the quartz substrate and the carbon surface did not provide a means of distinguishing the two regions. A simple technique based on the use of platinum plating to visualise the location of the electrochemically active region using SEM was developed. Using this technique correlation between the visually assessed SEM micrographs and that obtained from the Cottrell decay curve was obtained with suitable accuracy for calculation of capacitance and concentration of surface modifications.

Surface characterisation of the carbon film was carried out using Raman spectroscopy, XPS and the heterogeneous electron transfer of model analytes. The results of this work indicated that the surface formed by *in situ* pyrolysis was devoid of edge planes or a continuous basal region. The unique heterogeneous electron exchange properties were attributed to the presence of pendent groups, such as alkyne and polyaromatics. The surface concentration of the alkyne groups were determined, using stripping voltammetry, and was

found to occupy approximately $1x10^{-11}$ to $2x10^{-10}$ moles cm^{-2} of the surface. This work is possibly the first to report the presence of alkynes on the surface of a carbon film. The presence of such groups is predictable from the previously reported polymerisation mechanism of graphite formation from a hydrocarbon source.

The surface chemistry of the carbon film unifying all the results of this work was proposed. This proposal is based on the need to explain a carbon surface lacking either edge or basal plane heterogeneous electron transfer properties, particularly with respect to DA. The carbon film, as fabricated in this work also displayed well defined cathodic waves, at low scan rates during cyclic voltammetry of catechols, further indicating a unique surface chemistry. To account for this unique surface chemistry, whilst including an electrically conductive surface, the presence of aromatic and alkyne branch chains on the carbon surface was proposed.

The presence of pendent groups on the surface provided a unique opportunity for surface modification reactions. The alkyne groups were oxidised to carboxylic acid using a facile method utilising the immersion of the carbon film microelectrodes in ferrous sulfate followed by air drying. The presence and surface concentrations of the carboxylic acid groups was confirmed by changes in cyclic voltammetric response after derivatisation of the carboxylic groups. Using a previously reported technique of anodic oxidation of a diol to form a barrier to ascorbic acid, it was found short chain aliphatic alcohols also formed a barrier. The nature of the barrier, carboxylic acids, was previously proposed to be covalently bonded via an ether linkage to the graphene region. In this work the presence of carboxylic acid groups was established and their surface concentrations measured by cyclic voltammetry of the 2,4-dinitrobenzyl chloride carboxylic acid derivatives. The reaction pathway to the formation of a carbon carbon single bond attached through the alcohol β carbon atom, via carbocations to the graphene region was proposed.

To provide anti-fouling properties, for *in vivo* applications of the carbon film microelectrodes, aromatic nitro groups were utilised. By anodically oxidising dinitroanilines, in the presence of DBU, at the carbon film microelectrode a surface concentration of 10^{-10} moles cm^{-2} was achieved. At this surface concentration, after four hours *in vivo,* insignificant changes had occurred in the cyclic voltammetric limiting current and shape of the DA sigmodial curve. This indicates that the anti-fouling property of the modified carbon film surface is comparable with that of Nafion over four hours.

With the existence of two reaction sites, on the carbon film surface, this presented an opportunity for a dual modification of the carbon film surface. This was achieved using anodic oxidation of ethanol to react with the graphene region and 3,5-dinitroaniline with the pendent groups. This is possibly the first reported dual functional modification of a carbon electrode.

Also investigated in this work was the cathodic wave present in the cyclic voltammograms of DA. This had previously been reported when carrying out fast scan cyclic voltammetry at 300 and 2000 V s^{-1} at carbon fibre disc and cylinder microelectrode. It was attributed to the presence of an adsorbed species on the carbon fibre surface, with the amine functionality providing the electrostatic bond to the surface. In this work the carbon film displayed a very distinct cathodic wave present in the cyclic voltammetry of catechol at a 0.1 V s^{-1} scan rate. The cathodic wave in this work was well defined enabling the measurement of the area occupied by the adsorbed species ($\approx$ 50%). The presence of the well defined cathodic waves for the catechols, at slow scan rates used in this work, suggests that the hydroxyl groups, on the catecholamine, is providing the bonding to the surface. This further indicates the difference in surface chemistry between a carbon fibre and the carbon film fabricated in this work.

The carbon film not only provided a chemically unique surface suitable for the electrochemical detection of DA but also its inherent stability in the laboratory atmosphere

over 25 months which enables bulk fabrication of microelectrodes prior to experimentation. When these properties are combined with its low capacitance and quartz substrate it is almost an ideal microelectrode for fast cyclic voltammetry *in vivo* applications. If, during constant potential chronoamperometry *in vivo* studies a lower potential, such as 0.4 V is used instead of 0.9 V Ag|AgCl, to monitor the efflux of DA, the selectivity of the 2,4-dinitroaniline modified surface, are similar to that of Nafion. By using a reduced potential, a reduction in perturbation and fouling during monitoring of catecholamines during efflux could be expected.

The immediate application of the carbon film microelectrode, as well as *in vivo* studies, is *in vitro* studies. The use of a quartz substrate enabled a very thin Nafion coating, using the technique outlined in this work, to be applied to the surface of the carbon film microelectrode. This suggests together with the carbon film's inherit stability and low capacitance, would provide an ideal surface for chemical, electrochemical or polymer modification or as an unmodified microelectrode in applications of general electrochemical *in vitro* studies requiring millisecond responses to analyte concentration changes.

A commercial application of the unmodified carbon film microelectrodes is in the vegetable oil industry to determine the origins and monitor π complexing cations to minimise the dioxygen oxidation of vegetable oils during manufacture and storage. The advantage of using of a carbon film microelectrode in this application is the elimination of the need to ash the vegetable oil, use of expensive ultra-pure chemicals, expensive instrumentation and the detection of ferrous ions.

The pendent groups on the surface of the carbon film could, after conversion to carboxylic acids provide "amide linkers", thereby allowing existing surface modification techniques to be used in biosensor applications.

The existence of dual functionality presents the opportunity for close coupled reactions, such as chemical/electrochemical allowing enhanced analyte detection limits.

Possible future investigations, extending the knowledge generated in this work, are as follows:

Examination of the surface using Auger electron spectroscopy (AES) coupled with SEM, after π complexation with a heavy metal ion, would provide a visual distribution of the alkyne pendent groups. This information could then be used to optimise the surface chemistry by varying the pyrolysis temperature and gas composition.

The anti-fouling and selectivity, conferred by the nitro groups, could be further evaluated to determine the maximum possible *in vivo* exposure that is possible before signal deterioration occurs. With this information the anti-fouling and selectivity properties of additional nitro groups, perhaps using a dendritic structure could be investigated. The application of anti-fouling properties could be applied to other technologies, such as medical implants.

The unique surface of the carbon, as deposited in this work, is a fertile field for future electrochemical investigations. The discovery that by modifying the carbon film using 2,4-dinitroanilines has provided anti-fouling properties may open avenues to eliminate bio-fouling in many other applications.